AD

TECHNICAL REPORT 117

ON FLIGHT DYNAMICS OF MAGNUS ROTORS

AD 716345

Peter H. Zipfel

NOVEMBER 1970

D D C
RECEIVED
JAN 11 1971
B

Reproduced by
NATIONAL TECHNICAL
INFORMATION SERVICE
Springfield, Va. 22151

DEPARTMENT OF THE ARMY
Fort Detrick
Frederick, Maryland

This document has been approved for public release and sale; its distribution is unlimited.

50403

275

DEPARTMENT OF THE ARMY
Fort Detrick
Frederick, Maryland 21701

TECHNICAL REPORT 117

ON FLIGHT DYNAMICS OF MAGNUS ROTORS

Peter H. Zipfel

Munitions Development Division
COMMODITY DEVELOPMENT & ENGINEERING LABORATORIES

Project 1T061101A91A

November 1970

PREFACE

This report is the culmination of six years of Magnus Rotor research at Fort Detrick. The actual writing was carried out under the In-House Laboratory Independent Research Program (Project 1T061101A91A) with Dr. Harold N. Glassman as Director. This report was also submitted to the Faculty of the School of Engineering and Architecture of the Catholic University of America in partial fulfillment of the requirements for the degree of Doctor of Engineering.

The author is indebted to Mr. Carroll B. Buttler, Air Force Armament Laboratory, and Mr. Ron E. Davis, Arnold Research Organization, for an advance copy of their wind tunnel data. Many ideas in this report evolved during discussions with Mr. James E. Brunk, Alpha Research, and Mr. Abraham Flatau, Edgewood Arsenal. Their contributions are gratefully acknowledged.

ABSTRACT

Heinrich G. Magnus demonstrated experimentally, in 1852, that a body rotating in an air stream experiences a force that acts substantially normal to the air flow. An autorotating flight vehicle, designed to develop this Magnus force efficiently and to employ it as the major lift force in free flight, is called a Magnus rotor. It has been considered for application in areas such as the recovery of rocket boosters and aerial delivery. The underlying idea is to make the container serve as its own decelerator and thus eliminate the parachute. In this report the equations of motion of Magnus rotors are derived and their performance and stability analyzed and correlated with free flight tests.

Tensor concepts are used extensively in formulating the flight dynamical problem. In particular, the ordinary time derivative is replaced by a covariant time derivative, the Rotational Derivative, thus permitting an invariant formulation of the equations of motion, even under time-dependent coordinate transformations. As in airplane and missile dynamics, a reference flight is chosen and perturbation equations are developed. The reference flight of a Magnus rotor may be accelerated or decelerated. To determine its effect on the perturbation equations, a special tensorial formulation of the perturbations is introduced. It is also tailored to yield the aerodynamic forces in a simple McLaurin expansion. Because of the symmetry properties of Magnus rotors, certain aerodynamic derivatives are zero. An easy-to-apply rule is derived that tells which derivative of arbitrary order vanishes. The nonlinear aerodynamics are represented by derivatives up to the third order; with all

second order derivatives vanishing because of the symmetry properties of Magnus Rotors.

The perturbation equations are nonlinear nonautonomous ordinary differential equations of fifth order with three degrees of freedom: rolling, yawing, and sideslipping. Their stability is analyzed first for the simple but important case of linear aerodynamics and a steady-state reference flight; i.e., the governing equations are linear and autonomous. A simplified form of the roots is given. The roots describe three modes: nutation, undulation, and precession. If the nutational motions are of major concern, the perturbation equations can be reduced to two degrees of freedom: rolling and yawing. A further reduction to one degree of freedom is achieved by combining the roll and yaw angles to form the nutation angle and by employing the method of averaging. The result is a first order equation. Its stability is discussed. Necessary and sufficient conditions for limit cycles are derived, and it is shown that limit cycles can be avoided by proper design of the Magnus rotor.

The complete equations of motion are programmed in Fortran IV. Some sample computer runs show the trajectories and attitude motions of typical Magnus rotors under various initial conditions. They also validate the two- and one-degree-of-freedom perturbation equations and, in particular, verify the analytical prediction of limit cycles.

Thirty models flight tested represented eight different Magnus rotors: rectangular, triangular, and cylindrical shapes with different end plates and mass distributions. Their trajectories and attitude motions are

correlated with computer simulations whose aerodynamic input data are solely based on wind tunnel tests. The agreement is satisfactory. To measure the aerodynamic damping derivatives in free flight, the induced-nutation and limit-cycle methods are introduced. Two different Magnus rotor shapes were tested for limit cycles. The test results agree well with the predictions. It was found that larger end plates or a high moment of inertia about the spin axis can eliminate the limit cycle.

CONTENTS

		Page
	Acknowledgments	i
	Abstract	ii
	List of Tables	vii
	List of Illustrations	viii
1.	INTRODUCTION	1
2.	PROBLEM STATEMENT AND APPROACH	9
3.	TENSOR CONCEPTS IN FLIGHT DYNAMICS	13
	3.1 General Principles and Definitions	15
	3.2 Concept of Position	19
	3.3 Concept of Motion	22
4.	PERTURBATION EQUATIONS	34
5.	NORMALIZATION	43
	5.1 Dynamic-Normalized System	43
	5.2 Aero-Normalized System	45
	5.3 Discussion and Application	46
6.	FRAME AXES	51
7.	KINEMATICS	59
8.	REFERENCE FLIGHT	66
	8.1 Conditions for the Existence of a Planar Glide Phase	66
	8.2 Equations of Motion	74
9.	LINEAR MOMENTUM	79
10.	ANGULAR MOMENTUM	83
	10.1 Simplifications	83
	10.2 Equations in Component Form	88

Page

11. AERODYNAMIC FORCES 96

11.1 Functional Relationship 96

11.2 Taylor Series Expansion 99

11.3 Conditions for Vanishing Derivatives 108

11.4 Discussion 114

11.5 Applications 117

12. EQUATIONS OF MOTION 126

12.1 Lateral Perturbation Equations 126

12.2 Averaging the Reference Equations 130

12.3 Averaging the Lateral Perturbation Equations 134

12.4 Averaged Equations of Motion 138

13. STABILITY ANALYSIS 143

13.1 Reduction to a Fourth Order System 144

13.2 Stability of the First Approximation 149

13.3 Nutation Limit Cycles 155

14. COMPUTER SIMULATIONS AND TEST RESULTS 166

14.1 Computed Flight Histories 166

14.2 Validation of Assumptions 187

14.3 Flight Test Results 192

15. CRITICAL EVALUATION OF RESULTS 206

Nomenclature 209

Literature Cited 216

APPENDIXES

A. Proofs of Section 3.3 219

B. Computer Program MAGSIX 229

C. Magnus Rotor Data 240

LIST OF TABLES

Table No.	Title	Page
5.1	Defined Unit Scales of the Dynamic-Normalized System	44
5.2	Derived Unit Scales of the Dynamic-Normalized System	45
5.3	Defined Unit Scales of the Aero-Normalized System	46
5.4	Derived Unit Scales of the Aero-Normalized System	46
5.5	Dimensions and Unit Scales	48
6.1	Flight-Mechanical Frame Axes	54
6.2	Gyro-Mechanical Frame Axes	55
6.3	Coordinate Transformation Matrices	58
11.2	Lateral Derivatives	123
12.1	Equations of Motion	128
14.1	Computer Simulations	173
14.2	Validation of Order of Magnitude Estimates	188
14.3	Steady-State Nutation Frequencies	190
14.4	Analyzed Flight Tests	194
B.1	Data Sheet	232
B.2	Computer Symbols	233

LIST OF ILLUSTRATIONS

Figure No.	Title	Page
1.1	Typical Triangular, Cylindrical, and Rectangular Magnus Rotors	2
1.2	Perturbed Motions	6
4.1	The Two Kinds of Perturbations	39
6.1	Intersections of the Frame Axis with the Unit Sphere	56
7.1	Spherical Triangle	62
8.1	Location of Mass Elements	67
11.1	Aerodynamic Derivatives	121
13.1	Roll and Yaw Angles Projected on a Horizontal Plane	145
14.1	Transient Performance of Rectangular Magnus Rotor 1. Computer Run 13	174
14.2	Transient Trajectory of Rectangular Magnus Rotor 1. Computer Run 13	174
14.3	Transient Nutation of Rectangular Magnus Rotor 1. Computer Run 13	175
14.4	Transient Nutation of Rectangular Magnus Rotor 1. Computer Run 13	176
14.5	High Speed Transient Performance of Rectangular Magnus Rotor 1. Computer Run 15	176
14.6	High Speed Transient Trajectory of Rectangular Magnus Rotor 1. Computer Run 15	177
14.7	Lateral Motions With and Without Acceleration Term of Rectangular Magnus Rotor 1. Computer Runs 15 and 23	177
14.8	Performance of Accelerated Rectangular Magnus Rotor 1. Computer Runs 24 and 25	178
14.9	Lateral Motions With and Without Acceleration Term of Rectangular Magnus Rotor 1. Computer Runs 24 and 25	178

Figure No.	Title	Page
14.10	"Lift Down" High Speed Transient Performance of Rectangular Magnus Rotor 1. Computer Run 21	179
14.11	"Lift Down" High Speed Transient Trajectory of Rectangular Magnus Rotor 1. Computer Run 21	179
14.12	"Lift Down" Lateral Motions of Rectangular Magnus Rotor 1. Computer Run 21	180
14.13	High Speed, Low Spin Rate Transient Performance of Triangular Magnus Rotor 1. Computer Run 39	180
14.14	Transient Trajectory of Triangular Magnus Rotor 1. Computer Run 39	181
14.15	Transient Attitude Motions of Triangular Magnus Rotor 1. Computer Run 39	181
14.16	Low Speed, High Spin Rate Transient Performance of Cylindrical Magnus Rotor 1. Computer Run 40	182
14.17	Transient Trajectory of Cylindrical Magnus Rotor 1. Computer Run 40	182
14.18	Steady-State Limit Cycle of Cylindrical Magnus Rotor 4A. Computer Run 30	183
14.19	Dampened Nutation Cycles in Steady-State Flight of Cylindrical Magnus Rotor 11. Computer Run 31	184
14.20	Limit Cycle in Steady-State Flight of Rectangular Magnus Rotor 2. Computer Run 36	185
14.21	Dampened Nutation Cycles in Steady-State Flight of Rectangular Magnus Rotor 3. Computer Run 37	186
14.22	Comparison of Exact and Approximate Transient Nutation Frequencies of Rectangular Magnus Rotor 1. Computer Run 13	191
14.23	Flight Speed and Glide Angle of Rectangular Magnus Rotor 1. Flight Test July 26. Simulation Run 19	198
14.24	Spin Rate of Rectangular Magnus Rotor 1. Flight Test July 26. Simulation Run 19	198
14.25	Trajectory of Rectangular Magnus Rotor 1. Flight Test July 26. Simulation Run 19	199

Figure No.	Title	Page
14.26	Transient Nutation of Rectangular Magnus Rotor 1 with Initial Conditions from Flight Test July 26. Simulation Run 19	200
14.27	Transient Nutation of Rectangular Magnus Rotor 1. FlightTest July 26. Simulation Run 19	201
14.28	Induced Nutation of Rectangular Magnus Rotor 1. Flight Test July 26	201
14.29	Transient Performance of Rectangular Magnus Rotor 3. Flight Test June 10. Simulation Run 32	202
14.30	Steady-State Limit Cycle of Rectangular Magnus Rotor 2. Flight Test June 30	202
14.31	Transient Performance of Triangular Magnus Rotor 1. Flight Test June 30. Simulation Run 35	203
14.32	Transient Performance of Cylindrical Magnus Rotor 1. Flight Test June 10. Simulation Run 34	203
14.33	Induced Nutation of Cylindrical Magnus Rotor 1. Flight Test June 10	204
14.34	Induced Nutation of Cylindrical Magnus Rotor 3. Flight Test June 30	204
14.35	Transient Performance of Cylindrical Magnus Rotor 11. Flight Test June 30. Simulation Run 38	205
14.36	Steady-State Limit Cycle of Cylindrical Magnus Rotor 4. Flight Test June 30	205
B.1	MAGSIX Functional Chart	230
C.1	Rectangular Magnus Rotors 1, 2, and 3. Dimensions in Inches	240
C.2	Triangular Magnus Rotor 1. Dimensions in Inches	241
C.3	Cylindrical Magnus Rotors 1, 3, 4A, and 11. Dimensions in Inches	242

I. INTRODUCTION

Heinrich G. Magnus demonstrated experimentally, in 1852, that a body rotating in an air stream experiences a force that acts substantially normal to the air flow. An autorotating flight vehicle, designed to develop this Magnus force efficiently and to employ it as the major lift force in free flight, is called a Magnus rotor (MR). It consists of a center body, driving vanes, and, in most cases, endplates or ribs to assure proper orientation in free flight.

In general, the designer has much freedom in selecting the geometrical configuration so long as he provides driving vanes that generate a torque about an axis, the spin axis, and chooses a body with mirror symmetry relative to a plane normal to the spin axis. Any endplates will be arranged so that they are normal to the spin axis and the mirror symmetry is maintained. Five typical MR's are shown in Figure 1.1. They will be used to demonstrate and validate the analytical methods developed in this report. Some of the pertinent dimensions are: span b,* chord c, and endplate diameter d. The chord is defined as the diameter of that cylinder that fits tightly over the center body without driving vanes and is parallel to the spin axis. The reference area is $S = b \cdot c$.

The principal flight regime is the <u>planar steady-state glide phase</u>. It is characterized by a constant descent velocity of the center of mass along a straight line. The angle between this line and the horizon is the glide angle. While descending, part of the potential energy is

* All symbols are listed in Nomenclature, page 209

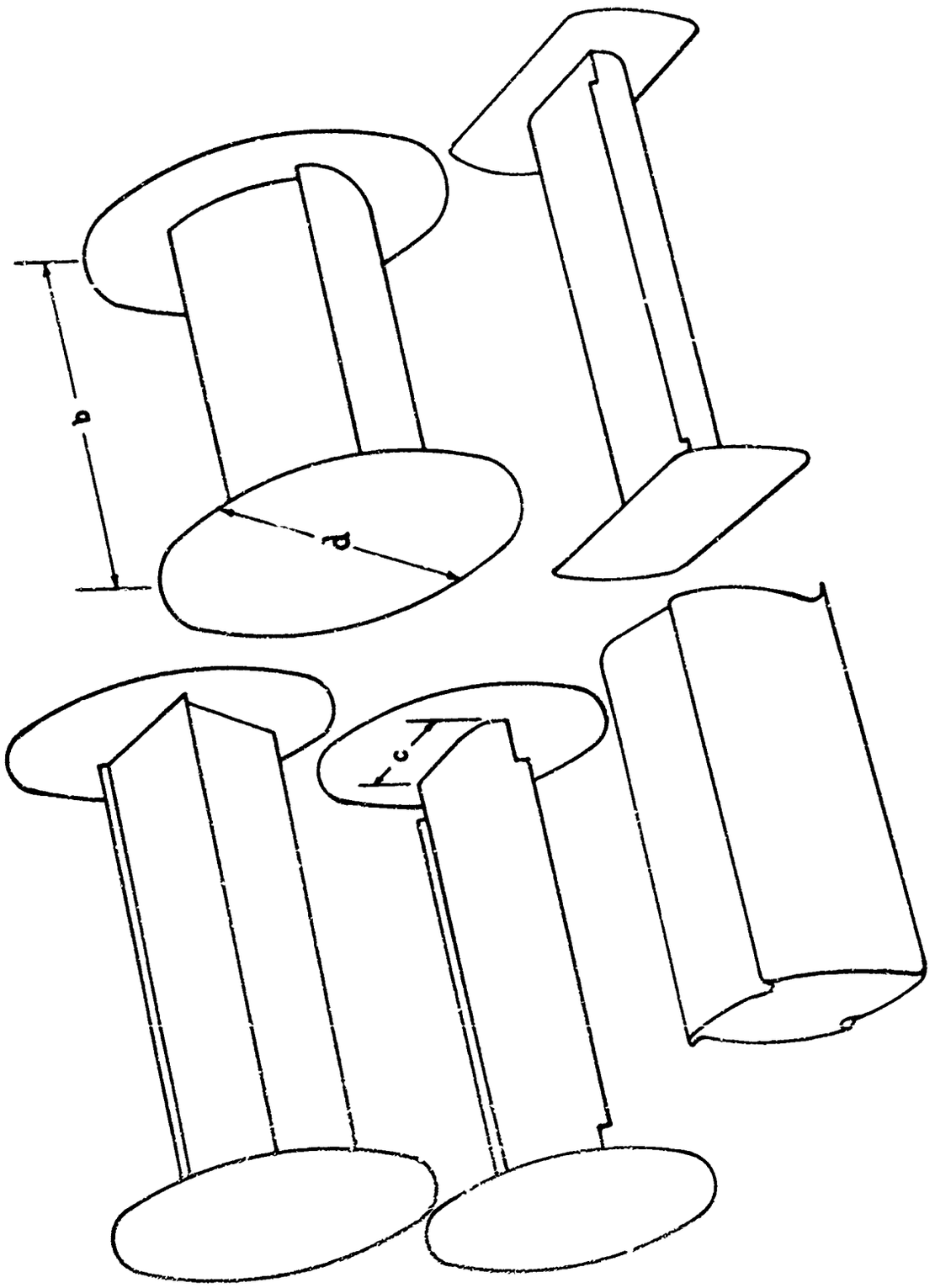

FIGURE 1.1 TYPICAL TRIANGULAR, CYLINDRICAL, AND RECTANGULAR MAGNUS ROTORS

converted via the driving vanes into kinetic energy, resulting in a constant rotation of the MR about a horizontal spin axis. The so generated aerodynamic circulation induces a Magnus force that is approximately normal to the flight velocity vector and the spin axis. Of particular importance is the ratio of the peripheral speed of the driving vanes to the flight speed of the MR. It is commonly referred to as the <u>tip-speed ratio</u> $\hat{\omega}$. In steady-state flight any MR with geometrical similar configuration has the same tip-speed ratio, regardless of size, weight, and mass distribution. We now define the planar steady-state glide phase as that part of the flight, when the angular velocity vector is constant and horizontal and the linear velocity vector is constant and normal to the angular velocity vector.

Unless the initial conditions match the steady-state values, the MR will go through some transient flight regimes. The most important one is the <u>planar transient glide phase</u>. It is defined as that part of the flight when the angular velocity vector is still horizontal and the linear velocity vector remains in a vertical plane normal to the angular velocity vector, but the absolute values of both vectors change in time.

The <u>planar glide phase</u> comprises both the steady-state and transient flight regimes. It is the flight phase that is of principal interest in any performance analysis.

Other flight regimes, like end-on flight, end-over rotation, or flat spin, are sometimes investigated. However, they are studied only to find out how to avoid them through proper design. They usually are not part of a performance analysis.

In recent years, the Magnus rotor principle has been considered for application in areas such as the recovery of rocket boosters, Brunk (1, 2)* and aerial delivery, Boehler (3) and Foshag (4). The MR also has been suggested for landing an instrumentation payload on Venus or Mars. The underlying idea is to make the container serve as its own decelerator and to eliminate the parachute. This is possible, because the high spin rate of an MR results in a drag coefficient between one and two (based on reference area S). In addition, the large angular momentum makes it insensitive to short-duration perturbations, and a lift-over-drag-ratio between one and three provides ample targeting range. With one of the several steering systems that have been proposed, the MR can be made to impact at a predetermined point. Thus, the MR is a precision decelerator system.

To discuss the flight dynamics of MR's in more detail, consider a particular application, say, the delivery of supplies from an aircraft to a ground station. The supplies are stored in the center body, and the MR is prespun and launched through the tail gate of the cargo plane. Ideally, if the initial conditions match the steady-state conditions and the flight is free of disturbances, the MR would descend in a planar steady-state glide phase. However, this is never satisfied. Usually, the spin rate and the velocity vector are mismatched. If no other disturbances occur, the MR would go through a planar transient glide phase until the steady-state values are reached; i.e., the MR would perform a planar glide phase. Again, this is an ideal case. The disturbances that can be expected are misalignments during the launch phase, wind gusts, and geometrical and

* All references are listed on pages 216 through 218

mass misalignments of the MR. They cause the MR to deviate from the planar glide phase. The question of "how much" must be answered by a stability analysis.

We are led to a similar stability analysis if we study the recovery of rocket boosters using the MR principle. After burn-out and separation, the booster goes through an arbitrary tumbling motion while picking up some spin with its driving vanes. The motion eventually transits into a nutational mode with a horizontal axis of nutation. The nutation damps out, and the steady-state velocity and rotation vectors are approached. The latter part of the flight, starting with a sufficiently small nutation-cone angle, can be considered as the planar glide phase of an MR with perturbations in the initial conditions.

The dynamics of an MR can best be explained in terms of a horizontally spinning gyroscope subjected to aerodynamic forces. The perturbations of the planar glide phase are rolling, yawing, and sideslipping (see Figure 1.2). They can perform three modes: nutation, precession, and undulation. The nutation and precession modes are those of a gyroscope with the modification that the nutation is aerodynamically damped. The undulation mode is a new mode that results from the aerodynamic forces created by sideslipping β. To these forces the MR responds with a precession that, in turn, changes β. The result is an unsteady precession; i.e., an undulation. The undulation mode can be oscillatory or aperiodic. In general, its motions are much slower than those of the nutation mode.

The MR is insensitive to short duration disturbances. However, even small long-duration disturbances can cause the MR to deviate considerably

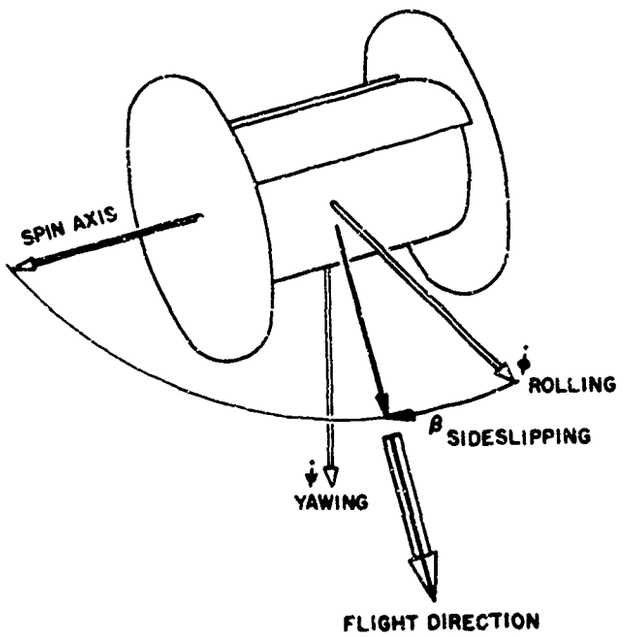

FIGURE 1.2 PERTURBED MOTIONS

from its planar glide phase. The most important such disturbance is a center of gravity offset along the spin axis. It causes the MR to precess horizontally at a constant rate.

To put the flight dynamics of MR's into perspective, we consider the dynamics of airplanes and spinning missiles. The MR shares the gyroscopic properties with the spinning missile. However, its spin axis is approximately normal to the flight direction and in a horizontal plane. This results in different perturbation equations. The equations of the missile are expressed in pitch, yaw, angle of attack, and sideslip angle and can be brought into a convenient complex form. The perturbations of an MR are rolling, yawing, and sideslipping, and the equations are not amenable

to the complex variable transformation. Here, the angle of attack is measured in the plane normal to the spin axis, between a driving vane and the roll axis. It plays the part of the roll angle in the missile case. Yet the roll orientation of a rapidly spinning missile is unimportant, while the angle of attack in the case of the MR influences the aerodynamic forces considerably, because of the shape of the center body and the driving vanes.

With regard to the symmetry of the external configuration, the MR has the mirror symmetrical properties of an aircraft rather than the rotational symmetry of a missile. That is why the aerodynamics of MR's are expressed in terms of airplane conventions, while borrowing the Magnus derivative notation from missile aerodynamics. The MR differs from an airplane by its high angular momentum and its rapidly changing angle of attack. But the perturbation equations can still be separated into longitudinal and lateral equations. The lateral equations describe the rolling, yawing, and sideslipping motions with a strong gyroscopic coupling in the roll and yaw equations.

In general, the moment of inertia tensor of an MR is not circular relative to the spin axis as is usually the case in spinning missile dynamics. This again shows that the orientation of the MR, expressed by the angle of attack, plays a more important part than the roll orientation of a missile. Summarizing, we note that the flight dynamics of MR's are a combination of airplane and spinning missile dynamics.

A historical review of the Magnus rotor principle was given by Foshag and Boehler (4). It suffices to mention that Maxwell (5) first discussed the phenomenon of a free-falling spinning card. Only recently

have the flight dynamics of Magnus rotors again attracted the interest of researchers. Brunk (1, 2) studied the equivalent problem of the dynamics of spinning missiles at a 90-degree complex angle of attack, developing a linear theory of the steady-state glide phase and employing a six-degree-of-freedom computer simulation. Millevolte (6) investigated the linear aspects of the dynamic stability of Vortex Gliders (Magnus rotors) during steady-state glide phase. The autorotational characteristics of various Magnus rotor shapes were studied by Bustamante (7, 8, 9) with particular emphasis on the spin degree-of-freedom. All these efforts have helped to explain some of the flight phenomena of MR's. But much research remains to be done until the flight dynamics of MR's are understood as well as aircraft and missile dynamics.

2. PROBLEM STATEMENT AND APPROACH

A properly designed MR will descend in a planar glide phase to the ground. The purpose of this report is to investigate the dynamics of the planar glide phase. For a complete analysis, the equations of motion must be derived, taking into account such effects as a noncircular moment of inertia ellipsoid, the rapidly rotating angle of attack, nonlinear aerodynamic forces, and the acceleration of the center of mass during the transient glide phase. But the equations should also be simple enough to be examined analytically. In particular, they should be suited for a stability analysis. This will yield the physical understanding of the flight phenomena and provide some simple relationships that are helpful in improving the design of an MR. To obtain the actual flight time histories, the equations must be programmed for computer. Finally, the required validation of these theoretical results can only come from the correlation of free-flight tests with computer runs.

To implement this program, we introduce the following basic assumptions:

1. The earth is an inertial reference frame and can be considered to be flat.

2. The MR is rigid with constant mass and is mirror symmetrical with respect to its external geometry and its mass distribution.

3. The material density of the MR is much greater than the density of the surrounding medium.

4. The perturbations of the planar glide phase are small.

5. The flight speed and spin rate do not drop below ten percent of their steady-state values.

Assumptions 1 to 4 are familiar from the flight dynamics of airplanes. Because MR motions are rapid and their distances traveled short compared with the earth's rotation and diameter, respectively, Assumption 1 is well justified. Assumption 2 enables one to focus on the flight dynamical problem by introducing the ideal MR. Aeroelastic and asymmetrical effects are of second order and are not treated in this report in detail. The high material density ratio, Assumption 3, is required to simplify the equations and to permit the use of an averaging process. It is always satisfied if air is the surrounding medium. The small perturbation assumption eliminates the trigonometric functions, and Assumption 5 assures that the equations of motion do not become singular.

The problem requires an approach on two different levels. The first part of this report supplies the mathematical tools to formulate the flight dynamics of MR's. It is mathematically rigorous. The second part, beginning with Chapter 8, deals with the engineering analysis of the flight dynamics of MR's. There, many assumptions must be introduced and much intuition and experimental evidence is needed to arrive at a manageable set of equations of motion.

The equations of motion consist of reference equations and perturbation equations. The reference flight of the perturbation equations is the planar glide phase. Since, in general, the center-of-mass of the MR is accelerated, care must be taken in deriving the perturbation equations. This is achieved by using the methods of tensor analysis and by introducing

the special concept of a Rotational Derivative. The definitions and theorems are summarized in Chapter 3 and applied in Chapter 4 to obtain a general formulation of the perturbation equations of atmospheric flight dynamics. In Chapter 5 the systems for normalizing the equations are introduced. The Dynamic-Normalized System is used to simplify the equations of motion, whereas the Aero-Normalized System is needed to arrive at the aerodynamic coefficients.

Up to Chapter 5, the development is general enough to apply to all atmospheric flight dynamic problems. With the introduction of the Flight-Mechanical and Gyro-Mechanical Frame Axes in Chapter 6, the specialization on MR's begins. After collecting some of the kinematical relationships in Chapter 7, the Reference Flight is defined in Chapter 8, and necessary and sufficient conditions are stated under which a planar glide phase is possible. Then, the perturbation equations are derived starting with the linear momentum in Chapter 9 and the angular momentum in Chapter 10. The formulation of the aerodynamic forces in terms of derivatives is executed in detail in Chapter 11. Again, the methods of tensor analysis are used to prove a theorem that establishes the conditions for vanishing derivatives of arbitrary order. This is the key to the nonlinear representation of the aerodynamic forces. In Chapter 12, the implicit dependence of the equations of motions on the rapidly rotating angle of attack is eliminated by the Method of Averaging. The perturbation equations are separated into Lateral and Longitudinal Equations. The longitudinal equations are dropped, and the final equations of motion (i.e., the reference equations of the planar glide phase and the lateral perturbation equations) are summarized.

The stability of the lateral perturbation equations is analyzed in

Chapter 13. The linear perturbation equations are used to discuss the stability of the first approximation. To analyze the effect of aerodynamic nonlinearities, the perturbation equations are reduced to a one-degree-of-freedom equation using the Method of Averaging. The conditions under which limit cycles occur are shown, as are the methods of avoiding them.

In Chapter 14, the theoretical methods are applied to several typical Magnus rotor shapes. The equations of motion are programmed for computer, and some typical flight histories are shown. The reduction of the perturbation equation to a one-degree-of-freedom equation is justified by comparison with the integration of the exact equations by computer. To validate the theoretical approach, approximately 30 flight tests were conducted. Some of the results are correlated with computer simulations whose aerodynamic input data are solely based on wind tunnel tests. Two new methods are introduced to measure the aerodynamic damping derivatives. They are the induced-nutation and limit-cycle methods. Finally, in Chapter 15, the contributions of this report are evaluated, the weak points exposed, and future work described.

The report is divided into chapters and sections. In each chapter the equations are numbered consecutively. If the equations are cross-referenced between different chapters, the chapter number precedes the equation number. The reader who is not interested in the mathematical development of the equations of motion can skip Chapters 3, 4, 8, 9, 10, and 11, and concentrate on the results in Chapters 12 through 15.

3. TENSOR CONCEPTS IN FLIGHT DYNAMICS

The formulation and interpretation of problems in flight dynamics can be a formidable task if many bodies and reference frames are involved. It is therefore important to have a concise mathematical language on hand to model the physical processes. In this chapter a tool will be introduced that is (i) capable of expressing dynamic problems in an invariant tensor form under time-dependent coordinate transformations and (ii) particularly tailored to problems whose major elements are rigid bodies.

To motivate the reader, we consider Newton's Second Law in its usual form:

$$\frac{d}{dt}(\vec{p}) = \vec{f} \tag{1}$$

where it is always understood that the time derivative is taken relative to an inertial frame. If we use a matrix formulation, we must specify the coordinate system of the vector components. Let $\mathcal{I}$ indicate an inertial coordinate system. Then Equation (1) is written as:

$$\frac{d}{dt}[p]^{\mathcal{I}} = [f]^{\mathcal{I}} \tag{2}$$

For a non-inertial coordinate system, say $]^{\mathcal{B}}$, the well known Euler transformation yields:

$$\frac{d}{dt}[p]^{\mathcal{B}} + [\Omega^{(\mathcal{B})(\mathcal{I})}]^{\mathcal{B}}[p]^{\mathcal{B}} = [f]^{\mathcal{B}} \tag{3}$$

where $[\Omega^{(\mathcal{B})(\mathcal{I})}]^{\mathcal{B}}$ is a skew-symmetric matrix describing the angular velocity of frame $(\mathcal{B})$ relative to frame $(\mathcal{I})$. Comparing Equations (2) and (3) we note that Newton's law may assume different forms, depending on

the coordinate system it is expressed in. Consequently, the formulation of Equation (2) is not invariant under a coordinate transformation. This is not a serious disadvantage if two frames suffice to formulate a problem. But, in flight dynamics, many frames usually are involved: inertial frame, earth frame, stability frame, wind frame, body frame, etc. Then it is desirable to work with an invariant (i.e., tensor) formulation in order not to lose sight of the physics of the problem. However, the transformations between the coordinate systems are time-dependent. We therefore need a tensor formulation that is invariant even under time-dependent coordinate transformations. This will be achieved by introducing the so-called rotational time derivative, $\mathcal{D}$. Newton's law then assumes the invariant tensor form with respect to all time-dependent coordinate transformations:

$$[\mathcal{D}^{(I)} p] = [f] \tag{4}$$

where $\mathcal{D}^{(I)}$ is the rotational time derivative relative to the inertial frame (I). Expressed in the coordinate systems $]^I$ and $]^B$, we obtain the forms equivalent to the Equations (2) and (3):

$$[\mathcal{D}^{(I)} p]^I = [f]^I \tag{5}$$

$$[\mathcal{D}^{(I)} p]^B = [f]^B \tag{6}$$

Before we can give the definition of the rotational time derivative, we shall state a few general principles and definitions on which the two fundamental concepts of "position" and "motion" are based. The fundamental kinematical theorems will then be formulated and proved. In later chapters it will be shown, using the MR as an example, how the new tools are applied

to problems in flight dynamics.

3.1 GENERAL PRINCIPLES AND DEFINITIONS

The three basic notions of classical mechanics are according to Truesdell (10):

a. Material Body. A body is a three dimensional differentiable manifold, the elements of which are called particles. It possesses a non-negative scalar measure that is called the mass distribution of the body. In particular, a body is called rigid if the distances between every pair of its particles are time-invariant.

b. Force. The force describes the action of the outside world on a body and the interaction between the different parts of the body. We distinguish between volume force (e.g., gravitational force) and surface force (e.g., aerodynamic force).

c. Euclidean Space-Time.

Classical mechanics is the investigation of the interaction of these three basic notions under four axioms (see Hamel (11)):

a. Time and space are homogeneous.

b. Space is isotropic.

c. Every effect must have its cause by which it is uniquely determined.

d. No particular length, velocity, or mass is singled out.

The surface forces of the force system depend on the kinematics of the body. This is expressed by the constitutive equation. From Axiom b, it

follows, as Noll (12) showed, that the constitutive equations are invariant under a rotation in space. He calls this the Principle of Material Indifference.

The general principles must be cast into a mathematical language in order to allow a concise formulation of the dynamic problem and make it amenable to mathematical analysis. We introduce two basic mathematical notions:

a. Point. A point is the mathematical model of a physical object whose spatial extension is irrelevant. Example: particle.

b. Frame. A frame is an unbounded continuous set of elements over the Euclidean three-space whose distances are time-invariant and which possesses, as a subset, at least three noncollinear points.

The following hypothesis will govern the modeling of dynamic problems:

> The mathematical notions of "point" and "frame" are sufficient to formulate any problem in classical dynamics.

This statement cannot be proven universally, because we do not know every conceivable problem in classical dynamics. However, it can be made plausible by considering the first two basic notions of classical mechanics. A body can be modeled by a frame or by points, depending on whether it is rigid or not. Forces can be expressed as the interaction of points or frames. Because dynamics is that branch of mechanics that deals with material bodies and forces as they interact in Euclidean space-time, the hypothesis appears to be justified sufficiently.

The mapping of the elements of a frame onto Euclidean three-space is

accomplished via coordinate systems.

DEFINITIONS: A coordinate system is an abstract entity embedded in Euclidean three-space that establishes a one-to-one correspondence between the elements of a frame and the ordered triple of algebraic numbers. A coordinate system is said to be associated with a frame if the one-to-one correspondence is time-invariant. All coordinate systems associated with one frame form a class, $\mathcal{C}$, with ∞^2 elements related by translation and rotation. The entity of all these classes over all frames are the allowable coordinate systems, where we restrict ourselves to right-handed orthogonal Cartesian coordinate systems. The group of allowable coordinate transformations are the transformations between allowable coordinate systems. They are, in general, functions of time. Only within one class are the transformations time-invariant.

We are now in a position to define the meaning of a tensor as it will be used throughout this report. The components of a first-order tensor in a coordinate system, say $]^B$, will be represented by lower case letters; e.g., $[x]^B$. Upper case letters are reserved for the components of second-order tensors; e.g., $[\bar{\delta}]^B$. The transformation matrix between two coordinate systems, say $]^B$ with respect to $]^A$, is abbreviated by $[T]^{BA}$. (See Jeffreys (13)).

DEFINITION: A first-order tensor (vector) is the abstract collection of ordered triples (i.e., components), each of which is associated with an allowable coordinate system and such that any two satisfy the transformation law

$$[x]^B = [T]^{BA}[x]^A \tag{7}$$

where $]^B$ and $]^A$ can be any allowable coordinate system. If we refer to this abstract collection, we write $[x]$. $[x]^B$ is just a particular element of $[x]$; i.e., the components expressed in the $]^B$ coordinate system.

A similar statement defines a second-order tensor (tensor) with Equation (7) replaced by:

$$[\mathfrak{T}]^B = [T]^{BA} [\mathfrak{T}]^A [T]^{BA^T} \tag{8}$$

$[\mathfrak{T}]$ again stands for the abstract collection of all ordered 9-tuples associated with all allowable coordinate systems. The superscript T indicates the transposed matrix. Higher-order tensors could be defined similarly. However, they will not be required.

The notation combines the features of the dyadic and the matrix formulations. For instance, $[\mathfrak{T}]$ is the abstract dyadic form that does not single out any coordinate system. $[\mathfrak{T}]^B$ is a 3 x 3 matrix whose elements are the components of the second-order tensor in the coordinate system $]^B$. For further reference, we also adopt the convention that a frame is represented by a capital letter in parenthesis, say (A) , and an element or point of the frame by the same capital letter A with a possible subscript. The coordinate systems associated with (A) also have the same capital letter, $]^A$, possibly modified by a subscript, $]^{A_k}$.

Thus far, we have assembled the basic mathematical elements needed to model kinematic problems. Two more concepts are required to establish the association between actual physical processes and the mathematical language. These are: position and motion.

3.2 CONCEPT OF POSITION

The position of a point C or a frame (B) is a relative concept in the sense that its definition requires a reference point R and a reference frame (R). In particular, the position of point C relative to point R is determined by the vector $[x_{CR}]$. To describe the position of the frame (B) relative to frame (R), we start with the definition of a frame given in Section 3.1. The three noncollinear points B_1, B_2, B_3 of frame (B) are referred to the three noncollinear points R_1, R_2, R_3 of frame (R) by the three vectors $[x_{B_iR_i}]$, $i=1,2,3$. Only six of the nine vector components are independent; i.e., a frame has six degrees of freedom.

An alternate and more useful way to describe the position of a frame is the distinction between location and orientation. Let B and R be two representative points of (B) and (R). $[x_{BR}]$ is then called the <u>location</u> of frame (B) relative to frame (R). The <u>orientation</u> of frame (B) relative to frame (R) is determined by the <u>rotation tensor</u> $[R^{(B)(R)}]$ whose definition is given below. By Euler's theorem on rigid bodies, and for that matter on frames, the general displacement is a rotation about some axis through a "fixed point." This "fixed point" is, in our case, an element that belongs to (B) and (R) and is not affected by the rotation. Since (B) and (R) are unbounded, such an element always exists. Location and orientation together describe the position of frame (B) relative to frame (R). Both $[x_{BR}]$ and $[R^{(B)(R)}]$ have three independent components; i.e., together they have the correct number to specify 6 degrees of freedom.

If $[n]$ is the unit vector of the axis of rotation and θ the angle of rotation, the rotation tensor is defined by:

$$[R^{(B)(R)}] = \cos\theta\,[E] + (1-\cos\theta)[n][n]^T + \sin\theta\,[N] \tag{9}$$

where $[E]$ is the unit tensor and $[N]$ the skew-symmetric tensor obtained from $[n]$. The derivation of this formula and the proof of the tensor property of $[R^{(B)(R)}]$ can be found in Jeffreys (13). We note further that the rotation tensor is orthonormal and that its determinant is +1 for proper and -1 for improper rotations. The trace is

$$R_{11} + R_{22} + R_{33} = 1 + 2\cos\theta \tag{10}$$

In flight dynamics it is customary to use a triad of orthogonal axes to represent a frame. But confusion very often arises because the axes of the triad and the coordinate axes are used as synonyms. Nothing could be more misleading. We will try to give an accurate account of the situation.

<u>DEFINITION</u>: A <u>triad</u> is a set of three orthonormal <u>base vectors</u> that connect one physically important point of a frame, the <u>base point</u>, with three other points of the frame.

The position of a frame, say (B), is uniquely determined by the position of its triad. The base point B defines the location and the base vectors $[b_1], [b_2], [b_3]$ the orientation relative to a reference frame (R). The rotation tensor $[R^{(B)(R)}]$ can be thought of as mapping the base vectors $[b_1], [b_2], [b_3]$ into the base vectors $[r_1], [r_2], [r_3]$ of the reference frame; namely,

$$[b_i] = [R^{(B)(R)}][r_i] \quad ; \quad i = 1,2,3 \tag{11}$$

Consider any two vectors $[X_{B_\mu B}]$ and $[X_{R_\mu R}]$, where B_μ and R_μ are any elements of (B) and (R), respectively. If $[X_{B_\mu B}]$ and $[X_{R_\mu R}]$ are composed

of the same linear combination of the base vectors $[b_1]$, $[b_2]$, $[b_3]$ and $[r_1]$, $[r_2]$, $[r_3]$, respectively, then the two vectors are related by

$$[x_{B_k B}] = [R^{(B)(R)}][x_{R_k R}] \tag{12}$$

because, if

$$[x_{B_k B}] = \gamma_1 [b_1] + \gamma_2 [b_2] + \gamma_3 [b_3] \tag{13}$$

and

$$[x_{R_k R}] = \gamma_1 [r_1] + \gamma_2 [r_2] + \gamma_3 [r_3] \tag{14}$$

then Equation (12) follows from Equation (11).

Now we are in a position to establish a relationship between the rotation tensor and the coordinate transformation.

<u>THEOREM</u>: Consider two arbitrary frames (B), (R) and choose $[x_{B_k B}]$ and $[x_{R_k R}]$ as outlined above. In particular, Equation (12) is supposed to be satisfied. Define two coordinate systems $]^B$ and $]^R$ in (B) and (R) respectively, such that

$$[x_{B_k B}]^B = [x_{R_k R}]^R \tag{15}$$

Then the following relationship holds:

$$[R^{(B)(R)}]^B = [R^{(B)(R)}]^R = [T]^{BR^T} \tag{16}$$

<u>PROOF</u>: From Equation (15) it follows that

$$[x_{B_k B}]^B = [T]^{BR^T}[x_{R_k R}]^B \tag{17}$$

and

$$[x_{B_k B}]^R = [T]^{BR^T} [x_{R_k R}]^R \tag{18}$$

Express Equation (12) first in the $]^B$ coordinate system and compare with Equation (17) and then in the $]^R$ coordinate system and compare with Equation (18). Equation (16) follows immediately.

It is very important to distinguish carefully between frame and space, triad and coordinate system, rotation tensor and coordinate transformation matrix. Frame, triad, and rotation are invariant tensor concepts, whereas space, coordinate system, and coordinate transformation are purely algebraic notions.

3.3 CONCEPT OF MOTION

The concept of motion is formulated by introducing time into the purely spatial concept of position; i.e., $[x_{BR}(t)]$ and $[R^{(B)(R)}(t)]$. Obviously, it is also a relative concept. It makes sense to talk about the motion of a point or a frame only with respect to another frame.

The time derivative $\frac{d}{dt}$ of a tensor is considered to operate on its components. It preserves the tensor character if the allowable coordinate systems are related by time-invariant coordinate transformations. However, in flight dynamics, it is very often necessary to express the time rate of change of a tensor relative to a reference frame in terms of the time rate of change of this tensor with respect to a moving body. Usually, this is achieved by introducing coordinate systems fixed with the reference frame

and the moving body and taking time derivatives of the corresponding components. The correction factor is given by Euler's transformation theorem. As Jeffreys (13) points out, the time derivative with respect to the moving body has lost its tensor properties, and one must continue to solve the remainder of the problem in one particular coordinate system.

We shall alleviate this shortcoming by introducing the concept of a rotational derivative. A <u>rotational derivative</u> is a time derivative of a tensor relative to an arbitrary frame; e.g., an inertial frame or body frame. It is also a tensor of the same order and therefore a covariant derivative with respect to the parameter t . The term "tensor" is understood here in the sense of the definition given in Section 3.1. If we use the rotational derivative instead of the ordinary time derivative, the time rate of change of a tensor, relative to a moving body, is still a tensor. In more general terms, we will be able to formulate the equations of motion in tensor form and carry out much of the analysis without recurring to the component form. For instance, we will be able to introduce perturbation equations that are not limited to a steady reference flight. However, before advancing into applications, we must lay a sound foundation for the rotational derivative. As far as I am aware, only Wrede (14) has reported a similar concept. But his approach is limited to vectors and restricted to one particular reference frame.

<u>DEFINITION</u>: Let $[p]$ be an arbitrary vector (first-order tensor) and $[P]$ an arbitrary tensor (second-order tensor). Furthermore, let (R) be an arbitrary frame. The rotational derivative of a vector and tensor with respect to the frame (R) is written in dyadic form:

$$[\mathcal{D}^{(R)}\{[p]\}] \quad , \quad [\mathcal{D}^{(R)}\{[P]\}]$$

or shorter

$$[\mathcal{D}^{(R)}\, p] \quad , \quad [\mathcal{D}^{(R)}\, P]$$

This is an abbreviation for the abstract collection of all component forms that arise from the allowable coordinate systems. For instance, let $]^{M}$ be any allowable coordinate system, and let $]^{R}$ be a coordinate system associated with the frame (R), where $[T]^{MR}$ is the possibly time-dependent transformation matrix. Then the components of the rotational derivative for a vector and tensor are defined:

$$[\mathcal{D}^{(R)}\, p]^{M} = \frac{d}{dt}[p]^{M} + [T]^{MR}\left(\frac{d}{dt}[T]^{MR^{T}}\right)[p]^{M} \tag{19}$$

$$[\mathcal{D}^{(R)} P]^{M} = \frac{d}{dt}[P]^{M} + [T]^{MR}\left(\frac{d}{dt}[T]^{MR^{T}}\right)[P]^{M} + [P]^{M}\left(\frac{d}{dt}[T]^{MR}\right)[T]^{MR^{T}} \tag{20}$$

Some of the important properties of the rotational derivative are:

<u>PROPERTY 1</u>: The rotational derivative of a vector $[p]$ relative to a frame (R) is a vector; i.e., let $(\bar{M})$ and $(\bar{\bar{M}})$ be any two frames with the associated coordinate systems $]^{\bar{M}}$ and $]^{\bar{\bar{M}}}$ and the transformation matrix $[T]^{\bar{M}\bar{\bar{M}}}$, then

$$[\mathcal{D}^{(R)}\, p]^{\bar{M}} = [T]^{\bar{M}\bar{\bar{M}}}\,[\mathcal{D}^{(R)}\, p]^{\bar{\bar{M}}} \tag{21}$$

<u>PROPERTY 2</u>: The rotational derivative of a tensor $[P]$ relative to a frame (R) is a tensor; i.e., let $(\bar{M})$ and $(\bar{\bar{M}})$ be any two frames with the associated coordinate systems $]^{\bar{M}}$ and $]^{\bar{\bar{M}}}$ and the transformation matrix $[T]^{\bar{M}\bar{\bar{M}}}$, then

$$[\mathcal{D}^{(R)} P]^{\bar{M}} = [T]^{\bar{M}\bar{\bar{M}}}\,[\mathcal{D}^{(R)} P]^{\bar{\bar{M}}}\,[T]^{\bar{M}\bar{\bar{M}}^{T}} \tag{22}$$

The second-order skew-symmetric tensors play an important role because they represent concepts like angular velocity, angular momentum, and torque. In Euclidean three-space, they have only three independent components and can therefore be contracted to a first-order tensor capacity (see Brillouin (15)). If we restrict ourselves to right-hand orthogonal Cartesian coordinate system, then the tensor capacity is determined uniquely. Such a first-order tensor capacity is called an <u>axial vector</u>.

<u>PROPERTY 3</u>: If the allowable coordinate systems are right-hand orthogonal Cartesian coordinate systems, then an axial vector $[\ell]$ has the same rotational derivative as a regular vector; i.e., let $(\bar{M})$ and $(\bar{\bar{M}})$ be any two frames with the associated coordinate systems $]^{\bar{M}}$ and $]^{\bar{\bar{M}}}$ and the transformation matrix $[T]^{\bar{M}\bar{\bar{M}}}$, then

$$[\mathcal{D}^{(R)}\ell]^{\bar{M}} = [T]^{\bar{M}\bar{\bar{M}}}[\mathcal{D}^{(R)}\ell]^{\bar{\bar{M}}} \tag{23}$$

The proofs of the three preceding properties are given in Appendix A.

<u>PROPERTY 4</u>: The rotational derivative is a linear operator.

<u>PROOF</u>: Let $[p_1]$ and $[p_2]$ be two arbitrary vectors and $]^M$ any coordinate system. The rotational derivative with respect to a reference frame expressed in the $]^M$ coordinate system is

$$[\mathcal{D}^{(R)}\{[p_1]+[p_2]\}]^M = \frac{d}{dt}([p_1]^M+[p_2]^M)+[T]^{MR}\left(\frac{d}{dt}[T]^{MR}\right)^T([p_1]^M+[p_2]^M) \tag{24}$$

$$[\mathcal{D}^{(R)}\{[p_1]+[p_2]\}]^M = [\mathcal{D}^{(R)}p_1]^M + [\mathcal{D}^{(R)}p_2]^M \tag{25}$$

Furthermore, let κ be a time-invariant scalar and $[p]$ any vector. We get

$$[\mathcal{D}^{(R)}\{\kappa[p]\}]^M = \frac{d}{dt}(\kappa[p]^M) + [T]^{MR}\left(\frac{d}{dt}[T]^{MR^T}\right)\kappa[p]^M \tag{26}$$

$$[\mathcal{D}^{(R)}\{\kappa[p]\}]^M = \kappa[\mathcal{D}^{(R)}p]^M \tag{27}$$

Equations (25) and (27) are the properties of a linear operator. They hold for any coordinate system. Therefore, we can write the properties in an invariant form:

$$[\mathcal{D}^{(R)}\{[p_1] + [p_2]\}] = [\mathcal{D}^{(R)}p_1] + [\mathcal{D}^{(R)}p_2] \tag{28}$$

$$[\mathcal{D}^{(R)}\{\kappa[p]\}] = \kappa[\mathcal{D}^{(R)}p] \tag{29}$$

It can easily be verified that the same properties hold for tensors.

<u>PROPERTY 5</u>: <u>Chain Rule</u>. Let $[B]$ be any tensor and $[p]$ be any vector. The following rule holds:

$$[\mathcal{D}^{(R)}\{[B][p]\}] = [\mathcal{D}^{(R)}B][p] + [B][\mathcal{D}^{(R)}p] \tag{30}$$

<u>PROOF</u>: Let $]^M$ be any coordinate system and consider the component form of Equation (30):

$$[\mathcal{D}^{(R)}\{[B][p]\}]^M = [\mathcal{D}^{(R)}B]^M[p]^M + [B]^M[\mathcal{D}^{(R)}p]^M \tag{31}$$

Write out the right-hand side using the definitions of Equations (19) and (20):

$$[\mathcal{D}^{(R)}\{[B][p]\}]^M = \left(\frac{d}{dt}[B]^M\right)[p]^M + [T]^{MR}\left(\frac{d}{dt}[T]^{MR^T}\right)[B]^M[p]^M +$$

$$+ [B]^M\left(\frac{d}{dt}[T]^{MR}\right)[T]^{MR^T}[p]^M + [B]^M\frac{d}{dt}[p]^M + [B]^M[T]^{MR}\left(\frac{d}{dt}[T]^{MR^T}\right)[p]^M$$

$$= \frac{d}{dt}\left([B]^M[p]^M\right) + [T]^{MR}\left(\frac{d}{dt}[T]^{MR^T}\right)[B]^M[p]^M + \tag{32}$$

$$+ [B]^M\left\{\left(\frac{d}{dt}[T]^{MR}\right)[T]^{MR^T} + [T]^{MR}\left(\frac{d}{dt}[T]^{MR^T}\right)\right\}[p]^M$$

The expression in the braces is zero because the first term is skew-symmetric:

$$\left(\frac{d}{dt}[T]^{MR}\right)[T]^{MR^T} = \left\{[T]^{MR}\frac{d}{dt}[T]^{MR^T}\right\}^T = -[T]^{MR}\frac{d}{dt}[T]^{MR^T} \tag{33}$$

This proves the chain rule.

The five properties of the rotational derivative are the more important characteristics that we will need in the sequel. In particular, we are now able to define linear and angular velocity.

<u>DEFINITION</u>: Let B be a point and (R) a reference frame containing a reference point R. The position of B relative to (R) is given by $[x_{BR}(t)]$. The velocity of B relative to (R) is defined by

$$[v_B^{(R)}] = [\mathcal{D}^{(R)} x_{BR}] \tag{34}$$

It is commonly called the <u>linear velocity</u> of point B.

<u>COMMENT</u>: Let R_1 and R_2 be two arbitrary points of (R). Then we have

$$[\mathcal{D}^{(R)} x_{BR_1}] = [\mathcal{D}^{(R)} x_{BR_2}] \tag{35}$$

because introducing

$$[x_{BR_1}] = [x_{BR_2}] + [x_{R_2R_1}] \tag{36}$$

and taking the rotational derivative relative to (R) yields:

$$[\mathcal{D}^{(R)} x_{BR_1}] = [\mathcal{D}^{(R)} x_{BR_2}] + [\mathcal{D}^{(R)} x_{R_2R_1}] \tag{37}$$

But

$$[\mathcal{D}^{(R)} x_{R_2R_1}] = [0] \tag{38}$$

because, for a coordinate system $]^R$ associated with (R)

$$[\mathcal{D}^{(R)} x_{R_2R_1}]^R = [\frac{d}{dt} x_{R_2R_1}]^R = [0]^R \tag{39}$$

Therefore, Equation (35) is correct, and we do not have to specify a special reference point to define the linear velocity uniquely. All that is needed is a reference frame. This is the explanation for the particular notation in Equation (34). It reduces to the familiar definition if we show its components in a $]^R$ coordinate system:

$$[v_0^{(R)}] = [\mathcal{D}^{(R)} x_{BR}]^R = \frac{d}{dt} [x_{BR}]^R \tag{40}$$

<u>DEFINITION</u>: Let (B) and (R) be two arbitrary frames whose orientation relative to each other is given by $[R^{(B)(R)}(t)]$. Let B_k and B be elements of (B) and connected by the vector $[x_{B_kB}]$. According to Equation (12) there exists a similar vector $[x_{R_kR}]$ in (R) such that

$$[x_{B_kB}] = [R^{(B)(R)}][x_{R_kR}] \tag{41}$$

Take the rotational derivative relative to (R) and use Property 5:

$$[\mathcal{D}^{(R)} x_{B_k B}] = [\mathcal{D}^{(R)} R^{(B)(R)}][x_{R_k R}] + [R^{(B)(R)}][\mathcal{D}^{(R)} x_{R_k R}] \tag{42}$$

The last term is zero. Substitute Equation (41) into Equation (42):

$$[\mathcal{D}^{(R)} x_{B_k B}] = [\mathcal{D}^{(R)} R^{(B)(R)}][R^{(B)(R)}]^T [x_{B_k B}] \tag{43}$$

and abbreviate

$$[\Omega^{(B)(R)}] = [\mathcal{D}^{(R)} R^{(B)(R)}][R^{(B)(R)}]^T \tag{44}$$

to get

$$[\mathcal{D}^{(R)} x_{B_k B}] = [\Omega^{(B)(R)}][x_{B_k B}] \tag{45}$$

$[\Omega^{(B)(R)}]$ is called the <u>angular velocity tensor</u> of frame (B) with respect to frame (R).

It is certainly a second-order tensor. Its skew-symmetric property is proved as follows. Consider

$$[\mathcal{D}^{(R)} \{ [R^{(B)(R)}][R^{(B)(R)}]^T \}] = [\mathcal{D}^{(R)} E] \tag{46}$$

We first show that $[\mathcal{D}^{(R)} E] = [0]$. For any coordinate system, say $]^B$:

$$\begin{aligned}
[\mathcal{D}^{(R)} E]^B &= \frac{d}{dt}[E]^B + [T]^{BR}\left(\frac{d}{dt}[T]^{BR^T}\right)[E]^B + \left(\frac{d}{dt}[T]^{BR}\right)[T]^{BR^T}[E]^B \\
&= [0]^B + [T]^{BR}\left(\frac{d}{dt}[T]^{BR^T}\right) + \left(\frac{d}{dt}[T]^{BR}\right)[T]^{BR^T} \qquad (47) \\
&= \frac{d}{dt}\left([T]^{BR}[T]^{BR^T}\right) = [0]
\end{aligned}$$

Therefore, Equation (46) becomes:

$$[\mathcal{D}^{(R)} R^{(B)(R)}][R^{(B)(R)}]^T + [R^{(B)(R)}][\mathcal{D}^{(R)} R^{(B)(R)}]^T = [0] \tag{48}$$

or by definition:

$$[\Omega^{(B)(R)}] + [\Omega^{(B)(R)}]^T = [0] \tag{49}$$

There is another important relationship linking the angular velocity tensor to coordinate transformation matrices:

$$[\Omega^{(B)(R)}]^R = \left(\frac{d}{dt}[T]^{BR^T}\right)[T]^{BR} \tag{50}$$

or

$$[\Omega^{(B)(R)}]^B = [T]^{BR}\frac{d}{dt}[T]^{BR^T} \tag{51}$$

Equation (50) is proved simply by taking the $]^R$ components of Equation (44) and employing Equation (16). Equation (51) follows then from Equation (50) by coordinate transformation.

Note that Equation (19) can be written, in view of Equation (51) as:

$$[\mathcal{D}^{(R)}p]^M = \frac{d}{dt}[p]^M + [\Omega^{(M)(R)}]^M[p]^M \tag{52}$$

However, a word of caution is necessary. Equation (52) may suggest that $\frac{d}{dt}[p]^M$ is a tensor because $[\mathcal{D}^{(R)}p]^M$ and, seemingly, $[\Omega^{(M)(R)}]^M[p]^M$ are tensors. But we know from Jeffreys (13) that neither term on the right-hand side of Equation (52) is a tensor. Only the sum is a tensor.

Before stating other important properties of the angular velocity tensor, we need to formulate the fundamental theorem of kinematics that governs the change of frames.

<u>THEOREM OF TRANSFORMATION OF FRAMES</u>. Let (A) and (B) be two arbitrary frames related by the angular velocity tensor $[\Omega^{(B)(A)}]$. Then for any vector $[p]$ the following relationship holds:

$$[\mathcal{D}^{(A)}p] = [\mathcal{D}^{(B)}p] + [\Omega^{(B)(A)}][p] \tag{53}$$

where every term is a first-order tensor.

The proof is somewhat lengthy and given in Appendix A. Note that Euler's theorem is a special case of Equation (53). Because if we choose the proper coordinate systems, we get:

$$\frac{d}{dt}[p]^A = [T]^{AB}\left\{\frac{d}{dt}[p]^B + [\Omega^{(B)(A)}]^B[p]^B\right\} \tag{54}$$

The additive property of angular velocity tensors will now be proved. Consider three arbitrary frames (A), (B), and (C). Apply Equation (53) three times:

$$[\mathcal{D}^{(A)}p] = [\mathcal{D}^{(B)}p] + [\Omega^{(B)(A)}][p] \tag{55}$$

$$[\mathcal{D}^{(B)}p] = [\mathcal{D}^{(C)}p] + [\Omega^{(C)(B)}][p] \tag{56}$$

$$[\mathcal{D}^{(A)}p] = [\mathcal{D}^{(C)}p] + [\Omega^{(C)(A)}][p] \tag{57}$$

Substituting Equations (56) and (57) into (55) and in view of the fact that $[p]$ is an arbitrary vector:

$$[\Omega^{(C)(A)}] = [\Omega^{(C)(B)}] + [\Omega^{(B)(A)}] \tag{58}$$

Notice the consistent sequence of superscripts.

Another useful property to remember is:

$$[\Omega^{(B)(A)}] = -[\Omega^{(A)(B)}] \tag{59}$$

It follows again from applying Equation (53) twice

$$[\mathcal{D}^{(A)} p] = [\mathcal{D}^{(B)} p] + [\Omega^{(B)(A)}][p] \tag{60}$$

$$[\mathcal{D}^{(B)} p] = [\mathcal{D}^{(A)} p] + [\Omega^{(A)(B)}][p] \tag{61}$$

and adding both equations.

Finally, we will prove a second important theorem:

<u>THEOREM OF ROTATION OF VECTORS</u>. Let (A) and (B) be two arbitrary frames related by the rotation tensor $[R^{(B)(A)}]$. Then for any vector $[p]$ the following holds:

$$[\mathcal{D}^{(A)} p] = [R^{(B)(A)}]^T [\mathcal{D}^{(B)} \{ [R^{(B)(A)}][p] \}] \tag{62}$$

This can be interpreted as follows: The rotational derivative of $[p]$ relative to (A) can also be evaluated by first rotating $[p]$ through $[R^{(B)(A)}]$ and then taking the rotational derivative relative to the likewise rotated frame, now called (B); then the result is rotated back through $[R^{(B)(A)}]^T$. This theorem is actually a consequence of the isotropic property of space, Axiom b of Section 3.1; i.e., taking the rotational derivative is invariant under spatial rotations of all points and frames involved.

<u>PROOF</u>. Apply the Chain Rule to the left side of Equation (62):

$$[\mathcal{D}^{(A)} p] = [R^{(B)(A)}]^T [\mathcal{D}^{(B)} R^{(B)(A)}][p] + [\mathcal{D}^{(B)} p] \tag{63}$$

and the Theorem of Transformation of Frames to the last term of Equation (63):

$$[\mathcal{D}^{(A)}\rho] = [R^{(B)(A)}]^T[\mathcal{D}^{(B)}R^{(B)(A)}][\rho] + [\mathcal{D}^{(A)}\rho] + [\Omega^{(A)(B)}][\rho] \quad (64)$$

It remains to be shown that

$$[R^{(B)(A)}]^T[\mathcal{D}^{(B)}R^{(B)(A)}] = -[\Omega^{(A)(B)}] \quad (65)$$

Let us start with a form equivalent to Equation (41)

$$[x_{R_k R}] = [R^{(R)(B)}][x_{B_k B}] \quad (66)$$

and take the rotational derivative relative to (R):

$$[0] = [\mathcal{D}^{(R)}R^{(R)(B)}][x_{B_k B}] + [R^{(R)(B)}][\mathcal{D}^{(R)}x_{B_k B}] \quad (67)$$

We compare the transposed form

$$[\mathcal{D}^{(R)}x_{B_k B}] = -[R^{(R)(B)}]^T[\mathcal{D}^{(R)}R^{(R)(B)}][x_{B_k B}] \quad (68)$$

with Equation (43) and conclude

$$[\Omega^{(B)(R)}] = -[R^{(R)(B)}]^T[\mathcal{D}^{(R)}R^{(R)(B)}] \quad (69)$$

But this is just the form of Equation (65).

4. PERTURBATION EQUATIONS

We shall apply the tensor concepts of Chapter 3 to shed light on the perturbation equations commonly used in flight dynamics. Two different perturbation methods can be distinguished. Their areas of application depend on the role the aerodynamic forces play. In space dynamics, where the aerodynamic forces are small, the first method is used. The second method applies to atmospheric flight dynamics where aerodynamic forces dominate.

Consider a rigid body subjected to aerodynamic and gravitational forces. Its mass and gravity center are assumed to coincide for all practical purposes. The Euler equations of mechanics are in the tensor formulation of Chapter 3:

$$[\mathcal{D}^{(I)} p^{(B)(I)}] = [f_a] + [f_g] \tag{1}$$

$$[\mathcal{D}^{(I)} \ell_B^{(B)(I)}] = [m_a] \tag{2}$$

The allowable coordinate systems are right-hand orthogonal Cartesian coordinate systems. $\mathcal{D}^{(I)}$ is the rotational derivative with respect to an inertial frame (I), $[p^{(B)(I)}]$ is the linear momentum of the body (B) relative to the inertial frame, and $[\ell_B^{(B)(I)}]$ is the angular momentum of the body relative to the inertial frame and referred to the mass center, B. $[f_a]$ and $[m_a]$ are the aerodynamic force and moment, respectively, and $[f_g]$ the gravitational force. Because the allowable coordinate systems are restricted to right-hand orthogonal Cartesian coordinate systems, the skew-symmetric angular momentum and aerodynamic moment tensors are written as axial vectors.

Consider two solutions of Equations (1) and (2). Call the first one the reference flight: $[p_{\kappa}^{(B)(I)}]$, $[\ell_{B\kappa}^{(B)(I)}]$. Call the second one the perturbed flight: $[p_{\rho}^{(B)(I)}]$, $[\ell_{B\rho}^{(B)(I)}]$. The κ and ρ below (B) indicate that the body frame is in a reference state or a perturbed state, respectively. To arrive at the so-called <u>first perturbation equations</u>, define the perturbations from the reference flight as the vector increments:

$$[\delta p^{(B)(I)}] = [p_{\rho}^{(B)(I)}] - [p_{\kappa}^{(B)(I)}] \tag{3}$$

$$[\delta \ell_{B}^{(B)(I)}] = [\ell_{B\rho}^{(B)(I)}] - [\ell_{B\kappa}^{(B)(I)}] \tag{4}$$

Because both the perturbed flight and the reference flight satisfy the equations of motion, and because the rotational derivative is a linear operator, we obtain from Equations (1) and (2) in view of Equations (3) and (4):

$$[\mathcal{D}^{(I)}\delta p^{(B)(I)}] = [f_a(\rho)] - [f_a(\kappa)] + [f_g(\rho)] - [f_g(\kappa)] \tag{5}$$

$$[\mathcal{D}^{(I)}\delta \ell_{B}^{(B)(I)}] = [m_a(\rho)] - [m_a(\kappa)] \tag{6}$$

where (κ) and (ρ) indicate that the respective functions are evaluated during reference or perturbed flight. The last two terms in Equation (5) cancel because the gravitational force is invariant under the flat-earth approximation. Define the perturbations of the aerodynamic force and moment as the vector increments

$$[\delta f_a] = [f_a(\rho)] - [f_a(\kappa)] \tag{7}$$

$$[\delta m_a] = [m_a(p)] - [m_a(r)] \tag{8}$$

We obtain then the first perturbation equations of a rigid body in free flight:

$$[\mathcal{D}^{(I)} \delta p^{(B)(I)}] = [\delta f_a] \tag{9}$$

$$[\mathcal{D}^{(I)} \delta l_B^{(B)(I)}] = [\delta m_a] \tag{10}$$

These are the most concise forms in which we can write the perturbation equations. They are valid in any allowable coordinate system, whether it is associated with an inertial system or some moving system.

To formulate the so-called <u>second perturbation equations</u>, we have to introduce a third frame, the stability frame (S). The aerodynamic forces are expressed in a coordinate system associated with this stability frame. Just as we have to distinguish between a body frame being in a reference state during reference flight and in a perturbed state during perturbed flight, so we have to define $\overset{(S)}{r}$ and $\overset{(S)}{p}$ as the stability frame in the reference state and perturbed state, respectively. The relationship between them is given by the orthonormal rotation tensor $[R_{\overset{(S)}{p}\overset{(S)}{r}}]$ that expresses the rotation of the frame $\overset{(S)}{p}$ with respect to the frame $\overset{(S)}{r}$. Finally, the angular velocity tensor $[\Omega^{(S)(I)}]$ describes the angular velocity of the stability frame (S) relative to the inertial frame (I).

Define the perturbations from the reference flight as the vector increments:

$$[\varepsilon p^{(B)(I)}] = [p_p^{(B)(I)}] - [R_p^{(S)}{}_r^{(S)}][p_r^{(B)(I)}] \tag{11}$$

$$[\varepsilon \ell_B{}^{(B)(I)}] = [\ell_{B\,p}^{(B)(I)}] - [R_p^{(S)}{}_r^{(S)}][\ell_{B\,r}^{(B)(I)}] \tag{12}$$

$$[\varepsilon \Omega^{(S)(I)}] = [\Omega_p^{(S)(I)}] - [R_p^{(S)}{}_r^{(S)}][\Omega_r^{(S)(I)}][R_p^{(S)}{}_r^{(S)}]^T \tag{13}$$

$$[\varepsilon f_a] = [f_a(p)] - [R_p^{(S)}{}_r^{(S)}][f_a(r)] \tag{14}$$

$$[\varepsilon m_a] = [m_a(p)] - [R_p^{(S)}{}_r^{(S)}][m_a(r)] \tag{15}$$

In writing Equations (12) and (15) in form of axial vectors, we must restrict the rotation tensor to the class of right-hand orthonormal rotations.

Let Equations (1) and (2) describe the equations of motion during a perturbed flight. Introducing Equations (11), (12), (14), and (15) then yields:

$$[\mathcal{D}^{(I)}\varepsilon p^{(B)(I)}] + [\mathcal{D}^{(I)}\{[R_p^{(S)}{}_r^{(S)}][p_r^{(B)(I)}]\}] = [\varepsilon f_a] + [R_p^{(S)}{}_r^{(S)}][f_a(r)] + [f_g(p)] \tag{16}$$

$$[\mathcal{D}^{(I)}\varepsilon \ell_B^{(B)(I)}] + [\mathcal{D}^{(I)}\{[R_p^{(S)}{}_r^{(S)}][\ell_{B\,r}^{(B)(I)}]\}] = [\varepsilon m_a] + [R_p^{(S)}{}_r^{(S)}][m_a(r)] \tag{17}$$

The second term on the left-hand side can be put in a more convenient form. In view of the Theorem of Transformations of Frames, Equation (3.53), we write for the linear momentum term:

$$[\mathcal{D}^{(I)}\{[R_p^{(S)}{}_r^{(S)}][p_r^{(B)(I)}]\}] = [\mathcal{D}_p^{(S)}\{[R_p^{(S)}{}_r^{(S)}][p_r^{(B)(I)}]\}] + [\Omega_p^{(S)(S)}][R_p^{(S)}{}_r^{(S)}][p_r^{(B)(I)}] \tag{18}$$

Apply the Theorem of Rotation of Vectors, Equation (3.62), and then again Equation (3.53) to the first term on the right-hand side:

$$[\mathcal{D}^{(S)}_{p}\{[R^{(S)}_{p\,n}][p^{(B)(I)}_{n}]\}] = [R^{(S)}_{p\,n}][\mathcal{D}^{(S)}_{n}\,p^{(B)(I)}_{n}]$$

$$= [R^{(S)(S)}_{p\,n}]\{[\mathcal{D}^{(I)}\,p^{(B)(I)}_{n}] + [\Omega^{(I)(S)}_{n}][p^{(B)(I)}_{n}]\} \tag{19}$$

and substitute Equation (19) into (18):

$$[\mathcal{D}^{(I)}\{[R^{(S)(S)}_{p\,n}][p^{(B)(I)}_{n}]\}] = [R^{(S)(S)}_{p\,n}][\mathcal{D}^{(I)}\,p^{(B)(I)}_{n}] +$$

$$+\{[\Omega^{(S)(I)}_{p}] - [R^{(S)(S)}_{p\,n}][\Omega^{(S)(I)}_{n}][R^{(S)(S)}_{p\,n}]^{T}\}[R^{(S)(S)}_{p\,n}][p^{(B)(I)}_{n}] \tag{20}$$

From Equations (16) and (20), after introducing the definition of Equation (13), we obtain:

$$\underline{[R^{(S)(S)}_{p\,n}][\mathcal{D}^{(I)}\,p^{(B)(I)}_{n}]} + [\mathcal{D}^{(I)}\varepsilon p^{(B)(I)}] + [\varepsilon\Omega^{(S)(I)}][R^{(S)(S)}_{p\,n}][p^{(B)(I)}_{n}]$$

$$= \underline{[R^{(S)(S)}_{p\,n}][f_a(n)]} + \underline{[R^{(S)(S)}_{p\,n}][f_g(n)]} - [R^{(S)(S)}_{p\,n}][f_g(n)] + [f_g(p)] + [\varepsilon f_a] \tag{21}$$

The underlined terms are the equations of motion, Equation (1), of the reference flight rotated by $[R^{(S)}_{p\,n}]$. They are satisfied identically.

Performing the same operations on the angular momentum Equation (17) yields an equivalent equation; however, without gravitational term. Both together are called the second perturbation equations of a rigid body in free flight. They are summarized below making use of the invariance of

the gravitational term; i.e., $[f_g(\rho)] = [f_g(n)]$

$$[\mathcal{D}^{(I)}\varepsilon p^{(B)(I)}] + [\varepsilon\Omega^{(S)(I)}][R^{(S)(S)}_{\rho n}][p^{(B)(I)}_{n}] = [\varepsilon f_a] + ([E] - [R^{(S)(S)}_{\rho n}])[f_g(n)] \quad (22)$$

$$[\mathcal{D}^{(I)}\varepsilon l_B^{(B)(I)}] + [\varepsilon\Omega^{(S)(I)}][R^{(S)(S)}_{\rho n}][l_{Bn}^{(B)(I)}] = [\varepsilon m_a] \quad (23)$$

where $[E]$ is a second order unit tensor.

<u>DISCUSSION</u>: The second perturbation equations determine the deviations from a reference flight that has been rotated by $[R^{(S)(S)}_{\rho n}]$. The second terms on the left-hand sides of Equations (22) and (23) are the correction factors. To see the advantage of the second perturbation method, compare Equation (7) with Equation (14). Figure 4.1 shows the quantities involved.

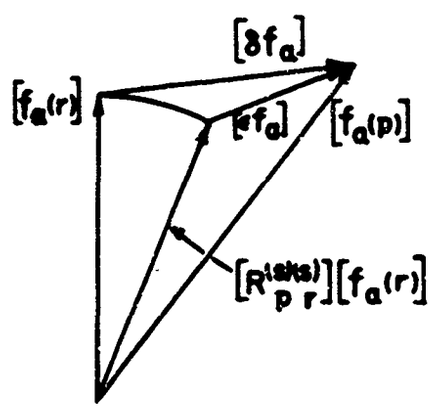

FIGURE 4.1 THE TWO KINDS OF PERTURBATIONS

$[\varepsilon f_a]$ contains the aerodynamic forces due to a deviation from the rotated reference flight only, while $[\delta f_a]$ also depends on this rotation. This difference can be seen if $[f_a(\rho)]$ is eliminated from Equations (7) and (14):

$$[\delta f_a] = [\varepsilon f_a] + \left([R^{(s)}{}_{\rho}{}^{(s)}{}_{\kappa}] - [E] \right) [f_a(\kappa)] \tag{24}$$

A more detailed discussion of why the second perturbation method is better suited to formulate the aerodynamic forces than the first one is given in Section 11.4.

Equations (22) and (23) reveal best the difference between the two perturbation methods. For applications, an alternate form of the second perturbation equations is sometimes more convenient. It is obtained simply by subtracting the reference equations of motion multiplied by $[R^{(s)}{}_{\rho}{}^{(s)}{}_{\kappa}]$ from the perturbed equations of motion:

$$[\mathcal{D}^{(\tau)} p_{\rho}{}^{(B)(\tau)}] - [R^{(s)}{}_{\rho}{}^{(s)}{}_{\kappa}][\mathcal{D}^{(\tau)} p_{\kappa}{}^{(B)(\tau)}] = [\varepsilon f_a] + \left([E] - [R^{(s)}{}_{\rho}{}^{(s)}{}_{\kappa}] \right) [f_g(\kappa)] \tag{25}$$

$$[\mathcal{D}^{(\tau)} l_{B\rho}{}^{(B)(\tau)}] - [R^{(s)}{}_{\rho}{}^{(s)}{}_{\kappa}][\mathcal{D}^{(\tau)} l_{B\kappa}{}^{(B)(\tau)}] = [\varepsilon m_a] \tag{26}$$

<u>COMMENT</u>: The second perturbation method can be considered as a generalization of the classical small disturbance method (see Etkin (16)). While the second perturbation equations are expressed in tensor form and therefore valid in any coordinate system, the classical disturbance equations hold only in one coordinate system, usually a stability or body system. For example, the definition of small disturbances for the velocities and the aerodynamic forces are:

$$\begin{Bmatrix} \varepsilon u \\ \varepsilon v \\ \varepsilon w \end{Bmatrix} = \begin{bmatrix} U_p \\ V_p \\ W_p \end{bmatrix}_p^s - \begin{bmatrix} U_r \\ V_r \\ W_r \end{bmatrix}_r^s ; \quad \begin{Bmatrix} \varepsilon L \\ \varepsilon M \\ \varepsilon N \end{Bmatrix} = \begin{bmatrix} L_p \\ M_p \\ N_p \end{bmatrix}_p^s - \begin{bmatrix} L_r \\ M_r \\ N_r \end{bmatrix}_r^s \tag{27}$$

where p and r indicate the perturbed and reference flights, respectively. During the perturbed flight the variables are measured in the stability coordinate system $]_p^s$ of the perturbed state, and during the reference flight they are measured in the stability coordinate system $]_r^s$ of the reference state. Because the two coordinate systems are not the same, the small disturbances in Equation (27) are not vector increments, but rather the scalar differences between components measured in two different coordinate systems. This can be a serious disadvantage if the time derivative of Equation (27) is taken:

$$\frac{d}{dt}\begin{Bmatrix} \varepsilon u \\ \varepsilon v \\ \varepsilon w \end{Bmatrix} = \frac{d}{dt}\begin{bmatrix} U_p \\ V_p \\ W_p \end{bmatrix}_p^s - \frac{d}{dt}\begin{bmatrix} U_r \\ V_r \\ W_r \end{bmatrix}_r^s \tag{28}$$

because it is very difficult to interpret the physical meaning of the last time derivative. The only alternative is to make it vanish by restricting the analysis to nonaccelerated reference flights. Another disadvantage of the classical approach lies in the effort required to think in three components. Errors might result from an intuition too badly strained.

The perturbation methods used in this report employ strictly tensorial concepts; i.e., invariants under allowable coordinate transformations. This

formulation was made possible by introducing the new concept of a rotational derivative to replace the time derivative. No restrictions have to be imposed on the reference flight, and the intuitional thinking process is improved.

5. NORMALIZATION

It is often possible to simplify the treatment of the equations of motion and, at the same time, to embrace a general class of related problems by normalizing the variables and parameters. This normalization process should be introduced early into the formulation of the equations and should be uniform for all components of a vector or tensor. There are two conflicting requirements to be satisfied when selecting the normalizing quantities: they should be constant in time and reduce the aerodynamic forces to the standard coefficient form. For instance, a constant reference flight speed usually is employed to normalize the equations of motion, but the actual variable flight speed is used to arrive at the aerodynamic coefficients. We shall therefore introduce two normalizing systems. Following Hopkin (17) we shall define a dynamic-normalized system for the equations of motion and an aero-normalized system for the aerodynamic forces.

5.1 DYNAMIC-NORMALIZED SYSTEM

Equations derived from the Euler equations of mechanics, Equations (4.1) and (4.2), allow three independent dimensions to be specified. In the "ordinary system" they are mass M, length L, and time T. The dynamic-normalized system is based on Mass M, Force F, and Velocity V. The relationships between the systems are:

ordinary system	dynamic-normalized system	
$M = M$	$M = M$	
$L = \frac{V^2 M}{F}$	$F = \frac{ML}{T^2}$	(1)
$T = \frac{VM}{F}$	$V = \frac{L}{T}$	

For our particular dynamic-normalized equations of motion, we select the following time-invariant quantities to define the unit scales of the three independent dimensions

Dimension	M	F	V
Unit Scale	m	$\frac{1}{2}\rho V_{ss}^2 S$	V_{ss}

TABLE 5.1 DEFINED UNIT SCALES OF THE DYNAMIC-NORMALIZED SYSTEM

where m is the vehicle's mass, S the reference area, V_{ss} the absolute value of the steady-state velocity, and ρ is some constant reference air density.

In specifying three dimensions, the dynamic-normalized system is a consistent dimensional set. By consistent we mean that the equations of motion remain unchanged when expressed in dynamic-normalized dimensions. There is no need to carry along artificial constants.

Any other dimension with its unit scale must be derived from the three basic dimensions. Thus, two of the dimensions in the ordinary system must be derived from the dynamic-normalized system as shown in Equation (1). Their derived unit scales are

Dimension	L	T
Unit Scale	$\frac{2m}{\rho S}$	$\frac{2m}{\rho V_{\infty} S} = \tau$

TABLE 5.2 DERIVED UNIT SCALES OF THE DYNAMIC-NORMALIZED SYSTEM

where we introduced the time parameter τ to abbreviate the time unit scale.

5.2 AERO-NORMALIZED SYSTEM

The functions expressing the aerodynamic forces are most conveniently formulated in the aero-normalized system. The three independent dimensions are specified to be length L, force F, and velocity V. The relationships between the ordinary and aero-normalized system are:

ordinary system	aero-normalized system	
$M = \frac{FL}{V^2}$	$L = L$	
$L = L$	$F = \frac{ML}{T^2}$	(2)
$T = \frac{L}{V}$	$V = \frac{L}{T}$	

and between the dynamic and aero-normalized system:

dynamic-normalized system	aero-normalized system	
$M = \frac{FL}{V^2}$	$L = \frac{MV^2}{F}$	
$F = F$	$F = F$	(3)
$V = V$	$V = V$	

The unit scales for the independent dimensions of the aero-normalized system are chosen such that the variables in the aerodynamic functions assume their simplest form:

Dimension	L	F	V
Unit Scale	ℓ	$\frac{1}{2}\rho V_n^2 S$	V_n

TABLE 5.3 DEFINED UNIT SCALES OF THE AERO-NORMALIZED SYSTEM

where ℓ is some reference length and V_n the absolute value of the velocity vector. Note that the unit scale for force and velocity are time-variant. Therefore, aero-normalized quantities should not be used where time derivatives must be taken, unless great care is being exercised.

If we adopt the three independent dimensions of the aero-normalized system as the three basic dimensions, the two dimensions, M and T, of the ordinary system are derived dimensions. Their derived unit scales are obtained from Equation (2):

Dimension	M	T
Unit Scale	$\frac{1}{2}\rho S \ell$	$\frac{\ell}{V_n}$

TABLE 5.4 DERIVED UNIT SCALES OF THE AERO-NORMALIZED SYSTEM

5.3 DISCUSSION AND APPLICATION

Throughout this study we shall use the dynamic-normalized system whenever dynamic problems arise. A horizontal bar will indicate a

dynamic-normalized quantity. For instance, the Euler equations of mechanics, Equations (4.1) and (4.2), become:

$$[\overline{\mathcal{D}^{(r)}}\,\overline{p^{(B)(r)}}] = [\overline{f_a}] + [\overline{f_g}] \tag{4}$$

$$[\overline{\mathcal{D}^{(r)}}\,\overline{\ell_B^{(B)(r)}}] = [\overline{m_a}] \tag{5}$$

where the dynamic-normalized rotational derivative is

$$\overline{\mathcal{D}^{(r)}} = \tau\,\mathcal{D}^{(r)} \tag{6}$$

with the time parameter τ defined in Table 5.2.

Similarly, the perturbation equations (4.9), (4.10) and (4.22), (4.23) expressed in the dynamic-normalized system receive just a bar above each quantity. There is one exception to this rule. The rotation tensor of the perturbation equations contains only elements that depend on angles. Because angles are already nondimensional quantities, the rotation tensor is not affected by a change in the dimensional system.

The aero-normalized system will only be employed to formulate the aerodynamic derivatives. Once the aerodynamic forces are combined with the rate of change of linear and angular momentum, we will express all terms in the dynamic-normalized system. A circumflex will designate an aero-normalized quantity.

Table 5.5 summarizes the dimensions and unit scales of some important physical quantities in the three systems.

PHYSICAL QUANTITY	ORDINARY SYSTEM		DYNAMIC-NORMALIZED		AERO-NORMALIZED	
	DIMENSION	UNIT	DIMENSION	UNIT	DIMENSION	UNIT
Mass, m'	M	Kg	M	m	$\frac{FL}{V^2}$	$\frac{\rho S \ell}{2}$
Length, $[s]$	L	m^* 1/	$\frac{V^2 M}{F}$	$\frac{2m}{\rho S}$	L	ℓ
Time, t	T	sec	$\frac{VM}{F}$	$\frac{2m}{\rho V_{ss} S}$	$\frac{L}{V}$	$\frac{\ell}{V_R}$
Linear Velocity, $[v]$	$\frac{L}{T}$	$\frac{m^*}{sec}$	V	V_{ss}	V	V_R
Linear Momentum, $[p]$	$\frac{ML}{T}$	$\frac{Kg\ m^*}{sec}$	MV	$m V_{ss}$	$\frac{FL}{V}$	$\frac{\rho}{2} V_R S \ell$
Force, $[F]$	$\frac{ML}{T^2}$	$\frac{Kg\ m^*}{sec^2}$	F	$\frac{1}{2}\rho V_{ss}^2 S$	F	$\frac{\rho}{2} V_R^2 S$
Angular Velocity, $[\omega]$	$\frac{1}{T}$	$\frac{1}{sec}$	$\frac{F}{VM}$	$\frac{\rho V_{ss} S}{2m}$	$\frac{V}{L}$	$\frac{V_R}{\ell}$
Angular Momentum, $[\ell]$	$\frac{ML^2}{T}$	$\frac{Kg\ m^{*2}}{sec}$	$\frac{M^2 V^3}{F}$	$\frac{2m^2 V_{ss}}{\rho S}$	$\frac{FL^2}{V}$	$\frac{\rho}{2} V_R S \ell^2$
Moment, $[m]$	$\frac{ML^2}{T^2}$	$\frac{Kg\ m^{*2}}{sec^2}$	MV^2	$m V_{ss}^2$	FL	$\frac{\rho}{2} V_R^2 S \ell$
Moment of Inertia, $[I]$	ML^2	$Kg\ m^{*2}$	$\frac{M^3 V^4}{F^2}$	$\frac{4m^3}{\rho^2 S^2}$	$\frac{FL^3}{V^2}$	$\frac{\rho}{2} S \ell^3$

1/ Asterisk is used in this table to distinguish between meter, m^*, mass of vehicle, m, and the symbol of the physical quantity mass, m'.

TABLE 5.5 DIMENSIONS AND UNIT SCALES

The relationship between the three different forms of one quantity are derived from the requirement that the equations must be dimensionally consistent. Some examples are given below:

$$m' = m\bar{m}' = \frac{\rho}{2} S \ell \hat{m}' \tag{7}$$

$$[s] = \frac{2m}{\rho S} [\bar{s}] = \ell [\hat{s}] \tag{8}$$

$$t = \frac{2m}{\rho V_{ss} S} \bar{t} = \frac{\ell}{V_R} \hat{t} \tag{9}$$

$$[v] = V_{ss} [\bar{v}] = V_R [\hat{v}] \tag{10}$$

$$[p] = m V_{ss} [\bar{p}] = \frac{\rho}{2} V_R S \ell [\hat{p}] \tag{11}$$

$$[f] = \frac{\rho}{2} V_{ss}^2 S [\bar{f}] = \frac{\rho}{2} V_R^2 S [\hat{f}] \tag{12}$$

$$[\omega] = \frac{\rho V_{ss} S}{2m} [\bar{\omega}] = \frac{V_R}{\ell} [\hat{\omega}] \tag{13}$$

$$[\ell] = \frac{2m^2 V_{ss}}{\rho S} [\bar{\ell}] = \frac{\rho}{2} V_R S \ell^2 [\hat{\ell}] \tag{14}$$

$$[m] = m V_{ss}^2 [\bar{m}] = \frac{\rho}{2} V_R^2 S \ell [\hat{m}] \tag{15}$$

$$[I] = \frac{4m^3}{\rho^2 S^2} [\bar{I}] = \frac{\rho}{2} S \ell^3 [\hat{I}] \tag{16}$$

If dynamic-normalized and aero-normalized variables are compared, two additional parameters are introduced for convenience:

mass parameter $\mu = \dfrac{2m}{\rho S l}$

velocity parameter $\bar{V}_r = \dfrac{V_r}{V_{ss}}$

From Equations (7) through (16) we obtain:

$$\hat{m}' = \mu \bar{m}' \tag{17}$$

$$[\hat{s}] = \mu [\bar{s}] \tag{18}$$

$$\hat{t} = \mu \bar{V}_r [\bar{t}] \tag{19}$$

$$[\hat{v}] = \frac{1}{\bar{V}_r} [\bar{v}] \tag{20}$$

$$[\hat{p}] = \frac{\mu}{\bar{V}_r} [\bar{p}] \tag{21}$$

$$[\hat{f}] = \frac{1}{\bar{V}_r^2} [\bar{f}] \tag{22}$$

$$[\hat{\omega}] = \frac{1}{\mu \bar{V}_r} [\bar{\omega}] \tag{23}$$

$$[\hat{l}] = \frac{\mu^2}{\bar{V}_r} [\bar{l}] \tag{24}$$

$$[\hat{m}] = \frac{\mu}{\bar{V}_r^2} [\bar{m}] \tag{25}$$

$$[\hat{I}] = \mu^3 [\bar{I}] \tag{26}$$

6. FRAME AXES

The modeling of the flight dynamic problem in this report requires an extensive use of physical and mathematical concepts. Many of them are defined in Chapter 3. It is particularly important that we understand the meanings of: frame, triad, and coordinate system.

Frames are the building stones for modeling rigid body problems. They represent physical concepts like earth frame, reference frame, body frame, etc. Three noncollinear frame points are sufficient to determine the position of a frame. However, many times a triad is used to represent a frame. It is defined by a right-hand orthonormal triad of base vectors and the base point; i.e., by four frame points. Therefore, two of the base vectors and the base point define a frame uniquely. Frames and their triads are physical concepts in the sense that they are invariants under allowable coordinate transformations. Thus, they can be cast into tensor formalism.

In contrast, a coordinate system is not a physical concept. All it does is to establish a one-to-one correspondence between the frame points and the ordered set of algebraic numbers. The set is called the coordinates of the point. However, knowing the coordinates of a point is not sufficient to locate a point because there are an infinite number of coordinate systems that can be associated with a particular frame. Only if we introduce another point of the frame as a reference point and if we form the coordinate differences, can we define the relative location of the point. Thus, we arrive at a displacement vector connecting both frame points. The coordinate differences are called the components of the displacement vector in a particular coordinate system. The abstract collection of the components

in all allowable coordinate systems constitutes the vector. The same collective point of view is used to define all other vectors and tensors. Knowing a set of components of a vector does not uniquely determine a coordinate system. It only fixes the set of coordinate systems generated by translational transformations. Thus, the location of the origin of the coordinate system is immaterial. In effect, all points of a frame are origins for the set of coordinate systems generated by translation.

The geometrical picture of a Cartesian coordinate system in a three-dimensional Euclidean space is modeled by three orthonormal axes. It is this geometrical analog that causes confusion because, intuitively, the geometrical picture is elevated to physical reality, even though we know that a coordinate system is a pure mathematical concept. However, in flight dynamic problems the notion of axes is too deeply rooted to be dispensed with. We will, therefore, retain this term but associate it with the physical concept of a triad. The base vectors of the triad will be called the <u>frame axes</u>. There exists a particular simple component form of the axes, the unit component form $\begin{bmatrix} 1 \\ 0 \\ 0 \end{bmatrix}$, etc. The set of coordinate systems, generated by translations, that provide this form are of special interest. They are usually meant, when we talk about a coordinate system associated with a frame.

To summarize, a frame is represented by a triad whose base vectors are called the frame axes. Two axes and their origin, the base point, define the position of a frame. The coordinate systems associated with a frame are purely mathematical concepts. There is always one set of them in which the axes attain a particular simple form. In a geometrical analog we would say that the coordinate axes of this set are parallel to the

frame axes. This set is used to express the components of a vector in a given frame.

Throughout this study we will use right-hand Cartesian coordinate systems and right-hand orthonormal triads. The base points of all triads coincide with the center of mass, $\mathcal{B}$, of the Magnus rotor (MR). There are two groups of frames: the flight mechanical frames, Table 6.1, and the gyro-mechanical frames, Table 6.2. The sequence of rotations of the flight mechanical frame axes is shown in Figure 6.1. It differs from that of conventional airplane dynamics (see Etkin (16)) because the singularity at glide angles $\gamma = \pm 90$ degree is undesirable. An MR in transient flight may perform a full loop, thus changing its glide angle 360 degree. We, therefore, prefer to locate the singularities at roll angles ± 90 degree. This is a better choice because, later on, the perturbation equations will be limited to small roll angles but the glide angle will remain unrestricted.

The singularity of the sequence of the gyro-mechanical frame axes is at $\eta = 0$. But this is just the position of the spin axes in reference flight. The gyro-mechanical frame axes, therefore, cannot be used to formulate the general perturbation equations. Nonetheless, they are useful to discuss the gyroscopic properties of MR's and, notably, to estimate the order of magnitude of certain terms.

FRAME	FRAME AXES		
	x_1	x_2	x_3
Earth frame, used as inertial frame (E)	horizontal and in the plane of the reference flight trajectory		parallel and in direction of gravity vector
Reference frame of reference flight $(R)_r$	parallel and in direction of velocity vector of mass center during reference flight	horizontal to the right	
Reference frame of perturbed flight $(R)_p$	parallel and in direction of the projection of the x_1^S - stability axis on the plane of the reference flight trajectory	horizontal to the right	
Yawing frame (Y)	coincides with x_1^S	parallel and in the direction of the projection of the spin axis on the x_1^R, x_2^R plane	
Stability frame (S)	parallel and in the direction of the projection of the velocity vector on the mirror symmetry plane x_1^B, x_3^B	positive spin axis	
Body frame (B)	parallel to principle moment of inertia axis, direction arbitrary	positive spin axis	
Wind frame (W)	parallel and in the direction of the linear velocity vector		coincident with x_3^S

TABLE 6.1 FLIGHT-MECHANICAL FRAME AXES

FRAME	FRAME AXES		
	x_1	x_2	x_3
Nodal frame (L)	line of nodes	horizontal to the right	parallel and in the direction of the projection of the spin axis into the vertical plane x_1^*, x_3^*
Nutation frame (N)	coincides with x_1^L	positive spin axis	
Body frame (B)	parallel to a principal moment of inertia axis, direction arbitrary	positive spin axis	

TABLE 6.2. GYRO-MECHANICAL FRAME AXES

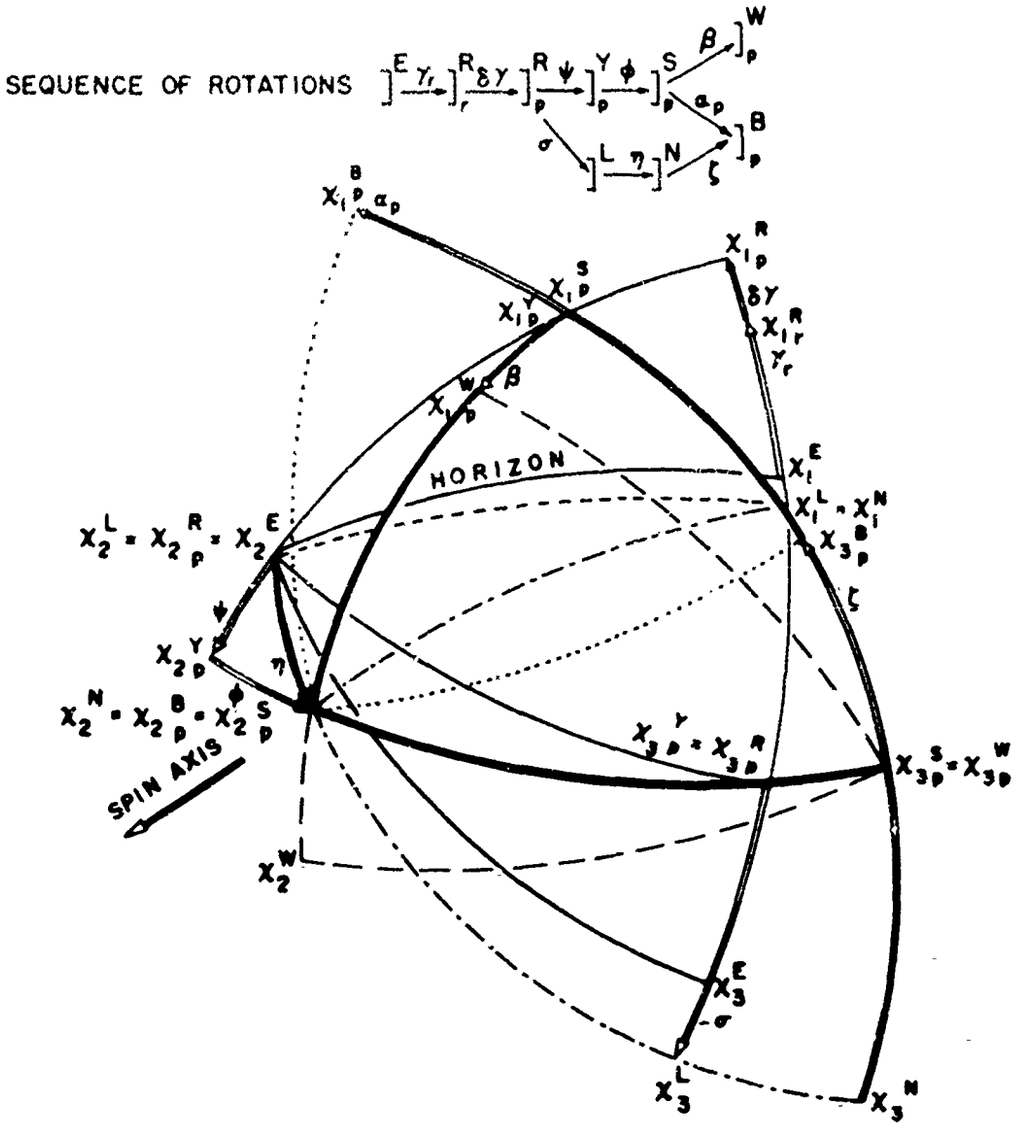

E = EARTH AXES	γ = GLIDE ANGLE
R = REFERENCE AXES	ψ = YAW ANGLE
Y = YAWING AXES	ϕ = ROLL ANGLE
S = STABILITY AXES	α = ANGLE OF ATTACK
W = WIND AXES	β = ANGLE OF SIDESLIP
B = BODY AXES	σ = NODE ANGLE
L = LINE OF NODE AXES	η = CONE ANGLE
N = NUTATION AXES	ζ = BODY ANGLE

FIGURE 6.1 INTERSECTIONS OF THE FRAME AXIS WITH THE UNIT SPHERE

Except for the earth frame, we must distinguish the individual flight mechanical frames during reference and perturbed flight. The definitions of the frame axes, given in Tables 6.1 and 6.2, can be applied to both flight states except for the reference axes. For the latter, both definitions are provided. Note that the following frame axes coincide during reference flight: $(w)_R = (S)_R = (Y)_R = (R)_R$. The nodal and nutation frame axes of the gyro-mechanical frames are not defined for the reference flight.

A definition of the spin axis remains to be given. The <u>spin axis</u> of an MR intersects the mirror plane orthonogally at the center of mass. Its positive direction is determined by the following <u>corkscrew rule</u>: Pick up an MR with your right hand such that the driving vanes offer the most resistance against a right-handed twist with your hand. The spin axis has then the same direction as the axial vector representing the twist.

Figure 6.1 presents the axes as they intersect the unit sphere. The lines are the great circles on the sphere connecting two axes. They carry the angles of rotation between the frame axes. These angles can be defined either by rotation tensors or transformation matrices. We choose to use here the transformation matrices. Associate with each frame a coordinate system that puts the components of the system axes in the simplest form $\begin{bmatrix} 1 \\ 0 \\ 0 \end{bmatrix}$, etc. The transformation matrices between these coordinate systems are given in Table 6.3.

$$[T]_{R}^{RE} = \begin{bmatrix} c\gamma_R & 0 & -s\gamma_R \\ 0 & 1 & 0 \\ s\gamma_R & 0 & c\gamma_R \end{bmatrix}; [T]_{P}^{RE} = \begin{bmatrix} c\gamma_P & 0 & -s\gamma_P \\ 0 & 1 & 0 \\ s\gamma_P & 0 & c\gamma_P \end{bmatrix}; [T]_{PR}^{RR} = \begin{bmatrix} c\delta\gamma & 0 & -s\delta\gamma \\ 0 & 1 & 0 \\ s\delta\gamma & 0 & c\delta\gamma \end{bmatrix}$$

$$[T]_{PP}^{YR} = \begin{bmatrix} c\psi & s\psi & 0 \\ -s\psi & c\psi & 0 \\ 0 & 0 & 1 \end{bmatrix}; [T]_{PP}^{SY} = \begin{bmatrix} 1 & 0 & 0 \\ 0 & c\phi & s\phi \\ 0 & -s\phi & c\phi \end{bmatrix}; [T]_{PP}^{WS} = \begin{bmatrix} c\beta & s\beta & 0 \\ -s\beta & c\beta & 0 \\ 0 & 0 & 1 \end{bmatrix}$$

$$[T]_{PP}^{BS} = \begin{bmatrix} c\alpha_P & 0 & -s\alpha_P \\ 0 & 1 & 0 \\ s\alpha_P & 0 & c\alpha_P \end{bmatrix}; [T]_{RR}^{BS} = \begin{bmatrix} c\alpha_R & 0 & -s\alpha_R \\ 0 & 1 & 0 \\ s\alpha_R & 0 & c\alpha_R \end{bmatrix}$$

$$[T]_{P}^{LQ} = \begin{bmatrix} c\sigma & 0 & -s\sigma \\ 0 & 1 & 0 \\ s\sigma & 0 & c\sigma \end{bmatrix}; [T]^{NL} = \begin{bmatrix} 1 & 0 & 0 \\ 0 & c\eta & s\eta \\ 0 & -s\eta & c\eta \end{bmatrix} [T]_{P}^{BN} = \begin{bmatrix} c\zeta & 0 & -s\zeta \\ 0 & 1 & 0 \\ s\zeta & 0 & c\zeta \end{bmatrix}$$

$$[T]_{PR}^{SS} = \begin{bmatrix} c\psi\, c\delta\gamma & s\psi & -c\psi\, s\delta\gamma \\ -c\phi\, s\psi\, c\delta\gamma + s\phi\, s\delta\gamma & c\phi\, c\psi & c\phi\, s\psi\, s\delta\gamma + s\phi\, c\delta\gamma \\ s\phi\, s\psi\, c\delta\gamma + c\phi\, s\delta\gamma & -s\phi\, s\psi & -s\phi\, s\psi\, s\delta\gamma + c\phi\, c\delta\gamma \end{bmatrix}$$

FOR SMALL ANGLES $\delta\gamma, \psi, \phi$:

$$[T]_{PR}^{SS} = \begin{bmatrix} 1 & \psi & -\delta\gamma \\ -\psi & 1 & \phi \\ \delta\gamma & -\phi & 1 \end{bmatrix}$$

TABLE 6,3 COORDINATE TRANSFORMATION MATRICES

7. KINEMATICS

All kinematic concepts have been introduced in Chapter 3. In particular, Equations (3.19) and (3.20) define the rotational derivatives of tensors and Equation (3.44) the angular velocity tensor. Here we shall concentrate on providing the formulas needed for the further development of the equations of motion.

One method of evaluating the angular velocity is given by Equations (3.50) and (3.51). But usually one tries to avoid the matrix multiplication and instead regards the angular velocity tensor as an axial vector and adds vectorially the individual components along the axes of rotation. As an example we shall evaluate the angular velocity vector $[\omega_p^{(S)(I)}]_p^S$ of the stability frame of the perturbed flight, $(S)_p$, relative to the inertial frame, (I), expressed in a coordinate system $]_p^S$ associated with $(S)_p$. Refer back to Figure 6.1 and read off:

$$[\omega_p^{(S)(I)}]_p^S = [\omega_{p\,p}^{(S)(Y)}]_p^S + [\omega_{p\,p}^{(Y)(R)}]_p^S + [\omega_p^{(R)(I)}]_p^S \tag{1}$$

To simplify the evaluation, express the last two terms in different coordinate systems:

$$[\omega_p^{(S)(I)}]_p^S = [\omega_{p\,p}^{(S)(Y)}]_p^S + [T]_{p\,p}^{S\,Y}[\omega_{p\,p}^{(Y)(R)}]_p^Y + [T]_{p\,p}^{S\,R}[\omega_p^{(R)(I)}]_p^R \tag{2}$$

with

$$[\omega_{p\,p}^{(S)(Y)}]_p^S = \begin{bmatrix} \dot{\phi} \\ 0 \\ 0 \end{bmatrix}_p^S ; [\omega_{p\,p}^{(Y)(R)}]_p^Y = \begin{bmatrix} 0 \\ 0 \\ \dot{\mu} \end{bmatrix}_p^Y ; [\omega_p^{(R)(I)}]_p^R = \begin{bmatrix} 0 \\ \dot{\gamma}_p \\ 0 \end{bmatrix}_p^R \tag{3}$$

Carrying out the multiplications yields:

$$[\omega_p^{(S)(I)}]_p^S = \begin{bmatrix} \dot{\phi} + \dot{\gamma}_p \sin\psi \\ \dot{\psi}\sin\phi + \dot{\gamma}_p \cos\psi\cos\phi \\ \dot{\psi}\cos\phi - \dot{\gamma}_p \cos\psi\sin\phi \end{bmatrix}_p^S \tag{4}$$

where the dot stands for the derivative $\frac{d}{dt}$. If we set $\dot{\gamma}_p = 0$ in Equation (4), we get

$$[\omega_p^{(S)(R)}]_p^S = \begin{bmatrix} \dot{\phi} \\ \dot{\psi}\sin\phi \\ \dot{\psi}\cos\phi \end{bmatrix}_p^S \tag{5}$$

and if we add $[\omega_p^{(B)(S)}]_p^S$ to Equation (5), we obtain

$$[\omega_p^{(B)(R)}]_p^S = \begin{bmatrix} \dot{\phi} \\ \dot{\alpha}_p + \dot{\psi}\sin\phi \\ \dot{\psi}\cos\phi \end{bmatrix}_p^S \tag{6}$$

Three more formulas are derived directly from Figure 6.1.

$$[\omega_r^{(S)(I)}]_r^S = \begin{bmatrix} 0 \\ \dot{\gamma}_r \\ 0 \end{bmatrix}_r^S \tag{7}$$

$$[\omega_p^{(R)(S)}]_r^S = \begin{bmatrix} 0 \\ \delta\dot{\gamma} \\ 0 \end{bmatrix}_r^S \tag{8}$$

$$[\omega_p^{(W)(S)}]_p^W = \begin{bmatrix} 0 \\ 0 \\ \dot{\beta} \end{bmatrix}_r^S \tag{9}$$

$$\left[\omega_{R}^{(B)(R)}\right]_{R}^{S} = \begin{bmatrix} 0 \\ \dot{\alpha}_R \\ 0 \end{bmatrix}_R^S \tag{10}$$

For further reference, we shall also need the time derivatives of Equations (6) and (10):

$$\frac{d}{dt}\left[\omega_{P}^{(B)(R)}\right]_{P}^{S} = \begin{bmatrix} \ddot{\phi} \\ \ddot{\alpha}_P + \ddot{\psi}\sin\phi + \dot{\psi}\dot{\phi}\cos\phi \\ \ddot{\psi}\cos\phi - \dot{\psi}\dot{\phi}\sin\phi \end{bmatrix}_P^S \tag{11}$$

$$\frac{d}{dt}\left[\omega_{R}^{(B)(R)}\right]_{R}^{S} = \begin{bmatrix} 0 \\ \ddot{\alpha}_R \\ 0 \end{bmatrix}_R^S \tag{12}$$

In Chapter 6 two groups of axis systems were introduced: the flight-mechanical and gyro-mechanical frame axes. The flight-mechanical frame axes are used to formulate the aerodynamic forces and the equations of motion. The purposes of introducing the gyro-mechanical frame axes are to establish the connection with the dynamics of gyroscopes and to obtain order of magnitude estimates for certain terms in the equations of motion. In the following we shall derive the relationships between the flight-mechanical angles ϕ and ψ and the gyro-mechanical angles δ and η, together with their time derivatives. This could be done via the appropriate coordinate transformations. However, to avoid lengthy matrix multiplications, we shall employ spherical trigonometry.

Consider the spherical triangle $(x_2^E, x_2^Y{}_P, x_2^S{}_P)$ of Figure 6.1 and reproduced in Figure 7.1.

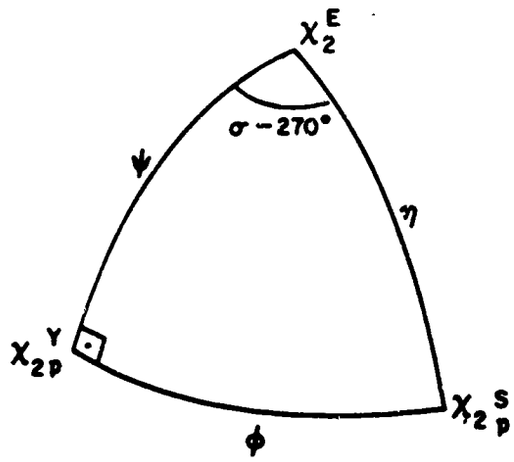

FIGURE 7.1 SPHERICAL TRIANGLE

We read off:

$$\sin\phi = \cos(90° - \eta)\cos(90° - \delta + 270°) \tag{13}$$

$$\sin\phi = \sin\eta\cos\delta \tag{14}$$

Similarly we get:

$$\sin(90° - \delta + 270°) = \tan\psi\tan(90° - \eta) \tag{15}$$

or

$$\tan\psi = -\tan\eta\sin\delta \tag{16}$$

The first time derivatives of Equations (14) and (16) are:

$$\dot{\phi} = \frac{-\dot{\delta}\sin\eta\sin\delta + \dot{\eta}\cos\eta\cos\delta}{(1-\sin^2\eta\cos^2\delta)^{1/2}} \tag{17}$$

$$\dot{\psi} = \frac{-\dot{\delta}\sin\eta\cos\eta\cos\delta - \dot{\eta}\sin\delta}{1-\sin^2\eta\cos^2\delta} \tag{18}$$

To simplify the expressions, we introduce the small-angle assumption. From Figure 7.1 we conclude that small angles ϕ and ψ imply a small angle η. With this assumption that the cone angle η is a small angle, we obtain from Equations (14), (16), (17), and (18)

$$\phi = \eta\cos\delta \tag{19}$$

$$\psi = -\eta\sin\delta \tag{20}$$

$$\dot{\phi} = -\eta\dot{\delta}\sin\delta + \dot{\eta}\cos\delta \tag{21}$$

$$\dot{\psi} = -\eta\dot{\delta}\cos\delta - \dot{\eta}\sin\delta \tag{22}$$

The second-order time derivatives are deduced from Equations (17) and (18). Again, assuming that η is a small angle, they become:

$$\ddot{\phi} = (-\eta\dot{\delta}^2 + \ddot{\eta})\cos\delta - (2\dot{\eta}\dot{\delta} + \eta\ddot{\delta})\sin\delta \tag{23}$$

$$\ddot{\psi} = (\eta\dot{\delta}^2 - \ddot{\eta})\sin\delta - (2\dot{\eta}\dot{\delta} + \eta\ddot{\delta})\cos\delta \tag{24}$$

Let us multiply Equation (21) by Equation (22) and Equation (14) by Equation (22), respectively:

$$\dot{\phi}\dot{\psi} = \frac{1}{2}(\eta^2\dot{\delta}^2 - \dot{\eta}^2)\sin 2\delta - \eta\dot{\eta}\dot{\delta}\cos 2\delta \tag{25}$$

$$\dot{\psi}\phi = \frac{1}{2}\left(-\eta^2\dot{\delta} - \eta^2\dot{\delta}\cos 2\delta - \eta\dot{\eta}\sin 2\delta\right) \tag{26}$$

Squaring the Equations (19) through (22) and adding the first two and last two equations yields:

$$\psi^2 + \phi^2 = \eta^2 \tag{27}$$

and

$$\dot{\psi}^2 + \dot{\phi}^2 = \eta^2\dot{\delta}^2 + \dot{\eta}^2 \tag{28}$$

For further reference we also give the time derivatives of the cone angle η and the node angle δ for small angles ϕ and ψ :

$$\dot{\eta} = \frac{\phi\dot{\phi} + \psi\dot{\psi}}{(\psi^2 + \phi^2)^{1/2}} \tag{29}$$

$$\dot{\delta} = \frac{-\phi\dot{\psi} + \psi\dot{\phi}}{\psi^2 + \phi^2} \tag{30}$$

All these equations will be used later to estimate the order of magnitude of certain terms. As an example, we want to show that the absolute value of $[\omega_p^{(S)(R)}]$ is of the order $\eta\dot{\delta}$; i.e.,

$$\| \omega_p^{(S)(R)} \| = \mathcal{O}\{\eta\dot{\delta}\} \tag{31}$$

From Equation (5) generate the absolute value and obtain in view of Equation (28):

$$\| \omega_p^{(S)(R)} \| = (\dot{\phi}^2 + \dot{\psi}^2)^{1/2} = (\eta^2\dot{\delta}^2 + \dot{\eta}^2)^{1/2} \tag{32}$$

Because the nutation rate $\dot{\delta}$ for common MR's is much greater than the decay of the cone angle η ; i.e.,

$$\sigma\{\dot{\delta}\} / \sigma\{\dot{\eta}\} \geqq 10^2 \tag{33}$$

and because $\eta = 0$ implies $\dot{\eta} = 0$, we receive the desired result

$$\| \omega_{\rho}^{(S)} {}_{\rho}^{(R)} \| \approx \eta \dot{\delta} \tag{34}$$

The time derivatives of all expressions are in real time. In later chapters we shall often need them in dynamic-normalized time. This can be achieved simply by substituting $\frac{d}{d\bar{t}}$ or a circle for $\frac{d}{dt}$ or a dot, respectively.

8. REFERENCE FLIGHT

Consider a Magnus rotor (MR) in free flight. Its most important flight regime is the descent in a vertical plane with horizontal spin axis. We call this flight condition the planar glide phase. It will serve as the reference or unperturbed flight for the stability investigations in later chapters. Before deriving the equations of this reference flight, we shall establish the conditions under which the MR is able to perform a planar glide phase.

8.1 CONDITIONS FOR THE EXISTENCE OF A PLANAR GLIDE PHASE

The equations for the planar glide phase were formulated by Brunk (1). They describe two translational and one rotational degrees of freedom of an MR. It is intuitively clear that a mirror-symmetrical MR can actually achieve a planar glide phase, provided that no external disturbances occur. However, we shall present a rigorous proof. Before we can formulate this proof, we must define mirror symmetry and the planar glide phase in mathematical terms. Let us begin by introducing the concept of a reflectional tensor that will lead us to the definition of mirror symmetry.

Consider a plane, P, normal to the MR's spin axis. The point of intersection with the spin axis is B. We consider two sets of displacement vectors. The first set connects the mass elements Δm_k ; $k = 1, 2, \cdots, n$ to the right of the plane P with the point B, $[s_{kB}]$. The right-hand side is the side of the positive spin axis. The second set connects the mass elements Δm_ℓ ; $\ell = 1, 2, \cdots, m$ to the left of the plane P with the point B, $[s_{\ell B}]$ (see Figure 8.1).

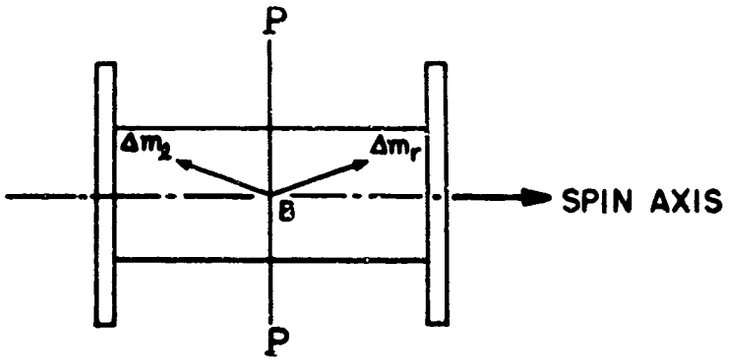

FIGURE 8.1 LOCATIONS OF MASS ELEMENTS

Let the subscript be chosen such that, if $k = \ell$, the displacement vector $[s_{\ell B}]$ is the mirror image of $[s_{kB}]$ with respect to the mirror plane P. This can be expressed mathematically by a tensor $[H]$ such that

$$[s_{\ell B}] = [H][s_{kB}] \tag{1}$$

In a body axis system, $[H]$ has the form

$$[H]^B = \begin{bmatrix} 1 & 0 & 0 \\ 0 & -1 & 0 \\ 0 & 0 & 1 \end{bmatrix}^B \tag{2}$$

It is symmetric and orthogonal with a value $\det\{[H]\} = -1$. We will refer to it as the <u>reflection tensor</u>. Any displacement vector in the plane P, $[s_{PB}]$, is reflected into itself; i.e.,

$$[s_{PB}] = [H][s_{PB}] \tag{3}$$

The reflectional tensor operates on a second-order tensor, $[A]$, as:

$$[A'] = [H][A][H]^T \tag{4}$$

If $[A]$ is skew-symmetric, say $[\Omega]$, then an equivalent form of Equation (4) is obtained for the axial vector $[\omega]$ of $[\Omega]$:

$$[\omega'] = -[H][\omega] \tag{5}$$

To prove this we write Equation (4) in subscript notation with summation convention:

$$\Omega'_{jk} = H_{jr}\,\Omega_{rs}\,H_{ks} \tag{6}$$

Contract the second-order tensor by multiplying both sides by ε_{ijk} and sum twice

$$\varepsilon_{ijk}\,\Omega'_{jk} = \varepsilon_{ijk}\,H_{jr}\,H_{ks}\,\Omega_{rs} \tag{7}$$

Because, from Jeffreys (13), page 72,

$$\varepsilon_{ijk}\,H_{jr}\,H_{ks} = \det(H)\,H_{il}\,\varepsilon_{lrs} \tag{8}$$

and $\det(H) = -1$, Equation (7) becomes

$$\varepsilon_{ijk}\,\Omega'_{jk} = -H_{il}\,\varepsilon_{lrs}\,\Omega_{rs} \tag{9}$$

The axial vectors of the skew-symmetric tensors are

$$\omega'_i = \frac{1}{2}\,\varepsilon_{ijk}\,\Omega'_{jk} \quad ; \quad \omega_l = \frac{1}{2}\,\varepsilon_{lrs}\,\Omega_{rs} \tag{10}$$

Therefore, we can write Equation (9) as

$$\omega_i' = -H_{il}\,\omega_l \tag{11}$$

which is in the form of Equation (5).

<u>DEFINITION</u>: An MR is said to have mirror-symmetrical <u>mass distribution</u> if, for every mass element Δm_k ; $k = 1, 2, \cdots, n$ located at $[s_{kB}]$, we can find a mass element $\Delta m_l = \Delta m_k$; $l = 1, 2, \cdots, n$ located at $[s_{lB}] = [H][s_{kB}]$.

<u>DEFINITION</u>: An MR is said to have a mirror-symmetrical <u>external configuration</u> if, for every surface element ΔA_k ; $k = 1, 2, \cdots, q$ at $[s_{kB}]$ we can find a surface element $\Delta A_l = \Delta A_k$; $l = 1, 2, \cdots, q$ located at $[s_{lB}] = [H][s_{kB}]$.

From the first definition, two properties of the mirror-symmetrical MR follow immediately: (i) its center of mass is in the mirror plane P , and (ii) its moment-of-inertia tensor is invariant under a reflectional tensor operation; i.e.,

$$[I^{(B)}{}_B] = [H][I^{(B)}{}_B][H]^T \tag{12}$$

To prove Equation (12), we express the moment-of-inertia tensor by its definition:

$$\begin{aligned}[H][I^{(B)}{}_B][H]^T = \sum_i \Delta m_i [s_{iB}]^T [s_{iB}][H][E][H]^T - \\ - \sum_i \Delta m_i [H][s_{iB}][s_{iB}]^T [H]^T\end{aligned} \tag{13}$$

where $\sum_i$; $i = 1, 2, \cdots, u$ is the summation of sufficiently small mass elements over the total MR. Let us separate the second term in Equation (13) into a right-hand contribution, $\sum_r$; $r = 1, 2, \cdots, n$ and a left-hand contribution, $\sum_l$; $l = 1, 2, \cdots, n$ with $n = \frac{1}{2}u$:

$$\sum_i \Delta m_i [H][s_{iB}][s_{iB}]^T[H]^T = \sum_r \Delta m_r [H][s_{rB}][s_{rB}]^T[H]^T + \sum_l \Delta m_l [H][s_{lB}][s_{lB}]^T[H]^T \tag{14}$$

Because the MR possesses mirror-symmetrical mass distribution, Equation (1) and its inverse $[s_{rB}] = [H][s_{lB}]$ holds for all $r = 1, 2, \cdots, n$. Thus, we write Equation (14)

$$\sum_i \Delta m_i [H][s_{iB}][s_{iB}]^T[H]^T = \sum_r \Delta m_r [s_{lB}][s_{lB}]^T + \sum_l \Delta m_l [s_{rB}][s_{rB}]^T \tag{15}$$

Furthermore, $\Delta m_r = \Delta m_l$ and $\sum_r = \sum_l$. Therefore,

$$\sum_i \Delta m_i [H][s_{iB}][s_{iB}]^T[H]^T = \sum_i \Delta m_i [s_{iB}][s_{iB}]^T \tag{16}$$

Substituting Equation (16) into Equation (13) delivers the desired proof:

$$[H][I^{(B)}{}_B][H]^T = \sum_i \Delta m_i \left\{ [s_{iB}]^T[s_{iB}][E] - [s_{iB}][s_{iB}]^T \right\} = [I^{(B)}{}_B] \tag{17}$$

Let us define now what we mean by planar glide phase.

<u>DEFINITION</u>: An MR performs a <u>planar glide phase</u> if three conditions are satisfied throughout the flight:

$$[\ell_{B\,n}^{(B)(I)}]^T [f_g] = 0 \tag{18}$$

$$[\ell_{B\,n}^{(B)(I)}]^T [\mathcal{D}^{(I)} p_n^{(B)(I)}] = 0 \tag{19}$$

$$[p_n^{(B)(I)}]^T [\mathcal{D}^{(I)} \ell_{B\,n}^{(B)(I)}] = 0 \tag{20}$$

<u>THEOREM</u>. The necessary and sufficient conditions for the existence of a planar glide phase are:

1. The MR possesses mirror symmetry with respect to its external geometry and the moment of inertia tensor satisfies Equation (12).

2. The perturbations during flight are limited to forces whose resultant vectors lie in the vertical plane and to horizontal moment vectors.

3. The initial conditions are:

a. Mirror plane is vertical; i.e., the gravitational force is contained in the plane:

$$[f_g] = [H][f_g] \tag{21}$$

b. The linear momentum vector is contained in a vertical plane:

$$[p_n^{(B)(I)}(0)] = [H][p_n^{(B)(I)}(0)] \tag{22}$$

c. The angular momentum vector is horizontal:

$$[\ell_{B\,n}^{(B)(I)}(0)] = -[H]^T [\ell_{B\,n}^{(B)(I)}(0)] \tag{23}$$

PROOF: We shall first give the initial orientation of the aerodynamic force and moment. As outlined in Section 11.3, the aerodynamic force must satisfy the relationship

$$[f_a(0)] = [f_a\{M_R, R_R, [S_{iB}(0)], [\hat{\omega}_R^{(B)(I)}(0)], [\hat{v}_{B_R}^{(I)}(0)]\}]$$

$$= [H]^T [f_a\{M_R, R_R, [H][S_{iB}(0)], -[H][\hat{\omega}_R^{(B)(I)}(0)], [H][\hat{v}_{B_R}^{(I)}(0)]\}] \tag{24}$$

where M_R and R_R are the Mach number and the Reynolds number, respectively. $[\hat{\omega}_R^{(B)(I)}(0)]$ and $[\hat{v}_{B_R}^{(I)}(0)]$ are the aero-normalized angular and linear velocities, respectively, of the MR relative to an inertial frame at time $t = 0$.

Because the surface is mirror symmetrical, we have:

$$[S_{iB}(0)] = [H][S_{iB}(0)] \tag{25}$$

From Equation (22):

$$[\hat{v}_{B_R}^{(I)}(0)] = [H][\hat{v}_{B_R}^{(I)}(0)] \tag{26}$$

and from Equation (23) with Equation (12):

$$[\hat{\omega}_R^{(B)(I)}(0)] = -[H][\hat{\omega}_R^{(B)(I)}(0)] \tag{27}$$

Therefore, Equation (24) has the form:

$$[f_a(0)] = [H][f_a(0)] \tag{28}$$

A similar procedure leads to:

$$[m_a(0)] = -[H][m_a(0)] \tag{29}$$

This means that initially the aerodynamic force is in a vertical plane and the aerodynamic moment is horizontal.

Now we shall show that Equations (18) through (20) are satisfied at $t = 0$. Equation (18) is automatically satisfied by Condition 3c of the theorem. Using the equation of motion, Equation (4.1), and premultiplying by $[\ell_{B_R}^{(B)(I)}(0)]^T$ gives:

$$[\ell_{B_R}^{(B)(I)}(0)]^T[\mathcal{D}^{(I)}p_R^{(B)(I)}] = [\ell_{B_R}^{(B)(I)}(0)]^T[f_a(0)] + [\ell_{B_R}^{(B)(I)}(0)]^T[f_g] \quad (30)$$

The right-hand side is zero because $[f_a(0)]$ and $[f_g]$ are in a vertical plane. Therefore, Equation (19) is also satisfied. Also, premultiply Equation (4.2) by $[p_R^{(B)(I)}(0)]$ and obtain

$$[p_R^{(B)(I)}(0)]^T[\mathcal{D}^{(I)}\ell_{B_R}^{(B)(I)}] = [p_R^{(B)(I)}(0)]^T[m_a(0)] \quad (31)$$

This is again zero, and Equation (20) is therefore also satisfied. Summarizing, we have at the initial time $t = 0$:

$$[\ell_{B_R}^{(B)(I)}(0)]^T[f_g] = 0 \quad (32)$$

$$[\ell_{B_R}^{(B)(I)}(0)]^T[\mathcal{D}^{(I)}p_R^{(B)(I)}] = 0 \quad (33)$$

$$[p_R^{(B)(I)}(0)]^T[\mathcal{D}^{(I)}\ell_{B_R}^{(B)(I)}] = 0 \quad (34)$$

which agrees with Equations (18) through (20). To arrive at these equations, we employed Conditions (1) and (3) of the theorem. It can easily be verified that, if any of these conditions is violated, then Equations (32) through (34) do not hold and, by definition, the MR is not in a planar glide phase initially. Therefore, for $t = 0$, Conditions (1) and (3) are the necessary and sufficient conditions for a planar glide phase.

To extend the reasoning to positive times, we interpret the Equations (32) through (34) as stating that, after a time increment δt, the linear momentum vector is still in the vertical plane and the angular momentum vector remains horizontal. Now we can again show that Equations (18) through (20) are satisfied for the time $t = \delta t$. However, because perturbations may be acting during the time increment, we must impose Condition (2) of the theorem. These admissible perturbations do not affect the restrictions on the linear and angular momentum vectors. But any other perturbation would force the linear momentum out of the vertical plane and/or the angular momentum from its horizontal attitude. Therefore, Conditions (1) through (3) are the necessary and sufficient conditions for a planar glide phase at $t = \delta t$. This process can be repeated for the next time increment, and so on. Thus, the theorem is proved.

8.2 EQUATIONS OF MOTION

We shall formulate the reference equations of motion in a coordinate system associated with the stability frame $\overset{(S)}{r}$ during reference flight (see Table 6.1). From Equations (5.4) and (5.5), we obtain:

$$\frac{d}{dt}\left[\overline{p_r^{(B)(I)}}\right]_r^S + \left[\overline{\Omega_r^{(S)(I)}}\right]_r^S \left[\overline{p_r^{(B)(I)}}\right]_r^S = \left[\overline{f_a(r)}\right]_r^S + \left[\overline{f_g(r)}\right]_r^S \tag{35}$$

$$\frac{d}{dt}\left[\overline{l_{Br}^{(B)(I)}}\right]_r^S + \left[\overline{\Omega_r^{(S)(I)}}\right]_r^S \left[\overline{l_{Br}^{(B)(I)}}\right]_r^S = \left[\overline{m_a(r)}\right]_r^S \tag{36}$$

From Section 8.1, we know that the linear momentum and the aerodynamic and gravitational forces remain in the vertical plane; i.e.,

$$[\overline{p_{\kappa}^{(B)(I)}}] = [H][\overline{p_{\kappa}^{(B)(I)}}] \tag{37}$$

$$[\overline{f_a(\kappa)}] = [H][\overline{f_a(\kappa)}] \tag{38}$$

$$[\overline{f_g}] = [H][\overline{f_g}] \tag{39}$$

and that the angular momentum and aerodynamic moment remain horizontal; i.e.,

$$[\overline{\ell_{B\,\kappa}^{(B)(I)}}] = -[H][\overline{\ell_{B\,\kappa}^{(B)(I)}}] \tag{40}$$

$$[\overline{m_a(\kappa)}] = -[H][\overline{m_a(\kappa)}] \tag{41}$$

With the reflection tensor

$$[H]_{\kappa}^{s} = \begin{bmatrix} 1 & 0 & 0 \\ 0 & -1 & 0 \\ 0 & 0 & 1 \end{bmatrix}_{\kappa}^{s} \tag{42}$$

Equations (37) through (41) require that some of the components in Equations (35) and (36) must be zero. We obtain the following result:

$$\begin{bmatrix} \dot{\bar{V}}_{\kappa} \\ 0 \\ -\bar{V}_{\kappa}\dot{\gamma}_{\kappa} \end{bmatrix}_{\kappa}^{s} = \begin{bmatrix} \overline{f_{a_1}(\kappa)} \\ 0 \\ \overline{f_{a_3}(\kappa)} \end{bmatrix}_{\kappa}^{s} + \frac{mg}{\frac{\rho}{2} V_{ss}^{2} S} \begin{bmatrix} -\sin\gamma_{\kappa} \\ 0 \\ \cos\gamma_{\kappa} \end{bmatrix}_{\kappa}^{s} \tag{43}$$

$$\begin{bmatrix} 0 \\ \bar{I}_y \dot{\bar{\omega}}_{\kappa} \\ 0 \end{bmatrix}_{\kappa}^{s} = \begin{bmatrix} 0 \\ \overline{m_{a_2}(\kappa)} \\ 0 \end{bmatrix}_{\kappa}^{s} \tag{44}$$

where $\bar{V}_n$ is the flight speed, $\bar{\omega}_n$ the spin rate about the spin axis, $\bar{I}_y$ the moment of inertia about the spin axis, and γ_n the glide angle. Equation (43) is the linear momentum equation with the first component along the flight path and the third component normal to it. The last terms on the right-hand side are the gravitational force components. The angular momentum Equation (44) consists of the component about the spin axis only.

We turn now to the determination of the aerodynamic forces. In Chapter 11, Equations (11.13) and (11.14), we shall show that the following functional relationships exist:

$$[\overline{f_a(n)}] = \bar{V}_n^2 [C_F \{ M_n, R_n, [b_k(n)]_n^s, [\hat{\omega}_{n\,n}^{(B)(S)}]_n^s, [\hat{v}_{B_n}^{(I)}]_n^s \}] \tag{45}$$

$$[\overline{m_a(n)}] = \frac{\bar{V}_n^2}{\mu} [C_M \{ \quad \text{SAME DEPENDENCE} \quad \}] \tag{46}$$

where we made the <u>ASSUMPTION</u>:

$$\| \hat{\omega}_n^{(S)(I)} \| << \| \hat{\omega}_n^{(B)(S)} \| \tag{47}$$

i.e., the maximum rate of change of glide angle is less than one percent of the spin rate. Furthermore, by definition, we have

$$[\hat{v}_{B_n}^{(I)}]_n^s = \begin{bmatrix} \hat{V}_n \\ 0 \\ 0 \end{bmatrix}_n^s = \begin{bmatrix} 1 \\ 0 \\ 0 \end{bmatrix}_n^s \tag{48}$$

Let

$$[\hat{\omega}_{n\,n}^{(B)(S)}]_n^s = \begin{bmatrix} 0 \\ \hat{\omega}_n \\ 0 \end{bmatrix}_n^s \tag{49}$$

and remember that $[b_k(r)]_r^s = [T]_{rr}^{BS^T} [b_k(r)]_r^B$ contains the only variable α_r. Then we can simplify the functional relationship in Equations (45) and (46).

$$[\overline{f_a(r)}] = \bar{V}_r^2 [C_F \{ M_r, R_r, \alpha_r, \hat{\omega}_r \}] \tag{50}$$

$$[\overline{m_a(r)}] = \frac{\bar{V}_r^2}{\mu} [C_M \{ M_r, R_r, \alpha_r, \hat{\omega}_r \}] \tag{51}$$

The lift and drag coefficients are introduced by the following definition:

$$\begin{bmatrix} C_D \\ 0 \\ C_L \end{bmatrix}_r^S = - \begin{bmatrix} C_{F_1}(r) \\ 0 \\ C_{F_3}(r) \end{bmatrix}_r^S \tag{52}$$

The spin torque coefficient is written as

$$\begin{bmatrix} 0 \\ C_M \\ 0 \end{bmatrix}_r^S = \begin{bmatrix} 0 \\ C_{M_2}(r) \\ 0 \end{bmatrix}_r^S \tag{53}$$

Experimental evidence justifies the following simplified functional forms for the coefficients:

$$C_D = C_D \{ M_r, R_r, \alpha_r \} \tag{54}$$

$$C_L = C_{L_{\hat{\omega}}} \{ M_r, R_r, \alpha_r \} \hat{\omega}_r \tag{55}$$

$$C_M = C_{M_a} \{ M_r, R_r, \alpha_r \} + C_{M_{d_{\hat{\omega}}}} \{ M_r, R_r, \alpha_r \} \hat{\omega}_r \tag{56}$$

where $C_D, C_L, C_{M_a}, C_{M_{d_{\hat{\omega}}}}$ must be determined experimentally. Substitute Equations (54) through (56) into Equations (43) and (44), and convert all

aero-normalized quantities into dynamic-normalized terms. The final result is:

$$\overset{\circ}{\bar{V}}_r = - C_D \bar{V}_r^2 - \frac{\tau}{V_{ss}} g \sin\gamma_r \tag{57}$$

$$\overset{\circ}{\gamma}_r = \frac{1}{\mu} C_{L_{\hat{\omega}}} \bar{\omega}_r - \frac{\tau}{V_{ss}} g \frac{1}{\bar{V}_r} \cos\gamma_r \tag{58}$$

$$\overset{\circ}{\bar{\omega}}_r = \frac{1}{\mu \bar{I}_y} \bar{V}_r^2 C_{M_a} + \frac{1}{\mu^2 \bar{I}_y} \bar{V}_r C_{M_{d\hat{\omega}}} \bar{\omega}_r \tag{59}$$

where we used the previously introduced assumption that the rate of change of glide angle is much smaller (<1%) than the spin rate.

$\bar{V}_r$, γ_r, and $\bar{\omega}_r$ are the dependent variables. The absolute value of the flight velocity $\bar{V}_r$ and the glide angle γ_r are the polar coordinates of the velocity vector. The dynamic-normalized spin rate $\bar{\omega}_r \equiv \overset{\circ}{\alpha}_r$ is related to the tip-speed ratio via $\bar{\omega}_r = \mu \bar{V}_r \hat{\omega}_r$. The aerodynamic coefficients depend implicitly on M_r, R_r, and α_r. For a discussion of the equations refer to Section 12.1.

9. LINEAR MOMENTUM

In this chapter we shall derive the equations that describe the perturbations of the linear momentum of an MR from the reference glide phase. The dynamic-normalized form of the Perturbation Equation (4.25) will be used:

$$[\overline{\mathcal{D}^{(I)}}\,\overline{p_{p}^{(B)(I)}}] - [R_{pn}^{(S)(S)}][\overline{\mathcal{D}^{(I)}}\,\overline{p_{pn}^{(n)(I)}}] = [\overline{\varepsilon f_a}] + \{[E] - [R_{pn}^{(S)(S)}]\}[\overline{f_g(n)}] \quad (1)$$

Our goal is to express the differential equations in a coordinate system associated with the perturbed stability frame $\overset{(S)}{p}$.

To begin with, let us concentrate on the first term in Equation (1). Equations (5.10) and (5.11) show that the linear momentum and linear velocity have the same value in a dynamic-normalized system. Therefore,

$$[\overline{\mathcal{D}^{(I)}}\,\overline{p_{p}^{(B)(I)}}] = [\overline{\mathcal{D}^{(I)}}\,\overline{v_{B_p}^{(I)}}] \quad (2)$$

For ease of calculation, we perform a transformation of frames from (I) to the wind frame $\overset{(W)}{p}$ in a perturbed state:

$$[\overline{\mathcal{D}^{(I)}}\,\overline{v_{B_p}^{(I)}}] = [\overline{\mathcal{D}_{p}^{(W)}}\,\overline{v_{B_p}^{(I)}}] + [\overline{\Omega_{p}^{(W)(S)}}][\overline{v_{B_p}^{(I)}}] + [\overline{\Omega_{p}^{(S)(I)}}][\overline{v_{B_p}^{(I)}}] \quad (3)$$

Furthermore, introduce the two convenient coordinate systems $]_p^S$ and $]_p^W$:

$$[\overline{\mathcal{D}^{(I)}}\,\overline{v_{B_p}^{(I)}}]_p^S = [T]_p^{WS}{}^T \left\{\frac{d}{dt}[\overline{v_{B_p}^{(I)}}]_p^W + [\overline{\Omega_{p}^{(W)(S)}}]_p^W[\overline{v_{B_p}^{(I)}}]_p^W\right\} + [\overline{\Omega_{p}^{(S)(I)}}]_p^S[\overline{v_{B_p}^{(I)}}]_p^S \quad (4)$$

where by definition:

$$[\overline{v_{B_p}^{(I)}}]_p^W = \begin{bmatrix} \bar{V}_p \\ 0 \\ 0 \end{bmatrix}_p^W \quad (5)$$

ASSUMPTION 1: Let the angles ϕ, ψ, β be small enough that the cosine of the angle can be replaced by one and the sine by the angle itself.

With this assumption, Equation (4) can be written out using the corresponding relationships derived in Chapters 6 and 7:

$$[\overline{\mathcal{D}^{(I)}}\,\overline{v_{B_p}^{(I)}}]_p^s = \begin{bmatrix} \overset{\circ}{\bar{V}}_p - (\dot{\beta} + \dot{\psi} - \phi\,\dot{\gamma}_p)\,\bar{V}_p\beta \\ \dot{\bar{V}}_p\beta + (\overset{\circ}{\beta} + \dot{\psi} - \phi\,\dot{\gamma}_p)\,\bar{V}_p \\ -\overset{\circ}{\gamma}_p\,\bar{V}_p + (\psi\,\dot{\gamma}_p + \overset{\circ}{\phi})\,\bar{V}_p\beta - \phi\,\dot{\psi}\,\bar{V}_p \end{bmatrix}_p^s \tag{6}$$

The second term on the left-hand side of Equation (1) becomes, if expressed in the $]_p^s$-coordinate system,

$$[R_{pr}^{(S)(S)}]_p^s\,[\overline{\mathcal{D}^{(I)}}\,\overline{p_r^{(B)(I)}}]_p^s = [T]_{pr}^{ss}\,[R_{pr}^{(S)(S)}]_r^s\,[\overline{\mathcal{D}^{(I)}}\,\overline{p_r^{(B)(I)}}]_r^s = [E]_{pr}^{ss}\,[\overline{\mathcal{D}^{(I)}}\,\overline{p_r^{(B)(I)}}]_r^s \tag{7}$$

which is the left-hand side of Equation (8.35). Both equations combined yield the perturbation of the linear momentum:

$$[\overline{\mathcal{D}^{(I)}}\,\overline{p_p^{(B)(I)}}]_p^s - [R_{pr}^{(S)(S)}]_p^s\,[\overline{\mathcal{D}^{(I)}}\,\overline{p_r^{(B)(I)}}]_p^s = \begin{bmatrix} \delta\overset{\circ}{\bar{V}} - (\overset{\circ}{\beta} + \dot{\psi} - \phi\,\overset{\circ}{\gamma}_p)\,\bar{V}_p\beta \\ \dot{\bar{V}}_p\beta + (\overset{\circ}{\beta} + \dot{\psi} - \phi\,\dot{\gamma}_p)\,\bar{V}_p \\ -(\dot{\gamma}_p\,\bar{V}_p - \dot{\gamma}_r\,\bar{V}_r) + (\psi\,\dot{\gamma}_p + \overset{\circ}{\phi})\,\bar{V}_p\beta - \phi\,\dot{\psi}\,\bar{V}_p \end{bmatrix}_p^s \tag{8}$$

where $\delta\bar{V}$ is the perturbation of the dynamic-normalized absolute value of the flight velocity, defined by

$$\delta\bar{V} = \bar{V}_p - \bar{V}_r \tag{9}$$

and its time derivative

$$\delta\overset{\circ}{\bar{V}} = \overset{\circ}{\bar{V}}_p - \overset{\circ}{\bar{V}}_r \tag{10}$$

<u>ASSUMPTION 2</u>: Let $\delta\bar{V} \ll \bar{V}_R$, $\delta\dot{\bar{V}} \ll \dot{\bar{V}}_R$. This is well justified because the angles ϕ, ψ, and β are small, and, therefore, disturbances will have a small effect on the change and rate of change of the total flight velocity.

Of particular interest for the further development is the second equation in Equation (8). Let us impose Assumption 2 and show that the term $\phi\,\dot{\gamma}_p\,\bar{V}_R$ can be neglected; i.e.,

$$\| \phi\,\dot{\gamma}_p \| \ll \| \dot{\psi} \| \tag{11}$$

To do that we convert Equation (11) into gyro-mechanical quantities using the Equations (7.19) and (7.22):

$$\| \dot{\gamma}_p\,\eta \cos\delta \| \ll \| -\eta\,\dot{\delta}\cos\delta - \dot{\eta}\sin\delta \| \tag{12}$$

For all MR's the rate of change of cone angle $\dot{\eta}$ is much smaller than the nutation rate $\dot{\delta}$; i.e.

$$\sigma\{\dot{\delta}/\dot{\eta}\} \geqq 10^2 \tag{13}$$

Therefore, even for a small cone angle η , we can replace Equation (12) for all practical purposes by

$$\| \dot{\gamma}_p\,\eta\cos\delta \| \ll \| \eta\,\dot{\delta}\cos\delta \| \tag{14}$$

and, therefore

$$\| \dot{\gamma}_p \| \ll \| \dot{\delta} \| \tag{15}$$

which says that, for the term $\phi\,\dot{\gamma}_p\,\bar{V}_R$ to be neglected, the rate of change of glide angle must be much smaller than the nutation rate. This is certainly satisfied $\left(\sigma\{\dot{\delta}/\dot{\gamma}_p\} \geqq 10^2 \right)$.

The same arguments also lead to a simplification of the first and third equation in Equation (8). Summarizing we get:

$$[\overline{\mathcal{D}^{(I)}}\,\overline{\rho^{(B)(I)}}]^{s}_{p} - [R^{(s)(s)}_{p\,n}]^{s}_{p}[\overline{\mathcal{D}^{(I)}}\,\overline{\rho^{(B)(I)}_{n}}]^{s}_{p} = \begin{bmatrix} \overset{\circ}{\delta\bar{V}} - (\overset{\circ}{\beta} + \overset{\circ}{\psi})\bar{V}_n\beta \\ \frac{d}{dt}(\bar{V}_n\beta) + \overset{\circ}{\psi}\,\bar{V}_n \\ -\delta\overset{\circ}{\gamma}\bar{V}_n + (\overset{\circ}{\phi}\beta - \phi\overset{\circ}{\psi})\bar{V}_n \end{bmatrix}^{s}_{p} \tag{16}$$

where

$$\delta\overset{\circ}{\gamma} = \overset{\circ}{\gamma}_p - \overset{\circ}{\gamma}_n \tag{17}$$

is the perturbation rate of the glide angle. The desired form of the perturbation equation is finally obtained by substituting Equation (16) into Equation (1) and expressing the last term of Equation (1) in the $]^{s}_{p}$ -coordinate system

$$\begin{bmatrix} \overset{\circ}{\delta\bar{V}} - (\overset{\circ}{\beta} + \overset{\circ}{\psi})\bar{V}_n\beta \\ \frac{d}{dt}(\bar{V}_n\beta) + \overset{\circ}{\psi}\,\bar{V}_n \\ -\delta\overset{\circ}{\gamma}\bar{V}_n + (\overset{\circ}{\phi}\beta - \phi\overset{\circ}{\psi})\bar{V}_n \end{bmatrix}^{s}_{p} = [\overline{\varepsilon f_a}]^{s}_{p} + \frac{\tau g}{V_{ss}} \begin{bmatrix} -\delta\gamma\cos\gamma_n \\ \psi\sin\gamma_n + \phi\cos\gamma_n \\ -\delta\gamma\sin\gamma_n \end{bmatrix}^{s}_{p} \tag{18}$$

The left-hand side represents the perturbations of the time rate of change of linear momentum from the reference flight. The first and third components are expressed in flight direction and normal to it in a vertical plane, respectively. They are nonlinear in ϕ, ψ and β . The second component gives the time rate of change of linear momentum along the spin axis. It is linear in ψ and β , and will be of major interest in the sequel. The terms on the right-hand are the perturbations of the aerodynamic forces and the gravitational contributions.

10. ANGULAR MOMENTUM

We shall derive the equations that describe the perturbations of the angular momentum of an MR from the reference glide phase. We begin with the dynamic-normalized form of Equation (4.23)

$$[\overline{\mathcal{D}^{(I)}}\,\varepsilon\,\overline{\mathcal{L}_{B}^{(B)(I)}}] + [\varepsilon\,\overline{\Omega^{(S)(I)}}][R_{p\,n}^{(S)(S)}][\overline{\ell_{B\,n}^{(B)(I)}}] = [\overline{\varepsilon\, m_a}] \tag{1}$$

Before converting to component form, we will show that Equation (1) can be simplified considerably by comparing the order of magnitudes of individual terms. Again, as in Chapter 9, we shall assume that ϕ , ψ , β are small angles. Then, because of Equation (7.27), the cone angle η is also small.

10.1 SIMPLIFICATIONS

SIMPLIFICATION 1: The major contribution to the perturbation of the angular velocity $[\varepsilon\omega^{(S)(I)}]$ comes from the rotation of the frame $\overset{(S)}{p}$ relative to $\overset{(R)}{p}$; i.e., the nutation rate is greater than the time rate of change of glide angle. This intuitively leads to the approximation:

$$[\overline{\varepsilon\omega^{(S)(I)}}] \approx [\overline{\omega_{p}^{(S)}\,{}_{p}^{(R)}}] \tag{2}$$

JUSTIFICATION: From definition Equation (4.13)

$$[\overline{\varepsilon\omega^{(S)(I)}}] = [\overline{\omega_{p}^{(S)(I)}}] - [R_{p\,n}^{(S)(S)}][\overline{\omega_{n}^{(S)(I)}}] = [\overline{\omega_{p\,p}^{(S)(R)}}] + [\overline{\omega_{p\,n}^{(R)(S)}}] + \left([E] - [R_{p\,n}^{(S)(S)}]\right)[\overline{\omega_{n}^{(S)(I)}}] \tag{3}$$

where the individual terms have the following order of magnitude

$$\|\overline{\omega_{p\,p}^{(S)(R)}}\| = \mathcal{O}\{\mathring{\delta}\eta\} \qquad \text{(see Equation (7.34))}$$

$$\|[E] - [R_{p\,n}^{(S)(S')}]\| = \mathcal{O}\{\eta\} \qquad \text{(see Table 6.3)}$$

$$\|\overline{\omega_{n}^{(S')(I)}}\| = \mathcal{O}\{\mathring{\gamma}_n\} \qquad \text{(see Equation (7.7))} \tag{4}$$

$$\|\overline{\omega_{p\,n}^{(R)(S')}}\| = \mathcal{O}\{\delta\mathring{\gamma}\} \qquad \text{(see Equation (7.8))}$$

Equation (2) is justified if

$$\|\overline{\omega_{p\,p}^{(S)(R)}}\| \gg \|[\overline{\omega_{p\,n}^{(R)(S')}}] + ([E] - [R_{p\,n}^{(S)(S')}])[\overline{\omega_{n}^{(S')(I)}}]\| \tag{5}$$

and it is certainly also justified if we can show that

$$\|\overline{\omega_{p\,p}^{(S)(R)}}\| \gg \|\overline{\omega_{p\,n}^{(R)(S')}}\| + \|[E] - [R_{p\,n}^{(S)(S')}]\|\,\|\overline{\omega_{n}^{(S')(I)}}\| \tag{6}$$

Expressed in order of magnitudes:

$$\|\mathcal{O}\{\eta\mathring{\delta}\}\| \gg \|\mathcal{O}\{\delta\mathring{\gamma}\}\| + \|\mathcal{O}\{\eta\}\|\,\|\{\mathring{\gamma}_n\}\| \tag{7}$$

The maximum time rate of change of glide angle $\mathring{\gamma}_n$ and its maximum perturbation $\delta\mathring{\gamma}$ are of the same order of magnitude. Furthermore, $\delta\mathring{\gamma}$ decreases as the magnitude of the disturbance decreases. We can therefore let the last term of Equation (7) be representative for the order of magnitude of the right-hand side of Equation (7). Because the rate of change of glide angle, $\mathring{\gamma}_n$, is much smaller than the nutation rate; i.e.,

$$\frac{\sigma\{\eta\dot{\delta}\}}{\sigma\{\eta\dot{\gamma}_r\}} = \frac{\sigma\{\dot{\delta}\}}{\sigma\{\dot{\gamma}_r\}} \geqq 10^2 \tag{8}$$

Equation (7) is satisfied, and, thus, Equation (2) is justified.

<u>SIMPLIFICATION 2</u>: Equation (1) can be reduced to:

$$[\overline{\mathcal{D}^{(R)}_p}\,\overline{\ell_{B\,p}^{(B)(I)}}] - [R^{(S)(S)}_{p\,r}][\overline{\mathcal{D}^{(S)}_r}\,\overline{\ell_{B\,r}^{(B)(I)}}] = [\overline{\varepsilon m_a}] \tag{9}$$

<u>JUSTIFICATION</u>: Introduce Simplification 1 into Equation (1) and refer the rotational derivative to the $\overset{(R)}{p}$ -frame, using the Theorem of Transformation of Frames, Equation (3.53):

$$[\overline{\mathcal{D}^{(R)}_p}\,\varepsilon\overline{\ell_B^{(B)(I)}}] + [\overline{\Omega^{(R)(I)}_p}][\varepsilon\overline{\ell_B^{(B)(I)}}] + [\overline{\Omega^{(S)(R)}_{p\,p}}][R^{(S)(S)}_{p\,r}][\overline{\ell_{B\,r}^{(B)(I)}}] = [\overline{\varepsilon m_a}] \tag{10}$$

The last two terms of Equation (10) have the following orders of magnitude

$$\begin{aligned} \|[\overline{\Omega^{(R)(I)}_p}][\varepsilon\overline{\ell_B^{(B)(I)}}]\| &= \sigma\{\dot{\gamma}_p\}\,\sigma\{\eta\,\|\overline{\ell_{B\,r}^{(B)(I)}}\|\} \\ \|[\overline{\Omega^{(S)(R)}_{p\,p}}][R^{(S)(S)}_{p\,r}][\overline{\ell_{B\,r}^{(B)(I)}}]\| &= \sigma\{\dot{\delta}\eta\}\,\sigma\{1\}\,\sigma\{\|\overline{\ell_{B\,r}^{(B)(I)}}\|\} \end{aligned} \tag{11}$$

Because

$$\frac{\sigma\{\dot{\delta}\eta\,\|\overline{\ell_{B\,r}^{(B)(I)}}\|\}}{\sigma\{\dot{\gamma}_r\eta\,\|\overline{\ell_{B\,r}^{(B)(I)}}\|\}} = \frac{\sigma\{\dot{\delta}\}}{\sigma\{\dot{\gamma}_r\}} \geqq 10^2 \tag{12}$$

the second term on the left-hand side of Equation (10) can be neglected. Substitute Equation (4.12) into Equation (10)

$$[\overline{\mathcal{D}^{(n)}_{p}}\,\overline{\ell_{B\,p}^{(B)(I)}}]-\left\{[\overline{\mathcal{D}^{(n)}_{p}}\,([R^{(S)(S)}_{p\,n}][\overline{\ell_{B\,n}^{(B)(I)}}])]+[\overline{\Omega^{(R)(S)}_{p\,p}}][R^{(S)(S)}_{p\,n}][\overline{\ell_{B\,n}^{(B)(I)}}]\right\}=[\overline{\varepsilon m_a}] \quad (13)$$

This can be brought into the form of Equation (9) if we first apply the Theorem of Transformation of Frames to the first term in the braces, generating $\mathcal{D}^{(S)}_{n}$ and then the Theorem of Rotation of Vectors to shift to $\mathcal{D}^{(S)}_{n} = \mathcal{D}^{(R)}_{n}$.

<u>SIMPLIFICATION 3</u>: Equation (9) can be further reduced to:

$$[\overline{\mathcal{D}^{(R)}_{p}}\,\overline{\ell_{B\,p\,p}^{(B)(R)}}]-[R^{(S)(R)}_{p\,n}][\overline{\mathcal{D}^{(R)}_{n}}\,\overline{\ell_{B\,n\,n}^{(B)(R)}}]=[\overline{\varepsilon m_a}] \quad (14)$$

<u>JUSTIFICATION</u>: Let

$$[\overline{\ell_{B\,p}^{(B)(I)}}]\equiv[\overline{I_{B\,p}^{(B)}}][\overline{\omega_{p}^{(B)(I)}}]=[\overline{I_{B\,p}^{(B)}}]\left([\overline{\omega_{p\,p}^{(B)(R)}}]+[\overline{\omega_{p}^{(R)(I)}}]\right)\equiv[\overline{\ell_{B\,p\,p}^{(B)(R)}}]+[\overline{\ell_{B\,p}^{(R)(I)}}] \quad (15)$$

$$[\overline{\ell_{B\,n}^{(B)(I)}}]\equiv[\overline{I_{B\,n}^{(B)}}][\overline{\omega_{n}^{(B)(I)}}]=[\overline{I_{B\,n}^{(B)}}]\left([\overline{\omega_{n\,n}^{(B)(S)}}]+[\overline{\omega_{n}^{(S)(I)}}]\right)\equiv[\overline{\ell_{B\,n\,n}^{(B)(S)}}]+[\overline{\ell_{B\,n}^{(S)(I)}}] \quad (16)$$

and substitute into Equation (9), recalling that $^{(S)}_{n} = {}^{(R)}_{n}$

$$[\overline{\mathcal{D}^{(R)}_{p}}\,\overline{\ell_{B\,p\,p}^{(B)(R)}}]-[R^{(S)(R)}_{p\,n}][\overline{\mathcal{D}^{(R)}_{n}}\,\overline{\ell_{B\,n\,n}^{(B)(R)}}]+[\overline{\mathcal{D}^{(R)}_{p}}\,\overline{\ell_{B\,p}^{(R)(I)}}]-[R^{(S)(R)}_{p\,n}][\overline{\mathcal{D}^{(R)}_{n}}\,\overline{\ell_{B\,n}^{(R)(I)}}]=[\overline{\varepsilon m_a}] \quad (17)$$

If we can show that, on the left-hand side, the last two terms are small compared with the first two terms, then Equation (14) is justified. Abbreviated, we have to prove that

$$\|A\| \gg \|B\| \quad (18)$$

where $\|B\|$ is expressed most conveniently in a $]^{S}_{n}$ coordinate system:

$$\|B\|=\left\|\frac{d}{dt}[\overline{\ell_{B\,p}^{(R)(I)}}]^{S}_{n}-[R^{(S)(S)}_{p\,n}]^{S}_{n}\frac{d}{dt}[\overline{\ell_{B\,n}^{(R)(I)}}]^{S}_{n}+[\overline{\Omega^{(R)(R)}_{n\,p}}]^{S}_{n}[\overline{\ell_{B\,p}^{(R)(I)}}]^{S}_{n}\right\| \quad (19)$$

The last term is zero, because $[\omega_{R\,P}^{(R)(R)}]$ is parallel to $[\ell_{B\,P}^{(R)(I)}]$. Therefore, the order of magnitude of $\|B\|$ is

$$\|B\| = \mathcal{O}\{\bar{I}_y \delta\ddot{\gamma}\} \tag{20}$$

The first two terms are expressed in a $]_P^S$ coordinate system:

$$\|A\| = \left\|\frac{d}{dt}[\overline{\ell_{B\,P}^{(B)(R)}}]_P^S - [E]_{PR}^{SS}\frac{d}{dt}[\overline{\ell_{B\,R}^{(B)(R)}}]_R^S + [\overline{\Omega_{P\,P}^{(S)(R)}}]_P^S[\overline{\ell_{B\,P}^{(B)(R)}}]_P^S\right\| \tag{21}$$

with the order of magnitudes

$$\|A\| = \|\mathcal{O}\{\bar{I}_y \delta\ddot{\alpha}\} + \mathcal{O}\{\eta\dot{\delta}\bar{I}_y\dot{\alpha}_P\}\| \tag{22}$$

where α is the angle of attack and $\bar{I}_y$ the dynamic-normalized moment of inertia about the spin axis.

Equation (18) is proven if we can show that

$$\mathcal{O}\{\bar{I}_y \eta\dot{\delta}\dot{\alpha}_P\} - \mathcal{O}\{\bar{I}_y \delta\ddot{\alpha}\} \gg \mathcal{O}\{\bar{I}_y \delta\ddot{\gamma}\} \tag{23}$$

The perturbation of the angular spin acceleration, $\delta\ddot{\alpha}$, depends on the magnitude of the disturbance. It usually does not exceed 10^3 rad/dnt^2 and decreases with decreasing disturbance. In contrast with this, $\mathcal{O}\{\dot{\delta}\dot{\alpha}_P\} = 5 \times 10^5$ rad/dnt^2. Thus, it remains to be shown that

$$\mathcal{O}\{\bar{I}_y \eta\dot{\delta}\dot{\alpha}_P\} \gg \mathcal{O}\{\bar{I}_y \delta\ddot{\gamma}\} \tag{24}$$

This is satisfied even for very small nutation angles η, because

$$\frac{\mathcal{O}\{\dot{\delta}\dot{\alpha}_P\}}{\mathcal{O}\{\delta\ddot{\gamma}\}} \geqq 10^3 \tag{25}$$

and, if $\eta = 0$, then $\delta\ddot{\gamma}$ must also be zero. This completes the justification of Equation (14).

DISCUSSION: Equation (14) will be used for further evaluation of the angular momentum. Its form is similar to Equation (4.26). However, it has some important simplifying features: (i) the rotational derivatives are referred to the reference frame and not to the inertial frame, and (ii) the total angular momentum is calculated relative to the reference frame; i.e., the contribution of the rotation between the reference frame and the inertial frame is neglected. These simplifications are possible because of the high angular spin momentum inherent in an MR. A somewhat less convenient, yet more elegant, form can be found by proceeding in a similar fashion:

$$[\overline{\mathcal{D}^{(R)}_{n}\, \ell_{B\,p\,n}^{(B)(R)}}] - [R^{(S)(R)}_{p\,n}][\overline{\mathcal{D}^{(R)}_{n}\, \ell_{B\,n\,n}^{(B)(R)}}] = [\overline{\varepsilon m_{a}}] \tag{26}$$

If $^{(R)}_{n}$ is replaced by (I), we arrive at Equation (4.26). This means that the disturbance of the rate of change of the angular momentum of an MR can be calculated as if the reference frame of the reference flight were an inertial system. Equation (14) goes even farther, permitting the reference frame of the perturbed flight to be considered as the inertial frame for calculating the rate of change of angular momentum of the perturbed MR.

10.2 EQUATIONS IN COMPONENT FORM

We shall express the rate of change of angular momentum in a coordinate system associated with the stability frame during perturbed flight. Before writing out the components, let us cast the moment of inertia tensor into a special form most suitable for further discussion.

Because the mass distribution of an MR is assumed to be mirror-symmetrical, the spin axis is always a principal moment-of-inertia axis. Some MR's have an inertia ellipsoid that is circular with reference to the spin axis; i.e., they have an inertia spheroid. However, others (e.g., wing rotors, see Boehler (3)) have noncircular or triaxial inertia ellipsoids. To treat both cases most easily, we separate the inertia ellipsoid into a mean spheroid and a perturbation ellipsoid. Correspondingly, we write the moment-of-inertia tensor during reference flight as

$$[I_{B\,r}^{(B)}] = [I_{B\,r}^{cir(B)}] + [\Delta I_{B\,r}^{(B)}] \tag{27}$$

and during perturbed flight as

$$[I_{B\,p}^{(B)}] = [I_{B\,p}^{cir(B)}] + [\Delta I_{B\,p}^{(B)}] \tag{28}$$

To show the advantage of this formulation, let us express the moment of inertia tensor

$$[I_{B\,p}^{(B)}]_p^B = \begin{bmatrix} I_1 & 0 & 0 \\ 0 & I_2 & 0 \\ 0 & 0 & I_3 \end{bmatrix}_p^B \tag{29}$$

in a $]_p^S$-coordinate system. After performing the proper transformations and introducing the double angle $2\alpha_p$, we obtain:

$$[I_{B\,p}^{(B)}]_p^S = \begin{bmatrix} \frac{1}{2}(I_1+I_3) & 0 & 0 \\ 0 & I_2 & 0 \\ 0 & 0 & \frac{1}{2}(I_1+I_3) \end{bmatrix}_p^S + \frac{1}{2}(I_3-I_1) \begin{bmatrix} -\cos 2\alpha_p & 0 & \sin 2\alpha_p \\ 0 & 0 & 0 \\ \sin 2\alpha_p & 0 & \cos 2\alpha_p \end{bmatrix}_p^S \tag{30}$$

Identify the first term as the mean circular moment of inertia tensor $[I_{B\,p}^{cir(B)}]_p^S$ and the second term as the perturbation inertia tensor

$[\Delta I_{B\,p}^{(B)}]_p^s$. An MR with circular or triangular cross-section has $I_3 = I_1$ and therefore maintains the first term only. For a triaxial inertia ellipsoid and high aspect ratio: $I_3 \approx I_1$, and the second term becomes small compared with the first term. Furthermore, we can regard the first term as that part of the moment-of-inertia tensor that is time-independent if expressed in a $]_p^s$-coordinate system. The time derivative with respect to the $]_p^s$ - coordinate system is obtained from the second term:

$$\frac{d}{dt}[\Delta I_{B\,p}^{(B)}]_p^s = \dot{\alpha}_p (I_3 - I_1) \begin{bmatrix} \sin 2\alpha_p & 0 & \cos 2\alpha_p \\ 0 & 0 & 0 \\ \cos 2\alpha_p & 0 & -\sin 2\alpha_p \end{bmatrix}_p^s \tag{31}$$

To evaluate Equation (14), we insert the dynamic-normalized form of Equations (27) and (28) and express the first term in a $]_p^s$ -coordinate system and the second term in a $]_R^s$ - coordinate system. The result is

$$\overline{[I_{B\,p}^{cir(B)}]_p^s} \frac{d}{dt}\overline{[\omega_{p\,p}^{(B)(R)}]_p^s} + \overline{[\Omega_{p\,p}^{(s)(R)}]_p^s}\,\overline{[I_{B\,p}^{cir(B)}]_p^s}\,\overline{[\omega_{p\,p}^{(B)(R)}]_p^s} +$$

$$+\frac{d}{dt}\left(\overline{[\Delta I_{B\,p}^{(B)}]_p^s}\right)\overline{[\omega_{p\,p}^{(B)(R)}]_p^s} + \overline{[\Delta I_{B\,p}^{(B)}]_p^s} \frac{d}{dt}\overline{[\omega_{p\,p}^{(B)(R)}]_p^s} + \overline{[\Omega_{p\,p}^{(s)(R)}]_p^s}\,\overline{[\Delta I_{B\,p}^{(B)}]_p^s}\,\overline{[\omega_{p\,p}^{(B)(R)}]_p^s} \tag{32}$$

$$-[E]_{p\,R}^{s\,s}\,\overline{[I_{B\,R}^{cir(B)}]_R^s} \frac{d}{dt}\overline{[\omega_{R\,R}^{(B)(R)}]_R^s} = \overline{[\varepsilon m_a]_p^s}$$

where we used the facts that

$$[T]_{p\,R}^{s\,s}\,[R_{p\,R}^{(s)(s)}]_R^s = [E]_{p\,R}^{s\,s} \tag{33}$$

and

$$[\Delta I_{B\,r}^{(B)}]_r^s\,[\omega_{r\,r}^{(B)(R)}]_r^s = [0]_r^s \tag{34}$$

which follows from the particular form of $[\Delta I_{B\,r}^{(B)}]_r^s$ as obtained by replacing ρ by r everywhere in Equation (30). The first and last lines in Equation (32) are the contributions of the circular part of the inertia ellipsoid, while the second line takes the deviations into consideration. For an MR with an inertia spheroid, the second line is, of course, zero.

To write out the components, we substitute Equations (30) and (31), and the proper equations from Chapter 7 into Equation (32). Assuming small angles ϕ, ψ, β and abbreviating

$$\frac{1}{2}(\bar{I}_3+\bar{I}_1) = \bar{I}\ ;\quad \frac{1}{2}(\bar{I}_3-\bar{I}_1) = \Delta\bar{I}\ ;\quad \bar{I}_2 = \bar{I}_y \tag{35}$$

we obtain, in view of Equation (8.44):

$$\begin{bmatrix} \bar{I}\ddot{\phi} + \{-\bar{I}_y\dot{\alpha}_\rho + (\bar{I}-\bar{I}_y)\dot{\psi}\phi\}\dot{\psi} \\ \bar{I}_y(\ddot{\alpha}_\rho + \ddot{\psi}\phi + \dot{\psi}\dot{\phi}) \\ \bar{I}\ddot{\psi} + \{\bar{I}_y\dot{\alpha}_\rho - (2\bar{I}-\bar{I}_y)\dot{\psi}\phi\}\dot{\phi} \end{bmatrix}_p^s +$$

$$+\Delta\bar{I}\begin{bmatrix} (\ddot{\psi}+2\dot{\alpha}_\rho\dot{\phi})\sin 2\alpha_\rho + \{-\ddot{\phi} + (2\dot{\alpha}_\rho + \dot{\psi}\phi)\dot{\psi}\}\cos 2\alpha_\rho \\ (\dot{\psi}^2-\dot{\phi}^2)\sin 2\alpha_\rho - 2\dot{\psi}\dot{\phi}\cos 2\alpha_\rho \\ \{\ddot{\phi} - (2\dot{\alpha}_\rho + \dot{\psi}\phi)\dot{\psi}\}\sin 2\alpha_\rho + (\ddot{\psi}+2\dot{\alpha}_\rho\dot{\phi})\cos 2\alpha_\rho \end{bmatrix}_p^s - \tag{36}$$

$$-\begin{bmatrix} 0 \\ \bar{I}_y\ddot{\alpha}_r \\ 0 \end{bmatrix}_p^s = [\overline{\varepsilon m_a}]_p^s$$

The quantities in Equation (36) have been grouped so that the terms containing $\mathring{\alpha}_p$ can be compared with the terms of $\mathring{\psi}\phi$.

<u>SIMPLICATION 4</u>: $\|\mathring{\psi}\phi\| << \|\mathring{\alpha}_p\|$ i.e., terms with $\mathring{\psi}\phi$ can be neglected.

<u>JUSTIFICATION</u>: From Equation (7.26), we have

$$\mathring{\psi}\phi = \frac{1}{2}\left\{-\eta^2\mathring{\delta} - \eta^2\mathring{\delta}\cos 2\delta - \eta\mathring{\eta}\sin 2\delta\right\} \tag{37}$$

Therefore, the order of magnitude is

$$\sigma\{\mathring{\psi}\phi\} = \sigma\{\eta^2\mathring{\delta}\} \tag{38}$$

The ratio between spin rate and nutation rate is approximately

$$\mathring{\alpha}_p / \mathring{\delta} \approx \bar{I} / \bar{I}_y \tag{39}$$

i.e., greater than one for most MR's.

Therefore,

$$\frac{\sigma\{\mathring{\alpha}_p\}}{\sigma\{\mathring{\psi}\phi\}} = \frac{\sigma\{\mathring{\alpha}_p\}}{\sigma\{\eta^2\mathring{\delta}\}} = \frac{\sigma\{\bar{I}/\bar{I}_y\}}{\sigma\{\eta^2\}} \geqq 10^2 \tag{40}$$

and Simplication 4 is justified.

<u>ASSUMPTION</u>: Let $\mathring{\alpha}_p \approx \mathring{\alpha}_r$. This is well justified because, by Assumption 1, Chapter 9, the deviation β from the reference flight velocity is limited to small angles.

Introduce Simplification 4 and this Assumption into Equation (36) and use the definition

$$\delta\ddot{\alpha} = \ddot{\alpha}_p - \ddot{\alpha}_n \tag{41}$$

Then the equations assume the form

$$\begin{bmatrix} \bar{I}\ddot{\phi} - \bar{I}_y\dot{\alpha}_n\dot{\psi} \\ \bar{I}_y(\delta\ddot{\alpha} + \ddot{\psi}\phi + \dot{\psi}\dot{\phi}) \\ \bar{I}\ddot{\psi} + \bar{I}_y\dot{\alpha}_n\dot{\phi} \end{bmatrix}^s_p + \Delta\bar{I}\begin{bmatrix} (\ddot{\psi} + 2\dot{\alpha}_n\dot{\phi})\sin 2\alpha_p - (\ddot{\phi} - 2\dot{\alpha}_n\dot{\psi})\cos 2\alpha_p \\ (\dot{\psi}^2 - \dot{\phi}^2)\sin 2\alpha_p - 2\dot{\psi}\dot{\phi}\cos 2\alpha_p \\ (\ddot{\phi} - 2\dot{\alpha}_n\dot{\psi})\sin 2\alpha_p + (\ddot{\psi} + 2\dot{\alpha}_n\dot{\phi})\cos 2\alpha_p \end{bmatrix}^s_p = [\overline{\varepsilon m_a}]^s_p \tag{42}$$

They are called roll, pitch, and yaw equations. The terms of the perturbation ellipsoid in the roll and yaw equation are strikingly symmetrical. This suggests the following theorem.

<u>THEOREM</u>: Consider an MR with a triaxial inertia ellipsoid that performs a perturbed flight along a planar reference trajectory. Assume angles ϕ, ψ, β are small. Let the inertia ellipsoid be decomposed into mean circular and perturbation ellipsoids, as shown in Equation (30). Then the rate of change of angular momentum calculated from the perturbation ellipsoid vanishes in the roll and yaw equations.

<u>PROOF</u>: Multiply the roll equation by i and the yaw equation by -1 and add:

$$\bar{I}(-\ddot{\psi} + i\ddot{\phi}) + i\bar{I}_y\dot{\alpha}_n(-\dot{\psi} + i\dot{\phi}) + \Delta\bar{I}\{i(\ddot{\psi} + i\ddot{\phi}) + 2\dot{\alpha}_n(\dot{\psi} + i\dot{\phi})\}\sin 2\alpha_p +$$

$$+ \Delta\bar{I}\{-(\ddot{\psi} + i\ddot{\phi}) + i2\dot{\alpha}_n(\dot{\psi} + i\dot{\phi})\}\cos 2\alpha_p = i\overline{\varepsilon m_{a_1}} - \overline{\varepsilon m_{a_3}} \tag{43}$$

Abbreviate this equation:

$$\bar{I}\ddot{T} + i\bar{I}_y\dot{\alpha}_n\dot{T} + \Delta\bar{I}(a\sin 2\alpha_p + b\cos 2\alpha_p) = i\overline{\varepsilon m_{a_1}} - \overline{\varepsilon m_{a_3}} \tag{44}$$

where Γ is the complex orientation angle used in missile dynamics (see Etkin (16)). The terms of the perturbation ellipsoid can be combined into one expression:

$$\Delta\bar{I}\sqrt{a^2+b^2}\ \sin\left(2\alpha_p + \tan^{-1}\frac{b}{a}\right) \tag{45}$$

But, because $a=-ib$, the square root in Equation (45) is zero. Therefore, Equation (44) reduces to

$$\bar{I}\ddot{\Gamma} + i\,\bar{I}_y\,\dot{\alpha}_n\,\dot{\Gamma} = i\,\overline{\varepsilon m_{a_1}} - \overline{\varepsilon m_{a_3}} \tag{46}$$

This completes the proof.

Similarly, the contribution of the perturbation ellipsoid to the pitch equation can be estimated by combining the two terms of $\Delta\bar{I}$. We obtain for the pitch equation in Equation (42):

$$\bar{I}_y\left(\ddot{\delta\alpha} + \ddot{\psi}\phi + \dot{\psi}\dot{\phi}\right) + \Delta\bar{I}\left(\dot{\psi}^2 + \dot{\phi}^2\right)\sin\left(2\alpha_p + \chi\right) = \overline{\varepsilon m_{a_2}} \tag{47}$$

with χ as a phase factor. The order of magnitude of the perturbation ellipsoid is based on Equation (7.28):

$$O\left\{\Delta\bar{I}\left(\dot{\psi}^2+\dot{\phi}^2\right)\sin\left(2\alpha_p+\chi\right)\right\} = O\left\{\Delta\bar{I}\,\eta^2\,\dot{\delta}^2\right\} \tag{48}$$

This is best compared with the last term of the spheroid (see Equation (7.25)):

$$O\left\{\bar{I}_y\,\dot{\psi}\dot{\phi}\right\} = O\left\{\bar{I}_y\,\eta^2\,\dot{\delta}^2\right\} \tag{49}$$

Even though the value of Equation (48) is of the same order as that of Equation (49), the contribution of the perturbation ellipsoid follows a

sine wave with twice the spin frequency. Therefore, its net effect is zero for all practical purposes.

With this additional information, we can put the angular momentum equations into their final form:

$$\begin{bmatrix} \bar{I}\ddot{\phi} - \bar{I}_y \dot{\alpha}_R \dot{\psi} \\ \bar{I}_y (\delta\ddot{\alpha} + \ddot{\psi}\phi + \dot{\psi}\dot{\phi}) \\ \bar{I}\ddot{\psi} + \bar{I}_y \dot{\alpha}_R \dot{\phi} \end{bmatrix}_p^s = \overline{[\varepsilon m_u]}_p^s \tag{50}$$

<u>DISCUSSION</u>: The assumption of small angles ϕ, ψ, β is the only major assumption that Equation (50) is based on. The other assumptions and simplifications are a consequence of either small angles or the high angular spin momentum. They are stated separately to clarify the exposition. However, note that we did not assume that the perturbation ellipsoid is small compared with the mean spheroid. Therefore, Equation (50) holds for any type of MR. The left-hand sides of the roll and yaw equations are linear in the perturbation variables ϕ and ψ with a time-dependent parameter $\dot{\alpha}_R$. They are decoupled from the pitch equation. The pitch equation is nonlinear.

11. AERODYNAMIC FORCES

In order to treat the aerodynamics of MR's from a general viewpoint, we shall employ a tensor formulation of the aerodynamic coefficients. The coefficients are expanded into a Taylor series, yielding the aerodynamic derivatives. Some of the derivatives are zero because the MR's external configuration is mirror symmetrical. A theorem will be derived that gives a quick answer as to which derivative of arbitrary order exists and which has to be zero.

11.1 FUNCTIONAL RELATIONSHIPS

ASSERTIONS:

The aerodynamic forces depend on the following quantities (see, for instance, Hopkin (17)):

a. External form (shape, roughness) of MR

b. Size of MR, represented by reference length ℓ

c. Properties of the air: pressure p , density ρ , viscosity ν

d. Position and motion of the MR with respect to the unperturbed air.

Three well justified assumptions will be made:

ASSUMPTIONS:

1. The parameters in Assertions a and b are constant for a particular flight of a particular MR.

   Justification: Because we are mostly interested in analyzing the stability of MR's, we do not consider effects of moving control surfaces or aeroelastic deflections.

2. The aerodynamic forces depend only on the linear and angular velocities of the MR with respect to air and not on the accelerations.

   Justification: This assumption is usually not justified in airplane aerodynamics. However, as Brunk (1) pointed out, the acceleration of bodies without lifting surfaces has only a small effect on the aerodynamic forces. So far, no experimental evidence has been found that contradicts this assumption.

3. The air is assumed to be at rest or in uniform rectilinear motion with respect to the inertial frame.

   Justification: It is too difficult to analyze the dynamics of a flight vehicle subjected to arbitrary wind conditions. Therefore, this assumption is commonly made. It yields satisfactory approximations, provided the air is not too turbulent.

From the assertions and assumptions, we shall derive the functional dependence of the aerodynamic forces. To express Assertion d in mathematical form, let the frame (A) represent the air, idealized by Assumption 3, and let frame (B) symbolize the MR. Then, according to Section 3.2, the position of the MR is given by the triad of base vectors $[b_k]$; $k = 1,2,3$. Note also, that by Equation (3.11), the base vectors $[b_k]$ are related to some base vectors, $[a_k]$, of frame (A) through the rotation tensor $[R^{(B)(A)}]$; namely,

$$[b_k] = [R^{(B)(A)}][a_k] \quad ; \; k = 1,2,3 \tag{1}$$

The motion of the MR relative to the air is determined by the linear velocity (see Equation (3.34)) of the center-of-mass B :

$$[v_B^{(A)}] = [\mathcal{D}^{(A)} x_{BA}] \tag{2}$$

and the angular velocity (see Equation (3.44))

$$[\Omega^{(B)(A)}] = [\mathcal{D}^{(A)} R^{(B)(A)}][R^{(B)(A)}]^T \tag{3}$$

From Assertions a through d we establish the following relationship of the aerodynamic force:

$$[f_a] = [f_1\{\text{FORM}, \text{SIZE}(\ell), \mu, \rho, V, [\Omega^{(B)(A)}], [v_B^{(A)}]\}] \tag{4}$$

Dimensional analysis and, in particular, the π -theorem permit us to eliminate the explicit dependence of the function f_1 from three of its variables. We choose to absorb the reference length ℓ , the air density ρ , and the absolute value of the velocity $\| v_B^{(A)} \| = V$. We obtain:

$$[f_a] = \rho V^2 \ell^2 [f_2\{\text{FORMFACTORS}, M, R, [b_k], \frac{\ell}{V}[\omega^{(B)(A)}], \frac{1}{V}[v_B^{(A)}]\}] \tag{5}$$

For geometrically similar MR's, the form factors are the same. Furthermore, ℓ^2 can be replaced by any other characteristic area, like $\frac{1}{2}S = b\ell$, where b is the span of the MR. Introducing the notation for aero-normalized quantities of Chapter 5.2, we can write Equation (5) as:

$$[f_a] = \frac{1}{2}\rho V^2 S [f_3\{M, R, [b_k], [\hat{\omega}^{(B)(A)}], [\hat{v}_B^{(A)}]\}] \tag{6}$$

The aerodynamic moment referred to the center of mass B has the same functional form. Dynamic-normalize the force and moment equations and introduce C_F , C_M as the aerodynamic force and moment coefficients to obtain:

$$[\overline{f_a}] = \bar{V}^2 [C_F \{ M, R, [b_k], [\hat{\omega}^{(B)(A)}], [\hat{v}_B^{(A)}] \}] \tag{7}$$

$$[\overline{m_a}] = \frac{\bar{V}^2}{\mu} [C_M \{ M, R, [b_k], [\hat{\omega}^{(B)(A)}], [\hat{v}_B^{(A)}] \}] \tag{8}$$

These two equations describe the aerodynamics of geometrically similar MR's.

11.2 TAYLOR SERIES EXPANSION

The perturbation Equations (4.22) and (4.23) or (4.25) and (4.26) require the aerodynamics to be expressed as perturbations defined by Equations (4.14) and (4.15). Their dynamic-normalized form is:

$$[\overline{\varepsilon f_a}] = [\overline{f_a(p)}] - [R_p^{(s)} {}_n^{(s)}] [\overline{f_a(n)}] \tag{9}$$

$$[\overline{\varepsilon m_a}] = [\overline{m_a(p)}] - [R_p^{(s)} {}_n^{(s)}] [\overline{m_a(n)}] \tag{10}$$

The aerodynamic functions on the right are evaluated from Equations (7) and (8). Because Equations (7) and (8) are valid for any flight trajectory, they also determine the aerodynamics of the reference flight and the perturbed flight. We need only introduce the proper notation to distinguish each case:

$$[\overline{f_a(p)}] = \bar{V}_p^2 [C_F(p)] = \bar{V}_p^2 [C_F \{ M_p, R_p, [b_k(p)], [\hat{\omega}_p^{(B)(s)}{}_p], [\hat{\omega}_p^{(s)(A)}], [\hat{v}_{B_p}^{(A)}] \}] \tag{11}$$

$$[\overline{m_a(p)}] = \frac{\bar{V}_p^2}{\mu} [C_M(p)] = \frac{\bar{V}_p^2}{\mu} [C_M \{ M_p, R_p, [b_k(p)], [\hat{\omega}_p^{(B)(s)}{}_p], [\hat{\omega}_p^{(s)(A)}], [\hat{v}_{B_p}^{(A)}] \}] \tag{12}$$

and

$$[\overline{f_a(n)}] = \bar{V}_n^2 [C_F(n)] = \bar{V}_n^2 [C_F\{M_n, R_n, [b_k(n)], [\hat{\omega}^{(B)(S)}_{n\,n}], [\hat{\omega}^{(S)(A)}_{n}], [\hat{v}_{B_n}^{(A)}]\}] \quad (13)$$

$$[\overline{m_a(n)}] = \frac{\bar{V}_n^2}{\mu} [C_M(n)] = \frac{\bar{V}_n^2}{\mu} [C_M\{M_n, R_n, [b_k(n)], [\hat{\omega}^{(B)(S)}_{n\,n}], [\hat{\omega}^{(S)(A)}_{n}], [\hat{v}_{B_n}^{(A)}]\}] \quad (14)$$

where we have separated the angular velocity into two parts:

$$[\hat{\omega}^{(B)(A)}_{p}] = [\hat{\omega}^{(B)(S)}_{p\,p}] + [\hat{\omega}^{(S)(A)}_{p}] \quad (15)$$

$$[\hat{\omega}^{(B)(A)}_{n}] = [\hat{\omega}^{(B)(S)}_{n\,n}] + [\hat{\omega}^{(S)(A)}_{n}] \quad (16)$$

The variables of the perturbed and unperturbed flights are related through

$$\delta\bar{V} = \bar{V}_p - \bar{V}_n \quad (17)$$

$$\delta M = M_p - M_n \quad (18)$$

$$\delta R = R_p - R_n \quad (19)$$

$$[\varepsilon b_k] = [b_k(p)] - [R^{(S)(S)}_{p\,n}][b_k(n)]; \quad k = 1,2,3 \quad (20)$$

$$[\varepsilon\hat{\omega}^{(B)(S)}] = [\hat{\omega}^{(B)(S)}_{p\,p}] - [R^{(S)(S)}_{p\,n}][\hat{\omega}^{(B)(S)}_{n\,n}] \quad (21)$$

$$[\varepsilon\hat{\omega}^{(S)(A)}] = [\hat{\omega}^{(S)(A)}_{p}] - [R^{(S)(S)}_{p\,n}][\hat{\omega}^{(S)(A)}_{n}] \quad (22)$$

$$[\varepsilon\hat{v}_B^{(A)}] = [\hat{v}_{B_p}^{(A)}] - [R^{(S)(S)}_{p\,n}][\hat{v}_{B_n}^{(A)}] \quad (23)$$

Substitute Equations (11) through (14) into (9) and (10). Because Assumption 2, Chapter 9, permits us to set $\bar{V}_p^2 \approx \bar{V}_r^2$, we can establish the following relationships:

$$[\overline{\varepsilon f_a}] = \bar{V}_r^2 [\varepsilon C_F] \tag{24}$$

$$[\overline{\varepsilon m_a}] = \frac{\bar{V}_r^2}{\mu} [\varepsilon C_M] \tag{25}$$

where we defined the perturbations of the aerodynamic coefficients as:

$$[\varepsilon C_F] = [C_F(p)] - [R_p^{(s)(s)}_r][C_F(r)] \tag{26}$$

$$[\varepsilon C_M] = [C_M(p)] - [R_p^{(s)(s)}_r][C_M(r)] \tag{27}$$

The problem we have to solve is how to express $[\varepsilon C_F]$ and $[\varepsilon C_M]$ in a form suitable for applications. The most common method is to expand $[C_F(p)]$ and $[C_M(p)]$ in a Taylor series about the reference values $[C_F(r)]$ and $[C_M(r)]$. As the "small" expansion variables, we choose $[\varepsilon \hat{v}_B^{(A)}]$ and $[\varepsilon \hat{\omega}^{(s)(A)}]$. Symbolically, we can write this as:

$$[C_F(p)] = [C_F(\varepsilon=0)] + \left[\frac{\partial C_{F_i}}{\partial \hat{v}_j}\right]_{\varepsilon=0} [\varepsilon \hat{v}_B^{(A)}] + \left[\frac{\partial C_{F_i}}{\partial \hat{\omega}_j}\right]_{\varepsilon=0} [\varepsilon \hat{\omega}^{(s)(A)}] + \cdots \tag{28}$$

$$[C_M(p)] = [C_M(\varepsilon=0)] + \left[\frac{\partial C_{M_i}}{\partial \hat{v}_j}\right]_{\varepsilon=0} [\varepsilon \hat{v}_B^{(A)}] + \left[\frac{\partial C_{M_i}}{\partial \hat{\omega}_j}\right]_{\varepsilon=0} [\varepsilon \hat{\omega}^{(s)(A)}] + \cdots \tag{29}$$

If we can show that

$$[C_F(\varepsilon=0)] = [R_p^{(s)(s)}_r][C_F(r)] \tag{30}$$

and

$$[C_M(\varepsilon=0)] = [R_p^{(s)(s)}_r][C_M(r)] \tag{31}$$

both are satisfied then, in view of Equations (26) and (27), $[\varepsilon C_F]$ and $[\varepsilon C_M]$ are expressed in a McLaurin series given on the right sides of Equations (28) and (29).

Let us demonstrate this procedure in more detail for $[\varepsilon C_F]$. From Equation (11), with Equations (17) through (23), we obtain for $[C_F(p)]$:

$$[C_F\{M_k+\delta M, R_n+\delta R, [\varepsilon b_k]+[R^{(s)(s)}_{p\,k}][b_k(n)], [\varepsilon\hat{\omega}^{(B)(s)}]+[R^{(s)(s)}_{p\,n}][\hat{\omega}^{(B)(s)}_{n\,n}],$$

$$[\varepsilon\hat{\omega}^{(s)(A)}]+[R^{(s)(s)}_{p\,n}][\hat{\omega}^{(s)(A)}_{n}], [\varepsilon\hat{\upsilon}_B^{(A)}]+[R^{(s)(s)}_{p\,n}][\hat{\upsilon}_{B_n}^{(A)}]\}]$$

$$=[C_F\{M_n, R_n, [R^{(s)(s)}_{p\,n}][b_k(n)], [R^{(s)(s)}_{p\,n}][\hat{\omega}^{(B)(s)}_{n\,n}], [R^{(s)(s)}_{p\,n}][\hat{\omega}^{(s)(A)}_{n}], [R^{(s)(s)}_{p\,n}][\hat{\upsilon}_{B_n}^{(A)}]\}] \tag{32}$$

$$+\left[\frac{\partial C_F}{\partial \hat{\upsilon}_B^{(A)}}\{M_p, R_p, [b_k(p)], [\hat{\omega}^{(B)(s)}_{p\,p}], [R^{(s)(s)}_{p\,n}][\hat{\omega}^{(s)(A)}_{n}], [R^{(s)(s)}_{p\,n}][\hat{\upsilon}_{B_n}^{(A)}]\}\right]_{\varepsilon=0}[\varepsilon\hat{\upsilon}_B^{(A)}]$$

$$+\left[\frac{\partial C_F}{\partial \hat{\omega}^{(s)(A)}}\{\text{ SAME DEPENDENCE }\}\right]_{\varepsilon=0}[\varepsilon\hat{\omega}^{(s)(A)}]+\cdots$$

The derivatives are evaluated at $[\varepsilon\hat{\upsilon}_B^{(A)}] = [\varepsilon\hat{\omega}^{(s)(A)}] = [0]$. According to Equation (30), we have to show that

$$[C_F\{M_n, R_n, [R^{(s)(s)}_{p\,n}][b_k(n)], [R^{(s)(s)}_{p\,n}][\hat{\omega}^{(B)(s)}_{n\,n}], [R^{(s)(s)}_{p\,n}][\hat{\omega}^{(s)(A)}_{n}], [R^{(s)(s)}_{p\,n}][\hat{\upsilon}_{B_n}^{(A)}]\}]$$

$$= [R^{(s)(s)}_{p\,n}][C_F\{M_n, R_n, [b_k(n)], [\hat{\omega}^{(B)(s)}_{n\,n}], [\hat{\omega}^{(s)(A)}_{n}], [\hat{\upsilon}_{B_n}^{(A)}]\}] \tag{33}$$

The proof is based on the Principle of Material Indifference, which follows from the isotropic property of space (see Section 3.1). That is: consider a physical process consisting of certain frames. The interactions of these frames produce the outcome. From the isotropic property of space, we conclude that, if the frames are subjected to a rotation, then the outcome is rotated by the same amount.

Apply this principle to our particular situation; i.e., let the generation of aerodynamic forces be the physical process. The frames involved are the body, stability, and air frames. The motions of the body frame with respect to the air frame and some scalar quantities of state determine the aerodynamics. Consider the special situation described by Equation (33). On the left, all vectorial variables, representing the frames and their interactions, are rotated by $[R^{(S)}_{p\ n}{}^{(S)}]$. According to the principle, the outcome on the left must be equal to the original outcome rotated by $[R^{(S)}_{p\ n}{}^{(S)}]$. But this is exactly the contents of the right-hand side of Equation (33). This completes the proof.

The McLaurin series of $[\varepsilon C_F]$ can now be obtained from Equation (32).

$$[\varepsilon C_F] = \left[\frac{\partial C_F}{\partial \hat{v}_B^{(A)}}\left\{M_p, R_p, [b_k(p)], [\hat{\omega}^{(B)(S)}_{p\ p}], [R^{(S)(S)}_{p\ n}][\hat{\omega}^{(S)(A)}_{n}], [R^{(S)(S)}_{p\ n}][\hat{v}^{(W)}_{B_n}]\right\}\right][\varepsilon \hat{v}_B^{(A)}]$$
$$+\left[\frac{\partial C_F}{\partial \hat{\omega}^{(S)(A)}}\left\{\text{SAME DEPENDENCE}\right\}\right][\varepsilon \hat{\omega}^{(S)(A)}] + \cdots \tag{34}$$

The expansion for $[\varepsilon C_M]$ is generated the same way and its derivatives have the same functional dependence.

<u>DISCUSSION</u>: Equation (34) differs from the classical expansions used in airplane and missile aerodynamics in two respects. First, it is formu-

lated in an invariant tensor concept, because it is valid in all allowable coordinate systems. Second, in airplane dynamics, the aerodynamic forces are expanded in terms of the linear and angular velocities of the aircraft with reference to the air frame. In the dynamics of spinning missiles, the variables to be expanded are the same linear velocities as in the airplane case; however, the angular velocities are the velocities of the nonspinning body frame with reference to the air frame. The spin angular velocity is usually treated as a constant parameter.

The aerodynamics of MR's follow the missile case as far as the selection of the variables in the expansion is concerned. The nonspinning body frame is here the perturbed stability frame $\overset{(s)}{\rho}$. But the aerodynamic treatment of the spin degree-of-freedom must be given more attention because of the complex geometrical shape of the MR's body section. Care has been taken in deriving Equation (34) to show this dependence clearly. It is given by $[b_\kappa(\rho)]$ and $[\hat{\omega}^{(B)}_{\rho}{}^{(S)}_{\rho}]$. Note that both quantities appear in the form associated with the perturbed flight, because they are not included in the expansion. The same holds for M_ρ and R_ρ . However, it is necessary that the derivatives are only functions of the reference variables. This can be partially achieved by introducing Assumption 2 of Chapter 9 and the Assumption of Chapter 10. They permit the simplifications:

$$
\begin{aligned}
M_\rho &\approx M_R \\
R_\rho &\approx R_R \\
[\hat{\omega}^{(B)}_{\rho}{}^{(S)}_{\rho}] &\approx [\hat{\omega}^{(B)}_{R}{}^{(S)}_{R}]
\end{aligned}
\tag{35}
$$

The discussion on how to treat $[b_k(p)]$, the orientation of the MR during perturbed flight, will be given below.

To relate the derivatives to the data obtained from wind tunnel tests, we must express Equation (34) in a coordinate system most suitable for applications. Because internal strain-gage balances promise the best test results, we choose the coordinate system $]^{s}_{p}$ associated with the perturbed stability frame as defined in Chapter 6. This agrees with missile testing practice. We get:

$$[\varepsilon C'_F]^{s}_{p} = \left[\frac{\partial C'_F}{\partial \hat{v}^{(A)}_{B}}\left\{M_p, R_p, [b_k(p)]^{s}_{p}, [\hat{\omega}^{(B)(S)}_{p\,p}]^{s}_{p}, [\hat{\omega}^{(S)(A)}_{r}]^{s}_{r}, [\hat{v}^{(A)}_{B_r}]^{s}_{r}\right\}\right]^{s}_{p} [\varepsilon \hat{v}^{(A)}_{B}]^{s}_{p}$$

$$+ \left[\frac{\partial C'_F}{\partial \hat{\omega}^{(S)(A)}}\left\{\text{SAME DEPENDENCE}\right\}\right]^{s}_{p} [\varepsilon \hat{\omega}^{(S)(A)}]^{s}_{p} + \cdots \tag{36}$$

The functional dependence of the derivatives can be simplified and written in a more concise form. Let the base vectors be expressed in body coordinates:

$$[b_k(p)]^{s}_{p} = [T]^{B\,s}_{p\,p}{}^{T} [b_k(p)]^{B}_{p} \tag{37}$$

$[b_k(p)]^{s}_{p}$ is therefore represented by α_p alone. Because, by definition,

$$[\hat{v}^{(A)}_{B_r}]^{s}_{r} = \begin{bmatrix} 1 \\ 0 \\ 0 \end{bmatrix}^{s}_{r} \tag{38}$$

the aero-normalized velocity is constant. Furthermore, we can assume that the effect of $[\hat{\omega}^{(S)(A)}_{r}]^{s}_{r}$ on the aerodynamics is small compared with $[\hat{\omega}^{(B)(S)}_{p\,p}]^{s}_{p}$. Using the simplifications of Equation (35) and the definition Equation (18) and Equation (8.48) we summarize:

$$[\varepsilon C_F']_p^s = \left[\frac{\partial C_F'}{\partial \hat{v}_B^{(A)}}\left\{M_n, R_n ; \alpha_p, \hat{\omega}_n\right\}\right]_p^s [\varepsilon \hat{v}_B^{(A)}]_p^s$$
$$+ \left[\frac{\partial C_F'}{\partial \hat{\omega}^{(S)(A)}}\left\{M_n, R_n, \alpha_p, \hat{\omega}_n\right\}\right]_p^s [\varepsilon \hat{\omega}^{(S)(A)}]_p^s + \cdots \tag{39}$$

So far we have shown only the linear terms of the expansions. A more concise notation will be required to express higher order terms. We introduce:

$$\left\{\begin{array}{c}[\varepsilon C_F']_p^s \\ \hline [\varepsilon C_M']_p^s\end{array}\right\} \quad \left\{\begin{array}{c}C_{F_\ell}' \\ \hline C_{M_\ell}'\end{array}\right\} \quad \left\{\begin{array}{c}C_{F_1}' \\ C_{F_2}' \\ C_{F_3}' \\ \hline C_{M_1}' \\ C_{M_2}' \\ C_{M_3}'\end{array}\right\} \quad \left\{\begin{array}{c}C_x' \\ C_y' \\ C_z' \\ \hline C_\ell' \\ C_m' \\ C_n'\end{array}\right\} = C_i' \tag{40}$$

$$\ell, a = 1,2,3$$
$$i, j = 1, \cdots, 6$$

$$\left\{\begin{array}{c}[\varepsilon \hat{v}_B^{(A)}]_p^s \\ \hline [\varepsilon \hat{\omega}^{(S)(A)}]_p^s\end{array}\right\} \quad \left\{\begin{array}{c}\hat{v}_a \\ \hline \hat{\omega}_a\end{array}\right\} \quad \left\{\begin{array}{c}\hat{v}_1 \\ \hat{v}_2 \\ \hat{v}_3 \\ \hline \hat{\omega}_1 \\ \hat{\omega}_2 \\ \hat{\omega}_3\end{array}\right\} \quad \left\{\begin{array}{c}\varepsilon\hat{u} \\ \varepsilon\hat{v} \\ \varepsilon\hat{w} \\ \hline \varepsilon\hat{p} \\ \varepsilon\hat{q} \\ \varepsilon\hat{r}\end{array}\right\} = z_j \tag{41}$$

The McLaurin expansions up to the third term become, if all partial derivatives are continuous:

$$C_{F_\ell} = \frac{\partial C_{F_\ell}}{\partial \hat{v}_a}\hat{v}_a + \frac{\partial C_{F_\ell}}{\partial \hat{\omega}_a}\hat{\omega}_a +$$

$$+\frac{1}{2!}\left(\frac{\partial^2 C_{F_\ell}}{\partial \hat{v}_a \partial \hat{v}_b}\hat{v}_a\hat{v}_b + 2\frac{\partial^2 C_{F_\ell}}{\partial \hat{v}_a \partial \hat{\omega}_b}\hat{v}_a\hat{\omega}_b + \frac{\partial^2 C_{F_\ell}}{\partial \hat{\omega}_a \partial \hat{\omega}_b}\hat{\omega}_a\hat{\omega}_b\right) + \tag{42}$$

$$+\frac{1}{3!}\left(\frac{\partial^3 C_{F_\ell}}{\partial \hat{v}_a \partial \hat{v}_b \partial \hat{v}_c}\hat{v}_a\hat{v}_b\hat{v}_c + 3\frac{\partial^3 C_{F_\ell}}{\partial \hat{v}_a \partial \hat{v}_b \partial \hat{\omega}_c}\hat{v}_a\hat{v}_b\hat{\omega}_c + 3\frac{\partial^3 C_{F_\ell}}{\partial \hat{v}_a \partial \hat{\omega}_b \partial \hat{\omega}_c}\hat{v}_a\hat{\omega}_b\hat{\omega}_c + \frac{\partial^3 C_{F_\ell}}{\partial \hat{\omega}_a \partial \hat{\omega}_b \partial \hat{\omega}_c}\hat{\omega}_a\hat{\omega}_b\hat{\omega}_c\right)$$

$$C_{M_\ell} = \frac{\partial C_{M_\ell}}{\partial \hat{v}_a}\hat{v}_a + \frac{\partial C_{M_\ell}}{\partial \hat{\omega}_a}\hat{\omega}_a +$$

$$+\frac{1}{2!}\left(\frac{\partial^2 C_{M_\ell}}{\partial \hat{v}_a \partial \hat{v}_b}\hat{v}_a\hat{v}_b + 2\frac{\partial^2 C_{M_\ell}}{\partial \hat{v}_a \partial \hat{\omega}_b}\hat{v}_a\hat{\omega}_b + \frac{\partial^2 C_{M_\ell}}{\partial \hat{\omega}_a \partial \hat{\omega}_b}\hat{\omega}_a\hat{\omega}_b\right) + \tag{43}$$

$$+\frac{1}{3!}\left(\frac{\partial^3 C_{M_\ell}}{\partial \hat{v}_a \partial \hat{v}_b \partial \hat{v}_c}\hat{v}_a\hat{v}_b\hat{v}_c + 3\frac{\partial^3 C_{M_\ell}}{\partial \hat{v}_a \partial \hat{v}_b \partial \hat{\omega}_c}\hat{v}_a\hat{v}_b\hat{\omega}_c + 3\frac{\partial^3 C_{M_\ell}}{\partial \hat{v}_a \partial \hat{\omega}_b \partial \hat{\omega}_c}\hat{v}_a\hat{\omega}_b\hat{\omega}_c + \frac{\partial^3 C_{M_\ell}}{\partial \hat{\omega}_a \partial \hat{\omega}_b \partial \hat{\omega}_c}\hat{\omega}_a\hat{\omega}_b\hat{\omega}_c\right)$$

with $\ell, a, b, c = 1, 2, 3$ and summation convention. Equations (42) and (43) can be combined formally and written in a concise form if we use C_i and z_j as defined in Equations (40) and (41).

$$C_i = \frac{\partial C_i}{\partial z_{j_1}} z_{j_1} + \frac{1}{2!}\frac{\partial^2 C_i}{\partial z_{j_1}\partial z_{j_2}} z_{j_1} z_{j_2} + \cdots + \frac{1}{k!}\frac{\partial^k C_i}{\partial z_{j_1}\cdots\partial z_{j_k}} z_{j_1}\cdots z_{j_k} + \cdots \tag{44}$$

with

$$i = 1, 2, \cdots, 6 \;;\; j_1, j_2, \cdots, j_k = 1, 2, \cdots, 6 \;;\; k = 1, 2, \cdots$$

and summation convention.

Let us abbreviate the derivatives by

$$\frac{\partial^k C_i}{\partial z_{j_1} \cdots \partial z_{j_k}} \equiv C_i^{j_1 j_2 j_3 \cdots j_k} \tag{45}$$

Then we can give a mixed matrix and subscript notation for the first three terms in Equation (44):

$$\begin{aligned} \{C_i\} = \{C_i^{j_1}\}^T \{z_{j_1}\} + \frac{1}{2!} \{z_{j_1}\}^T \{C_i^{j_1 j_2}\} \{z_{j_2}\} + \\ + \frac{1}{3!} \left(\{z_{j_1}\}^T \left(\{C_i^{j_1 j_2 1}\} + \{C_i^{j_1 j_2 2}\} + \cdots + \{C_i^{j_1 j_2 6}\} \right) \{z_{j_2}\} \right) \{z_{j_3}\} \end{aligned} \tag{46}$$

where the indices run over the same numbers as in Equation (44) but the summation convention is replaced by matrix multiplications. The notation $\{\ \}$ is used to indicate a 6-dimensional vector space and to contrast it against the 3-dimensional Euclidean space, $[\ ]$. To give an example for Equation (45), we convert back a derivative to physically meaningful nomenclature using the notation of Equations (40) and (41).

$$C_4^{346} = \frac{\partial^3 C_4}{\partial z_3 \partial z_4 \partial z_6} = \frac{\partial^3 C_\ell}{\partial \varepsilon \hat{w} \, \partial \varepsilon \hat{p} \, \partial \varepsilon \hat{r}} \tag{47}$$

11.3 CONDITIONS FOR VANISHING DERIVATIVES

In evaluating the aerodynamics of a particular flight vehicle, important information can be derived just by investigating the conditions imposed by the symmetrical properties of the external shape. Maple and Synge (18) conducted a thorough study of the aerodynamic symmetry of projectiles. Their findings are limited to missiles, because they base their method

on the complex variable presentation of velocities and forces. In airplane and Magnus Rotor dynamics, the forces are not amenable to this treatment. Charters (19) developed a method that permits one to decide which first order derivative is zero because of symmetry conditions.

In this section we shall derive an existence theorem for derivatives of arbitrary order. It will be based on the principle of material indifference (see Section 3.1) and on the property of the reflection tensor as introduced in Section 8.1. Even though we shall use the MR to formulate the proof, the theorem applies equally as well to airplanes with mirror symmetry.

We start out with an argument similar to that in Section 11.2; i.e., the Principle of Material Indifference requires that rotating the elements that produce a physical process, is equivalent to rotating the outcome of the process. However, instead of using $[R^{(s)}_{p}{}^{(s)}_{n}]$ as the rotation tensor, we use the reflection tensor $[H]$. Specifically, let the perturbations of the aerodynamic forces, $[\varepsilon C_F]$ and $[\varepsilon C_M]$, be the physical process. Its outcome is determined by the perturbed motions that are described by the motions of the body and stability frames relative to the air frame. Equation (34), for instance, delineates the functional dependencies for the force disturbances. Now, the principle of material indifference postulates the following relationship:

$$[\varepsilon C_F\{M_\rho, R_\rho, [H][b_k], -[H][\hat{\omega}^{(B)(S)}_{\rho\,\rho}], -[H][R^{(S)(S)}_{\rho\,n}][\hat{\omega}^{(S)(A)}_{n}],$$

$$[H][R^{(S)(S)}_{\rho\,n}][\hat{\nu}^{(A)}_{B_n}]; [H][\varepsilon\hat{\nu}^{(A)}_{B}], -[H][\varepsilon\hat{\omega}^{(S)(A)}]\}] = \tag{48}$$

$$=[H][\varepsilon C_F\{M_\rho, R_\rho, [b_k], [\hat{\omega}^{(B)(S)}_{\rho\,\rho}], [R^{(S)(S)}_{\rho\,n}][\hat{\omega}^{(S)(A)}_{n}], [R^{(S)(S)}_{\rho\,n}][\hat{\nu}^{(A)}_{B_n}], [\varepsilon\hat{\nu}^{(A)}_{B}], [\varepsilon\hat{\omega}^{(S)(A)}]\}]$$

where $[b_k]$ are the base vectors of frame (B). The justification for writing the skew-symmetric tensors as axial vectors, even though they are subjected to a reflectional tensor, is given by Equation (8.5).

Let us show now that

$$[b_k] = [H][b_k] \tag{49}$$

$$[\hat{\omega}^{(B)(S)}_{\rho\,\rho}] = -[H][\hat{\omega}^{(B)(S)}_{\rho\,\rho}] \tag{50}$$

$$[R^{(S)(S)}_{\rho\,n}][\hat{\omega}^{(S)(A)}_{n}] = -[H][R^{(S)(S)}_{\rho\,n}][\hat{\omega}^{(S)(A)}_{n}] \tag{51}$$

$$[R^{(S)(S)}_{\rho\,n}][\hat{\nu}^{(A)}_{B_n}] = [H][R^{(S)(S)}_{\rho\,n}][\hat{\nu}^{(A)}_{B_n}] \tag{52}$$

Equation (49) is given by Equation (8.25). The Equations (51) and (52) follow from Equations (8.37) and (8.41), using Equation (8.12). To prove Equation (50), we take recourse to the definition of $[\hat{\omega}^{(B)(S)}_{\rho\,\rho}]$ and multiply out:

$$\begin{bmatrix} 0 \\ \frac{d}{d\hat{t}}\alpha_n \\ 0 \end{bmatrix}_p^s = - \begin{bmatrix} 1 & 0 & 0 \\ 0 & -1 & 0 \\ 0 & 0 & 1 \end{bmatrix}_p^s \begin{bmatrix} 0 \\ \frac{d}{d\hat{t}}\alpha_n \\ 0 \end{bmatrix}_p^s \tag{53}$$

Because Equations (49) through (52) hold, we do not have to show them explicitly in Equation (48). The conditions that the aerodynamics of mirror-symmetrical MR's must obey are then given for the force perturbations by Equation (48). The same reasoning leads to the conditions for the moment perturbations, where we have to recall that the moment is an axial vector. Summarizing we have:

$$[\varepsilon C_F\{[H][\varepsilon\hat{v}_B^{(A)}], -[H][\varepsilon\hat{\omega}^{(S)(A)}]\}] = [H][\varepsilon C_F\{[\varepsilon\hat{v}_B^{(A)}], [\varepsilon\hat{\omega}^{(S)(A)}]\}] \tag{54}$$

$$[\varepsilon C_M\{[H][\varepsilon\hat{v}_B^{(A)}], -[H][\varepsilon\hat{\omega}^{(S)(A)}]\}] = -[H][\varepsilon C_M\{[\varepsilon\hat{v}_B^{(A)}], [\varepsilon\hat{\omega}^{(S)(A)}]\}] \tag{55}$$

From these equations we shall formulate the conditions for vanishing derivatives expressed in the $]_p^s$-coordinate system. To arrive at a concise formulation, we use the subscript notation as defined in Equations (40) and (41). The elements of the rotation tensor $[H]$ expressed in the $]_p^s$-coordinate system will be written as h_{ij}. Using summation convention we obtain,

$$\varepsilon C_{F_\ell}\{h_{ad}\hat{v}_d, -h_{be}\hat{\omega}_e\} = h_{\ell n}\varepsilon C_{F_n}\{\hat{v}_a, \hat{\omega}_b\} \tag{56}$$

$$\varepsilon C_{M_\ell}\{h_{ad}\hat{v}_d, -h_{be}\hat{\omega}_e\} = -h_{\ell n}\varepsilon C_{M_n}\{\hat{v}_a, \hat{\omega}_b\} \tag{57}$$

To combine both equations, let us introduce the six-component vectors z_j and C_i of Equations (40) and (41). Because it can be shown that

$$\left\{ \frac{h_{ad}\ \hat{v}_d}{-h_{be}\ \hat{\omega}_e} \right\} = (-1)^{j+1} z_j \quad ; \ j = 1, \cdots, 6 \tag{58}$$

and

$$\left\{ \frac{h_{\ell n}\ \varepsilon C_{F_n}}{-h_{\ell n}\ \varepsilon C_{M_n}} \right\} = (-1)^{i+1} C_i \quad ; \ i = 1, \cdots, 6 \tag{59}$$

we can combine Equations (56) and (57) and arrive at the most concise form in which the mirror symmetry conditions can be expressed:

$$C_i \left\{ (-1)^{j+1} z_j \right\} = (-1)^{i+1} C_i \left\{ z_j \right\} \tag{60}$$

For the functional form $C_i\{z_j\}$, introduce the series expansion, Equation (44)

$$\begin{aligned} &(-1)^{j_1+1} C_i^{j_1} z_{j_1} + \frac{1}{2!}(-1)^{j_1+1}(-1)^{j_2+1} C_i^{j_1 j_2} z_{j_1} z_{j_2} + \cdots \\ &+ \frac{1}{k!}(-1)^{j_1+1} \cdots (-1)^{j_k+1} C_i^{j_1 \cdots j_k} z_{j_1} z_{j_2} \cdots z_{j_k} = (-1)^{i+1} C_i^{j_1} z_{j_1} + \\ &+ \frac{1}{2!}(-1)^{i+1} C_i^{j_1 j_2} z_{j_1} z_{j_2} + \cdots + \frac{1}{k!}(-1)^{i+1} C_i^{j_1 \cdots j_k} z_{j_1} z_{j_2} \cdots z_{j_k} \end{aligned} \tag{61}$$

Comparing terms of equal power yields

$$C_i^{j_1 j_2 \cdots j_k} = (-1)^{\sum_k j_k + k + i + 1} C_i^{j_1 j_2 \cdots j_k} \tag{62}$$

For instance, the condition for the linear terms $C_i^{j_1} = (-1)^{j_1+1+i+1} C_i^{j_1}$ can be rewritten as $C_i^{j_1}(-1)^{j_1+1} = (-1)^{i+1} C_i^{j_1}$ which is in the form of Equation (61). Equation (62) is satisfied if either the power of (-1)

is even or the derivative is zero. We summarize the results in the following theorem.

<u>THEOREM</u>: Assume that the MR possesses a mirror-symmetrical external configuration as defined in Section 8.1. Let

$$C_i^{j_1 j_2 \cdots j_k} \equiv \frac{\partial^k C_i}{\partial z_{j_1} \partial z_{j_2} \cdots \partial z_{j_k}}$$

be an aerodynamic derivative of the disturbed flight in the notation of Equations (40) and (41), where

$i = 1, 2, \ldots, 6$ indicates the force or moment component

$k = 1, 2, \ldots, 6$ indicates the order of the derivative

$j_k = 1, 2, \ldots, 6$ indicates the linear or angular velocity component of disturbance

The existence of the derivative is determined by a function $f(\gamma)$ defined as:

$f(+1) =$ derivative exists

$f(-1) =$ derivative vanishes

where $\gamma = (-1)^{\sum_k j_k + i + k + 1}$

<u>EXAMPLE</u>: Does the derivative $\dfrac{\partial^3 C_m}{\partial \varepsilon \hat{v} \, \partial \varepsilon \hat{q} \, \partial \varepsilon \hat{q}} \equiv C_5^{255}$ exist? We have:

$$i = 5, \quad k = 3, \quad j_1 = 2, \quad j_2 = 5, \quad j_3 = 5$$

$$\gamma = (-1)^{2+5+5+5+3+1} = (-1)^{21} = -1$$

therefore $f(-1)$ = derivative does not exist. The theorem is easy to apply and particularly helpful if nonlinear aerodynamic effects must be considered. It is not only applicable to MR's but also to aircraft with mirror symmetry.

11.4 DISCUSSION

The purpose of this discussion is to answer two questions: (i) why is the stability frame introduced, and (ii) why is the second perturbation method used rather than the first one (see Chapter 4)?

In airplane dynamics, the stability coordinate system is introduced to simplify the expressions for the aerodynamic forces. Because it is related to the body coordinate system by a time invariant transformation (see Etkin (16)), it is also a body coordinate system. To investigate the aerodynamics of spinning missiles, a non-rolling body coordinate system is defined, which permits the forces to be expressed in an associated aeroballistic coordinate system. This coordinate system is not a body coordinate system. In MR dynamics, the situation is similar. The attention is focused on nutational and precessional motions, and the spin degree-of-freedom is only of interest as far as it affects these motions. Therefore, as in missile dynamics, a non-rolling body coordinate system is introduced. However, because the major flight direction is normal to the spin axis, the aeroballistic coordinate system, as defined in NOLR 1241 (20), cannot be used for MR's. Instead we employ the stability coordinate system as given in the same report. The x-axis is parallel to the projection of the velocity vector on the mirror plane, and the y-axis is parallel to the

spin axis. This coordinate system suggests the introduction of the stability frame, which is given by the spin axis, the projection of the velocity vector on the mirror plane, and the center of mass, $\mathcal{B}$. The motions of the stability frame with respect to the air frame constitute the nutation and precession of an MR. We distinguish between a stability frame during reference flight $\overset{(S)}{n}$ and during perturbed flight $\overset{(S)}{p}$. Because the deviations of $\overset{(S)}{p}$ from $\overset{(S)}{n}$ are assumed to be small, a Taylor expansion can be generated in the variables $[\varepsilon \hat{\omega}_{\mathcal{B}}^{(A)}]$ and $[\varepsilon \hat{\omega}_{p}^{(S)(A)}]$, which permits the most convenient treatment of the flight dynamical problem.

Another important reason for introducing the stability frame lies in the method of measuring aerodynamic forces in a wind tunnel. The internal strain gage balance is best suited to determine the aerodynamic derivatives of a spinning MR. It is aligned with the spin axis, fixed with reference to the mass center of the MR, and directly related to the projection of the velocity vector on the mirror plane. In short, the strain gage balance constitutes the stability frame in wind tunnel measurements.

Note also that the mirror-symmetry conditions can be used to the same advantage in a stability coordinate system as in a body coordinate system. This is based on the fact that the reflection tensor of mirror symmetry has the same simple form in both coordinate systems.

Why is the second perturbation method used? Consider the aerodynamic forces acting on an MR in perturbed flight. The perturbations of the aerodynamic forces are caused by kinematic and aerodynamic effects. Varying attitude angles produce the kinematic effect by changing the direction of the aerodynamic force vectors without changing their magnitude. This

is described by an expression like $[R_p^{(S)}{}_n^{(S)}][\overline{f_a(n)}]$ (see Equation (4.14)). It can easily be evaluated. On the other side, the aerodynamic effect is difficult to determine. It is generated by the perturbation variables $[\varepsilon \hat{v}_B^{(A)}]$ and $[\varepsilon \hat{\omega}_p^{(S)(A)}]$ as they alter the fluid flow around the MR. As an example, consider the side force component acting on an MR. If the MR is rolled through ϕ, the side force changes its direction by ϕ but not its magnitude. However, an MR that alters its flight direction experiences a different magnitude of the side force because of the different fluid pattern.

Thus, we are led to define a vectorial force increment that focuses attention on the aerodynamic effect:

$$[\overline{\varepsilon f_a}] = [\overline{f_a(p)}] - [R_p^{(S)}{}_n^{(S)}][\overline{f_a(n)}] \tag{63}$$

Because it is independent of the attitude angles, its Taylor expansion assumes the simplest form, as derived in Section 11.2. In contrast, the force perturbation

$$[\overline{\delta f_a}] = [\overline{f_a(p)}] - [\overline{f_a(n)}] \tag{64}$$

is a function of the attitude angles and therefore unnecessarily complicates the Taylor expansion.

To illustrate this, we compare the perturbation $[\varepsilon C_F]_p^S$ of Equation (36) with the perturbation $[\delta C_F]_p^S$, derived in a similar fashion:

$$[\delta C_F]_p^S = \left[\frac{\partial C_F}{\partial \hat{v}_B^{(A)}}\left\{M_p, R_p, [b_k(p)]_p^S, [\hat{\omega}_p^{(B)(S)}]_p^S, [\hat{\omega}_n^{(S)(A)}]_p^S, [\hat{v}_{B_n}^{(A)}]_p^S\right\}\right]_p^S [\varepsilon \hat{v}_B^{(A)}]_p^S \tag{65}$$

$$+ \left[\frac{\partial C_F}{\partial \hat{\omega}^{(S)(A)}}\left\{ \quad \text{same dependence} \quad \right\}\right]_p^S [\varepsilon \hat{\omega}^{(S)(A)}]_p^S + \cdots$$

Because $[\hat{\omega}_{n}^{(S)(A)}]$ and $[\hat{v}_{B_n}^{(A)}]$ are known in a $]_n^S$ coordinate system, we must introduce the coordinate transformation $[T]_{pn}^{SS}$ to express them in the $]_p^S$ coordinate system, as required in Equation (65). Thus, the derivatives become a function of the angles ϕ, ψ, and $\delta\gamma$.

11.5 APPLICATIONS

So far we have not specified the components of the expansion variables $[\varepsilon\hat{v}_B^{(A)}]_p^S$ and $[\varepsilon\hat{\omega}^{(S)(A)}]_p^S$. By Assumption 3 of Section 11.1, the air frame can be used as inertial frame. Therefore, we can write

$$[\varepsilon\hat{v}_B^{(A)}]_p^S = [\varepsilon\hat{v}_B^{(I)}]_p^S \tag{66}$$

$$[\varepsilon\hat{\omega}^{(S)(A)}]_p^S = [\varepsilon\hat{\omega}^{(S)(I)}]_p^S \tag{67}$$

and thus establish the connection between the rate of change of linear and angular momentum and the formulation of the aerodynamic forces.

The linear velocity perturbation is, by definition, Equation (4.11), and in view of Equation (5.10)

$$[\varepsilon\hat{v}_B^{(I)}] = [\hat{v}_{B_p}^{(I)}] - [R_{pn}^{(S)(S)}][\hat{v}_{B_n}^{(I)}] \tag{68}$$

Expression in a $]_p^S$ coordinate system and transformation into a more convenient form results in:

$$[\varepsilon\hat{v}_B^{(I)}]_p^S = [T]_{pp}^{WS\,T}[\hat{v}_{B_p}^{(I)}]_p^W - [R_{pn}^{(S)(S)}]_p^S[T]_{pn}^{SS}[\hat{v}_{B_n}^{(I)}]_n^S \tag{69}$$

Let us substitute Equation (8.47) and the equivalent definition

$$[\hat{\mathcal{V}}_{B_p}^{(I)}]_p^w = \begin{bmatrix} \hat{V}_p \\ 0 \\ 0 \end{bmatrix}_p^w \tag{70}$$

into Equation (69) and write, in view of the notation of Equation (41)

$$[\varepsilon\hat{\mathcal{V}}_B^{(A)}]_p^s = [\varepsilon\hat{\mathcal{V}}_B^{(I)}]_p^s = \begin{bmatrix} \varepsilon\hat{u} \\ \varepsilon\hat{v} \\ \varepsilon\hat{w} \end{bmatrix}_p^s = \begin{bmatrix} \delta\hat{V} \\ \hat{V}_p\beta \\ 0 \end{bmatrix}_p^s \tag{71}$$

where

$$\delta\hat{V} = \frac{V_p - V_r}{V_r} \; ; \; \hat{V}_p = \frac{V_p}{V_r} \; ; \; \hat{V}_r = \frac{V_r}{V_r} = 1 \tag{72}$$

The relationship with the dynamic-normalized velocity perturbation is obtained from Equation (5.20):

$$[\overline{\varepsilon\mathcal{V}_B^{(I)}}]_p^s = \bar{V}_r[\varepsilon\hat{\mathcal{V}}_B^{(I)}]_p^s = \bar{V}_r\begin{bmatrix} \varepsilon\hat{u} \\ \varepsilon\hat{v} \\ \varepsilon\hat{w} \end{bmatrix}_p^s = \begin{bmatrix} \overline{\delta V} \\ \bar{V}_p\beta \\ 0 \end{bmatrix}_p^s \tag{73}$$

where

$$\overline{\delta V} = \frac{\delta V}{V_{ss}} \; ; \; \bar{V}_p = \frac{V_p}{V_{ss}} \; ; \; \bar{V}_r = \frac{V_r}{V_{ss}} \tag{74}$$

Therefore, the velocity components are:

$$\begin{bmatrix} \varepsilon\hat{u} \\ \varepsilon\hat{v} \\ \varepsilon\hat{w} \end{bmatrix}_p^s = \begin{bmatrix} \overline{\delta V}/\bar{V}_r \\ (\bar{V}_p/\bar{V}_r)\beta \\ 0 \end{bmatrix}_p^s = \begin{bmatrix} \overline{\delta V}/\bar{V}_r \\ \beta \\ 0 \end{bmatrix}_p^s = \begin{bmatrix} \delta\hat{V} \\ \beta \\ 0 \end{bmatrix}_p^s \tag{75}$$

because we can set, according to Assumption 2 of Chapter 9:

$$\frac{\bar{V}_p}{\bar{V}_r} = \frac{V_p}{V_{ss}}\frac{V_{ss}}{V_r} \approx 1 \tag{76}$$

The angular velocity perturbation is, by definition, Equation (4.13), and in view of Equation (5.13):

$$[\varepsilon\hat{\omega}^{(s)(I)}] = [\hat{\omega}_p^{(s)(I)}] - [R_p^{(s)}{}_n^{(s)}][\hat{\omega}_n^{(s)(I)}] \tag{77}$$

with V_n / ℓ as the aero-normalizing unit. This can be replaced by $[\hat{\omega}_p^{(s)}{}_n^{(s)}]$, as shown in Simplification 1 of Section 10.1. Using Equation (7.5) and in view of the notation of Equation (43), we obtain

$$[\varepsilon\hat{\omega}^{(s)(A)}]_p^s = [\varepsilon\hat{\omega}^{(s)(I)}]_p^s = \begin{bmatrix} \varepsilon\hat{p} \\ \varepsilon\hat{q} \\ \varepsilon\hat{r} \end{bmatrix}_p^s = [\hat{\omega}_p^{(s)}{}_n^{(s)}]_p^s = \begin{bmatrix} \hat{\dot{\phi}} \\ \phi\hat{\dot{\psi}} \\ \hat{\dot{\psi}} \end{bmatrix}_p^s \tag{78}$$

where

$$\hat{\dot{\phi}} = \frac{\ell}{V_n}\frac{d}{dt}\phi \quad ; \quad \hat{\dot{\psi}} = \frac{\ell}{V_n}\frac{d}{dt}\psi \tag{79}$$

The relationship with the dynamic-normalized velocity perturbation is obtained from Equation (5.23):

$$[\overline{\varepsilon\omega^{(s)(A)}}]_p^s = \mu\bar{V}_n[\varepsilon\hat{\omega}^{(s)(A)}]_p^s = \mu\bar{V}_n\begin{bmatrix} \varepsilon\hat{p} \\ \varepsilon\hat{q} \\ \varepsilon\hat{r} \end{bmatrix}_p^s \tag{80}$$

where

$$[\overline{\varepsilon\omega^{(s)(A)}}]_p^s \approx [\overline{\omega_p^{(s)}{}_n^{(s)}}]_p^s = \begin{bmatrix} \mathring{\phi} \\ \phi\mathring{\psi} \\ \mathring{\psi} \end{bmatrix}_p^s \tag{81}$$

and

$$\mathring{\phi} = \tau\frac{d}{dt}\phi \quad ; \quad \mathring{\psi} = \tau\frac{d}{dt}\psi \tag{82}$$

Therefore the relationship is:

$$\begin{bmatrix} \varepsilon\hat{p} \\ \varepsilon\hat{q} \\ \varepsilon\hat{r} \end{bmatrix}^s_p = \begin{bmatrix} \mathring{\Phi}/\mu\bar{V} \\ \Phi\mathring{\psi}/\mu\bar{V} \\ \mathring{\psi}/\mu\bar{V} \end{bmatrix}^s_p = \begin{bmatrix} \hat{\dot{\Phi}} \\ \Phi\hat{\dot{\psi}} \\ \hat{\dot{\psi}} \end{bmatrix}^s_p \tag{83}$$

Now we shall use the theorem of Section 11.3 to write out the derivatives up to the third order for the three coefficients C_y, C_ℓ, and C_n. These coefficients are particularly important for the further development of the theory. Since the i's in C_i are even numbers for all three coefficients, the theorem has the same form. A schematic summary is given in Table 11.1, based on the matrix notation of Equation (46). The expansion of the three coefficients up to third order consists of 774 derivatives. This number is cut in half by the theorem and further reduced, because pairs of the mixed derivatives are equal. Moreover, some of the derivatives must be zero because, by the definition of the stability coordinate system, $\varepsilon\hat{w} = 0$. However, there are still 84 derivatives to be evaluated.

The determination of these derivatives is probably the most difficult task in Magnus rotor dynamics. Some information can be found in Brunk (1,2) and Bustamante (7). However, much research is still to be done in this field. A combination of engineering intuition, experimental results, and mathematical analysis must be employed to arrive at quantitative values. The final verification will come through free flight tests.

Here, we do not intend to treat this area of Magnus Rotor Dynamics exhaustively. We shall rather concentrate on some aspects that are required for the latter part of this report.

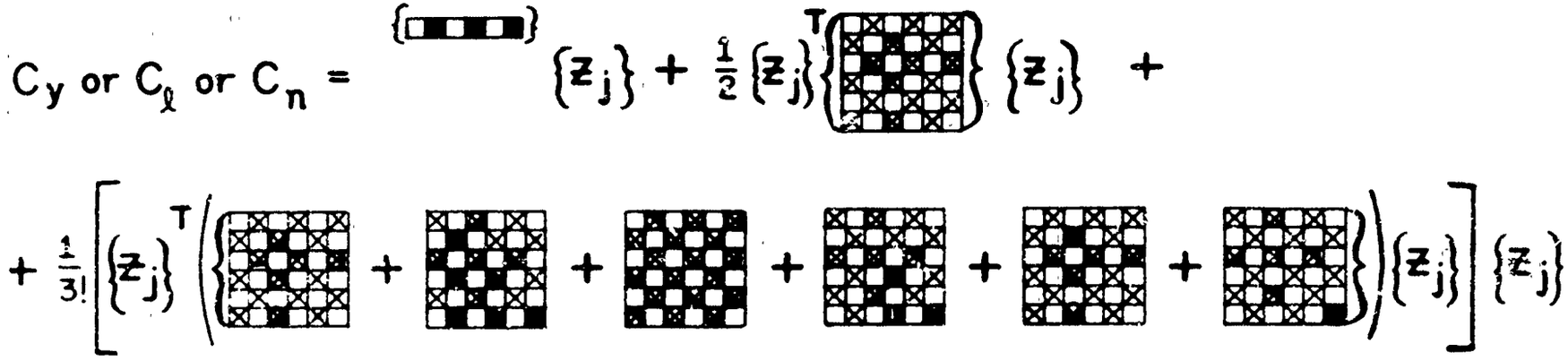

- ⊠ DERIVATIVE EXISTS ACCORDING TO EXISTENCE THEOREM
- ⊠ DERIVATIVE IS ZERO BECAUSE $\varepsilon \hat{w} = 0$
- ■ DERIVATIVES TO BE EVALUATED

MATRICES ARE SYMMETRIC

FIGURE 11.1 AERODYNAMIC DERIVATIVES

To begin with, we want to show that the dependence of the coefficients C_y, C_ℓ, and C_n on $\varepsilon\hat{u}$ and $\varepsilon\hat{q}$ can be neglected. Equation (75) yields $\varepsilon\hat{u} = \delta\hat{V}$; i.e., $\varepsilon\hat{u}$ is the perturbation of the flight velocity. But the flight velocity appears only in terms of Reynolds number and Mach number in the coefficients, and small changes of the Reynolds number and Mach number have a negligible effect on the coefficients. By Equation (83), $\varepsilon\hat{q} = \phi\hat{\dot{\psi}}$. Because of the small angle assumption, $\varepsilon\hat{q}$ is small compared with $\varepsilon\hat{p}$ and $\varepsilon\hat{r}$, and its influence on the coefficients can therefore be disregarded. This simplification means that, in the terminology of Chapter 12, the lateral aerodynamics are decoupled from the longitudinal motions. Thus, the number of derivatives to be evaluated is further reduced. The remaining ones are marked by a black square in Table 11.1. They are summarized in Table 11.2 in the same arrangement. We shorten the list further by two reasonable arguments:

<u>ARGUMENT 1</u>: The side force does not depend on the $\hat{p}$ and $\hat{r}$ angular velocities.

<u>ARGUMENT 2</u>: The gyroscopic coupling moment is much greater than the comparable aerodynamic coupling.

The derivatives thus deleted are marked by a corresponding sign in Table 11.2. Fourteen of them remain to be evaluated. According to Equation (39), they are still functions of M_R, R_R, α_p, and $\hat{\omega}_R$. C_{y_β} and $C_{y_{\beta^3}}$ are the linear and cubic side-force derivatives. They are mainly due to the drag force caused by the component of the flight velocity along the spin axis. Therefore, C_{y_β} is usually negative and decreases with the increasing size of the end plates. For MR's without end plates, $C_{y_{\beta^3}}$ can

$$C_{y_\beta} \quad \cancel{C_{y_{\hat{p}}}} \quad \cancel{C_{y_{\hat{r}}}} \quad C_{y_{\beta^3}}$$

$$\cancel{C_{y_{\beta^2\hat{p}}}} \quad \cancel{C_{y_{\beta\hat{p}^2}}} \quad \cancel{C_{y_{\hat{p}^3}}}$$

$$\cancel{C_{y_{\beta^2\hat{r}}}} \quad \cancel{C_{y_{\beta\hat{p}\hat{r}}}} \quad \cancel{C_{y_{\beta\hat{r}^2}}} \quad \cancel{C_{y_{\hat{p}^2\hat{r}}}} \quad \cancel{C_{y_{\hat{p}\hat{r}^2}}} \quad \cancel{C_{y_{\hat{r}^3}}}$$

$$C_{l_\beta} \quad C_{l_{\hat{p}}} \quad \cancel{C_{l_{\hat{r}}}} \quad C_{l_{\beta^3}}$$

$$C_{l_{\beta^2\hat{p}}} \quad C_{l_{\beta\hat{p}^2}} \quad C_{l_{\hat{p}^3}}$$

$$\cancel{C_{l_{\beta^2\hat{r}}}} \quad \cancel{C_{l_{\beta\hat{p}\hat{r}}}} \quad \cancel{C_{l_{\beta\hat{r}^2}}} \quad \cancel{C_{l_{\hat{p}^2\hat{r}}}} \quad \cancel{C_{l_{\hat{p}\hat{r}^2}}} \quad \cancel{C_{l_{\hat{r}^3}}}$$

$$C_{n_\beta} \quad \cancel{C_{n_{\hat{p}}}} \quad C_{n_{\hat{r}}} \quad C_{n_{\beta^3}}$$

$$\cancel{C_{n_{\beta^2\hat{p}}}} \quad \cancel{C_{n_{\beta\hat{p}^2}}} \quad \cancel{C_{n_{\hat{p}^3}}}$$

$$C_{n_{\beta^2\hat{r}}} \quad \cancel{C_{n_{\beta\hat{p}\hat{r}}}} \quad C_{n_{\beta\hat{r}^2}} \quad \cancel{C_{n_{\hat{p}^2\hat{r}}}} \quad \cancel{C_{n_{\hat{p}\hat{r}^2}}} \quad C_{n_{\hat{r}^3}}$$

/ Neglected because of Argument 1.

\ Neglected because of Argument 2.

TABLE 11.2 LATERAL DERIVATIVES

become important. The dependence of both derivatives on $\hat{\omega}_R$ is weak and is therefore dropped in most applications.

The rolling derivatives C_{ℓ_β} and $C_{\ell_{\beta^3}}$ are referred to as the linear and cubic Magnus moment derivatives. They are caused by a shift of the Magnus lift force along the spin axis due to the sideslip angle β. Because the Magnus lift is approximately proportional to the tip speed ratio, $\hat{\omega}_R$, the Magnus moment derivatives will also strongly depend on $\hat{\omega}_R$. To express this dependence explicitly, we expand the derivatives in power series of $\hat{\omega}_R$. For the linear Magnus moment derivative, we have, for instance:

$$C_{\ell_\beta} = C_{\ell_{\beta_0}}\{M_R, R_R, \alpha_p\} + C_{\ell_{\hat{\omega}_\beta}}\{M_R, R_R, \alpha_p\}\,\hat{\omega}_R + \cdots \tag{84}$$

If $\hat{\omega}_R = 0$, the Magnus lift is zero. Consequently, the constant term in the expansion can be neglected. Because of insufficient wind tunnel data, the linear term is retained only. Thus, the linear coefficients of the power series, $C_{\ell_{\hat{\omega}_\beta}}$ and $C_{\ell_{\hat{\omega}_{\beta^3}}}$, are usually meant by Magnus moment derivatives. They are important for the stability of the nutation mode and can, in particular, cause a nutation limit cycle.

The yawing moment derivatives C_{n_β} and $C_{n_{\beta^3}}$ are generated by the shift of the drag force along the spin axis. In the first approximation, they are independent of $\hat{\omega}_R$ because the drag force is independent of $\hat{\omega}_R$. They mostly affect the stability of the undulation mode.

The aerodynamic damping is expressed in the derivatives $C_{\ell_{\hat{p}}}$, $C_{\ell_{\hat{p}^3}}$, $C_{n_{\hat{R}}}$, and $C_{n_{\hat{R}^3}}$. $C_{\ell_{\hat{p}}}$ and $C_{n_{\hat{R}}}$ are always negative. In the stability analysis, only their sums, $C_{\ell_{\hat{p}}} + C_{n_{\hat{R}}}$ and $C_{\ell_{\hat{p}^3}} + C_{n_{\hat{R}^3}}$, have to be known.

These derivatives cannot be measured in conventional wind tunnels. They require either a curved working section as in the old NACA Langley Stability Tunnel or some free-flight simulations.

The remaining mixed derivatives $C_{l_{\beta^2\hat{p}}}$, $C_{l_{\beta\hat{p}^2}}$, $C_{n_{\beta^2\hat{r}}}$, and $C_{n_{\beta\hat{r}^2}}$ express the aerodynamic damping of a yawed MR. Again, the rolling moment derivatives are expanded in $\hat{\omega}_r$, and the linear terms are written as $C_{l_{\hat{\omega}\beta^2\hat{p}}}$ and $C_{l_{\hat{\omega}\beta\hat{p}^2}}$. No experimental data have been obtained on these derivatives.

For further reference, let us write out some components of Equations (24) and (25) using the derivatives of Table 11.2 and the format of Table 11.1. Equations (75) and (83) introduce the dynamic-normalized variables.

$$[\overline{\varepsilon f_{a_2}}]_p^s = \bar{V}_r^2 \left(C_{y_\beta} \beta + \frac{1}{6} C_{y_{\beta^3}} \beta^3 \right) \tag{85}$$

$$\begin{aligned}[\overline{\varepsilon m_{a_1}}]_p^s = \frac{\bar{V}_r^2}{\mu} \Big\{ & C_{l_{\hat{\omega}\beta}} \hat{\omega}_r \beta + \frac{1}{\mu \bar{V}_r} C_{l_{\hat{p}}} \dot{\phi} + \frac{1}{6} C_{l_{\hat{\omega}\beta^3}} \hat{\omega}_r \beta^3 + \\ & + \frac{1}{6\mu\bar{V}_r} C_{l_{\hat{\omega}\beta^2\hat{p}}} \beta^2 \dot{\phi} + \frac{1}{6(\mu\bar{V}_r)^2} C_{l_{\hat{\omega}\beta\hat{p}^2}} \beta \dot{\phi}^2 + \frac{1}{6(\mu\bar{V}_r)^3} C_{l_{\hat{p}^3}} \dot{\phi}^3 \Big\}\end{aligned} \tag{86}$$

$$\begin{aligned}[\overline{\varepsilon m_{a_3}}]_p^s = \frac{\bar{V}_r^2}{\mu} \Big\{ & C_{n_\beta} \beta + \frac{1}{\mu \bar{V}_r} C_{n_{\hat{r}}} \dot{\psi} + \frac{1}{6} C_{n_{\beta^3}} \beta^3 + \\ & + \frac{1}{6\mu\bar{V}_r} C_{n_{\beta^2\hat{r}}} \beta^2 \dot{\psi} + \frac{1}{6(\mu\bar{V}_r)^2} C_{n_{\beta\hat{r}^2}} \beta \dot{\psi}^2 + \frac{1}{6(\mu\bar{V}_r)^3} C_{n_{\hat{r}^3}} \dot{\psi}^3 \Big\}\end{aligned} \tag{87}$$

12. EQUATIONS OF MOTION

Thus far, all the required details have been derived for the perturbation equations of an MR in planar glide phase. What is left is to investigate the possibility of separating the equations into lateral and longitudinal perturbation equations and to eliminate the dependence on the rapidly rotating angle of attack.

12.1 LATERAL PERTURBATION EQUATIONS

The perturbation equations are given by Equations (9.18) and (10.50). We observe that the second component of Equation (9.18) and the first and third components of Equation (10.50) can be evaluated without knowing the solution of the remaining three components, provided that the aerodynamic forces can be separated accordingly. Borrowing from airplane terminology, we call this set the lateral perturbation equations and the remaining three equations the longitudinal perturbation equations. Notice that the lateral equations are decoupled from the longitudinal equations but the converse is not true. The lateral perturbation equations are the side force, rolling, and yawing equations, with the side slip angle β, roll angle ϕ, and yaw angle ψ as the perturbations. The longitudinal perturbation equations consist of the two flight-path equations and the pitch equation, with the increments of the flight speed $\delta\bar{V}$, glide angle $\delta\gamma$, and the angle of attack $\delta\alpha$ as the perturbations.

Now we want to justify the separation of the aerodynamic forces into the same two groups so that the lateral forces can be evaluated without

knowing the longitudinal motions. Equations (11.85) through (11.87) provide part of the justification. They do not depend on the variables $\delta\gamma$ and $\delta\bar{V}$. But the aerodynamic derivatives do depend on $\alpha_p = \alpha_R + \delta\alpha$ implicitly, as seen from Equation (11.84). However, in Section 12.3 we shall show that the dependency on α_p can be averaged over one revolution resulting in a zero net effect. Therefore, the lateral equations are entirely decoupled from the longitudinal equations. They are summarized in Table 12.1 together with the equations of the reference flight.

<u>DISCUSSION</u>: The equations of motion are presented in their dynamic-normalized form (see Chapter 5). The crossbar indicates that the quantity is measured in dynamic-normalized units, and the circle stands for the time derivative with respect to the dynamic-normalized time $\bar{t}$.

Equations (1) through (3) are Equations (8.57) through (8.59). The first equation is the force equation tangent to the flight path, while the second is the normal force equation. The moment equation about the spin axis is given by the third equation. There are two major assumptions that must be satisfied:

1. The MR is mirror symmetrical with respect to its external geometry and its mass distribution.

2. The rate of change of glide angle is much smaller than the rate of change of the angle of attack; i.e., $\mathring{\gamma}_R << \mathring{\alpha}_R$

Furthermore, the condition $\bar{V}_R \neq 0$ must be imposed to keep the coefficients finite. Otherwise, the equations must be revised. The aerodynamic coefficients are still a function of Mach number M_R, Reynolds number R_R, and angle of attack α_R. If the initial flight speed of a particular problem does not reach into the compressible regime, and if the air density

REFERENCE FLIGHT

1) $\dot{\bar{V}}_R = -C_D \bar{V}_R^2 - \frac{\tau g}{V_{ss}} \sin\gamma_R$

2) $\dot{\gamma}_R = \frac{C_{L\hat{\omega}}}{\mu} \bar{\omega}_R - \frac{\tau g}{V_{ss}\bar{V}_R} \cos\gamma_R$

3) $\dot{\bar{\omega}}_R = \frac{C_{M\alpha}}{\mu \bar{I}_y} \bar{V}_R^2 + \frac{C_{M_d\hat{\omega}}}{\mu^2 \bar{I}_y} \bar{V}_R \bar{\omega}_R$

DEPENDENT VARIABLES

$\bar{V}_R$	flight speed
γ_R	glide angle
$\bar{\omega}_R$	spin rate
β	sideslip angle
ϕ	roll angle
ψ	yaw angle

CONSTANT PARAMETERS

g	gravitational constant
τ	time parameter
μ	mass parameter
$\bar{I}_y$	spin moment-of-inertia
$\bar{I}$	transverse moment-of-inertia
V_{ss}	steady-state flight speed

LATERAL PERTURBATIONS

$$
\begin{array}{l}
4)\\ 5)\\ 6)\\ 7)\\ 8)
\end{array}
\begin{bmatrix} \dot{\beta} \\ \dot{\hat{\phi}} \\ \dot{\hat{\psi}} \\ \dot{\phi} \\ \dot{\psi} \end{bmatrix}
=
\begin{bmatrix}
-\frac{\dot{\bar{V}}_R}{\bar{V}_R} + \bar{V}_R C_{y_\beta} & 0 & -1 & \frac{\tau g \cos\gamma_R}{\bar{V}_R V_{ss}} & \frac{\tau g \sin\gamma_R}{\bar{V}_R V_{ss}} \\
\frac{\bar{V}_R \bar{\omega}_R}{\mu^2 \bar{I}} C_{l_{\hat{\omega}\beta}} & \frac{\bar{V}_R}{\mu^2 \bar{I}} C_{l_{\hat{p}}} & \frac{\bar{I}_y \bar{\omega}_R}{\bar{I}} & 0 & 0 \\
\frac{\bar{V}_R^2}{\mu \bar{I}} C_{n_\beta} & -\frac{\bar{I}_y \bar{\omega}_R}{\bar{I}} & \frac{\bar{V}_R}{\mu^2 \bar{I}} C_{n_{\hat{r}}} & 0 & 0 \\
0 & 1 & 0 & 0 & 0 \\
0 & 0 & 1 & 0 & 0
\end{bmatrix}
\begin{bmatrix} \beta \\ \hat{\phi} \\ \hat{\psi} \\ \phi \\ \psi \end{bmatrix}
+
\begin{bmatrix}
\frac{1}{6} \bar{V}_R C_{y_{\gamma\beta^3}} \beta^3 \\
\frac{\bar{V}_R \bar{\omega}_R}{6\mu^2 \bar{I}} C_{l_{\hat{\omega}\beta^3}} \beta^3 + \frac{1}{6\mu^4 \bar{I} \bar{V}_R} C_{l_{\hat{p}^3}} \dot{\hat{\phi}}^3 + \frac{\bar{\omega}_R}{6\mu^3 \bar{I}} C_{l_{\hat{\omega}\beta^2\hat{p}}} \beta^2 \dot{\hat{\phi}} + \frac{\bar{\omega}_R}{6\mu^4 \bar{I} \bar{V}_R} C_{l_{\hat{\omega}\beta\hat{p}^2}} \beta \dot{\hat{\phi}}^2 \\
\frac{\bar{V}_R^2}{6\mu \bar{I}} C_{n_{\beta^3}} \beta^3 + \frac{1}{6\mu^4 \bar{I} \bar{V}_R} C_{n_{\hat{r}^3}} \dot{\hat{\psi}}^3 + \frac{\bar{V}_R}{6\mu^2 \bar{I}} C_{n_{\beta^2\hat{r}}} \beta^2 \dot{\hat{\psi}} + \frac{1}{6\mu^3 \bar{I}} C_{n_{\beta\hat{r}^2}} \beta \dot{\hat{\psi}}^2 \\
0 \\
0
\end{bmatrix}
$$

TABLE 12.1 EQUATIONS OF MOTION

changes only little during the flight, the aerodynamic coefficients can be considered to be a function of α_R only. In Section 12.2, we will show that even this dependence can be eliminated and that, under those conditions, the aerodynamic coefficients can be considered to be constants. The equations of the reference flight are highly nonlinear and cannot be simplified further. They must be solved by computer.

Equations (4) through (8) describe the lateral perturbations of an MR during the planar glide phase. They are referred to the coordinate system $\mathcal{J}_p^s$ associated with the stability frame $\overset{(s)}{p}$ of the perturbed motions. Equation (4) is the force equation along the spin axis. Its first term on the right includes the inertial force component $-\dot{\bar{V}}/\bar{V}_R$ caused by the acceleration of the mass during the reference flight. The last two linear terms are the gravitational contributions. The moment Equation (5) is similar in structure to Equation (6). The first terms on the right are the aerodynamic moments about the roll axis $X_1{}_p^s$ and the yaw axis $X_3{}_p^s$, respectively. The following two terms are the aerodynamic damping and the gyroscopic coupling and vice versa, respectively. All nonlinear aerodynamic contributions are collected in the right matrix. In addition to the two assumptions already stated in the previous paragraph, the lateral perturbation equations are valid under the following major conditions:

3. The angles β, $\dot{\Phi}$, Ψ remain small throughout the flight.

4. The aerodynamic forces depend on the linear and angular velocities only and not on the accelerations.

The small-angle assumption means that the sine of an angle is replaced by the angle itself and the cosine is set equal to one. For an engineering

analysis, angles up to 20 degree can be admitted. This causes errors of 2% and 6%, in the sine and cosine, respectively, at 20 degree. One of the consequences of this assumption is that the nonlinear behavior of the aerodynamic forces must occur at small angles in order to be correctly analyzed by these equations.

The aerodynamic coefficients are functions of M_R, R_R, and α_p. As in the case of the reference flight, we can gain much information by limiting ourselves to the dependence on α_p alone. And again, in Section 12.3, we shall show that this dependence can be neglected if certain conditions are satisfied. Also, the value $\bar{V}_R = 0$ must be excluded in order that the coefficients are finite. In Table 12.1, the perturbation equations are separated into linear and nonlinear parts. If we neglect the nonlinear part, and if we consider the steady-state glide phase only, the perturbation equations are linear differential equations with constant coefficients and therefore easy to solve. If we consider the transient glide phase, the equations remain linear but become nonautonomous. Adding the nonlinear aerodynamic terms makes the equations nonlinear and nonautonomous; i.e., for solutions, we have to rely on a digital computer.

12.2 AVERAGING THE REFERENCE EQUATIONS

In this section we shall give a mathematical justification for the intuitive reasoning that the effect of α_R on the reference flight can be averaged over one revolution, provided that α_R changes rapidly enough. The method of averaging, as developed by Bogoliubov and Mitropolsky (21),

will be employed. In particular, we refer to the "Case of the Rapidly Rotating Phase", as outlined in Chapter 5, Paragraph 25 of their book, and assume that the reader is familiar with this part.

The underlying idea is to introduce a transformation composed of the averaged state and small vibrations due to α_R. This leads to the averaged equations of motion that are independent of α_R. The vibrations are described by a power series in terms of a small parameter $1/\lambda$, and, thus, the averaged equations will have the same power series expansion. The search for such a large parameter λ requires a slight change of the equations of the reference flight. In view of Equation (5.23) and Equation (5.13), we obtain

$$\bar{\omega}_R = \mu \bar{V}_R \hat{\omega}_R = \mu \bar{V}_R \frac{\omega_R \ell}{V_R} \frac{V_{SS}}{V_{SS}} \frac{\omega_{SS}}{\omega_{SS}} = \mu \hat{\omega}_{SS} \frac{\omega_R}{\omega_{SS}} \tag{9}$$

and define

$$\lambda = \mu \hat{\omega}_{SS} \tag{10}$$

For common MR's, λ is a large parameter compared with the circular frequencies of the solution, because $\hat{\omega}_{SS}$ is of the order of one, and μ, the density ratio between the MR and air, is of the order of 10^3. Representative circular frequencies of the solution are of the order of 10^{-1}. Substitute Equation (9) into Equations (1), (2), and (3):

$$\mathring{\bar{V}}_R = -C_D \bar{V}_R^2 - \frac{\tau g}{V_{SS}} \sin \gamma_R \tag{11}$$

$$\mathring{\gamma}_R = C_{L\hat{\omega}} \hat{\omega}_{SS} \frac{\omega_R}{\omega_{SS}} - \frac{\tau g}{V_{SS} \bar{V}_R} \cos \gamma_R \tag{12}$$

$$\frac{d}{d\bar{t}}\left(\frac{\omega_n}{\omega_{ss}}\right) = \frac{C_{M_\alpha}}{\mu^2 \bar{I}_y \hat{\omega}_{ss}} \bar{V}_n^2 + \frac{C_{M_{d\hat{\omega}}}}{\mu^2 \bar{I}_y} \bar{V}_n \frac{\omega_n}{\omega_{ss}} \tag{13}$$

with

$$\frac{d}{d\bar{t}} \alpha_n = \mu \frac{\omega_n}{\omega_{ss}} \tag{14}$$

The new variable is $\frac{\omega_n}{\omega_{ss}}$, the percentage of the spin rate relative to its steady-state value. We abbreviate these equations to obtain a corresponding form used in Ref. 21:

$$\frac{dy_k}{d\bar{t}} = Y_k(\alpha_n, y_1, y_2, y_3) \quad ; \; k = 1,2,3 \tag{15}$$

$$\frac{d\alpha_n}{d\bar{t}} = \lambda y_3 \tag{16}$$

where the state vector is:

$$\begin{bmatrix} y_1 \\ y_2 \\ y_3 \end{bmatrix} = \begin{bmatrix} \bar{V}_n \\ \gamma_n \\ \omega_n/\omega_{ss} \end{bmatrix} \tag{17}$$

According to page 417 of Ref. 21, the transformations

$$y_k = \tilde{y}_k + \frac{1}{\lambda} \sum_{n=1}^{\infty} \frac{1}{n\tilde{y}_3} \left\{ -G_{k,n} \cos n\tilde{\alpha}_n + F_{k,n} \sin n\tilde{\alpha}_n \right\} + O\left\{\frac{1}{\lambda^2}\right\} \tag{18}$$

$$\alpha_n = \tilde{\alpha}_n - \frac{1}{\lambda} \sum_{n=1}^{\infty} \frac{1}{n^2 \tilde{y}_3^2} \left\{ F_{3,n} \cos n\tilde{\alpha}_n + G_{3,n} \sin n\tilde{\alpha}_n \right\} + O\left\{\frac{1}{\lambda^2}\right\} \tag{19}$$

generate the averaged equations:

$$\frac{d\tilde{y}_k}{d\bar{t}} = Y_{k,0} - \frac{1}{\lambda}\sum_{\substack{n,q \\ n\neq 0}}^{\infty} \frac{1}{2n\tilde{y}_3}\left\{\frac{\partial F_{k,n}}{\partial \tilde{y}_q} G_{q,n} - \frac{\partial G_{k,n}}{\partial \tilde{y}_q} F_{q,n}\right\} + \tag{20}$$

$$+\frac{1}{\lambda}\sum_{n=1}^{\infty}\frac{1}{2\tilde{y}_3^2 n}\left\{F_{k,n}G_{3,n} - G_{k,n}F_{3,n}\right\} + \mathcal{O}\left\{\frac{1}{\lambda^2}\right\}$$

$$\frac{d\tilde{\alpha}_n}{d\bar{t}} = \lambda\tilde{y}_3 + \mathcal{O}\left\{\frac{1}{\lambda^2}\right\} \tag{21}$$

where the tilde denotes the averaged variable. $Y_{k,0}$ is the first term in the Fourier expansion:

$$Y_k = Y_{k,0} + \sum_{n=1}^{\infty}\left\{F_{k,n}\cos n\tilde{\alpha}_n + G_{k,n}\sin n\tilde{\alpha}_n\right\} \tag{22}$$

with the Fourier coefficients still being a function of the $\tilde{y}_k$'s . In order that the second terms on the right of the Equations (18), (19), and (20) remain small, we must put a restriction on $\tilde{y}_3 = \frac{\tilde{\omega}_n}{\omega_{ss}}$. We require that $\tilde{y}_3 \geq 0.1$; i.e., that the spin rate never drops below 10% of its steady state value. Now, because λ is a large value (10^3) and the terms of $Y_{k,0}$ are of the order of one, it suffices to let the zeroth order approximation

$$\frac{d\tilde{y}_k}{d\bar{t}} = Y_{k,0}(\tilde{y}_i) \tag{23}$$

represent the equations of motion of the reference flight. The error committed is given by Equation (18).

12.3 AVERAGING THE LATERAL PERTURBATION EQUATIONS

We would like to use the same averaging method to eliminate the dependence of the lateral perturbation equations from α_p. However, the method given in Ref. 21 is only applicable to autonomous differential equations, whereas the coefficients of the lateral perturbation equations depend on the state of the reference equation; i.e., we have to deal with a nonautonomous case. Fortunately, the coefficients change slowly in time compared with α_p so that the averaging method can be extended to the lateral perturbation equations. We shall outline the procedure below, again closely following the book by Bogoliubov and Mitropolsky (21).

The lateral perturbation Equations (4) through (8) will be abbreviated as:

$$\frac{dx_k}{d\bar{t}} = X_k(\alpha_p, x_i, \bar{t}) \quad ; \; k = 1, \cdots, 5 \; ; \; i = 1, \cdots, 5 \tag{24}$$

Notice that the rapidly rotating phase α_p is different from the previous case. We therefore cannot use Equation (14) directly. But we can still take the same large parameter $\lambda = \mu \hat{\omega}_{ss}$ if we include a correction term $A(x_k, \bar{t})$. Thus, we form

$$\frac{d\alpha_p}{d\bar{t}} = \lambda \frac{\omega_n(\bar{t})}{\omega_{ss}} + A(x_k, \bar{t}) \tag{25}$$

where $A(x_k, \bar{t})$ is small compared with $\lambda \dfrac{\omega_n(\bar{t})}{\omega_{ss}}$ by the Assumption of Section 10.2.

As in Ref. 21, Equation (25.2), let us introduce the transformations

$$x_k = \tilde{x}_k + \sum_{n=1}^{\infty} \frac{1}{\lambda^n} \xi_k^{(n)}(\tilde{\alpha}_p, \tilde{x}_i, \bar{t}) \tag{26}$$

$$\alpha_p = \tilde{\alpha}_p + \sum_{n=1}^{\infty} \frac{1}{\lambda^n} U_n(\tilde{\alpha}_p, \tilde{x}_i, \bar{t}) \tag{27}$$

with the difference that the coefficients of the power series are also time-dependent. They will reduce Equations (24) and (25) to the form

$$\frac{d\tilde{x}_k}{d\bar{t}} = \sum_{n=0}^{\infty} \frac{1}{\lambda^n} X_k^{(n)}(\tilde{x}_i, \bar{t}) \tag{28}$$

$$\frac{d\tilde{\alpha}_p}{d\bar{t}} = \lambda \frac{\omega_r(\bar{t})}{\omega_{ss}} + \sum_{n=0}^{\infty} \frac{1}{\lambda^n} \Omega_n(\tilde{x}_i, \bar{t}) \tag{29}$$

Substitute Equations (26) and (27) into Equation (24):

$$\begin{aligned} &\frac{d\tilde{x}_k}{d\bar{t}} + \frac{1}{\lambda}\left(\frac{\partial \xi_k^{(1)}}{\partial \tilde{\alpha}_p}\frac{d\tilde{\alpha}_p}{d\bar{t}} + \frac{\partial \xi_k^{(1)}}{\partial \bar{t}} + \frac{\partial \xi_k^{(1)}}{\partial \tilde{x}_q}\frac{d\tilde{x}_q}{d\bar{t}}\right) + \frac{1}{\lambda^2}\left(\frac{\partial \xi_k^{(2)}}{\partial \tilde{\alpha}_p}\frac{d\tilde{\alpha}_p}{d\bar{t}} + \right. \\ &\left. + \frac{\partial \xi_k^{(2)}}{\partial \tilde{x}_q}\frac{d\tilde{x}_q}{d\bar{t}} + \frac{\partial \xi_k^{(2)}}{\partial \bar{t}}\right) = X_k\left(\tilde{\alpha}_p + \frac{1}{\lambda}U_1(\tilde{\alpha}_p, \tilde{x}_i, \bar{t}) + \cdots + \tilde{x}_j + \frac{1}{\lambda}\xi_j^{(1)}(\tilde{\alpha}_p, \tilde{x}_i, \bar{t}) + \cdots, \bar{t}\right) \end{aligned} \tag{30}$$

Then, similarly insert Equations (26) and (27) into Equation (25):

$$\begin{aligned} &\frac{d\tilde{\alpha}_p}{d\bar{t}} + \frac{1}{\lambda}\left\{\frac{\partial U_1}{\partial \tilde{\alpha}_p}\frac{d\tilde{\alpha}_p}{d\bar{t}} + \frac{\partial U_1}{\partial \tilde{\alpha}_p}\frac{d\tilde{\alpha}_p}{d\bar{t}} + \frac{\partial U_1}{\partial \bar{t}} + \frac{\partial U_1}{\partial \tilde{x}_q}\frac{d\tilde{x}_q}{d\bar{t}}\right\} + \frac{1}{\lambda^2}\left\{\frac{\partial U_2}{\partial \tilde{\alpha}_p}\frac{d\tilde{\alpha}_p}{d\bar{t}} + \right. \\ &\left. + \frac{\partial U_2}{\partial \tilde{x}_q}\frac{d\tilde{x}_q}{d\bar{t}} + \frac{\partial U_2}{\partial \bar{t}}\right\} = \lambda \frac{\omega_r(\bar{t})}{\omega_{ss}} + A\left\{\tilde{x}_k + \frac{1}{\lambda}\xi_k^{(1)}(\tilde{\alpha}_p, \tilde{x}_i, \bar{t}) + \cdots, \bar{t}\right\} \end{aligned} \tag{31}$$

We want to show now that the partial derivatives $\frac{\partial \xi_k^{(1)}}{\partial \bar{t}}$ and $\frac{\partial U_1}{\partial \bar{t}}$ are of order $\frac{1}{\lambda}$ relative to their preceding term. By Equations (26) and (27), $\xi_k^{(1)}$ and U_1 are the first "vibrations" of the solution vectors x_k and α_p, respectively. Their gradients relative to $\tilde{\alpha}_p$ are certainly of the same order of magnitude or greater than their gradients with respect

to the slowly changing time $\bar{t}$. Furthermore, because $\frac{d\tilde{\alpha}_p}{d\bar{t}} = \mathcal{O}(\lambda)$, we obtain the desired result:

$$\lambda \frac{\partial \xi_k^{(1)}}{\partial \bar{t}} \approx \frac{\partial \xi_k^{(1)}}{\partial \tilde{\alpha}_p} \frac{d\tilde{\alpha}_p}{d\bar{t}} \tag{32}$$

$$\lambda \frac{\partial U_1}{\partial \bar{t}} \approx \frac{\partial U_1}{\partial \tilde{\alpha}_p} \frac{d\tilde{\alpha}_p}{d\bar{t}} \tag{33}$$

Substitute Equations (28) and (29) into Equations (30) and (31) and compare equal powers of λ^0 , λ^{-1} :

$$X_k^{(0)}(\tilde{x}_i,\bar{t}) + \frac{\partial \xi_k^{(1)}}{\partial \tilde{\alpha}_p} \frac{\omega_n(\bar{t})}{\omega_{ss}} = X_k(\tilde{\alpha}_p, \tilde{x}_i, \bar{t}) + \underline{\frac{\partial X_k}{\partial \bar{t}} d\bar{t}} \tag{34}$$

$$\begin{aligned} &X_k^{(1)}(\tilde{x}_i,\bar{t}) + \frac{\partial \xi_k^{(1)}}{\partial \tilde{\alpha}_p} \Omega_0(\tilde{x}_i,\bar{t}) + \frac{\partial \xi_k^{(1)}}{\partial \tilde{x}_q} X_q^{(0)}(\tilde{x}_i,\bar{t}) + \frac{\partial \xi_k^{(2)}}{\partial \tilde{\alpha}_p} \frac{\omega_n(\bar{t})}{\omega_{ss}} = \\ &= \frac{\partial X_k}{\partial \tilde{\alpha}_p} U_1(\tilde{\alpha}_p, \tilde{x}_i, \bar{t}) + \frac{\partial X_k}{\partial \tilde{x}_q} \xi_q^{(1)}(\tilde{\alpha}_p, \tilde{x}_i, \bar{t}) \end{aligned} \tag{35}$$

$$\begin{aligned} &\Omega_1(\tilde{x}_i,\bar{t}) + \frac{\partial U_1}{\partial \tilde{\alpha}_p} \Omega_0(\tilde{x}_i,\bar{t}) + \frac{\partial U_1}{\partial \tilde{x}_q} X_q^{(0)}(\tilde{x}_i,\bar{t}) + \frac{\partial U_2}{\partial \tilde{\alpha}_p} \frac{\omega_n(\bar{t})}{\omega_{ss}} = \\ &= \frac{\partial A}{\partial \tilde{x}_q} \xi_q^{(1)}(\tilde{\alpha}_p, \tilde{x}_i, \bar{t}) \end{aligned} \tag{36}$$

$$\Omega_0(\tilde{x}_i,\bar{t}) + \frac{\partial U_1}{\partial \tilde{\alpha}_p} \frac{\omega_n(\bar{t})}{\omega_{ss}} = A(\tilde{x}_i,\bar{t}) + \underline{\frac{\partial A}{\partial \bar{t}} d\bar{t}} \tag{37}$$

These equations correspond to the Equations (25.4) of Ref. 21, but contain two more partial derivatives with respect to time (underlined terms). We want to show that these partials can be neglected and begin with the term of Equation (30). Compare $\Sigma_k(\tilde{\alpha}_p, \tilde{x}_i, \bar{t})$ with $\frac{\partial \Sigma_k}{\partial \bar{t}} d\bar{t}$. Because Σ_k changes slowly in $\bar{t}$, we have

$$\frac{\partial \Sigma_k}{\partial \bar{t}} d\bar{t} \ll \Sigma_k(\tilde{\alpha}_p, \tilde{x}_i, \bar{t}) \tag{38}$$

The same reasoning holds for Equation (33); i.e.,

$$\frac{\partial A}{\partial \bar{t}} d\bar{t} \ll A(\tilde{x}_i, \bar{t}) \tag{39}$$

Therefore, partial derivatives with respect to time do not occur in terms with powers of λ^0 and λ^{-1}. Rather they appear in terms with λ^{-2} and higher order. But, because the averaging method is based on the first two powers only, we can carry over the results from Bogoliubov and Mitropolsky directly. The only difference lies in the implicit time-dependence of some of the terms in the Equations (34) through (37). This does not pose any problem, because there are no further operations on the time $\bar{t}$ as the solution of the averaging method is developed. The time $\bar{t}$ is just another parameter.

From Equations (25.16), (25.17), and (25.18) of Ref. 21, we obtain the result that the transformation

$$x_k = \tilde{x}_k + \frac{1}{\lambda} \sum_{n=1}^{\infty} \frac{\omega_{ss}}{n\omega_k(\bar{t})} \left\{ -G_{k,n}(\tilde{x}_i, \bar{t}) \cos n\tilde{\alpha}_p + F_{k,n}(\tilde{x}_i, \bar{t}) \sin n\tilde{\alpha}_p \right\} + O\left\{\frac{1}{\lambda^2}\right\} \tag{40}$$

$$\alpha_p = \tilde{\alpha}_p + O\left\{\frac{1}{\lambda^2}\right\} \tag{41}$$

generates the averaged equations

$$\frac{d\tilde{x}_k}{d\bar{t}} = X_{k,0}(\tilde{x}_i,\bar{t}) - \frac{1}{\lambda}\sum_{\substack{n,q\\ n\neq 0}}^{\infty}\frac{\omega_{ss}}{2n\omega_n(\bar{t})}\left\{\frac{\partial F_{k,n}}{\partial \tilde{x}_q}G_{q,n} - \frac{\partial G_{k,n}}{\partial \tilde{x}_q}F_{q,n}\right\} + O\left(\frac{1}{\lambda^2}\right) \quad (42)$$

$$\frac{d\tilde{\alpha}_p}{d\bar{t}} = \lambda\frac{\omega_n(\bar{t})}{\omega_{ss}} + A_0(\tilde{x}_k,\bar{t}) + O\left(\frac{1}{\lambda^2}\right) \quad (43)$$

where the following Fourier expansion was used:

$$X_k(\tilde{\alpha}_p,\tilde{x}_i,\bar{t}) = X_{k,0}(\tilde{x}_i,\bar{t}) + \sum_{n=1}^{\infty}\left\{F_{k,n}(\tilde{x}_i,\bar{t})\cos n\tilde{\alpha}_p + G_{k,n}(\tilde{x}_i,\bar{t})\sin n\tilde{\alpha}_p\right\} \quad (44)$$

Again, as in the previous section, we will be satisfied by the zeroth order approximation of the lateral perturbation equations

$$\frac{d\tilde{x}_k}{d\bar{t}} = X_{k,0}(\tilde{x}_i,\bar{t}) \quad (45)$$

The error incurred is given by Equation (40).

12.4 AVERAGED EQUATIONS OF MOTION

We have arrived at the major set of equations describing the flight dynamics of MR's in the planar glide phase. They are given by Equations (23) and (45) and have the same form as the equations of Table 12.1, except for a tilde over the variables to indicate the averaging process. In the sequel, we only shall deal with these averaged equations and drop the tilde for simplicity. Equations (1) through (8) of Table 11.1 represent then the equations of motion, averaged over α_R and α_p, respectively, and, thus, the aerodynamic coefficients and derivatives are only functions of the Mach and Reynolds numbers. We summarize the major assumptions for these equations:

1. The MR is mirror symmetrical with respect to its external geometry and its mass distribution.

2. $\dot{\gamma}_n \ll \dot{\alpha}_n$

3. β , ϕ , ψ are small angles, i.e. less than 20°.

4. The aerodynamic forces depend on the linear and angular velocities only and not on the accelerations.

5. The density ratio between the MR and the surrounding medium is large; i.e., $\mu \geq \mathcal{O}(10^2)$ which results in a spin rate high enough to justify the averaging process.

6. The flight speed and the spin rate do not drop below ten percent of their steady-state values; i.e.,

$$\bar{V}_n \geqq 0.1\,\bar{V}_{ss} = 0.1$$

$$\bar{\omega}_n \geqq 0.1\,\bar{\omega}_{ss}$$

The value of "ten percent" is somewhat arbitrary. It should emphasize that neither the flight velocity nor the spin rate should become too small to invalidate the averaging process. The reference values $\bar{V}_{ss}$ and $\bar{\omega}_{ss}$ are chosen because they are simple characteristic constants of a particular MR.

The averaged equations of motion of the planar glide phase are considered to be the most important set of equations for the flight dynamics of Magnus rotors because they cover most of the motions of interest. They describe the dynamics of an MR released from a launcher and the motions of a randomly released MR after some initial transient motions. This assumes that the MR was properly designed so that it is actually able to achieve a steady-state glide phase. If this is not the case, the MR may slip into

one of the undesirable flight phases like "end-on flight," "end-over rotation" or "top mode." Our equations would not be applicable to these flight regimes. The averaged equations of motion are also capable of describing the influence of nonlinear aerodynamic forces that might occur at small sideslip angles β and give the effect of the accelerated center of mass on the lateral perturbation equations. But it should be emphasized that, by Assumption 5, the dynamics of very light MR's in air or common MR's in water may not be well presented by the averaged equations.

The longitudinal perturbation equations will not be investigated further, because they only add some small corrections to the flight speed, spin rate, and glide angle of the reference flight.

There are two important extensions of the equations of motion, Table 12.1, that should be mentioned. First, we can supplement the homogeneous lateral perturbation equations by inhomogeneous terms, representing an external side force and an external torque about the roll and yaw axes. We shall omit the details. The other extension allows for a slow turning of the spin axis in a horizontal plane. This turning or spiraling is observed very often in free flight, whenever the flight models were not balanced carefully enough before test. It is caused by a slight mass asymmetry resulting in a small shift of the center of gravity along the spin axis. Let this displacement between the geometrical center and the gravitational center be "a", and make it positive for a shift along the positive spin axis. Suppose that the MR is in a steady-state glide phase. The time rate of change of angular momentum then balances the gravitational torque:

$$[\mathcal{D}^{(E)} \ell_B^{(B)(E)}] = [M_g] = am[g] \tag{46}$$

To introduce the proper coordinate systems, consider the vertical plane normal to the steady-state angular momentum vector. This is the plane we refer to when we speak about the equations of the reference flight, Table 12.1, of the planar glide phase. It was taken to be fixed in the earth frame (E) and therefore also fixed relative to an inertial frame (I). Now, we still require that this plane is normal to the steady-state angular momentum vector but lift the restriction that it is fixed relative to an earth frame. Call this plane the guiding plane, and let $]^P$ be the associated coordinate system with the x_1^P-axis horizontal and in the direction of flight and the x_3^P-axis in the direction of the gravitational vector. Express Equation (46) in this coordinate system, and note that, for small center-of-gravity displacements, the angular momentum vector does not change relative to the guiding plane. We obtain:

$$[\Omega^{(P)(E)}]^P [\ell_B^{(B)(E)}]^P = am[g]^P \tag{47}$$

which reduces to

$$-\frac{d\Psi}{dt} I_y \omega_{ss} = amg \tag{48}$$

where $\frac{d\Psi}{dt}$ is the angular velocity of the guiding plane about a vertical axis:

$$\frac{d\Psi}{dt} = -\frac{amg}{I_y \omega_{ss}} \tag{49}$$

So far we have assumed that the MR is in a quasi-steady-state glide phase; i.e., the absolute value of the angular momentum vector is constant while

the vector turns in a horizontal plane. We can extend this to other flight regimes, such as perturbations in quasi-steady-state glide phase and transient glide phase, as long as the time rate of change of the angular momentum vector with respect to the guiding plane is small relative to $\|[\Omega^{(P)(E)}]^P[\ell_G^{(G)(E)}]^P\|$. Under this condition, we solve the equations of motion, Table 12.1, with reference to the guiding plane and then perform a coordinate transformation $[T]^{PE}$ to obtain the solution relative to the earth frame. The transformation angle is given by Equation (49). In short, the case of the turning of an MR due to slight mass asymmetry is reduced to a coordinate transformation.

13. STABILITY ANALYSIS

Suppose we are interested in evaluating the performance of a given MR. It would suffice to analyze the equations of the reference flight only. But for the results to be a good approximation of the actual behavior, the particular MR must be stable with respect to the reference flight. Otherwise, any perturbations would cause the MR to deviate too far from the reference flight. A stability analysis, therefore, has to proceed a performance evaluation. Other problem areas that are solved with the methods of a stability analysis are the identification of the important design parameters, the improvement of a particular MR design, and the response of an MR to disturbances.

The stability analysis is based on the lateral perturbation Equations (12.4) through (12.8) of Table 12.1. They are a fifth-order system of nonlinear nonautonomous ordinary differential equations. We shall first show that, under certain assumptions, a transformation reduces them to a fourth-order system. Then we shall discuss the asymptotic stability of the first approximation in general terms, using a theorem by Malkin (22). The simplest but also most important case is the stability in the planar steady-state glide phase with linear behavior of the aerodynamic forces. The associated equations are linear and autonomous. They were already investigated by Millivolte (6). Here, we shall only summarize the results and give some simplified expressions for the roots of the characteristic equation. To treat certain aspects of the nonlinear nonautonomous case, the equations are reduced first to the two degrees of freedom: rolling and yawing. Then, the yaw and roll angle are combined to form the nutation

cone angle, resulting, via the method of averaging, in a first-order nonlinear and nonautonomous differential equation. Its stability is discussed in detail, and necessary and sufficient conditions for limit cycles are given.

13.1 REDUCTION TO A FOURTH ORDER SYSTEM

To simplify the notation, we shall abbreviate the equations of the planar glide phase; i.e., the reference equations of Table 12.1, by

$$\dot{y}_k = f_k(y_i) \quad ; \quad k = 1,2,3 \; ; \quad i = 1,2,3 \tag{1}$$

with the state vector $y_1 = \bar{V}_n$, $y_2 = \gamma_n$, $y_3 = \bar{\omega}_n$. The lateral perturbation equations, Table 12.1, are abridged by

$$\mathring{x}_\ell = a_{\ell m}(\bar{t})\, x_m + g_\ell(x_n, \bar{t}) \; ; \quad \ell, m, n = 1, \cdots, 5 \tag{2}$$

with the state vector $x_1 = \beta$, $x_2 = \mathring{\phi}$, $x_3 = \mathring{\psi}$, $x_4 = \phi$, $x_5 = \psi$.
We shall also refer to Equation (2) in a special matrix form:

$$\begin{bmatrix} \dot{\beta} \\ \mathring{\mathring{\phi}} \\ \mathring{\mathring{\psi}} \\ \mathring{\phi} \\ \mathring{\psi} \end{bmatrix} = \begin{bmatrix} a_{11} & 0 & -1 & a_{14} & a_{15} \\ a_{21} & a_{22} & a_{23} & 0 & 0 \\ a_{31} & -a_{23} & a_{33} & 0 & 0 \\ 0 & 1 & 0 & 0 & 0 \\ 0 & 0 & 1 & 0 & 0 \end{bmatrix} \begin{bmatrix} \beta \\ \mathring{\phi} \\ \mathring{\psi} \\ \phi \\ \psi \end{bmatrix} \begin{bmatrix} g_1 \beta^3 \\ g_{21}\beta^3 + g_{22}\mathring{\phi}^3 + g_{23}\beta^2\mathring{\phi} + g_{24}\beta\mathring{\phi}^2 \\ g_{31}\beta^3 + g_{32}\mathring{\psi}^3 + g_{33}\beta^2\mathring{\psi} + g_{34}\beta\mathring{\psi}^2 \\ 0 \\ 0 \end{bmatrix} \tag{3}$$

The elements are found by comparison with the lateral perturbation equations of Table 12.1.

A salient feature of Equation (3) is that it admits a one parametric family of stationary solutions; i.e., the state vector

$$(x_\ell)_s = \{0, 0, 0, -\lambda \tan \gamma_n, \lambda\} \tag{4}$$

satisfies the Equation (3) for any value of λ . The physical explanation follows from Figure 13.1. It shows the roll and yaw angles of the

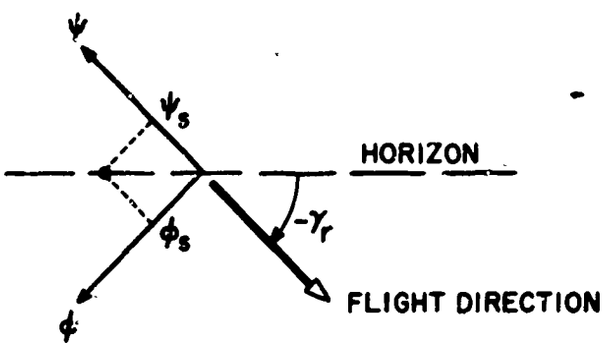

FIGURE 13.1 ROLL AND YAW ANGLES PROJECTED ON A HORIZONTAL PLANE

spin axis projected on a horizontal plane and the glide angle plotted in negative direction. If the spin axis is horizontal, the ratio of roll to yaw angle is

$$\frac{\phi_s}{\psi_s} = -\tan \gamma_n \tag{5}$$

This is the same ratio we obtain from the last two components, ϕ_s and ψ_s of Equation (4). Therefore, the stationary solutions imply a horizontal spin axis. In particular, it means that, once the perturbations have

dampened out and the MR has achieved its steady-state flight, its spin axis will be horizontal though it may be heading in another direction. The MR has no heading stability. Such a behavior indicates that one eigenvalue of the $a_{\ell m}$ matrix is zero. This can easily be checked by actually evaluating the characteristic equation.

Under certain simplifying assumptions, this zero root can be removed by a transformation resulting in a fourth order system of differential equations. The details follow. Introduce the new roll angle Φ about a horizontal axis:

$$\Phi = \frac{\tau g}{V_{ss}} \frac{1}{\bar{V}_R} \left\{ \phi \cos\gamma_R + \psi \sin\gamma_R \right\} \tag{6}$$

and take the time derivative with respect to the dynamic-normalized time

$$\dot{\Phi} = \frac{\tau g}{V_{ss}} \left\{ -\frac{\dot{\bar{V}}_R}{\bar{V}_R^2} \left(\phi \cos\gamma_R + \psi \sin\gamma_R \right) + \frac{1}{\bar{V}_R} \left(\dot{\phi} \cos\gamma_R + \dot{\psi} \sin\gamma_R \right) \right. \\ \left. + \frac{\dot{\gamma}_R}{\gamma_R} \left(-\phi \sin\gamma_R + \psi \cos\gamma_R \right) \right. \tag{7}$$

The last term is much smaller than the preceding term because ϕ, ψ are small angles and the glide angle γ_R changes much slower than the roll and yaw angles executing nutational motions. Without this term and in view of Equation (6), we get

$$\dot{\Phi} = -\frac{\dot{\bar{V}}_R}{\bar{V}_R} \Phi + \frac{\tau g \cos\gamma_R}{V_{ss} \bar{V}_R} \dot{\phi} + \frac{\tau g \sin\gamma_R}{V_{ss} \bar{V}_R} \dot{\psi} \tag{8}$$

Substitute Equations (6) and (8) into Equation (3):

$$\begin{bmatrix} \dot{\beta} \\ \dot{\phi} \\ \dot{\psi} \\ \dot{\Phi} \end{bmatrix} = \begin{bmatrix} a_{11} & 0 & -1 & 1 \\ a_{21} & a_{22} & a_{23} & 0 \\ a_{31} & -a_{23} & a_{33} & 0 \\ 0 & a_{14} & a_{15} & -\frac{\dot{\bar{V}}_R}{\bar{V}_R} \end{bmatrix} \begin{bmatrix} \beta \\ \dot{\phi} \\ \dot{\psi} \\ \Phi \end{bmatrix} + \begin{bmatrix} g_1(\beta, \dot{\phi}, \dot{\psi}, \bar{t}) \\ g_2(\beta, \dot{\phi}, \dot{\psi}, \bar{t}) \\ g_3(\beta, \dot{\phi}, \dot{\psi}, \bar{t}) \\ 0 \end{bmatrix} \tag{9}$$

and abbreviate

$$\dot{z}_q = b_{qs}(\bar{t}) z_s + g_q(z_1, z_2, z_3, \bar{t}) \quad ; \; q, s = 1, \cdots, 4 \tag{10}$$

The order of the system of differential equations has been reduced by one and the dependence on ψ and ϕ replaced by Φ. In other words, the dependence on the heading of the MR has been eliminated. A check of the eigenvalues of b_{qs} will show that the zero root has also been removed. The remaining eigenvalues of b_{qs} are identical with the non-zero eigenvalues of b_{qs} because the transformation of variables is linear.

We succeeded in removing the zero root through a simple transformation. This root was independent of the shape or mass of the particular MR under consideration and was present in the transient and steady-state glide phases. It also could happen that one of the other eigenvalues assumes a zero real value. But this is only possible for a very special combination of shape and mass distribution and therefore unlikely to occur. We shall not deal with this case any further.

We now ask whether asymptotic stability of the first approximation of Equation (9) implies asymptotic stability of the nonlinear system? A theorem by Malkin (22) p. 322 provides the conditions under which the answer is affirmative:

If the equations of the first approximation are regular and if all its characteristic numbers are positive, then the unperturbed motions of Equation (10) are asymptotically stable, provided the functions $g_q(z_1, z_2, z_3, \bar{t})$ satisfy in $|z_q| \leqq H$ = constant, $t \geqq 0$ the inequality:

$$|g_q(z_1, z_2, z_3, \bar{t})| < A\left(|z_1| + |z_2| + |z_3| + |z_4|\right)^m \qquad A > 0\ ,\ m > 1 \tag{11}$$

We shall show that Equation (9) satisfies these conditions. A necessary and sufficient condition for the first approximation to be regular is, according to Malkin (22) p. 294 that

$$\lim_{\bar{t} \to \infty} \frac{1}{\bar{t}} \int_0^{\bar{t}} b_{ss}\, d\bar{t} = \text{CONSTANT} < \infty\ ;\ s = 1, 2, 3, 4 \tag{12}$$

Consider the elements of the trace of $b_{qs}(\bar{t})$. They approach either a constant or zero value as time increases. Therefore, Equation (12) is satisfied. The characteristic number of a function $f(\bar{t})$ is defined (Malkin (22) p. 283) by

$$\pi(f) = -\lim_{\bar{t} \to \infty} \sup \frac{\ln|f(\bar{t})|}{\bar{t}} \tag{13}$$

To find the characteristic numbers of the first approximation,

$$\mathring{z} = b_{qs}(\bar{t})\, z_s \tag{14}$$

separate the matrix b_{qs} into a constant part c_{qs} and a variable part $d_{qs}(\bar{t})$. The elements of $d_{qs}(\bar{t})$ be chosen such that:

$$\lim_{\bar{t} \to \infty} d_{qs}(\bar{t}) = 0 \quad ; \quad q, s = 1, \cdots, 4 \tag{15}$$

This is always possible because the solutions of the reference Equations (12.1) through (12.3) of Table 12.1 tend to constant values as time increases. C_{qs} is just the matrix of the autonomous case; i.e., the matrix of the first approximation of the lateral perturbation equations in steady-state glide phase:

$$\dot{z}_q = C_{qs} z_s \tag{16}$$

A theorem by Malkin (22) p. 305 states that, if Equation (15) is satisfied, the characteristic numbers of Equation (14) are equal to the characteristic numbers of Equation (16). But the characteristic numbers of an autonomous linear system, Equation (16), are the negative values of the real parts of the eigenvalues of the matrix C_{qs}. Therefore, if Equation (16) is asymptotically stable, all its characteristic numbers are positive, and, consequently, all characteristic numbers of the first approximation, Equation (14), are positive. The conditions, Equation (11), are satisfied because the nonlinear aerodynamic functions q_q are power series expansions of z_1, z_2, and z_3 and because $\bar{V}_n = 0$ is excluded. We conclude that asymptotic stability of the first approximation, Equation (14), implies asymptotic stability of the nonlinear Equation (10). Moreover, asymptotic stability of Equation (14) is simply established if the autonomous Equation (16) is asymptotically stable.

13.2 STABILITY OF THE FIRST APPROXIMATION

The important stability theorem has already been stated in the previous section; namely, that asymptotic stability of the autonomous linear perturba-

tion Equation (16) implies the asymptotic stability of the nonautonomous linear Equation (14). We can extend this to Equation (2); separate the $a_{\ell m}(\bar{t})$ matrix into constant and time-dependent parts as at the end of the previous section:

$$\mathring{x}_\ell = a_{\ell m}(\bar{t})\, x_m = \left(h_{\ell m} + p_{\ell m}(\bar{t}) \right) x_m \tag{17}$$

Again, $p_{\ell m}(\bar{t})$ tends to zero as time increases. But now, instead of asymptotic stability, only stability can be inferred. We conclude that, if the equilibrium of the autonomous perturbation equations

$$\mathring{x}_\ell = h_{\ell m} x_m \tag{18}$$

is stable, the equilibrium of the nonautonomous Equation (17) is stable too.

We have shown that the issue of stability can be reduced to the simple problem of the stability of the linear autonomous perturbation equations. However, a word of caution is necessary. The perturbation equations are valid only so long as the angles ϕ, ψ, β remain small throughout the flight. This can always be satisfied for sufficiently small initial conditions z_{0_q}. But for an engineering analysis the initial conditions cannot always be made arbitrarily small. Then, we have to ask whether a particular solution of an asymptotically stable system, Equation (14), stays within the small angle limits, say ε, for all times $\bar{t} > \bar{t}_0$ for some small initial conditions; i.e.,

$$\| z_q(\bar{t}, z_{0_q}, \bar{t}_0) \| < \varepsilon \quad \text{FOR ALL} \quad \bar{t} \geq \bar{t}_0 , \; \| z_{0_q} \| < \delta < \varepsilon \tag{19}$$

The search for an answer leads to theorems that establish an upper bound on the solution vector. See Bellman (23) p. 44, Cesari (24) p. 48, and

Zubov (25) p. 78. However, all bounds include arbitrary constants that cannot be predetermined. The only way, therefore, to judge whether the Condition (19) is satisfied for a particular MR is to actually calculate the solutions for some representative initial conditions by computer.

In general, the eigenvalues of the matrix $h_{\ell m}$ or c_{qs} are evaluated by computer. But for design purposes, we can use simplified formulas that have been shown to be accurate within $\pm$ 5% for common MR configurations. The simplification is based on the overriding effect of the gyroscopic coupling term a_{23} (see Equation (3)). More specifically, it is assumed that

$$\begin{aligned} &a_{23} \gg a_{22} \text{ and } a_{33} \\ &a_{23}^2 \gg a_{21} \text{ and } a_{31} \text{ and } a_{11} \end{aligned} \tag{20}$$

The result is that the pair of roots of the so-called <u>nutation mode</u> are approximated by:

$$\bar{s}_N = \bar{\xi}_N \pm i\bar{\eta}_N = \frac{1}{2a_{23}}\left\{(a_{22}+a_{33})a_{23} - a_{21}\right\} \pm i\, a_{23} \tag{21}$$

where

$$\bar{\xi}_N = \frac{\bar{V}_{ss}}{2\mu^2 \bar{I}_y}\left\{ (C_{\ell\hat{\beta}} + C_{n\hat{R}})\frac{\bar{I}_y}{\bar{I}} - C_{\ell\hat{\omega}_\beta} \right\} \tag{22}$$

$$\bar{\eta}_N = \frac{\bar{I}_y}{\bar{I}}\,\bar{\omega}_{ss} \tag{23}$$

The other pair of roots of the <u>undulation mode</u> are:

$$\bar{s}_U = \bar{\xi}_U \pm \bar{\eta}_U = \frac{1}{2}\left(a_{11} + \frac{a_{21}}{a_{23}}\right) \pm \sqrt{\frac{1}{4}\left(a_{11} + \frac{a_{21}}{a_{23}}\right)^2 + \frac{1}{a_{23}}(a_{31}a_{14} - a_{21}a_{15})} \tag{24}$$

where

$$\bar{\xi}_u = \frac{\bar{V}_{ss}}{2}\left(C_{y_\beta} + \frac{1}{\mu^2 \bar{I}_y} C_{l_{\hat{\omega}_\beta}}\right) \tag{25}$$

$$\bar{\eta}_u = \left\{ \bar{\xi}_u^2 + \frac{\tau q}{\mu^2 \bar{I}_y \bar{\omega}_{ss} \bar{V}_{ss}}\left(\mu \bar{V}_{ss} C_{n_\beta} \cos\gamma_{ss} - \bar{\omega}_{ss} C_{l_{\hat{\omega}_\beta}} \sin\gamma_{ss}\right)\right\}^{1/2} \tag{26}$$

The dimensions of the roots are radians per dynamic-normalized unit time. This result can be verified by multiplying out the nutation and undulation roots. The approximate characteristic equation thus obtained agrees with the characteristic equation of the matrix $h_{\ell m}$ subjected to the simplifications of Equation (20).

The nutation roots are always conjugate complex with a nutation frequency of

$$\dot{\delta} = \frac{\bar{I}_y}{\bar{I}} \bar{\omega}_{ss} \tag{27}$$

just as in the case of a classical gyroscope. Equation (22) determines the aerodynamic damping. The damping derivatives $C_{l_{\hat{p}}}$ and $C_{n_{\hat{r}}}$, which are always negative, are opposed by a usual negative Magnus moment derivative $C_{l_{\hat{\omega}_\beta}}$. The higher the moment-of-inertia ratio $\bar{I}_y / \bar{I}$, the higher the nutation rate and the more effective the aerodynamic damping. The undulation roots can be conjugate complex or both real. Their rate of change of amplitude is generally two orders of magnitude less than that of the nutation mode. In gyroscopic terms, the undulation mode of an MR is the unsteady precession caused by aerodynamic torques. It would not be present in a vacuum. In the oscillatory case, a necessary and sufficient condition for asymptotic stability of the undulation mode is:

$$C_{y_\beta} + \frac{1}{\mu^2 \bar{I}_y} C_{\ell_{\hat{\omega}_\beta}} < 0 \tag{28}$$

and, because C_{y_β} is negative for most practical MR's:

$$C_{y_\beta} < -\frac{1}{\mu^2 \bar{I}_y} C_{\ell_{\hat{\omega}_\beta}} \tag{29}$$

This is always satisfied for a negative Magnus moment $C_{\ell_{\hat{\omega}_\beta}}$. If the undulation mode is purely exponential, Equation (28) is only a necessary condition. Without giving the details, we remark that the sufficient condition can be derived from Equation (24) Thus, we have seen that the important aerodynamic derivatives are $C_{\ell_{\hat{\omega}_\beta}}$ C_{y_β}, and the sum $C_{\ell_{\hat{\beta}}} + C_{n_{\hat{R}}}$ and the important mass parameter is $\bar{I}_y / \bar{I}$.

The effect of the acceleration of the center of mass on the lateral perturbation equations is limited to the matrix element

$$a_{11} = -\frac{\dot{\bar{V}}_R}{\bar{V}_R} + C_{y_\beta} \bar{V}_R \tag{30}$$

In steady-state it is desirable to have a highly negative C_{y_β}, as can be seen from Equation (28). This can be generalized to the transient case by saying that the more negative a_{11} is, the smaller the deviation of the solution vector from the unperturbed flight for a given set of initial conditions. Therefore, we conclude from Equation (30) that the effect of a decelerated center of mass is destabilizing whereas acceleration tends to stabilize the perturbations. Some sample solutions in support of this statement will be given in Chapter 14.

We have indicated that the undulation mode is much slower than the nutation mode. Consequently, one can identify them as two separate motion

histories and would like to investigate them separately. If the nutational motions are of main interest, one can assume that the center of mass remains in the plane defined by the planar glide phase. This implies that $\beta = -\psi$ and therefore reduces the perturbation equations to two degrees of freedom, namely, rolling and yawing. We obtain from Equation (3):

$$\begin{bmatrix} \ddot{\phi} \\ \ddot{\psi} \\ \dot{\psi} \end{bmatrix} = \begin{bmatrix} a_{22} & a_{23} & -a_{21} \\ -a_{23} & a_{33} & -a_{31} \\ 0 & 1 & 0 \end{bmatrix} \begin{bmatrix} \dot{\phi} \\ \dot{\psi} \\ \psi \end{bmatrix} + \begin{bmatrix} -g_{21}\psi^3 + g_{22}\dot{\phi}^3 + g_{23}\psi^2\dot{\phi} - g_{24}\psi\dot{\phi}^2 \\ -g_{31}\psi^3 + g_{32}\dot{\psi}^3 + g_{33}\psi^2\dot{\psi} - g_{34}\psi\dot{\psi}^2 \\ 0 \end{bmatrix} \tag{31}$$

or abbreviated:

$$\dot{\zeta}_n = u_{nt}(\bar{t})\zeta_t + w_n(\zeta_1, \zeta_2, \zeta_3, \bar{t}) \; ; \; n,t = 1,2,3 \tag{32}$$

The eigenvalues of the matrix u_{nt} are with the assumptions, Equation (20):

$$\bar{s}_N = \bar{\xi}_N \pm i\bar{\eta}_N = \frac{1}{2a_{23}}\left\{ (a_{22} + a_{33})a_{23} - a_{21} \right\} \pm i a_{23} \tag{33}$$

$$\bar{\xi}_u = \frac{1}{a_{23}^2}\left(a_{22}a_{31} + a_{23}a_{21} \right) \tag{34}$$

We again recognize in Equation (33) the roots of the nutation mode, Equation (21). The undulation mode is represented by only one real root, Equation (34). In steady-state glide phase it has the form:

$$\bar{\xi}_u = \frac{\bar{V}_{ss}}{\mu^2 \bar{I}_y^2}\left\{ \frac{V_{ss}^2}{\mu\, \bar{\omega}_{ss}^2} C_{l\hat{p}} C_{n\beta} + \bar{I}_y C_{l\hat{\omega}_\beta} \right\} \tag{35}$$

which has no common features either with Equation (25) or Equation (26). But then we do not attempt to analyze the undulation mode with Equation (31).

13.3 NUTATION LIMIT CYCLES

In the previous section we showed that the stability of the perturbation equations can be determined from the linear autonomous perturbation equations. But this requires initial conditions small enough, so that the state vector remains sufficiently small. In an engineering analysis, the investigation is focused not only on the question of stability, but also on the motions of MR's, resulting from realistic initial conditions. For a majority of MR's, the first approximation is still satisfactory. However, wind tunnel tests show that for certain configurations, the rolling and yawing moment coefficients are not approximated satisfactorily by the linear derivatives only. Even for small angles β, higher order derivatives must be considered. This can lead, as observed in flight tests, to limit cycles of the nutational motions; i.e., a coning motion about a horizontal axis with constant cone angle.

For the first part of this section, we shall concentrate on the most important aerodynamic nonlinearities, namely, g_{21} and g_{31} (see Equation (31)). This case is also more easily treated than if other nonlinearities are included. Afterwards the effect of the nonlinear damping derivatives, g_{22} and g_{32}, will be discussed. The complete set of nonlinearities will not be studied because little is known about the values of the mixed derivatives g_{23}, g_{24}, g_{33}, and g_{34}.

We can begin our analysis of limit cycles with the two-degrees-of-freedom Equation (31) because this phenomenon is basically a nutational motion. First, we perform a transformation of variables from the flight mechanical angles ϕ and ψ to the gyro mechanical cone angle η and

node angle δ . This is accomplished by substituting Equations (7.19) through (7.24) in Equation (31). The relevant angle for the nutational motions is the cone angle η , whereas we shall not be particularly interested in the value of the node angle δ . From the observed exponential damping of the nutation mode we also expect that a first-order differential equation in η is a reasonably good approximation. Guided by these physical considerations, we eliminate $\ddot{\eta}$ from the two equations just obtained by multiplying the first equation by $\sin\delta$ and the second equation by $\cos\delta$ and adding both equations. Arranging terms in form of a differential equation in η yields:

$$\begin{aligned}
&\dot{\eta}\{-2\dot{\delta} + a_{23} + (a_{33}-a_{22})\cos\delta\sin\delta\} + \\
&+\eta\{-\ddot{\delta} + (a_{22}\sin^2\delta + a_{33}\cos^2\delta)\dot{\delta} - a_{21}\sin^2\delta - a_{31}\sin\delta\cos\delta\} \\
&+\eta^3\{-g_{21}\sin\delta - g_{21}\cos\delta\}\sin^3\delta = 0
\end{aligned} \tag{36}$$

This equation cannot be solved as it stands. It would have to be supplemented by an equation in δ . However, in the following we shall show that, if we can approximate $\dot{\delta}$ and $\ddot{\delta}$ by some known quantities, and if we consider δ as a rapidly rotating phase, the averaging method of Bogoliubov and Mitropolsky can again be applied and Equation (36) reduced to a solvable first-order differential equation.

From the linear theory, we have for the nutation frequency, in view of Equation (21):

$$\dot{\delta} \approx a_{23} \tag{37}$$

Because this does not depend on the aerodynamic derivatives, we can assume that the nonlinear aerodynamic effect is also small and that

Equation (37) holds also for Equation (36). In steady-state glide phase, $\ddot{\delta} = 0$. In the transient glide phase, $\dot{\delta}$ changes like the slowly-changing a_{23}. Therefore, we can assume that:

$$\|\ddot{\delta}\| \ll \|(a_{22} + a_{33})\dot{\delta}\| \tag{38}$$

Furthermore, it is easily justifiable to drop the last term in the first line of Equation (36) because

$$\|(a_{33}-a_{22})\cos\delta\sin\delta\| \approx \|(a_{33}-a_{22})\tfrac{1}{2}\sin 2\delta\| \ll \|-2\dot{\delta}+a_{23}\| \approx \|a_{23}\| \tag{39}$$

With those simplifications, Equation (36) reduces to

$$\begin{aligned}\dot{\eta} = {} & \left(a_{22}\sin^2\delta + a_{33}\cos^2\delta - \frac{a_{21}}{a_{23}}\sin^2\delta - \frac{a_{31}}{a_{23}}\sin\delta\cos\delta\right)\eta \\ & - \left(\frac{g_{21}}{a_{23}}\sin^4\delta + \frac{g_{31}}{a_{23}}\sin^3\delta\cos\delta\right)\eta^3\end{aligned} \tag{40}$$

This equation is similar to Equation (12.24) with the rapidly rotating phase δ. We abbreviate:

$$\frac{d\eta}{d\bar{t}} = N(\delta, \eta, \bar{t}) \tag{41}$$

and express the rate of change of the phase by

$$\frac{d\delta}{d\bar{t}} = a_{23} = \lambda' \frac{\omega_n(\bar{t})}{\omega_{ss}} \tag{42}$$

where, in view of Equation (12.9), the large parameter becomes:

$$\lambda' = \frac{\bar{I}_y}{\bar{I}}\mu\,\hat{\omega}_{ss} = \frac{\bar{I}_y}{\bar{I}}\lambda \tag{43}$$

The time-dependence of Equation (41) is due to the a_{lm}, g_{21}, and g_{31} in Equation (40). As in Section 12.3, this is a "slow" time-dependence, and, therefore, the results obtained there can be carried over directly.

Corresponding to Equations (12.40) and (12.41), we introduce the transformations

$$\eta = \tilde{\eta} + \frac{1}{\lambda'} \sum_{n=1}^{\infty} \frac{\omega_{ss}}{n\omega_n(\bar{t})} \left\{ -G_n(\tilde{\eta},\bar{t}) \cos n\tilde{\delta} + F_n(\tilde{\eta},\bar{t}) \sin n\tilde{\delta} \right\} + O\left(\frac{1}{\lambda'^2}\right) \quad (44)$$

$$\delta = \tilde{\delta} + O\left(\frac{1}{\lambda'^2}\right) \quad (45)$$

which generate the averaged equations (see Equations (12.42) and (12.43)):

$$\frac{d\tilde{\eta}}{d\bar{t}} = N_0(\tilde{\eta},\bar{t}) - \frac{1}{\lambda'} \sum_{n=1}^{\infty} \frac{\omega_{ss}}{2n\,\omega_n(\bar{t})} \left\{ \frac{\partial F_n}{\partial \tilde{\eta}} G_n - \frac{\partial G_n}{\partial \tilde{\eta}} F_n \right\} + O\left(\frac{1}{\lambda'^2}\right) \quad (46)$$

$$\frac{d\tilde{\delta}}{d\bar{t}} = \lambda' \frac{\omega_n(\bar{t})}{\omega_{ss}} + O\left(\frac{1}{\lambda'^2}\right) \quad (47)$$

when the following Fourier expansion was used:

$$N(\tilde{\delta},\tilde{\eta},\bar{t}) = N_0(\tilde{\eta},\bar{t}) + \sum_{n=1}^{\infty} \left\{ F_n(\tilde{\eta},\bar{t}) \cos n\tilde{\delta} + G_n(\tilde{\eta},\bar{t}) \sin n\tilde{\delta} \right\} \quad (48)$$

To determine the Fourier coefficients, convert the powers of the trigonometric functions in Equation (40) into multiples of the phase angle δ, and compare coefficients of the same harmonics with Equation (48). The result is:

$$N_0 = \frac{1}{2a_{23}} \left\{ (a_{22} + a_{33}) a_{23} - a_{21} \right\} \tilde{\eta} - \frac{3}{8} \frac{g_{21}}{a_{23}} \tilde{\eta}^3 \quad (49)$$

$$F_2 = \frac{1}{2a_{23}} \left\{ (-a_{22} + a_{33}) a_{23} + a_{21} \right\} \tilde{\eta} + \frac{1}{2} \frac{g_{21}}{a_{23}} \tilde{\eta}^3 \quad (50)$$

$$G_2 = -\frac{1}{2}\frac{a_{31}}{a_{23}}\tilde{\eta} - \frac{1}{4}\frac{g_{31}}{a_{23}}\tilde{\eta}^3 \tag{51}$$

$$F_4 = -\frac{1}{8}\frac{g_{21}}{a_{23}}\tilde{\eta}^3 \tag{52}$$

$$G_4 = \frac{1}{8}\frac{g_{31}}{a_{23}}\tilde{\eta}^3 \tag{53}$$

Substitute Equations (49) through (53) into Equations (44) and (46):

$$\begin{aligned}\eta = \tilde{\eta} &+ \frac{1}{4a_{23}^2}\left\{\left(a_{31}\tilde{\eta} + \frac{g_{31}}{2}\tilde{\eta}^3\right)\cos 2\tilde{\delta} + \left\{\left(\left(-a_{22}+a_{33}\right)a_{23}+a_{21}\right)\tilde{\eta} + g_{21}\tilde{\eta}^3\right\}\sin 2\tilde{\delta}\right\} \\ &- \frac{1}{32\,a_{23}^3}\left\{g_{31}\tilde{\eta}^3\cos 4\tilde{\delta} + g_{21}\tilde{\eta}^3\sin 4\tilde{\delta}\right\} + O\left(\frac{1}{\lambda'^2}\right)\end{aligned} \tag{54}$$

$$\begin{aligned}\frac{d\tilde{\eta}}{d\tilde{t}} &= \frac{1}{2a_{23}}\left\{\left[\left(a_{22}+a_{33}\right)a_{23} - a_{21}\right]\tilde{\eta} - \frac{3}{4}g_{21}\tilde{\eta}^3\right\} - \\ &- \frac{1}{16\,a_{23}^3}\left\{\left[\left(-a_{22}+a_{33}\right)a_{23} + a_{21}\right]g_{21} - 2a_{31}g_{21}\right\}\tilde{\eta}^3 + O\left(\frac{1}{\lambda'^2}\right)\end{aligned} \tag{55}$$

Writing out the individual terms yields the final equations:

$$\eta = \tilde{\eta} + \frac{1}{4}\left(\frac{\bar{I}}{\bar{I}_y}\right)^2 \frac{1}{\bar{\omega}_n^2}\left\{\left[C_{n_\beta}\tilde{\eta} + \frac{1}{12}C_{n_{\beta^3}}\tilde{\eta}^3\right]\frac{\bar{V}_n^2}{\mu\bar{I}}\cos 2\tilde{\delta} + \right.$$

$$\left. + \left[\left(\left(-C_{\ell_{\hat{p}}} + C_{n_{\hat{r}}}\right)\frac{\bar{I}_y}{\bar{I}} + C_{\ell_{\hat{\omega}_\beta}}\right)\tilde{\eta} + \frac{1}{6}C_{\ell_{\hat{\omega}_{\beta^3}}}\tilde{\eta}^3\right]\frac{\bar{V}_n\bar{\omega}_n}{\mu^2\bar{I}}\sin 2\tilde{\delta}\right\} - \tag{56}$$

$$-\frac{1}{192}\left(\frac{\bar{I}}{\bar{I}_y}\right)^2\frac{\bar{V}_n}{\mu\bar{I}\,\bar{\omega}_n^2}\left\{\bar{V}_n C_{n_{\beta^3}}\tilde{\eta}^3\cos 4\tilde{\delta} + \frac{\bar{\omega}_n}{\mu}C_{\ell_{\hat{\omega}_{\beta^3}}}\tilde{\eta}^3\sin 4\tilde{\delta}\right\} + O\left\{\frac{1}{\lambda^{12}}\right\}$$

$$\overset{\circ}{\tilde{\eta}} = \frac{1}{2}\frac{\bar{V}_n}{\mu^2\bar{I}_y}\left\{\left[\left(C_{\ell_{\hat{p}}} + C_{n_{\hat{r}}}\right)\frac{\bar{I}_y}{\bar{I}} - C_{\ell_{\hat{\omega}_\beta}}\right]\tilde{\eta} - \frac{1}{8}C_{\ell_{\hat{\omega}_{\beta^3}}}\tilde{\eta}^3\right\} -$$

$$-\frac{1}{96}\frac{\bar{V}_n^3\bar{I}}{\mu^3\bar{I}_y^3\bar{\omega}_n^2}\left\{\left[-C_{\ell_{\hat{p}}} + C_{n_{\hat{r}}}\right)\frac{\bar{I}_y}{\bar{I}} + C_{\ell_{\hat{\omega}_\beta}}\right]C_{n_{\beta^3}} - 2C_{n_\beta}C_{\ell_{\hat{\omega}_{\beta^3}}}\right\}\tilde{\eta}^3 + O\left(\frac{1}{\lambda^{12}}\right) \tag{57}$$

The equations above were arranged in the following way: in Equation (56), the terms between the first pair of braces are the second harmonics, and the expressions between the second pair of braces are the fourth harmonics of the first-order corrections of η . The averaged equation of motion of the cone angle, Equation (57), displays the zeroth order approximation within the first braces and the first-order correction between the second braces. From Equation (55), we see that the accuracy of the zeroth approximation depends on the nutation frequency $\overset{\circ}{\delta} = a_{23} = \frac{\bar{I}_y}{\bar{I}}\bar{\omega}_n$. The greater the moment of inertia ratio $\bar{I}_y/\bar{I}$ and the spin rate $\bar{\omega}_n$, the better the approximation. An estimate of the error incurred is obtained from Equation (56). In the sequel we shall first investigate the zeroth order approximation and then look into the possible error.

The simplest case is obtained if all nonlinear terms are dropped:

$$\overset{\circ}{\tilde{\eta}} = \frac{1}{2}\frac{\bar{V}_R}{\mu^2 \bar{I}_y}\left\{\left(C_{l_{\hat{p}}} + C_{n_{\hat{r}}}\right)\frac{\bar{I}_y}{\bar{I}} - C_{l_{\hat{\omega}_\beta}}\right\}\tilde{\eta} \tag{58}$$

The root of this equation agrees with the real part of the nutation root, Equation (22); i.e., the decay of η equals the exponential decrease of the envelope of the nutation mode. This result was to be expected if the averaging method is a physically justifiable process.

Now we consider the nonlinear zeroth order approximation:

$$\overset{\circ}{\tilde{\eta}} = \frac{1}{2}\frac{\bar{V}_R}{\mu^2 \bar{I}_y}\left\{\left[\left(C_{l_{\hat{p}}} + C_{n_{\hat{r}}}\right)\frac{\bar{I}_y}{\bar{I}} - C_{l_{\hat{\omega}_\beta}}\right]\tilde{\eta} - \frac{1}{8}C_{l_{\hat{\omega}_{\beta^3}}}\tilde{\eta}^3\right\} \tag{59}$$

and note first that it is independent of $C_{n_{\beta^3}}$; i.e., in the zeroth approximation, the effect of $C_{n_{\beta^3}}$ cancels over one nutation cycle. A necessary condition for the existence of a limit cycle is $\overset{\circ}{\tilde{\eta}} = 0$ and $\tilde{\eta} \neq 0$, yielding:

$$\tilde{\eta}^2_{LC} = 8\,\frac{\left(C_{l_{\hat{p}}} + C_{n_{\hat{r}}}\right)\frac{\bar{I}_y}{\bar{I}} - C_{l_{\hat{\omega}_\beta}}}{C_{l_{\hat{\omega}_{\beta^3}}}} \tag{60}$$

Only the real and positive value is physically of interest. To determine whether a limit cycle will actually occur, the stability at η_{LC} must be investigated. We have the simple conditions

$$\left.\frac{\partial \overset{\circ}{\tilde{\eta}}}{\partial \tilde{\eta}}\right|_{LC} < 0 \qquad \text{stable limit cycle}$$

$$\left.\frac{\partial \overset{\circ}{\tilde{\eta}}}{\partial \tilde{\eta}}\right|_{LC} > 0 \qquad \text{unstable limit cycle} \tag{61}$$

where Equation (59) furnishes the relationship:

$$\left.\frac{\partial \dot{\tilde{\eta}}}{\partial \tilde{\eta}}\right|_{LC} = -\frac{\bar{V}_n}{\mu^2 \bar{I}_y}\left\{\left(C_{\ell_\beta} + C_{n_{\hat{R}}}\right)\frac{\bar{I}_y}{\bar{I}} - C_{\ell_{\hat{\omega}_\beta}}\right\} \tag{62}$$

which is according to Equation (22):

$$\left.\frac{\partial \dot{\tilde{\eta}}}{\partial \tilde{\eta}}\right|_{LC} = -2\bar{\xi}_N \tag{63}$$

Consequently, the conditions expressed in Equation (61) are equivalent to

$$\begin{aligned} &\bar{\xi}_N > 0 \qquad \text{stable limit cycle} \\ &\bar{\xi}_N < 0 \qquad \text{unstable limit cycle} \end{aligned} \tag{64}$$

By stable limit cycle we mean that any solution of Equation (59) tends toward the limit cycle, provided it initiated closely enough to $\tilde{\eta}_{LC}$. If the limit cycle is unstable, the solution will diverge from it, no matter how close to $\tilde{\eta}_{LC}$ it originated. Summarizing, we state: the necessary and sufficient condition for an MR to experience a nutation limit cycle is that $\tilde{\eta}_{LC}$, evaluated from Equation (60), has a positive value and that the nutation root is unstable; i.e., $\bar{\xi}_N > 0$.

Next we want to show that this condition can only be satisfied if the linear Magnus moment derivative $C_{\ell_{\hat{\omega}_\beta}}$ is negative. The damping derivatives $C_{\ell_{\hat{p}}}$ and $C_{n_{\hat{R}}}$ can only be negative. In order for $\bar{\xi}_N$ to be positive, $C_{\ell_{\hat{\omega}_\beta}}$ must be negative. If $C_{\ell_{\hat{\omega}}}$ is a nonlinear function of β in the range $\pm$ 20°, a negative $C_{\ell_{\hat{\omega}_\beta}}$ will be accompanied by a positive $C_{\ell_{\hat{\omega}_{\beta^3}}}$, and, thus, Equation (60) has a positive value.

The cone angle of the limit cycle, $\tilde{\eta}_{LC}$, does not depend on the state of the planar trajectory. Therefore, once it has reached $\tilde{\eta}_{LC}$, an MR will maintain this cone angle, even though it might still be in

the transient glide phase. Consider Equation (59). The rate of change of $\dot{\tilde{\eta}}$ in the transient glide phase is proportional to the only variable $\bar{V}_n$. The higher the velocity, the greater $\dot{\tilde{\eta}}$.

In general, it is undesirable for an MR to nutate in a stable limit cycle because it is detrimental to its performance. A properly designed MR must satisfy two conditions: the limit cycle is unstable, and the nutation root is stable. Both are fulfilled by $\bar{\xi}_N < 0$. Then any nutational motion of the spin axis will converge into a horizontal attitude. To avoid a limit cycle, the designer can choose a configuration with positive $C_{\ell_{\hat{\omega}_p}}$. However, because these shapes are not very common, he might accept a negative $C_{\ell_{\hat{\omega}_p}}$ but assure a negative $\bar{\xi}_N$ value by increasing the $\bar{I}_y / \bar{I}$ ratio or providing larger end plates to increase the aerodynamic damping derivatives. We conclude that it is very important to assure a stable nutation mode. An unstable nutation mode will either lead to a limit cycle, if $C_{\ell_{\hat{\omega}}}$ is sufficiently nonlinear, or to a divergent nutation and an ensuing tumbling motion.

The zeroth approximation predicts a circular limit cycle; i.e., the spin axis moves on the surface of a circular cone. To estimate the deviations from the circular motions, we consider the second harmonics of the first-order approximation of Equation (56) and write them in the form

$$\eta_{LC} = \tilde{\eta}_{LC}\left\{1 + A\cos 2\tilde{\delta} + B\sin 2\tilde{\delta}\right\} = \tilde{\eta}_{LC}\left\{1 + F\sin(2\tilde{\delta} + \chi)\right\} \quad (65)$$

where:

$$F = \left(A^2 + B^2\right)^{1/2} \quad ; \quad \chi = \tan^{-1}\frac{B}{A} \quad (66)$$

$$A = \frac{1}{4}\left(\frac{\bar{I}}{\bar{I}_y}\right)^2 \frac{\bar{V}_n^{\,2}}{\bar{\omega}_n^2 \mu \bar{I}} \left(C_{n_\beta} + \frac{1}{12} C_{n_{\beta^3}} \tilde{\eta}_{LC}^{\,2} \right) \tag{67}$$

$$B = \frac{1}{4}\left(\frac{\bar{I}}{\bar{I}_y}\right)^2 \frac{\bar{V}_n}{\bar{\omega}_n \mu^2 \bar{I}} \left[\left(-C_{\ell_{\hat{p}}} + C_{n_{\hat{r}}}\right)\frac{\bar{I}_y}{\bar{I}} + C_{\ell_{\hat{\omega}_\beta}} + \frac{1}{6} C_{\ell_{\hat{\omega}_{\beta^3}}} \tilde{\eta}_{LC}^{\,2} \right] \tag{68}$$

From Equation (65), it follows that the maximum deviation is given by F and occurs at $2\tilde{\delta} + \chi = \frac{\pi}{2}$ or

$$\tilde{\delta}_{max} = \frac{1}{2} \cot^{-1} \frac{B}{A} \tag{69}$$

We now extend our investigation to include the effect of the nonlinear damping derivatives $C_{\ell_{\hat{p}^3}}$ and $C_{n_{\hat{r}^3}}$. This means that, in Equation (31), the nonlinear terms g_{21}, g_{22}, g_{31}, and g_{32} are taken to be different from zero. The analysis proceeds just like in the first part of this section. However, we have to deal with the $\dot{\phi}^3$ and $\dot{\psi}^3$ expressed in gyromechanical angles that are quite awkward. To simplify the expressions, we restrict the validity of the ensuing equations to cone angles $2^\circ < \eta < 20^\circ$. Then we can use the approximate relationships:

$$\dot{\phi}^3 = -\eta^3 \dot{\delta}^3 \sin^3 \delta \tag{70}$$

$$\dot{\psi}^3 = -\eta^3 \dot{\delta}^3 \cos^3 \delta \tag{71}$$

After averaging the equations over one nutation cycle, we obtain the result equivalent to the Equations (54) and (55)

$$\eta = \tilde{\eta} + \frac{1}{4a_{23}^2}\Big\{\left(a_{31}\tilde{\eta} + \tfrac{1}{2}g_{31}\tilde{\eta}^3\right)\cos 2\tilde{\delta} + \Big[\left((-a_{22}+a_{33})a_{23}+a_{21}\right)\tilde{\eta} +$$

$$+ \left(\underline{(-g_{22}+g_{32})a_{23}^3} + g_{21}\right)\tilde{\eta}^3\Big]\sin 2\tilde{\delta} - \tag{72}$$

$$-\frac{1}{32a_{23}^2}\Big\{g_{31}\tilde{\eta}^3\cos 4\tilde{\delta} - \Big[\underline{(g_{22}+g_{32})a_{23}^2} - g_{21}\Big]\tilde{\eta}^3\sin 4\tilde{\delta}\Big\} + O\left(\frac{1}{\lambda^{12}}\right)$$

$$\frac{d\tilde{\eta}}{d\bar{t}} = \frac{1}{2a_{23}}\Big\{\Big[(a_{22}+a_{33})a_{23} - a_{21}\Big]\tilde{\eta} + \frac{3}{4}\Big[\underline{(g_{22}+g_{32})a_{23}^3} - g_{21}\Big]\tilde{\eta}^3\Big\} -$$

$$-\frac{1}{16a_{23}^3}\Big\{\Big[(-a_{22}+a_{33})a_{23}+a_{21}\Big]g_{31} - 2\Big[\underline{(-g_{22}+g_{32})a_{23}^2} + g_{21}\Big]a_{31}\Big\}\tilde{\eta}^3 + O\left(\frac{1}{\lambda^{12}}\right) \tag{73}$$

The underlined terms constitute the effect of the nonlinear aerodynamic damping. Like before we can find a limit cycle at

$$\tilde{\eta}_{LC}^2 = 8\,\frac{\left(C_{\ell_{\hat{p}}} + C_{n_{\hat{r}}}\right)\frac{\bar{I}_y}{\bar{I}} - C_{\ell_{\hat{\omega}_\beta}}}{C_{\ell_{\hat{\omega}_{\beta^3}}} - \left(\frac{\bar{I}_y}{\bar{I}}\right)^3\left(\frac{\bar{\omega}_n}{\mu\bar{V}_n}\right)^2\left(C_{\ell_{\hat{p}^3}} + C_{n_{\hat{r}^3}}\right)} \tag{74}$$

if, and only if, the right-hand side is positive and the nutation root is unstable. Compare Equation (74) with Equation (60). We have stated earlier that $C_{\ell_{\hat{\omega}_{\beta^3}}}$ is positive most of the time. Therefore, if $C_{\ell_{\hat{p}^3}} + C_{n_{\hat{r}^3}}$ are positive (i.e., if damping diminishes for higher nutation rates), the cone angle of the limit cycle is larger than that given by Equation (60). For increased damping at high nutation rates, the limit cycle will be smaller.

14. COMPUTER SIMULATIONS AND TEST RESULTS

In this chapter, the dynamics of actual Magnus rotor flight models are investigated. The basic configurations are shown in Figure 1.1, and they are classified by the form of the cross-sections as cylindrical, triangular, and rectangular Magnus rotors. Some sample trajectories are calculated, using the equations of motion from Table 12.1, as programmed for computer in Appendix B. The mass and aerodynamic input data are given in Appendix C. Wind tunnel data from NACA Langley, Aerojet General, and Arnold Research Organization are used to obtain the aerodynamic derivatives. To validate the assumptions of the previous chapters, order-of-magnitude comparisons are made of the pertinent terms. Finally, the Magnus rotor models were flight tested, and the results are correlated with computer simulations.

14.1 COMPUTED FLIGHT HISTORIES

The calculations of the trajectories and attitude motions are based on the equations of motion (Table 12.1), with the additional simplifying assumptions that the aerodynamic coefficients and the air density are constant. This implies aerodynamic coefficients independent of the Reynolds and Mach numbers and a short flight during which the air density does not change appreciably. Because we are mostly concerned with transient and short-time attitude motions, the last assumption is not very restrictive. Moreover, the computer program is easily extended to include a variable

density atmosphere. To limit the calculations to the incompressible flight region is a more serious restriction. It had to be made to simplify the calculations and because of the lack of reliable transonic and supersonic wind tunnel data. The justification for neglecting the dependence on the Reynolds number will be given next.

Extensive studies have been performed to investigate the Reynolds number effect on externally driven, smooth cylinders, e.g., those of Van Aken and Kelly (26) and Swanson (27). Van Aken and Kelly show that the Magnus lift coefficient is sensitive to changes in Reynolds number if (i) the test Reynolds number is close to the critical value of the nonspinning cylinder, and (ii) the tip-speed ratio is below 0.6. The critical Reynolds number for smooth cylinders is approximately 4×10^5. They explain this sensitivity by the flow separation on the bottom and the top of the cylinder caused by the flow transition from laminar to turbulent and vice versa. For tip-speed ratios above 0.6 and at high supercritical Reynolds numbers, no Reynolds number effect was observed.

The MR's investigated in this chapter have a steady-state Reynolds number between 10^5 to 3×10^5 and a steady-state tip speed ratio between 0.4 and 1.2. In the transient glide phase, we experience a Reynolds number range of 10^4 to 10^6 and a tip-speed range of 0.1 to 20. Thus, the MR's are well within the critical range. However, because an MR is never a smooth cylinder but always has sharp driving vanes, no laminar flow is expected to develop and no flow transition can occur. Therefore, even for low Reynolds numbers, the MR should fly supercritically, and the dependence of the aerodynamic coefficients on the Reynolds number can be neglected. The limited wind tunnel tests that have been conducted support this assumption.

The purpose of this section is to provide a broad sample of flight histories for the reader so that he can develop a "feel" for the flight dynamics of MR's. Table 14.1, page 173, summarizes the computer simulations. The MR's are the same as the models used in the flight tests. Their most important physical characteristics are included in the table. For more details, refer to the run sheets and drawings in Appendix C.

The first flight histories, Run 13, simulate a typical low speed release of a rectangular MR from a helicopter with a transient nutational motion about a horizontal axis. They are graphed in Figures 14.1 through 14.4. Flight speed, glide angle, and spin rate are highly dampened. A small overshoot occurs first in the flight speed, which causes a delayed overshoot in the spin rate and the glide angle. The transient nutation is also dampened with an increasing cyclic frequency according to the increase of the spin rate. The vacuum approximation for the nutation frequency, Equation (13.37), is in real time:

$$\Omega_N = \dot{\delta} = \frac{I_y}{I} \gamma \omega_R \tag{1}$$

It correlates very closely with the actual nutation frequency of Figure 14.4. The Rectangular MR 1 has a steady-state lift/drag (L/D) ratio of 2.16 and a steady-state tip speed ratio $\hat{\omega}_{SS}$ of 1.13. It is the best performer of all shapes investigated in this report.

Its high transient spin-up potential is illustrated in Figures 14.5 and 14.6. The initial linear and rotational kinetic energy is converted into potential energy, resulting in a full loop. This Computer Run 15 simulates the launch of an MR with overspin from an aircraft. It is assumed that the spin axis is rolled 3 degrees from the horizontal. The

ensuing lateral motions are shown in Figure 14.7. To show the influence of the deceleration of the center of mass on the stability, as discussed in Section 13.2, the equations of motion were solved again in Run 23, but without the acceleration term $\dot{\bar{V}}_R / \bar{V}_R$. The result is a more stable lateral motion. Therefore, in agreement with Section 13.2, the effect of the decelerated center of mass is destabilizing.

To show that an accelerated center of mass is stabilizing, a typical flight history is graphed in Figures 14.8 and 14.9. Run 25 is the solution of the complete equations of motion, while the acceleration term has been deleted in Run 24. Much effort was spent in Chapters 3 through 10 to derive the perturbation equations of an MR about an accelerated reference flight. Figures 14.7 and 14.9 justify the travail.

Refer back to the end of Chapter 6 for the definition of a positive spin axis. The MR is said to be launched with a positive spin if the angular velocity vector has the same direction as the spin axis. All pre-spun MR's are launched with a positive spin because, in the other case, the driving vanes would de-spin the MR immediately, causing it to tumble until it reorients itself and picks up positive spin. On the other hand, an MR can be released with a positive or negative horizontal linear velocity component. In Computer Run 15, it is positive. This is the normal case. It is also called the "lift-up" launch, because the lift force initially points upward. A launch with a negative horizontal linear velocity component is the "lift-down" case. Figures 14.10 through 14.12 show such a "lift-down" flight history. The initial conditions are those of Run 15, except for a negative horizontal linear velocity component. The effect can be seen in Figure 14.11. As a charged particle in a magnetic

field, the MR is subjected for the first two seconds to a centripetal force, the Magnus lift, resulting in a near circular trajectory. Because the overspin is so high, it loops again before reaching the steady-state glide phase.

Next, we simulate the flight of a triangular MR in the Figures 14.13 through 14.15. We assume that the MR is launched with a high horizontal linear velocity component, low spin rate, and a roll angle of 3 degree. The MR rapidly picks up spin and climbs to approximately 30 meter above release while losing much of its velocity. Consequently, even though the spin rate is still high, the Magnus lift force is small and the MR starts descending towards its steady-state glide phase. The Triangular MR 1 is not as good a performer as the Rectangular MR 1. Its steady-state values are L/D = 1.50 and $\hat{\omega}_{ss}$ = 0.77. The attitude motions, Figure 14.15, exhibit a transient nutation that is quickly dampened out. The roll and yaw angles reach a steady-state value of $\phi_s = -0.13$ degree and $\psi_s = 0.20$ degree. This means, according to Figure 13.1, that the MR is heading in a new direction with its spin axis still horizontal. A check is provided by Equations (13.5) and (13.6). The change in heading angle Ψ is calculated from:

$$\Psi = \left(\psi_s^2 + \phi_s^2\right)^{1/2} \tag{2}$$

A simulation of the release of a cylindrical MR is shown in Figures 14.16 and 14.17. It is launched with a small linear velocity and a high spin rate. Because of the high moment of inertia about the spin axis, the Cylindrical MR 1 loses its rotational speed only slowly. In Figure 14.16 the steady-state values are not yet reached. They are: $V_{ss} = 23.7$ m/sec

$\omega_{ss} = 1574$ RPM ; $\gamma_{ss} = -42.3°$. With a L/D = 1.10 and $\hat{\omega}_{ss}$ = 0.53, the Cylindrical MR 1 is the poorest performer among the three shapes investigated so far. It was also assumed that initially $\beta = 3$ degree. Because of the small linear velocity at launch, the sideslip vanishes quickly. After 1.5 sec of flight time, it is below 0.1 degree. The effect on the roll and yaw angle is negligible.

So far the aerodynamic stability coefficients of the MR's behaved sufficiently linear to be represented by the linear stability derivatives only. Now we shall investigate two Magnus rotor shapes whose rolling moment coefficients exhibit a nonlinear behavior at the origin. They are the cylindrical MR without end plates and the rectangular MR with cut-off end plates. The nutational motions in steady-state glide phase are simulated for each shape with two different moment of inertia rations I/I_y. First, we choose for the cylindrical MR 4A, I/I_y = 2.19, which, according to Equation (13.60), results in a limit cycle with η_{LC} = 12.5 degree. The result is plotted in Figure 14.18. In particular, note the circular motion as predicted by the zeroth order approximation (see Section 13.3). The corrections are indeed small. Furthermore, in good agreement is the approximated nutation frequency Ω_N = 9.63 CPS, as calculated from Equation (1), with the exact nutation frequency Ω_N = 9.80 CPS from Computer Run 30. In Section 13.3 we stated that one way to eliminate the limit cycle is to decrease the ratio I/I_y. Figure 14.19 shows the result for I/I_y = 1.28. The other possibility is to increase the damping by end plates. This was demonstrated by Computer Run 40.

A similar result is obtained for the rectangular MR with cut-off end plates. The noncircular end plates lower the aerodynamic damping and

generate a nonlinear behavior of the rolling and yawing moment coefficients. Equation (13.60) predicts a steady-state limit cycle at $\eta_{uc} = 1.36$ degree, which is in very close agreement with Figure 14.20. We also notice again that the limit cycle is very nearly circular, as predicted by the zeroth approximation. A decrease of the I/I_y ratio to 8.50 dampens the nutation cycle. This is demonstrated by Computer Run 37 in Figure 14.21, using the initial conditions of Run 36. The other method of eliminating the limit cycle (i.e., the increase in aerodynamic damping through larger end plates) leads back to the circular end plates of the Rectangular MR 1, as exemplified in the Figures 14.1 to 14.4.

FIGURES	RUN	CONFIGURATION	END PLATE	I/I_y	MASS KG	μ	SEE* FIG.	SIMULATION
14.1-14.4	13	RECT. MR 1	Circular	6.70	1.500	841	C.1	Transient nutation
14.5-14.7	15,23	RECT. MR 1	Circular	6.70	1.500	841	C.1	Deceleration from high speeds. Effect of deceleration.
14.8-14.9	24,25	RECT. MR 1	Circular	6.70	1.500	841	C.1	Accelerated flight. Effect of acceleration.
14.10-14.12	21	RECT. MR 1	Circular	6.70	1.500	841	C.1	"Lift-down" deceleration from high speeds.
14.13-14.15	39	TRIA. MR 1	Circular	4.40	2.395	549	C.2	Deceleration from high speed and low spin rate.
14.16-14.17	40	CYL. MR 1	Circular	2.41	3.148	1450	C.3	Deceleration from low speed and high spin rate.
14.18	30	CYL. MR 4A	None	2.19	2.137	1060	C.3	Limit cycle.
14.19	31	CYL. MR 11	None	1.28	2.580	1280	C.3	Dampened nutation cycles.
14.20	36	RECT. MR 2	Cut-off	12.00	1.607	965	C.1	Limit cycle.
14.21	37	RECT. MR 3	Cut-off	8.50	1.367	829	C.1	Dampened nutation cycles.

* Figure numbers refer to Appendix C.

TABLE 14.1 COMPUTER SIMULATIONS

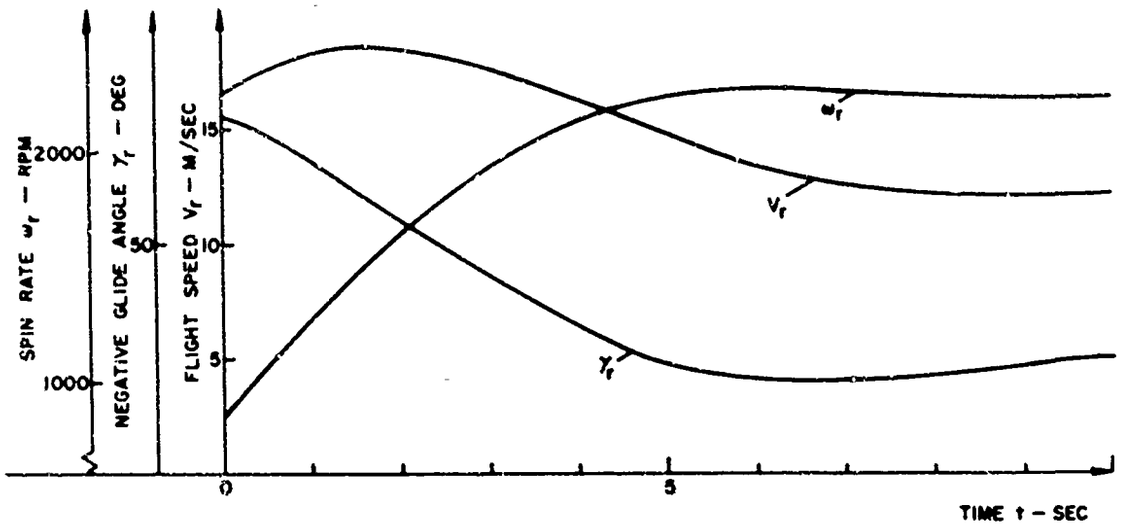

FIGURE 14.1 TRANSIENT PERFORMANCE OF RECTANGULAR MAGNUS ROTOR 1. COMPUTER RUN 13

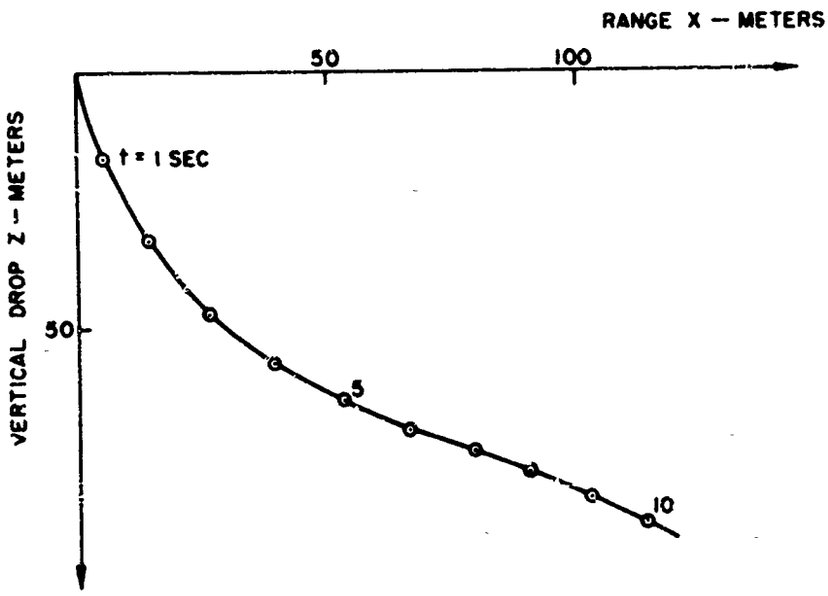

FIGURE 14.2 TRANSIENT TRAJECTORY OF RECTANGULAR MAGNUS ROTOR 1. COMPUTER RUN 13

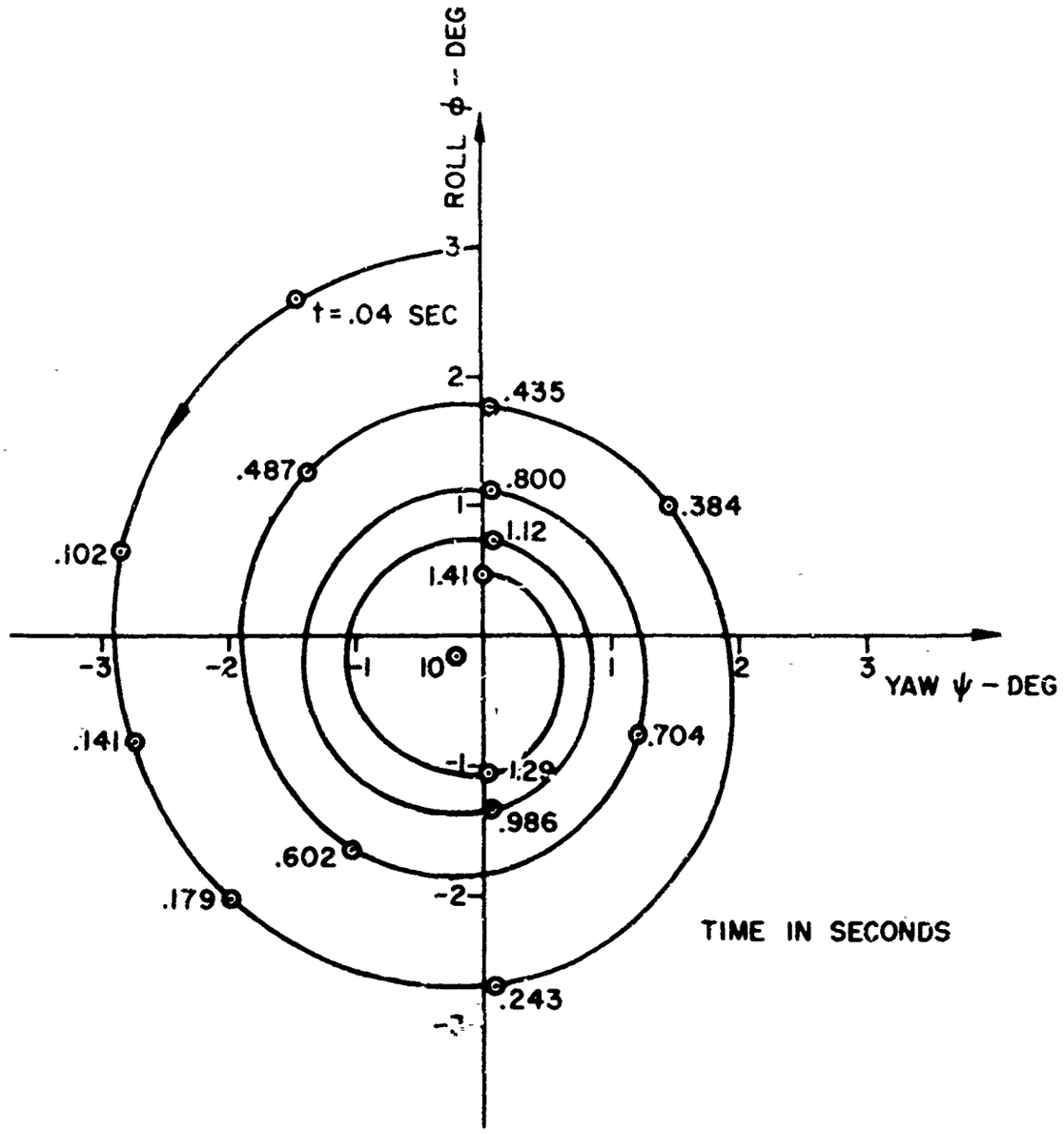

FIGURE 14.3 TRANSIENT NUTATION OF RECTANGULAR MAGNUS ROTOR 1. COMPUTER RUN 13

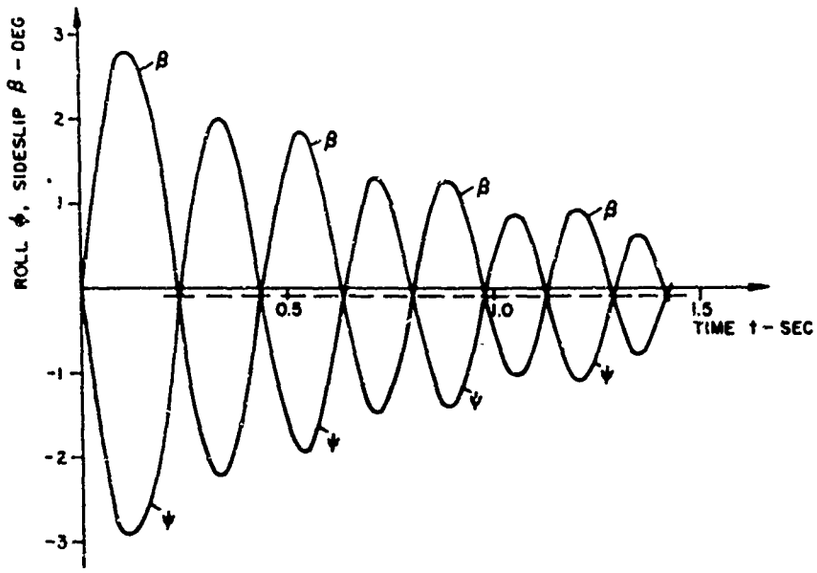

FIGURE 14.4 TRANSIENT NUTATION OF RECTANGULAR MAGNUS ROTOR 1.COMPUTER RUN 13

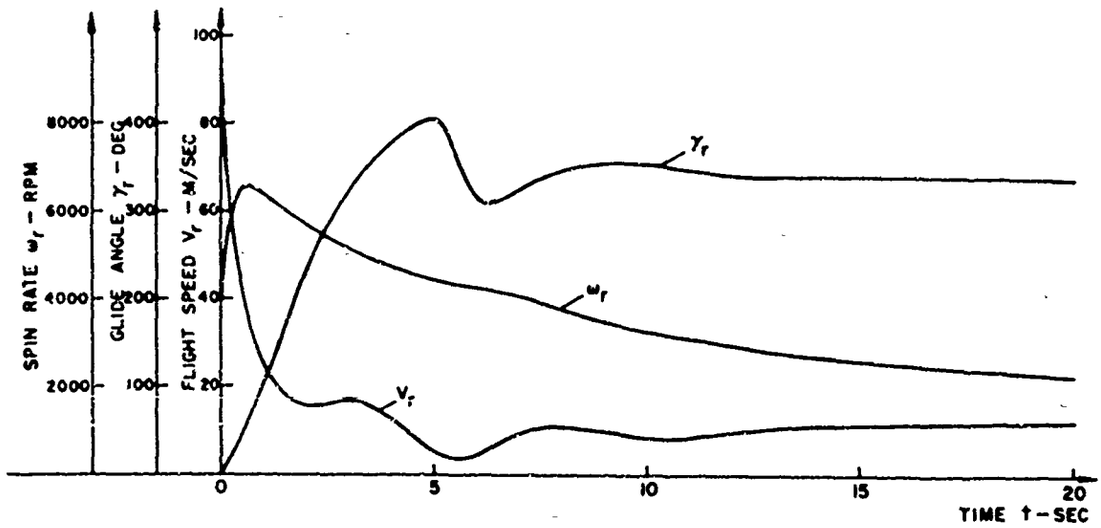

FIGURE 14.5 HIGH SPEED TRANSIENT PERFORMANCE OF RECTANGULAR MAGNUS ROTOR 1. COMPUTER RUN 15

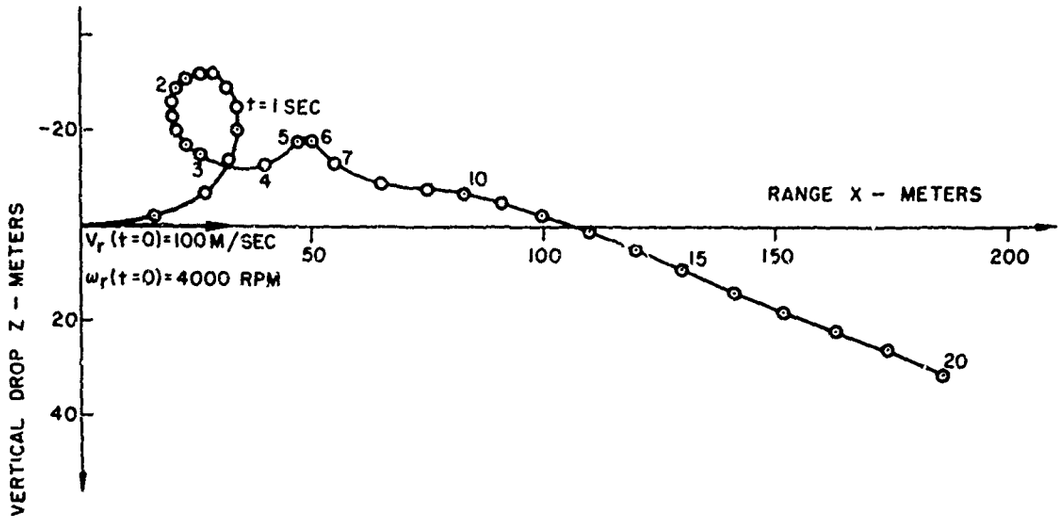

FIGURE 14.6 HIGH SPEED TRANSIENT TRAJECTORY OF RECTANGULAR MAGNUS ROTOR 1 COMPUTER RUN 15

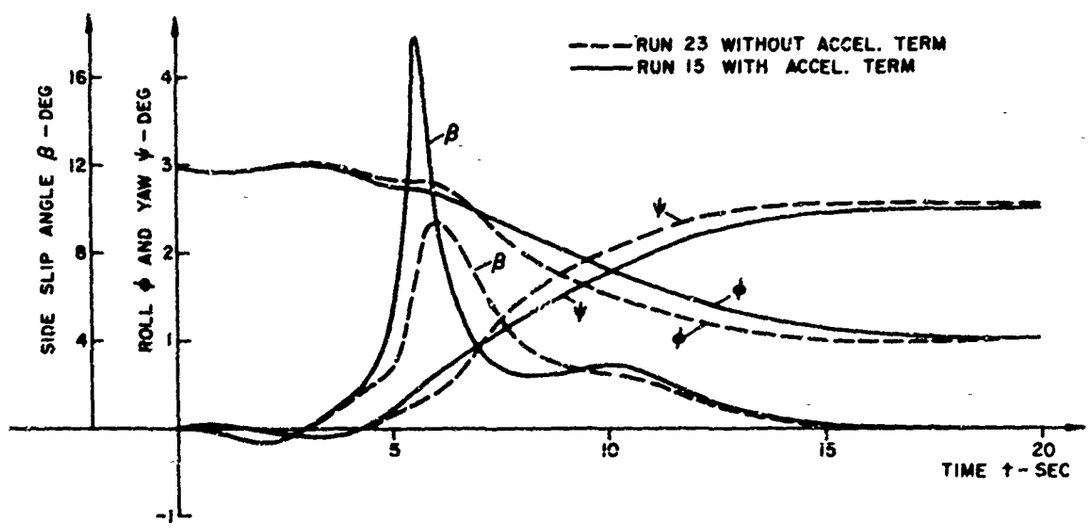

FIGURE 14.7 LATERAL MOTIONS WITH AND WITHOUT ACCELERATION TERM OF RECTANGULAR MAGNUS ROTOR 1. COMPUTER RUNS 15 AND 23

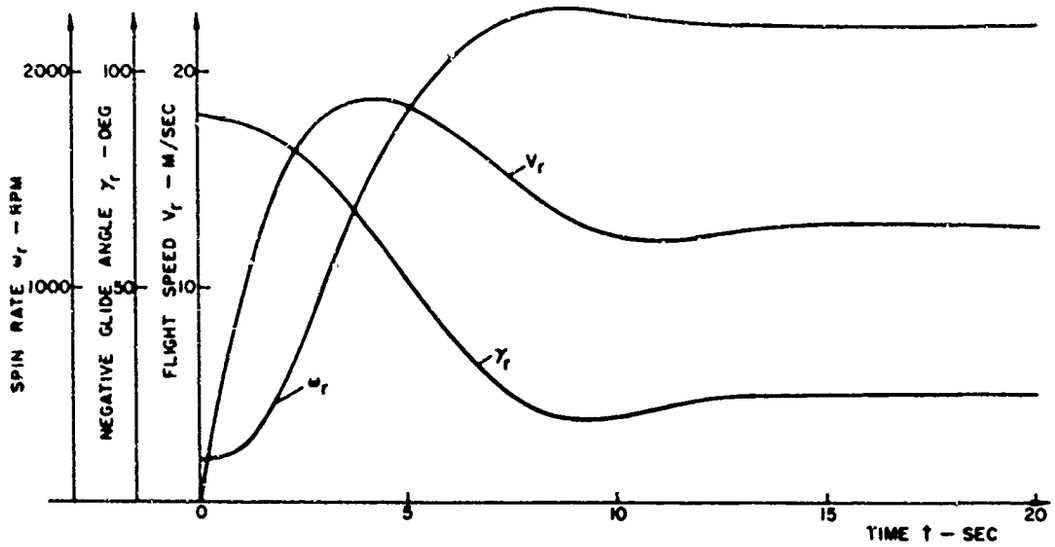

FIGURE 14.8 PERFORMANCE OF ACCELERATED RECTANGULAR MAGNUS ROTOR 1. COMPUTER RUNS 24 AND 25

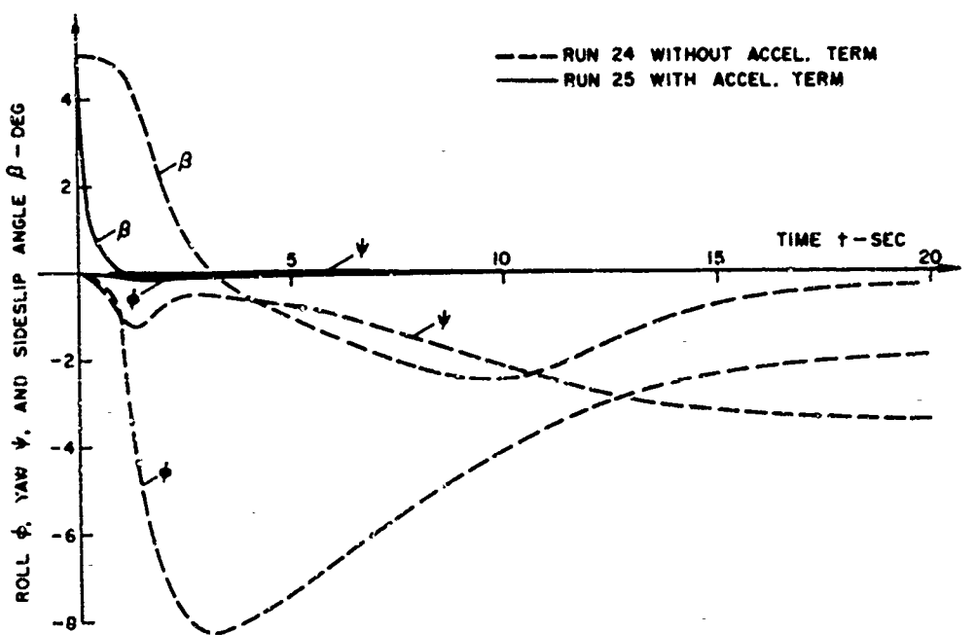

FIGURE 14.9 LATERAL MOTIONS WITH AND WITHOUT ACCELERATION TERM OF RECTANGULAR MAGNUS ROTOR 1. COMPUTER RUNS 24 AND 25

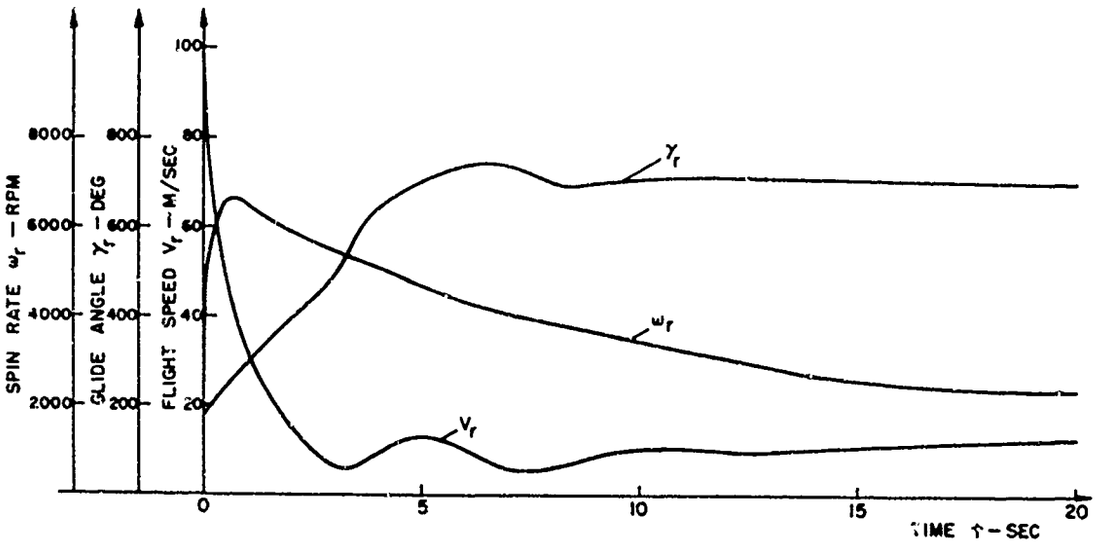

FIGURE 14.10 "LIFT-DOWN" HIGH SPEED TRANSIENT PERFORMANCE OF RECTANGULAR MAGNUS ROTOR 1. COMPUTER RUN 21

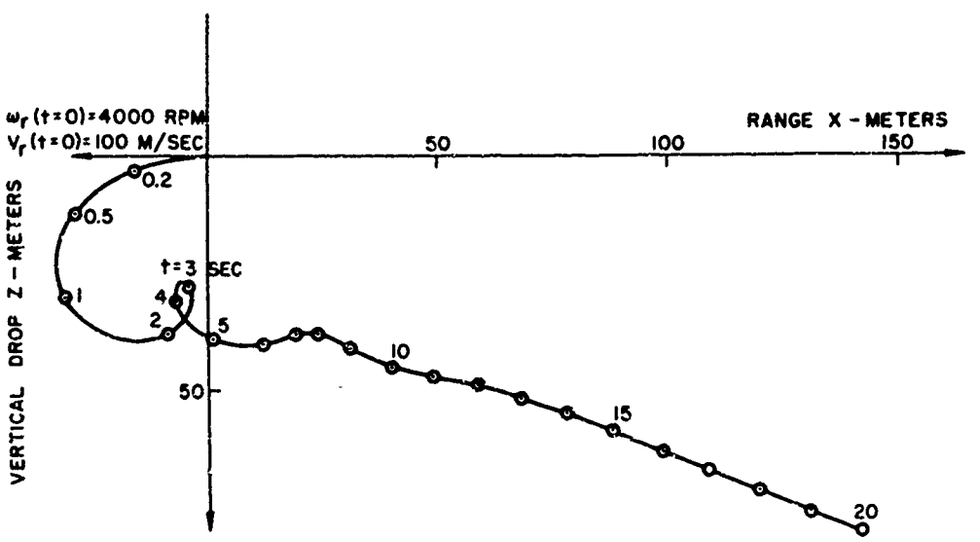

FIGURE 14.11 "LIFT-DOWN" HIGH SPEED TRANSIENT TRAJECTORY OF RECTANGULAR MAGNUS ROTOR 1. COMPUTER RUN 21

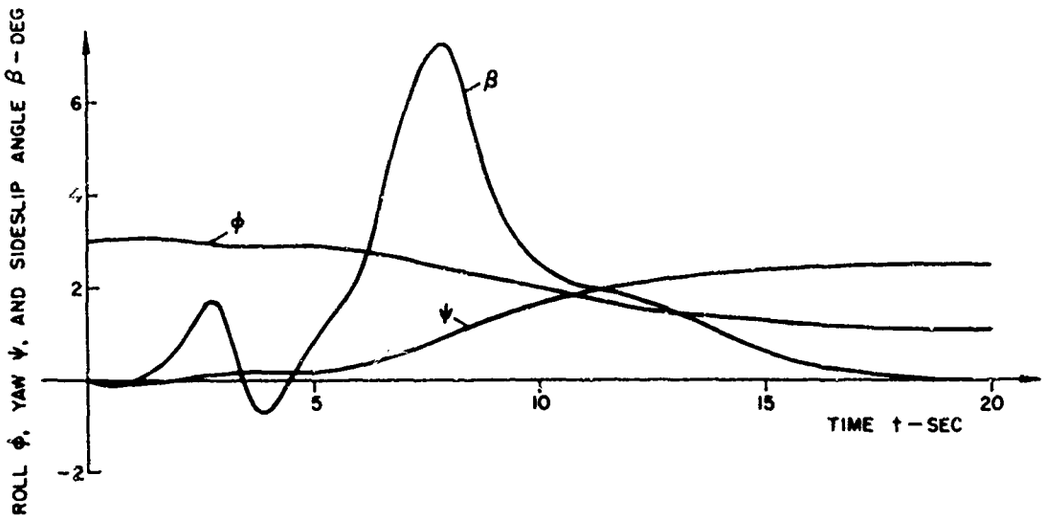

FIGURE 14.12 "LIFT-DOWN" LATERAL MOTIONS OF RECTANGULAR MAGNUS ROTOR 1. COMPUTER RUN 21

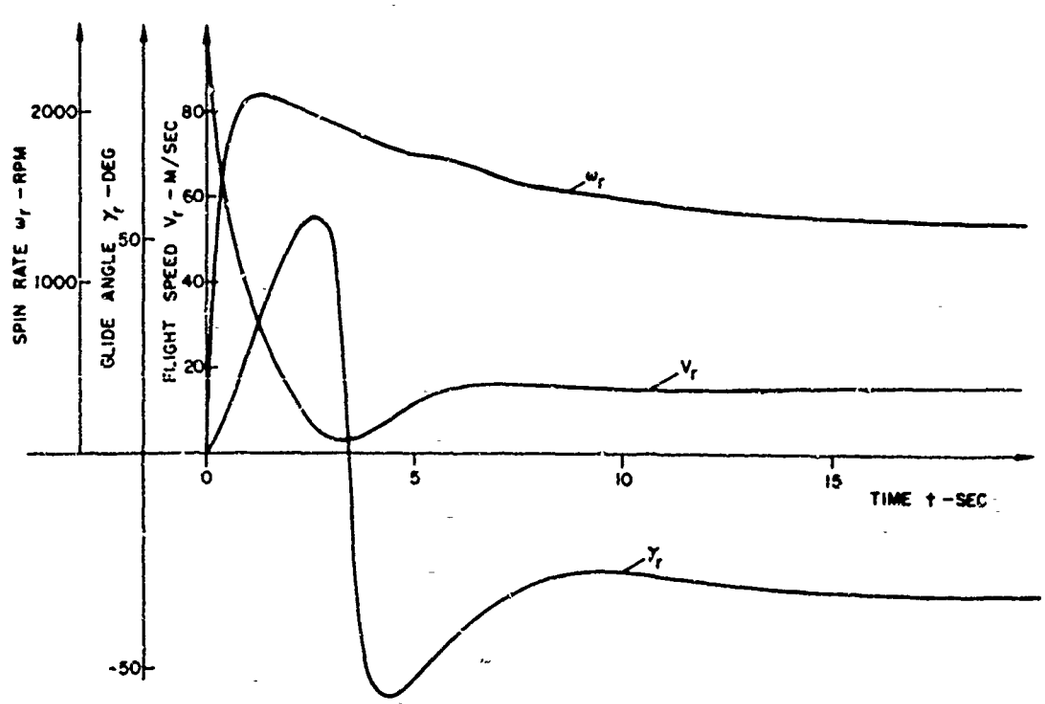

FIGURE 14.13 HIGH SPEED, LOW SPIN RATE TRANSIENT PERFORMANCE OF TRIANGULAR MAGNUS ROTOR 1. COMPUTER RUN 39

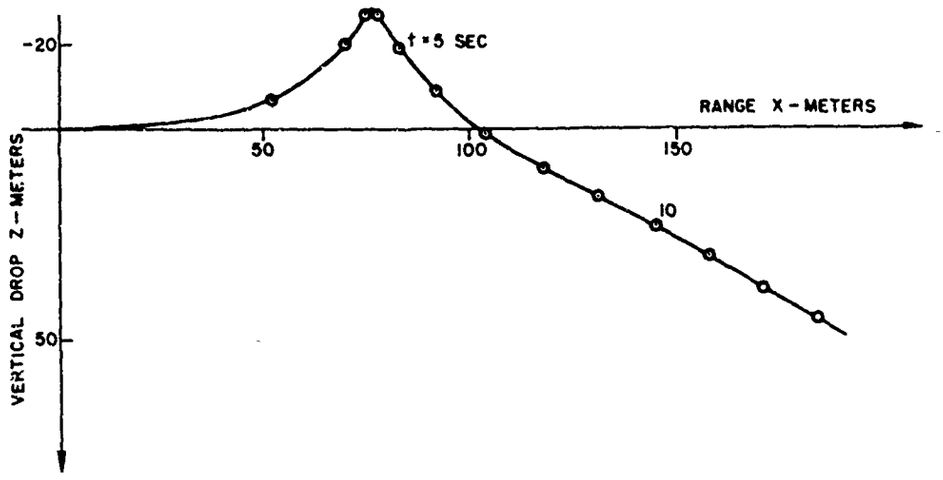

FIGURE 14.14 TRANSIENT TRAJECTORY OF TRIANGULAR MAGNUS ROTOR 1. COMPUTER RUN 39

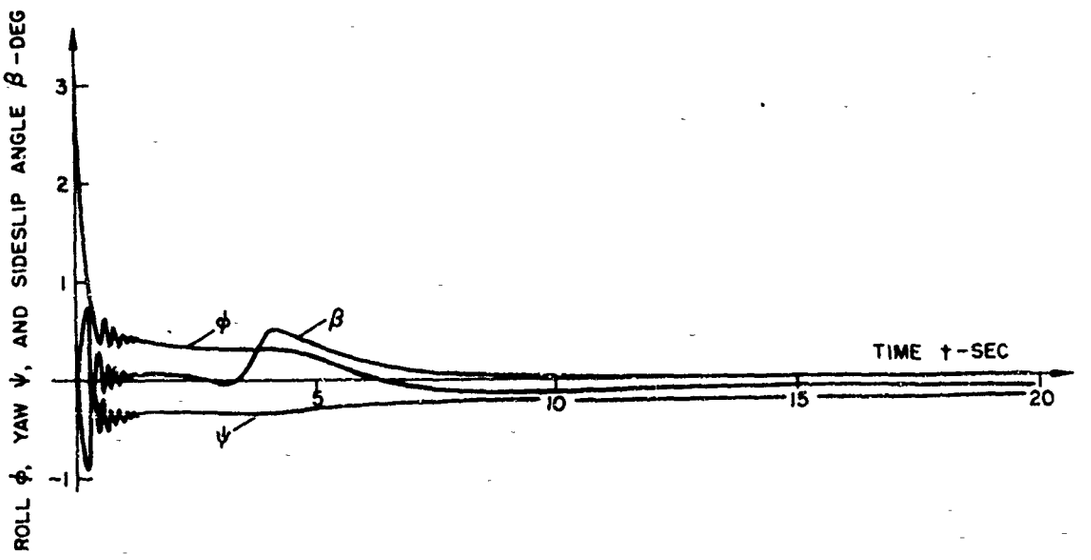

FIGURE 14.15 TRANSIENT ATTITUDE MOTIONS OF TRIANGULAR MAGNUS ROTOR 1. COMPUTER RUN 39

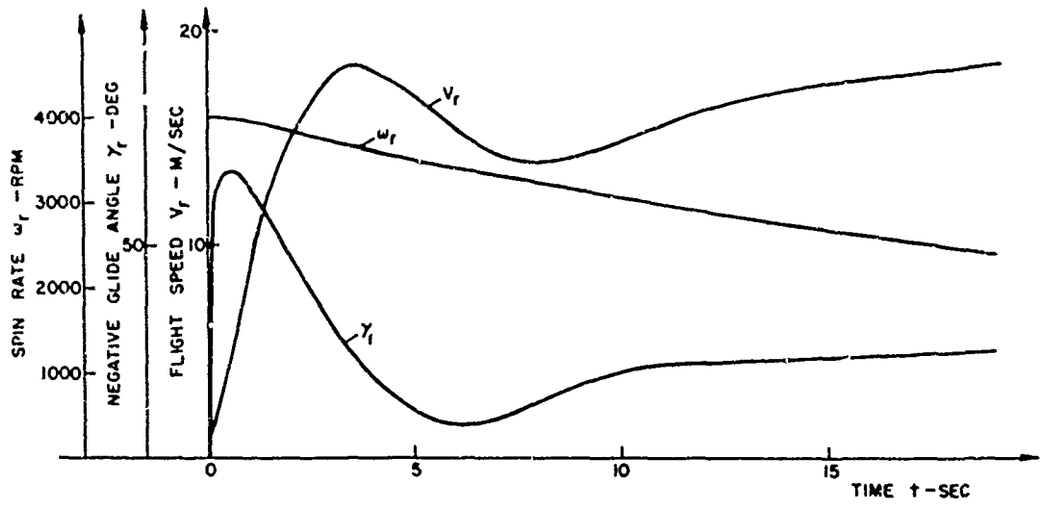

FIGURE 14.16 LOW SPEED; HIGH SPIN RATE TRANSIENT PERFORMANCE OF CYLINDRICAL MAGNUS ROTOR 1. COMPUTER RUN 40

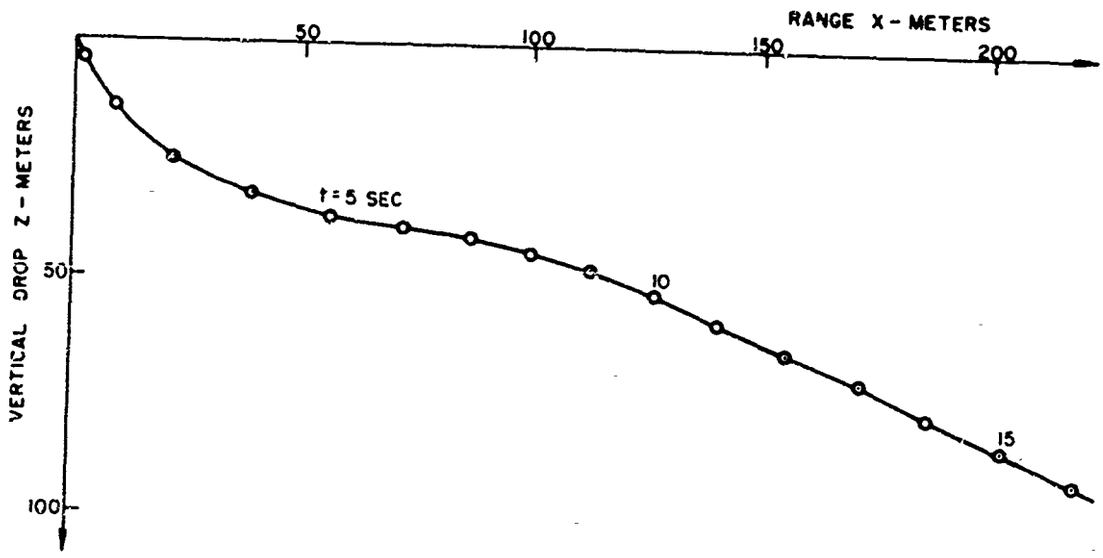

FIGURE 14.17 TRANSIENT TRAJECTORY OF CYLINDRICAL MAGNUS ROTOR 1. COMPUTER RUN 40

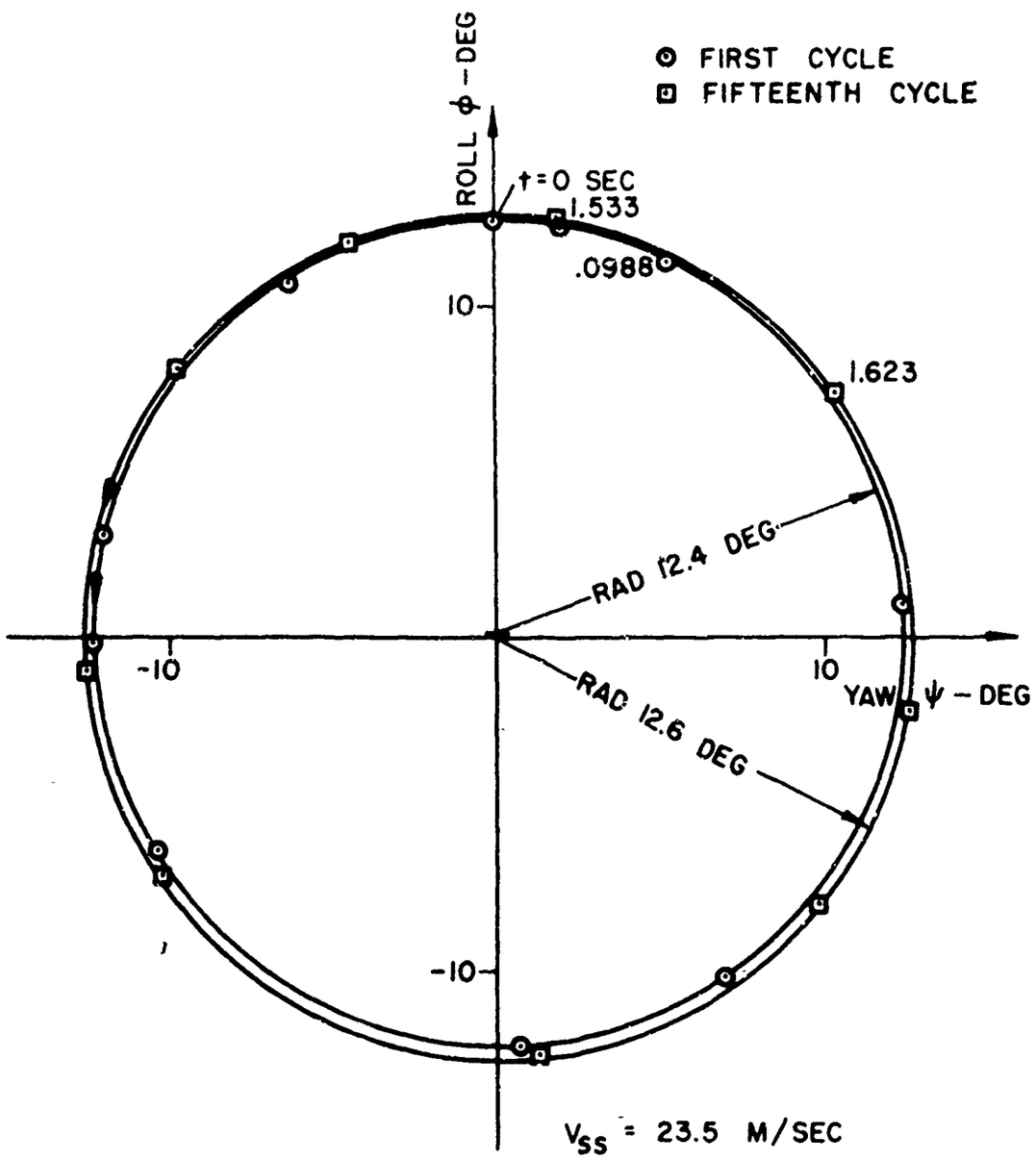

V_{SS} = 23.5 M/SEC

Ω_N = 9.80 CPS

ω_{SS} = 1266 RPM

γ_{SS} = -57 DEG

FIGURE 14.18 STEADY-STATE LIMIT CYCLE OF CYLINDRICAL MAGNUS ROTOR 4A. COMPUTER RUN 30

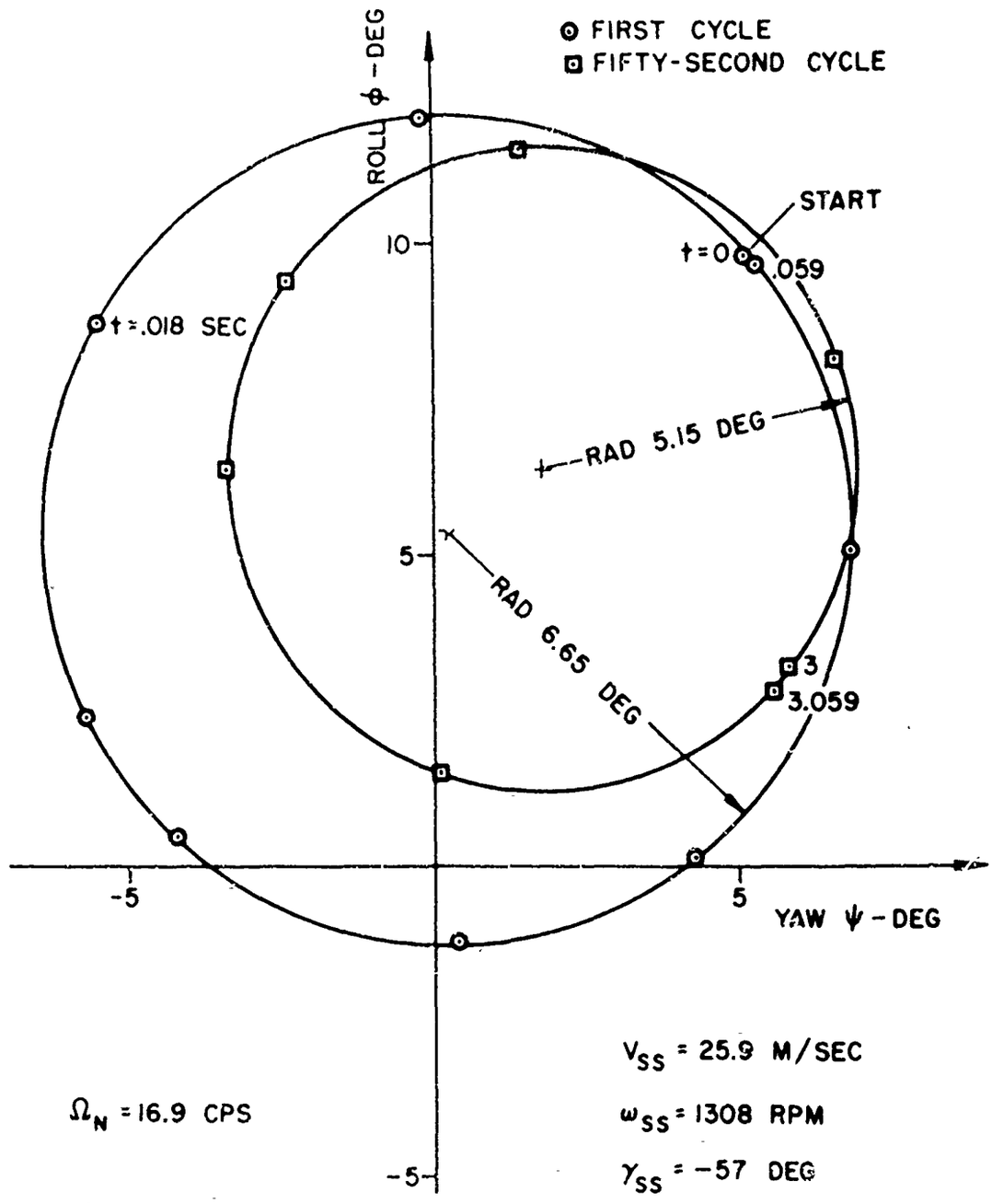

FIGURE 14.19 DAMPENED NUTATION CYCLES IN STEADY-STATE FLIGHT OF CYLINDRICAL MAGNUS ROTOR 11. COMPUTER RUN 31

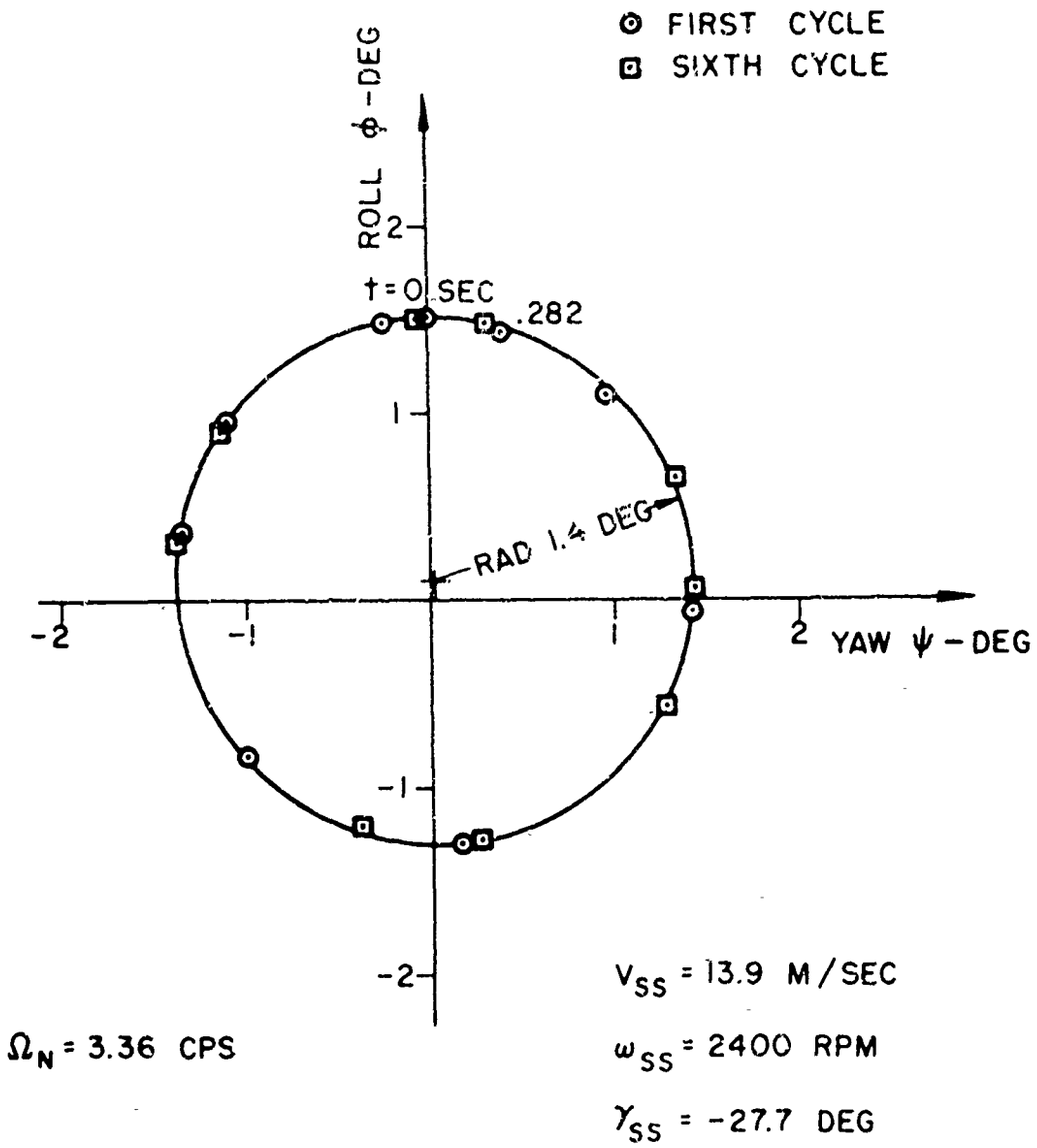

FIGURE 14.20 LIMIT CYCLE IN STEADY-STATE FLIGHT OF RECTANGULAR MAGNUS ROTOR 2. COMPUTER RUN 36

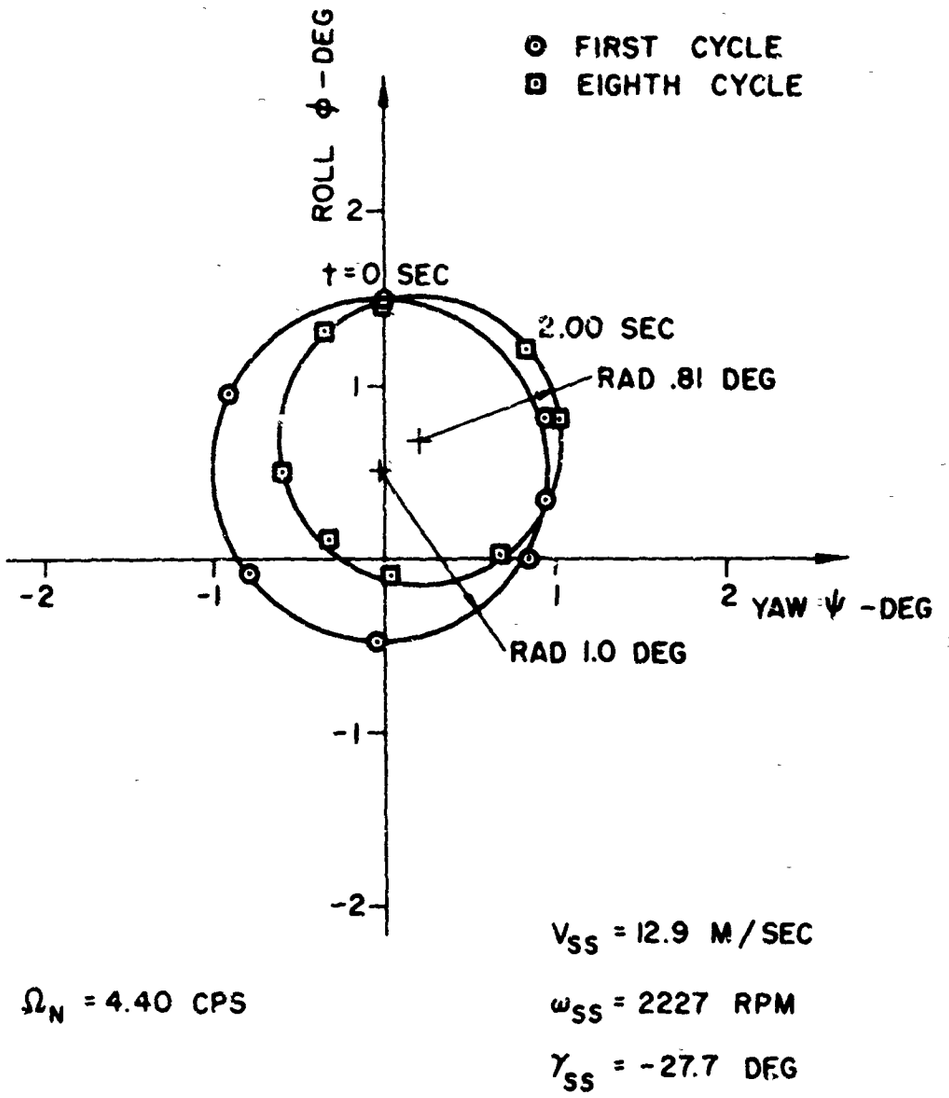

FIGURE 14.21 DAMPENED NUTATION CYCLES IN STEADY-STATE FLIGHT OF RECTANGULAR MAGNUS ROTOR 3. COMPUTER RUN 37

14.2 VALIDATION OF ASSUMPTIONS

Let us go back to the earlier chapters and scrutinize the assumptions in view of the flight simulations of the previous Section 14.1. In Chapter 2, the basic Assumption 3 can be directly related to the mass parameter $\mu = 2m/\rho S l$, as it has been done in Assumption 5 of Section 12.4. The individual values for our Magnus rotor models satisfy the condition $\mathcal{O}(\mu) \geqq 10^2$, as shown in Table 14.1. Furthermore, a check shows that Assumptions 3 and 6 of Section 12.4 hold for all computer simulations. The justification for Assumption 2 will be part of the following outline.

During the derivation of the equations of motion, we have made several order-of-magnitude estimates to simplify some of the terms. The more important ones are summarized in Table 14.2. The first three estimates should be greater than 100. The next order-of-magnitude term relates to Equation (10.25), which includes the unknown term $\delta\ddot{\gamma} = \ddot{\gamma}_p - \ddot{\gamma}_n$. However, from the previous computer runs, we know that $\ddot{\gamma}_n$ changes slowly for most parts of the flight. Therefore, the perturbation $\delta\ddot{\gamma}$ is also a small term. To verify Equation (10.25), it is left to show that $\mathcal{O}\{\delta\dot{\alpha}_p\}$ is large throughout the trajectory and in particular at the maximum value of $\ddot{\gamma}_n$, where the largest $\delta\ddot{\gamma}$ can be expected. This value is given in Table 14.2. The order of magnitude requirements on the remaining estimates are only $\geqq 10$ because they are used to arrive at simplified formulas, which can always be checked out by the exact computer calculations.

ORDER OF MAGNITUDE	REFERENCE	RUN 13	TIME SEC	RUN 15	TIME SEC	RUN 40	TIME SEC	
$\sigma\{\dot{\alpha}_n / \dot{\gamma}_n\} \geq 100$	Eq. 8.47	790	2	254	5.6	41	3.5	
$\sigma\{\dot{\delta} / \dot{\eta}\} \geq 100$	Eq. 9.13	263	0.2	2000	9	258	0.5	
$\sigma\{\dot{\delta} / \dot{\gamma}_n\} \geq 100$	Eq. 10.8	118	2	38	5.6	17	3.5	
$\sigma\{\dot{\delta}\dot{\alpha}_p\}$ @ max $\dot{\gamma}_n$	Eq. 10.25	245	2	1.2×10^4	5.6	10^3	3.5	
$\sigma\{(a_{22}+a_{33})\dot{\delta} / \dot{\delta}^2\} \geq 10$	Eq. 13.38	19	0	2	0	2	0	
$\sigma\{a_{23} / a_{22}\} \geq 10$	Eq. 13.20	33	0	743	0	6.5	0	
$\sigma\{a_{23} / a_{33}\} \geq 10$	Eq. 13.20	14	0	314	0	2.7	0	
$\sigma\{a_{23}^2 / a_{21}\} \geq 10$	Eq. 13.20	33	0	1575	0.7	33	1.3	
$\sigma\{a_{23}^2 / a_{31}\} \geq 10$	Eq. 13.20	11	0	9×10^4	0	2.7	0	
$\sigma\{a_{23}^2 / a_{11}\} \geq 10$	Eq. 13.20	588	0	4.5×10^4	20	270	0	

TABLE 14.2 VALIDATION OF ORDER OF MAGNITUDE ESTIMATES

As a sample we use three computer runs. Run 13 represents a typical drop test, while Runs 15 and 40 give some extreme release conditions. In Table 14.2, the minimum values of the order-of-magnitude terms during a particular run are given, together with their times of occurrence. Run 13 fulfills all conditions. Two of the order-of-magnitude estimates in Run 15 and six in Run 40 are not satisfied. But in all cases this is due to the extreme transient behavior and lasts only a fraction of the total flight. The closer to the steady-state glide phase, the better the conditions hold. Therefore, even though the order of magnitude estimates are not satisfied throughout, computer Runs 15 and 40 simulate the flights of the respective MR's accurately enough.

At the conclusion of Section 13.2, we introduced the two-degrees-of-freedom lateral equations of motion to study the nutational motions. The simplifications were based on the assumption that $\beta = -\psi$. To validate this assumption, the initial conditions of Run 13 were chosen so that only the nutation mode would be excited. The transient time history of β and ψ are shown in Figure 14.4. Because the initial conditions were not matched exactly, a constant ψ value of 0.1 degree is superimposed. If we disregard this effect, β and $-\psi$ are equal within 3%. An even better agreement is found in Run 30. There is no constant ψ and $\beta = -\psi$ within 0.5% accuracy. In Run 36 β and $-\psi$ are within 3%.

An important assumption that leads to the one-degree-of-freedom equation of Section 13.3 is expressed in Equation (13.37). Table 14.3 compares the approximate and exact values. They lie within 2% of each other. An equally good agreement of the transient nutation frequencies is given in Figure 14.22.

RUN	NUTATION FREQUENCY (CPS) FROM $\delta^{o} = a_{33}$	COMPUTER RUN
30	9.63	9.80
31	17.08	16.90
36	3.33	3.36
37	4.36	4.40

TABLE 14.3 STEADY-STATE NUTATION FREQUENCIES

Finally, we want to show that the zeroth order approximation of the one-degree-of-freedom equation of motion, Equation (13.59), gives an accurate account of the nutational motions. The test case is the prediction of a limit cycle. We refer to the Figures 14.18 and 14.20. In both cases the nutation angle calculated from Equation (13.60) is within 3% of the value obtained from the exact Computer Runs 30 and 36. Furthermore, the zeroth order approximation requires a circular limit cycle. This is well demonstrated in the Figures 14.18 and 14.20.

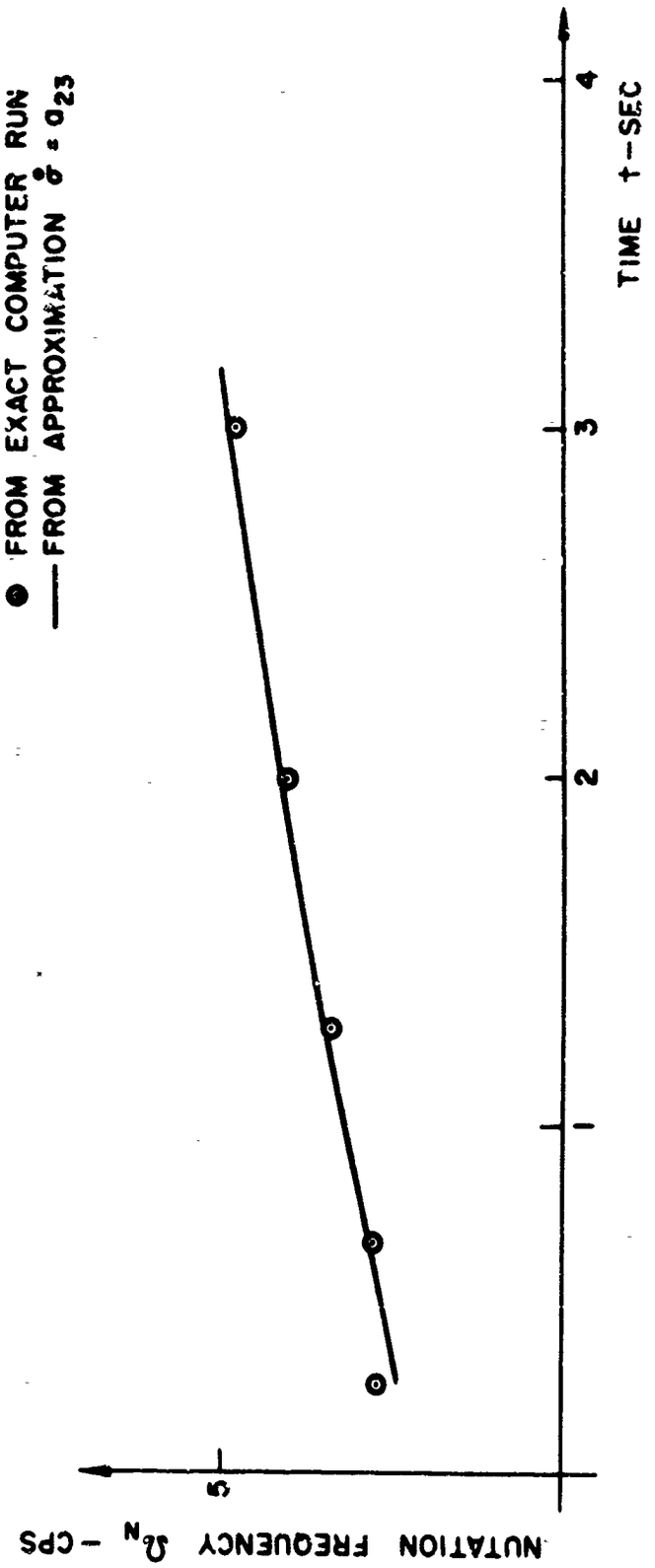

FIGURE 14.22 COMPARISON OF EXACT AND APPROXIMATE TRANSIENT NUTATION FREQUENCIES OF RECTANGULAR MAGNUS ROTOR 1. COMPUTER RUN 13

14.3 FLIGHT TEST RESULTS

The flight tests were conducted between June 1968 and June 1970. The test area was equipped with two man-operated turrets to track the flight models. One turret carried a high-speed 16-mm Millikan movie camera with an 800-mm telephoto lens. The angles of the turrets were recorded digitally in half-second time intervals and fed into a computer to yield space coordinates, velocity and glide angle. To obtain the attitude angles, the film was processed through a photoanalyzer.

Prior to each test a pilot balloon was released and tracked. The balloon data were used by the computer to correct the MR tracking results for the mean wind. The flight models were launched from a hovering helicopter either by hand or by a so-called jo-jo method; i.e., a canvas wrapped around the MR provided the initial spin rate. This limited the release conditions to low speed and small spin rates.

Several error sources must be considered when interpreting the data:

1. Human error. The turret operator follows the MR through a monocular with a solid view angle of 0.6 degree, the same as the angle of the 800-mm camera lens. No corrections are made if the model is not centered on the film.
2. Mechanical error. Backlash in the encoders and gear boxes amounts to approximately 0.3 degree.
3. Wind error. Changes in wind speed and direction during test and local gusts cannot be accounted for.
4. Helicopter downwash error. At release the helicopter rotor blades induce a downward velocity on the MR. No correction is made for this effect.

5. Photoanalyzer error. The two attitude angles ψ and ϕ are projected on the plane film surface. A separate estimate of ψ and ϕ can only be made with an error of 25%. However, for the nutation and limit cycle tests, only the projection of the nutation cone angle η on a plane is required. If the MR flies straight towards the camera, this angle can be measured within $\pm$ 0.25 degree.

Thirty MR's representing 8 different types were drop tested. The best test of each category was analyzed. They are summarized in Table 14.4. The purpose of the tests was to validate some of the theoretical predictions, to show the influence of end plates and moment-of-inertia ratios, and to develop test methods to determine the nutational damping derivatives.

To achieve the proper moment-of-inertia ratios, various materials (aluminum, steel, brass, acrylic plastic, styrofoam) were used to build the flight models. Great care was taken to avoid mass unbalances. In Models RECT. MR 1, CYL. MR 1, and CYL. MR 3, a special impulse fixture was added to induce a nutational motion. The impulse was generated by two cylindrical tubes, located at both ends of the MR normal to the spin axes, containing one to 2.5 grams of black powder. An electronic timer fired two MK 1 Squibs, which in turn set off the black powder charges.

FIGURES	IDENTIFICATION	END PLATE	I/I_y	MASS KG.	TEST PURPOSE	DATA REFERENCE*
14.23-14.28	RECT. MR 1	Circular	6.70	1.500	Trajectory, transient nutation, induced nutation	Fig.C.1; Run 19
14.29	RECT. MR 3	Cut-off	8.50	1.367	No limit cycle	Fig.C.1; Run 32
14.30	RECT. MR 2	Cut-off	12.00	1.607	Limit cycle	Fig.C.1; Run 36
14.31	TRIA. MR 1	Circular	4.40	2.395	Trajectory, transient nutation	Fig.C.2; Run 35
14.32,14.33	CYL. MR 1	Circular	2.41	3.148	Induced nutation	Fig.C.3; Run 34
14.34	CYL. MR 3	Circular	2.50	3.242	Induced nutation	Fig.C.3; Run 41
14.35	CYL. MR 11	None	2.19	2.137	Limit cycle	Fig.C.3; Run 38
14.36	CYL. MR 4A	None	1.28	2.580	No limit cycle	Fig.C.3; Run 30

* Figure and Run Numbers refer to Appendix C.

TABLE 14.4 ANALYZED FLIGHT TESTS

The first flight test results are shown in Figures 14.23 through 14.28, together with the computer simulation Run 19. A disturbance was introduced through impulse fixtures at 13.5 seconds into the flight. The induced nutational motion was analyzed from the film and graphed in Figure 14.28; it produced a 7% drop in the spin rate (see Figure 14.24). Its influence on the flight speed and glide angle, Figure 14.23, is less certain because wind, mechanical, and human errors can introduce an inaccuracy of the order ± 5%. But the result of the analytical investigation seems to be confirmed because the effect of lateral perturbations on the reference flight is small.

All results of the flight test of July 26 (Figures 14.23 through 14.27) are in good agreement with the computer simulation. This is due to the relatively weak wind (12 ft/sec) blowing from the turrets to the helicopter and the fact that the RECT. MR 1 flew straight towards the camera, such remaining only a short time in the downwash of the helicopter rotor. A transient nutation was also observed and recorded in Figure 14.27. The computer simulation shows a slowly changing rolling motion superimposed over the nutational motion. The photoanalyzer does not allow the extraction of such a slow motion from the film. Otherwise the agreement of the nutational frequencies and amplitudes is satisfactory.

To determine the aerodynamic damping derivatives from free-flight, the <u>Induced-Nutation Method</u> was tried out. An impulse is initiated during steady-state flight and the nutational response analyzed (see Figure 14.28). The time-to-halve-the-amplitude, t_{H_N}, and Equation (13.22) yield the damping derivatives:

$$C_{\ell_{\hat{p}}} + C_{n_{\hat{r}}} = \frac{\bar{I}}{\bar{I}_y}\left\{ C_{\ell_{\omega_\beta}} - \frac{1.386\,\tau\,\mu^2\,\bar{I}_y}{t_{H_N}} \right\} \tag{3}$$

The result, $C_{\ell_{\hat{p}}} + C_{n_{\hat{r}}}$ = -21.4, agrees well with NACA's value of -19.62 measured in the Langley Stability Tunnel. Notice also the constant nutation frequency throughout the decay. This confirms the linear perturbation equation as a good model of the flight dynamics.

The effect of cutting off the end plates at two sides is given next. We tested two models with different moment-of-inertia ratios, the Rectangular MR's 2 and 3. Because the aerodynamic coefficients behave nonlinearly at small sideslip angles, the possibility of limit cycles must be investigated. According to Equation (13.60), the Rectangular MR 3 is not capable of a limit cycle (See Figure 14.21). Its moment-of-inertia ratio $\bar{I}/\bar{I}_y$ is too low and its nutation mode, Equation (13.21), is stable. This was confirmed by a flight test. The transient performance is given in Figure 14.29. An increase in the $\bar{I}/\bar{I}_y$ ratio leads to a limit cycle. For the Rectangular MR 2, we calculated η_{LC} = 1.36 degree. The flight yielded η_{LC} = 1.25 degree as shown in Figure 14.30. The measured frequency of 3.75 CPS also compares favorably with Simulation Run 36, Figure 14.20, of 3.36 CPS.

In Figure 14.31, the flight test of the Triangular MR 1 is compared with the computer simulation. The model disintegrated after 9 seconds of flight time. Except for the spin history, the correlation is poor. This is probably due to the strong winds of 35 ft/sec during the test.

To obtain the unknown damping derivatives for the cylindrical MR with end plates, the induced-nutation method was used. Figure 14.32 shows such a typical transient flight performance. The correlation of the calculated with the measured flight speed is poor because of human error during the early tracking phase. Figures 14.33 and 14.34 give the decay of the nutation mode for the Cylindrical MR's 1 and 3. Using Equation (3) we obtain $C_{\ell_{\hat{p}}} + C_{n_{\hat{r}}}$ = -35 from Figure 14.33 and -27 from Figure 14.34. The mean value -31 will be used.

Without end plates the cylindrical MR exhibits a nonlinear behavior of the rolling and yawing moment coefficients. For $\bar{I}/\bar{I}_y$ = 1.28, the nutation mode is stable (see Figure 14.19), and no limit cycle is predicted by Equation (13.60). This was confirmed by the flight test of the Cylindrical MR 11. Its transient performance is correlated with the computer simulation in Figure 14.35. Again, because of the high winds, the glide angle and the flight speed do not check out well. If the $\bar{I}/\bar{I}_y$ ratio is increased to 2.19, a limit cycle exists, as shown by the computer simulation, Figure 14.20, and the flight test result, Figure 14.36.

There is an alternate method, the so-called <u>Limit-Cycle Method</u>, to measure damping derivatives from free-flight tests. It can be used if, through proper choice of the $\bar{I}/\bar{I}_y$ ratio, the MR performs steady-state limit cycles. The limit cycle cone angle η_{LC} is measured and the damping derivatives are evaluated from Equation (13.60):

$$C_{\ell_{\hat{p}}} + C_{n_{\hat{r}}} = \frac{\bar{I}}{\bar{I}_y}\left\{ C_{\ell_{\hat{\omega}_\beta}} + \frac{\eta_{LC}^2 C_{\ell_{\hat{\omega}_\beta}}}{8} \right\} \tag{4}$$

From Figure 14.36 we obtain for the Cylindrical Magnus Rotor 4A without end plates: $C_{\ell_{\hat{p}}} + C_{n_{\hat{r}}}$ = -3.2.

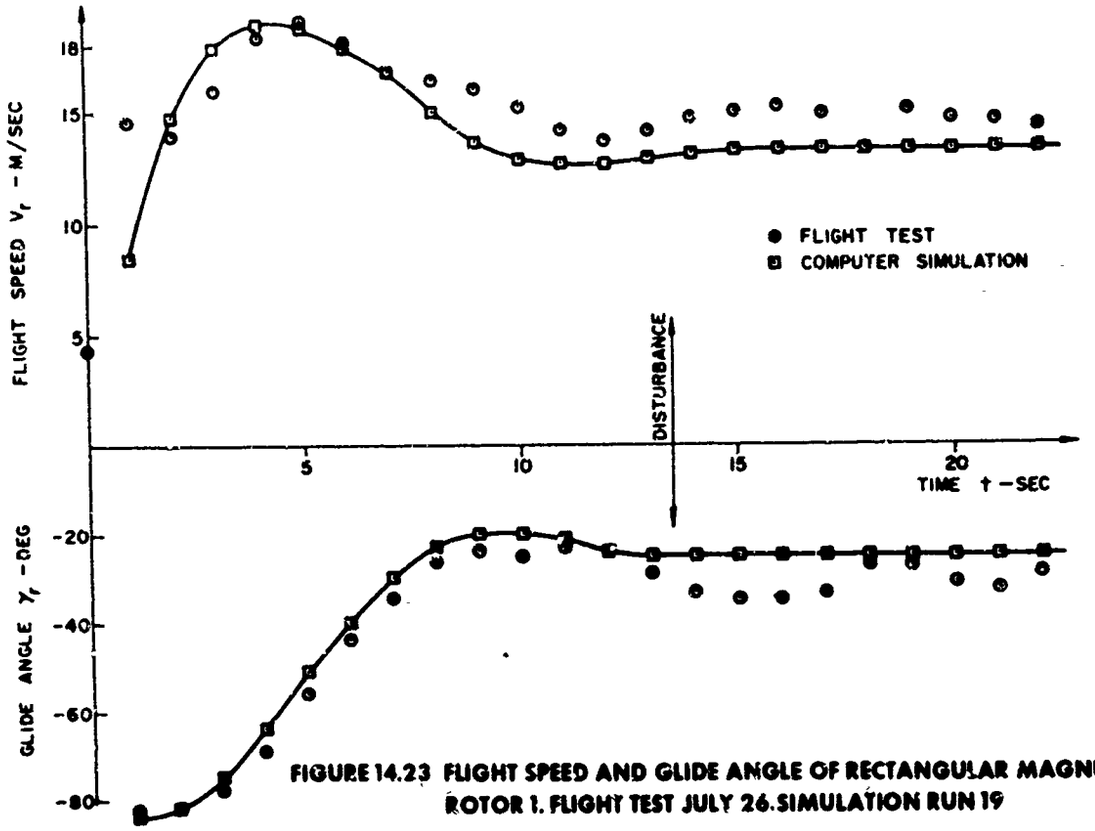

FIGURE 14.23 FLIGHT SPEED AND GLIDE ANGLE OF RECTANGULAR MAGNUS ROTOR 1. FLIGHT TEST JULY 26. SIMULATION RUN 19

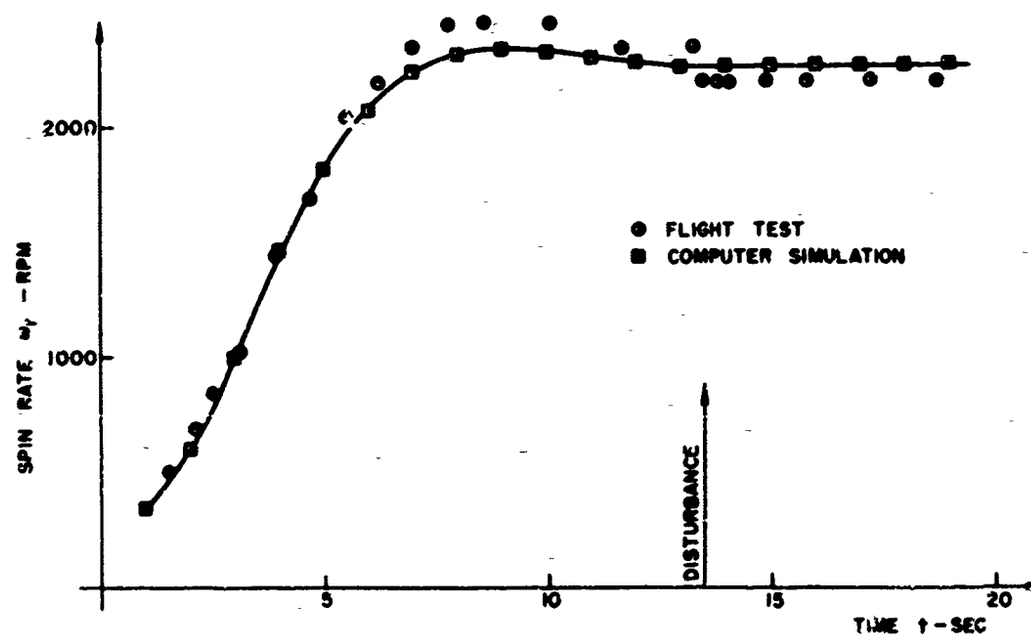

FIGURE 14.24 SPIN RATE OF RECTANGULAR MAGNUS ROTOR 1. FLIGHT TEST JULY 26. SIMULATION RUN 19

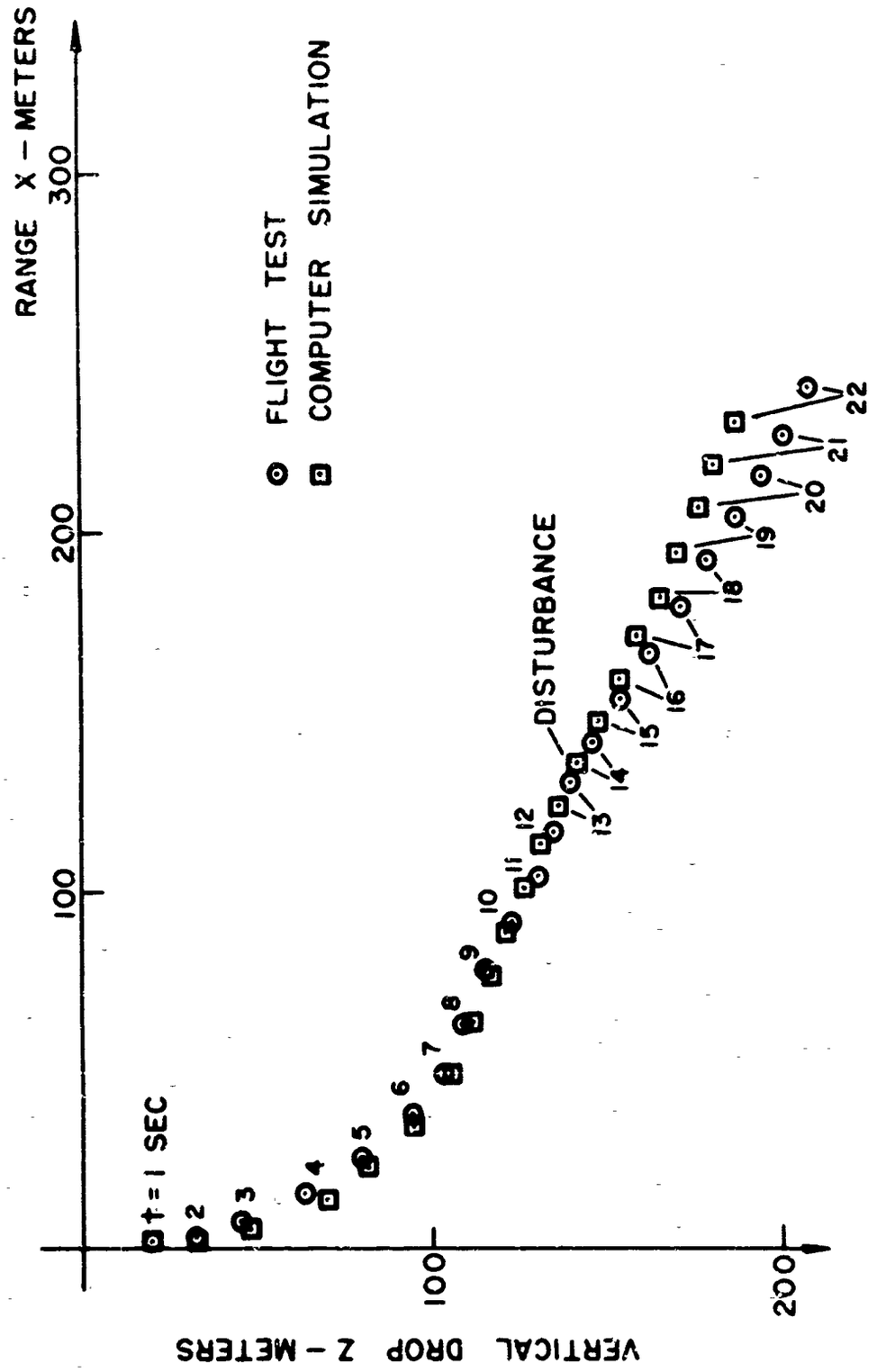

FIGURE 14.25 TRAJECTORY OF RECTANGULAR MAGNUS ROTOR 1. FLIGHT TEST JULY 26. SIMULATION RUN 19

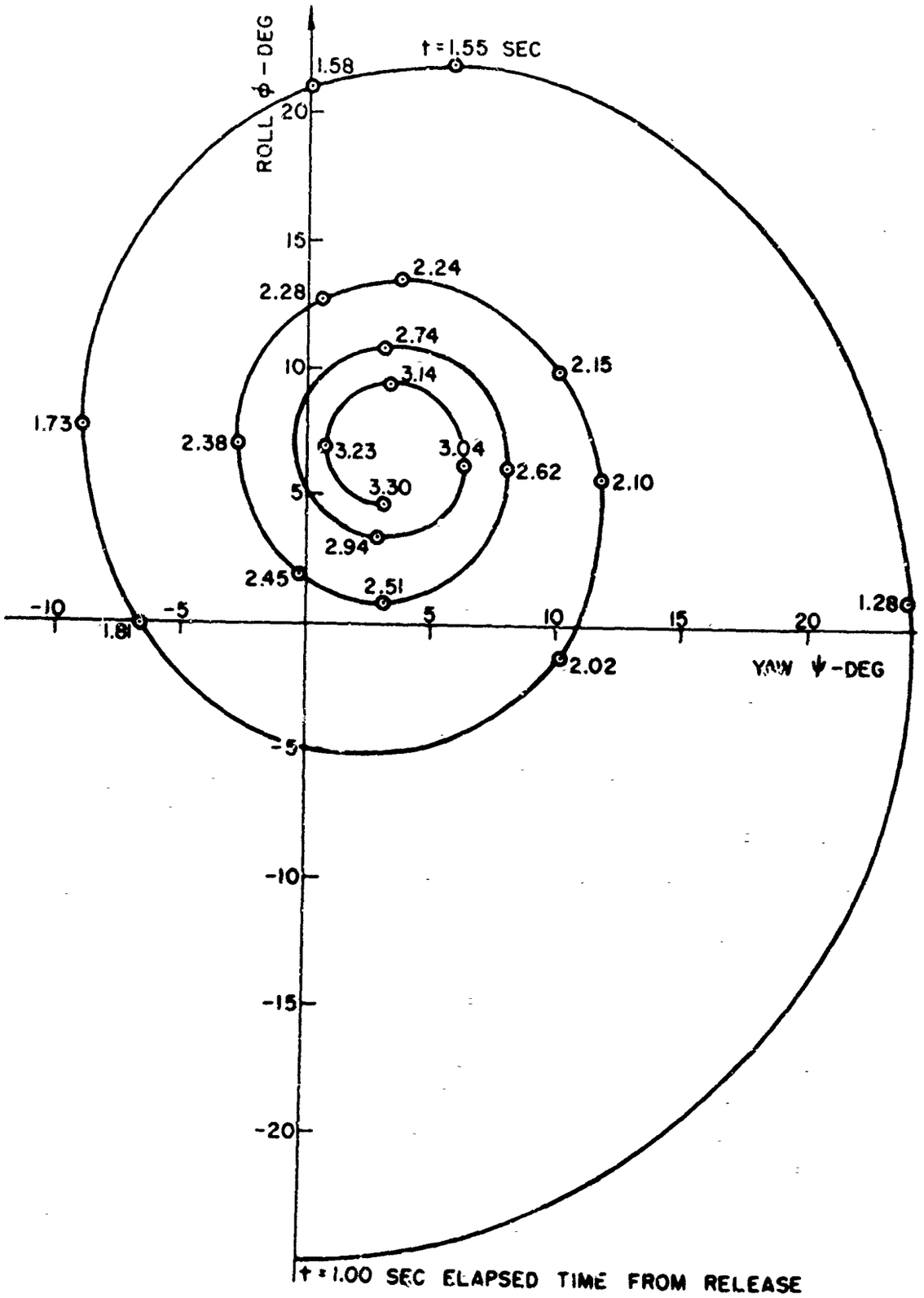

FIGURE 14.26 TRANSIENT NUTATION OF RECTANGULAR MAGNUS ROTOR 1 WITH INITIAL CONDITIONS FROM FLIGHT TEST JULY 26. SIMULATION RUN 19

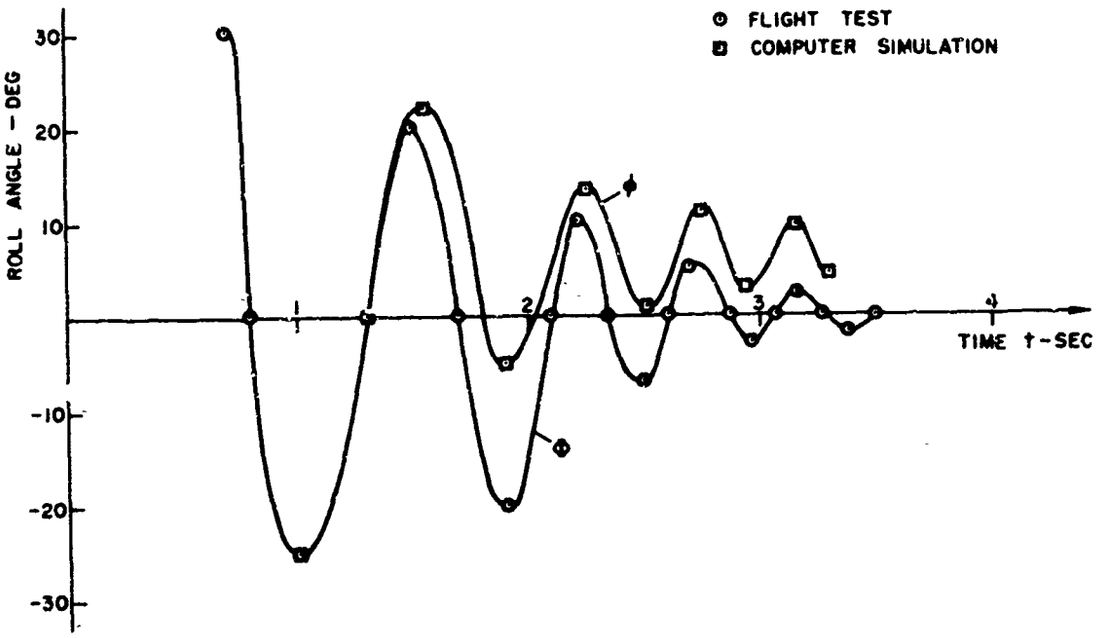

FIGURE 14.27 TRANSIENT NUTATION OF RECTANGULAR MAGNUS ROTOR 1. FLIGHT TEST JULY 26. SIMULATION RUN 19

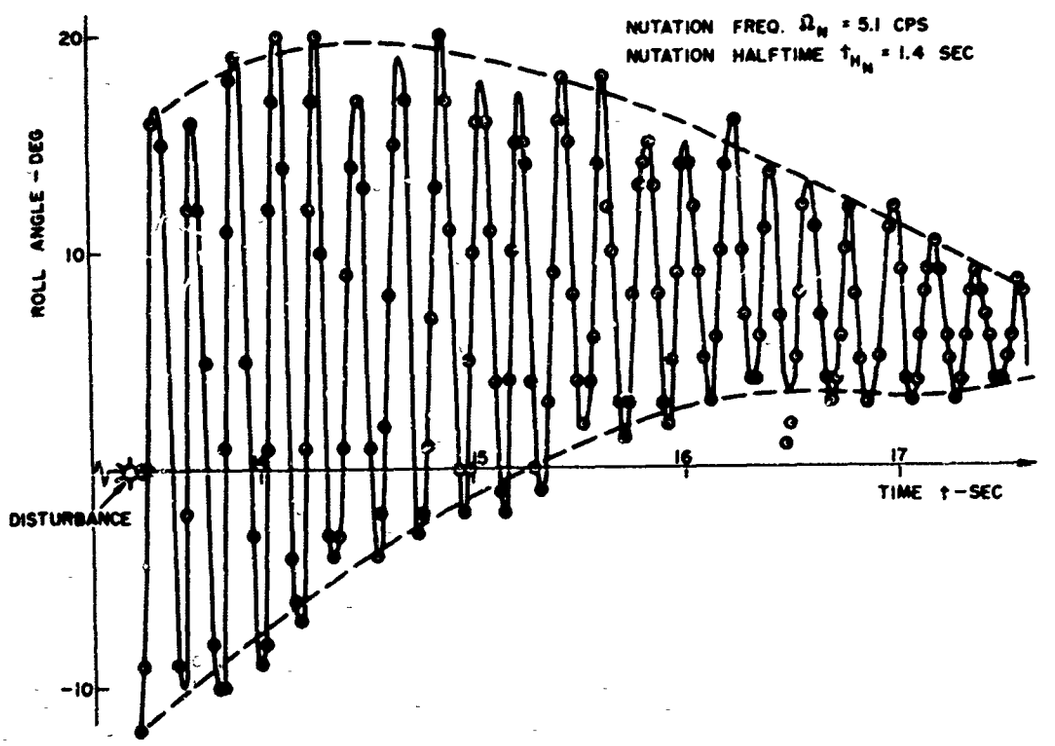

FIGURE 14.28 INDUCED NUTATION OF RECTANGULAR MAGNUS ROTOR 1. FLIGHT TEST JULY 26

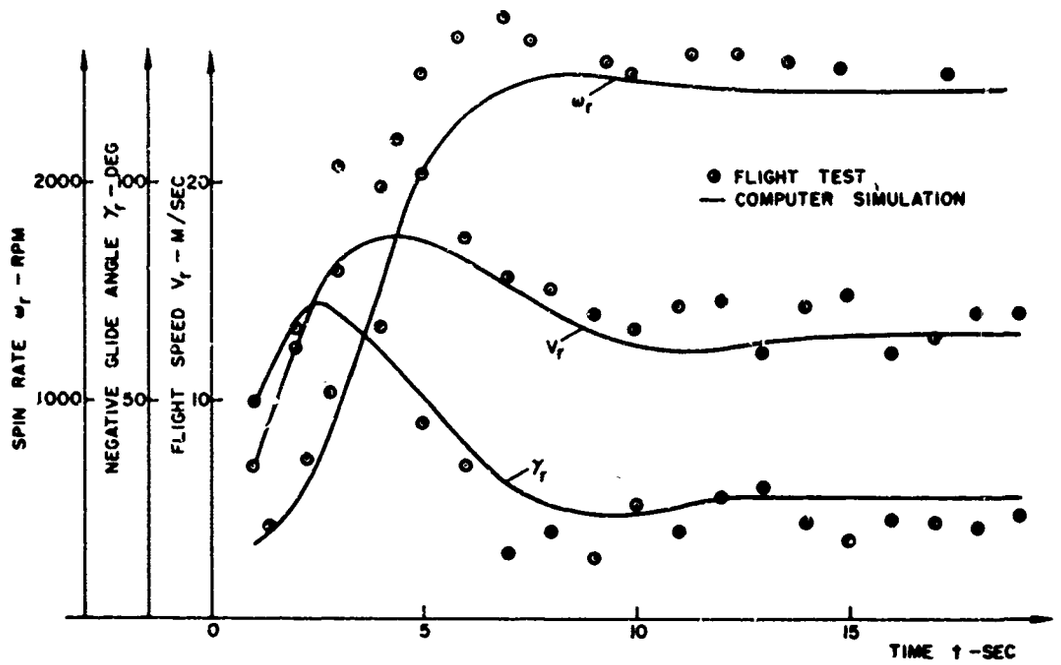

FIGURE 14.29 TRANSIENT PERFORMANCE OF RECTANGULAR MAGNUS ROTOR 3. FLIGHT TEST JUNE 10. SIMULATION RUN 32

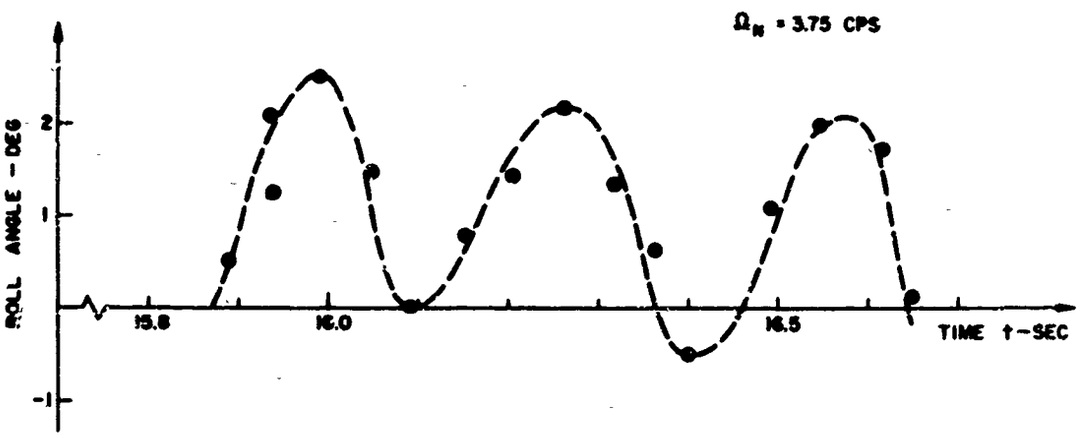

FIGURE 14.30 STEADY-STATE LIMIT CYCLE OF RECTANGULAR MAGNUS ROTOR 2. FLIGHT TEST JUNE 30

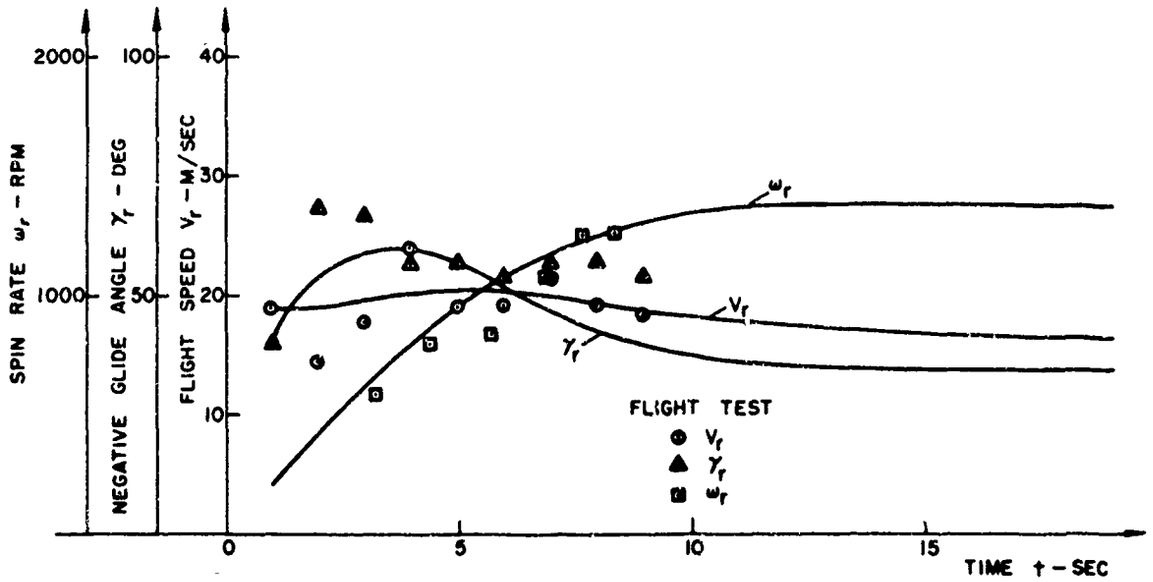

FIGURE 14.31 TRANSIENT PERFORMANCE OF TRIANGULAR MAGNUS ROTOR 1. FLIGHT TEST JUNE 30. SIMULATION RUN 35

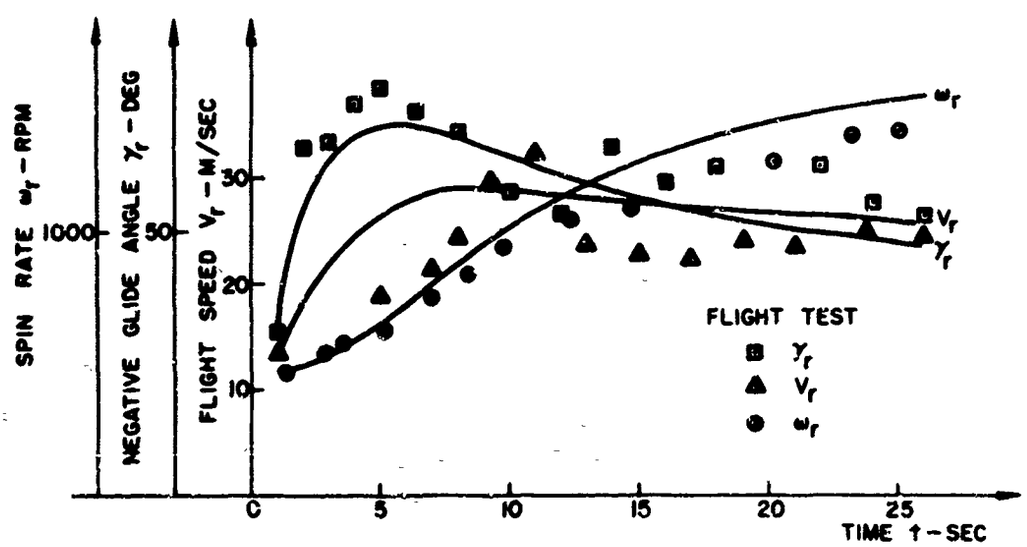

FIGURE 14.32 TRANSIENT PERFORMANCE OF CYLINDRICAL MAGNUS ROTOR 1. FLIGHT TEST JUNE 10. SIMULATION RUN 34

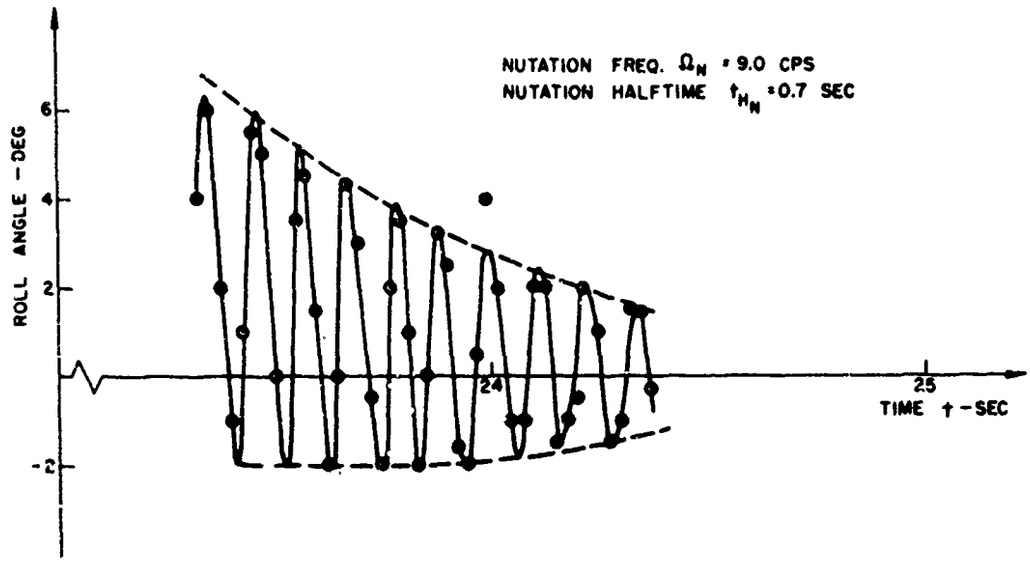

FIGURE 14.33 INDUCED NUTATION OF CYLINDRICAL MAGNUS ROTOR 1. FLIGHT TEST JUNE 10

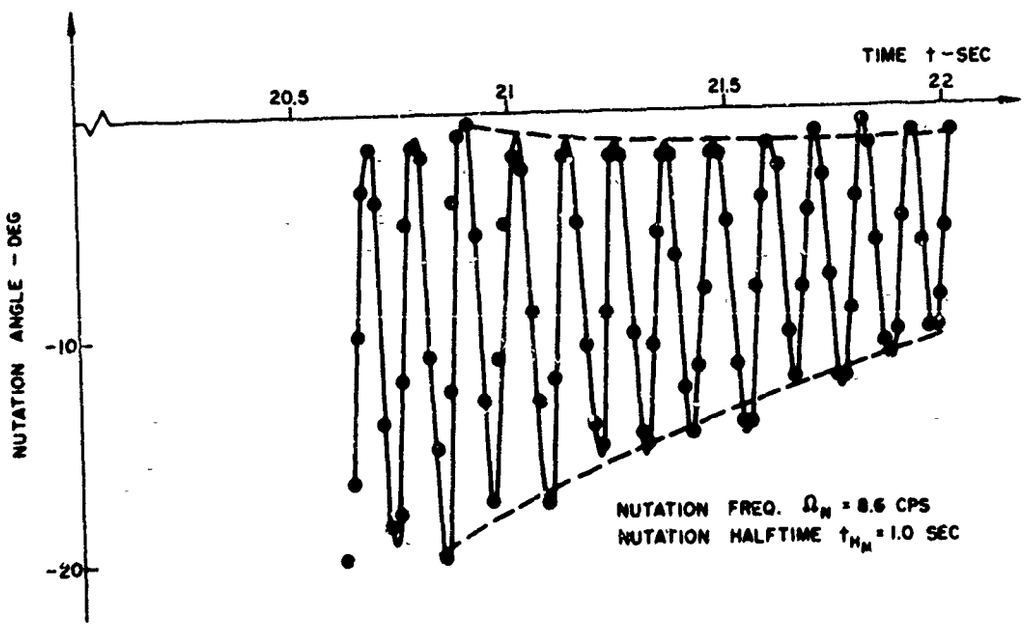

FIGURE 14.34 INDUCED NUTATION OF CYLINDRICAL MAGNUS ROTOR 3. FLIGHT TEST JUNE 30

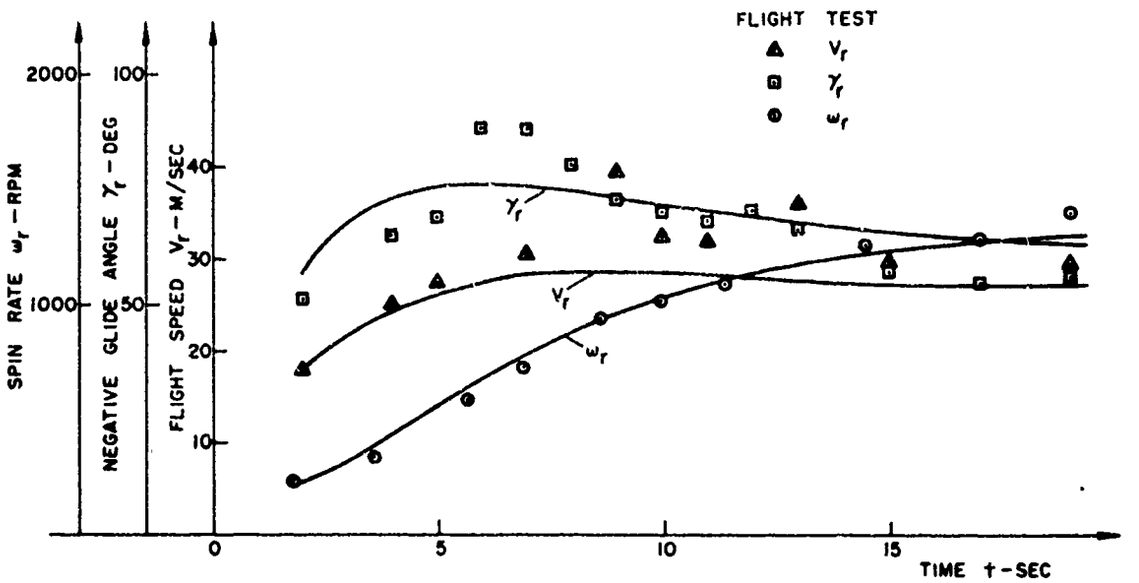

FIGURE 14.35 TRANSIENT PERFORMANCE OF CYLINDRICAL MAGNUS ROTOR 11. FLIGHT TEST JUNE 30. SIMULATION RUN 38

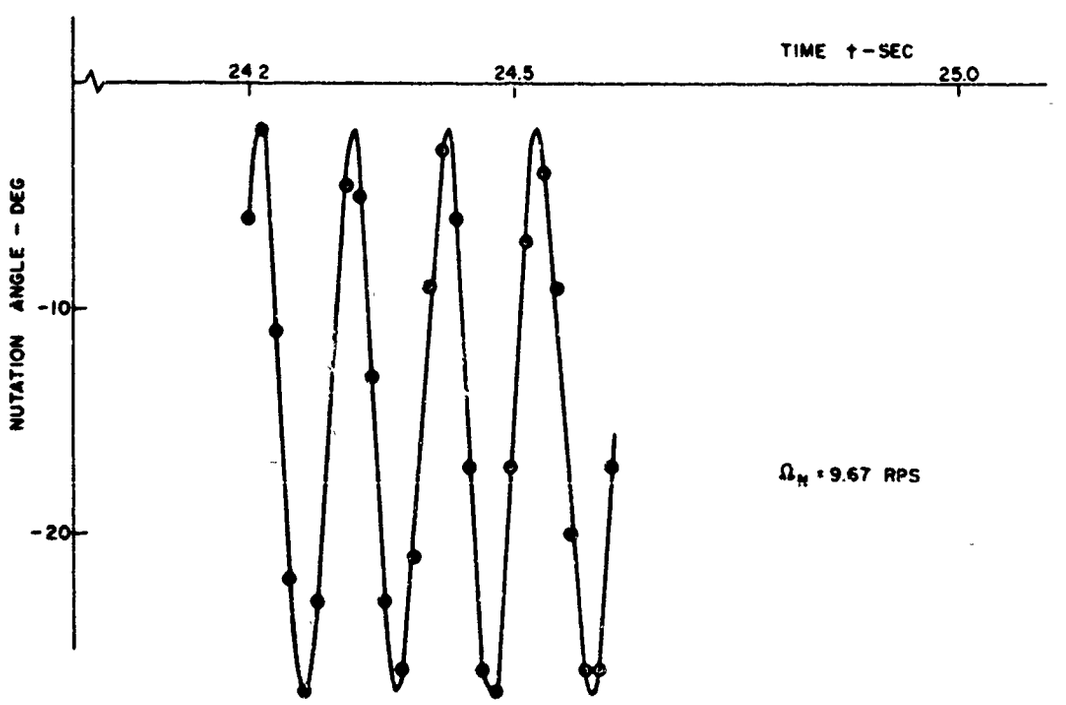

FIGURE 14.36 STEADY-STATE LIMIT CYCLE OF CYLINDRICAL MAGNUS ROTOR 4A. FLIGHT TEST JUNE 30

15. CRITICAL EVALUATION OF RESULTS

The contributions of this report are in two areas: the formulation of flight dynamical problems in general and the flight dynamics of Magnus rotors (MR) in particular. As is so often the case, the general formulation evolved from the specific requirements of Magnus rotor dynamics: the reference flight of the perturbation equations can be under acceleration, nonlinear aerodynamics must be included, and many coordinate systems are involved. Tensor algebra is the natural remedy for too many coordinate systems. It presents the equations in an invariant form, valid in all coordinate systems. In flight dynamics, most coordinate transformations are time dependent. To preserve the invariant form of the equations of motion, the rotational derivative was introduced to replace the ordinary time derivative. Then, for instance, Newton's Second Law can truly be written in an invariant form for inertial or noninertial coordinate systems.

The tensor formulation of the perturbation equations is carried out as far as possible, leading to a generalization of the classical small disturbance method and to a particularly convenient series expansion of the aerodynamic forces. No restrictions have to be placed on the reference flight. It can be accelerated or decelerated.

The state-of-the-art of Magnus rotor dynamics has been advanced in several respects. The perturbation equations of the steady-state glide phase are extended into the transient glide phase. The nonlinearities of the aerodynamic forces are taken into account by derivatives up to the

third order. A simple theorem states which derivative must vanish because of the mirror symmetry of MR's. This considerably reduces the number of derivatives. A one-degree-of-freedom perturbation equation is introduced by combining the roll and yaw angles into the single nutation angle and using the method of averaging. With this equation, necessary and sufficient conditions are derived for the existence of nutational limit cycles. Other intuitive concepts have been given a sound mathematical basis: the effect of a noncircular moment of inertia ellipsoid can be neglected, and the influence of the rapidly rotating angle of attack is averaged out over one revolution.

To back up the analytical results of this report, an extensive flight test program has been conducted. Two new methods proved to be successful in determining the otherwise difficult to obtain damping derivatives. They are the induced-nutation and the limit-cycle methods. The first one requires some external energy source that induces a nutational motion in steady-state flight, while the second one can be applied to MR's capable of limit cycles by the proper choice of the moment of inertia ratio. A good correlation was obtained between the analytically predicted and the free-flight limit cycles.

The agreement between the simulated trajectories and the test results is only satisfactory. This is mainly due to the high winds encountered during testing and mechanical and human tracking errors. A more accurate tracking facility should be used for further testing, and the wind should not exceed 5 knots. Also, the acquisition of attitude angles from high-speed film is not accurate enough to determine the roll and yaw angles

separately. The MR should be equipped with on-board instruments such as accelerometers or gyromagnetic sensors, and the measurements recorded on the ground.

The accuracy of the computer simulations depends on the quality of the wind tunnel data. Because of the high spin rate, the aerodynamic coefficients of an MR are difficult to measure. Improved testing methods should be developed. In particular, more transient wind tunnel tests should be conducted. They would provide a better basis for the formulation of the transient behavior of the aerodynamic coefficients than has been attempted in Chapter 11. No theoretical analysis of the aerodynamics of MR's was conducted. This is an area which requires more research. It is particularly important to improve the understanding of the airflow around MR's and to derive methods for the theoretical evaluation of aerodynamic derivatives.

Except for Section 12.4, the ideal MR postulated by Assumption 2 of Chapter 2 occupied our interest throughout this report. Such aberrations as configurational and mass asymmetries were not discussed in detail. Because they usually are small, they can be treated as external disturbances of the ideal MR. Their effect should be studied further. An especially fruitful area of research may be the resonance instability of MR's.

The general tensorial formulation of flight dynamics, as outlined in Chapters 3 to 5, was successfully applied to the dynamics of MR's. This method should also be employed to formulate the flight of missiles and airplanes and thus be developed into a general tool of flight dynamics.

NOMENCLATURE

CONVENTIONS

$[a]$	Vector in Euclidean three-space. Lower case letter.
$[A]$	Second-order tensor in Euclidean three-space. Upper case letter.
$]^B$	Right-handed orthogonal Cartesian coordinate system called B.
$[\ ]^B$	Components of a vector or tensor expressed in the $]^B$-coordinate system.
$[T]^{BA}$	Transformation matrix of coordinate system $]^B$ with respect to coordinate system $]^A$.
(A)	Frame A. Upper case letter.
$(A)_n$	Frame A during reference flight.
$(A)_p$	Frame A during perturbed flight.
A	Point A. Upper case letter.
$[x_{BA}]$	Displacement vector of point B with respect to point A. Arrow points to B.
$[R^{(B)(A)}]$	Rotation tensor of frame (B) with respect to frame (A).
$[\Omega^{(B)(A)}]$	Skew-symmetric angular velocity tensor of frame (B) with respect to frame (A).
$\frac{d}{dt} = (\dot{\ })$	Time derivative. Operates on the components of a tensor.
$\frac{d}{d\bar{t}} = (\overset{\circ}{\ })$	Time derivative, dynamic-normalized.
$\mathcal{D}^{(A)}$	Rotational time derivative with respect to frame (A).

$\overline{\mathcal{D}}^{(A)}$	Rotational time derivative, dynamic-normalized.
$\| \ \|$	Absolute value sign and matrix norm.

SYMBOLS

(A)	Air frame.
a	Center-of-gravity offset along spin axis.
B	Center of mass of Magnus rotor.
(B)	Body frame.
$(B)_R$	Body frame during reference flight.
$(B)_P$	Body frame during perturbed flight.
b	Span.
c	Chord.
$[C_F]$	Aerodynamic force coefficient vector.
$[C_M]$	Aerodynamic moment coefficient axial vector.
$C_D = D/qS$	Drag coefficient.
$C_L = L/qS$	Lift coefficient.
$C_{L_{\hat{\omega}}} = C_L / \hat{\omega}_R$	Magnus lift coefficient.
$C_{M_a} = M_a / qSl$	Accelerating spin torque.
$C_{M_{d_{\hat{\omega}}}} = M_d / qSl\hat{\omega}_R$	Damping spin torque.
$C_x = X/qS$	Axial force coefficient.
$C_y = Y/qS$	Side force coefficient.
$C_z = Z/qS$	Normal force coefficient.
$C_l = L/qSl$	Rolling moment coefficient.
$C_m = M/qSl$	Pitching moment coefficient.
$C_n = N/qSl$	Yawing moment coefficient.

$C_{y_\beta} = \partial C_y / \partial \beta$	Side force derivative.
$C_{y_{\beta^3}} = \partial^3 C_y / \partial \beta^3$	Cubic side force derivative.
$C_{\ell_{\hat{\omega}_\beta}} = \partial C_\ell / \partial \beta \hat{\omega}_r$	Magnus moment derivative.
$C_{\ell_{\hat{\omega}_\beta^3}} = \partial^3 C_\ell / \partial \beta^3 \hat{\omega}_r$	Cubic Magnus moment derivative.
$C_{n_\beta} = \partial C_n / \partial \beta$	Yawing moment derivative.
$C_{n_{\beta^3}} = \partial^3 C_n / \partial \beta^3$	Cubic yawing moment derivative.
$C_{\ell_{\hat{p}}} = \partial C_\ell / \partial \varepsilon \hat{p}$	Roll damping derivative.
$C_{\ell_{\hat{p}^3}} = \partial C_\ell / \partial \varepsilon \hat{p}^3$	Cubic roll damping derivative.
$C_{n_{\hat{r}}} = \partial C_n / \partial \varepsilon \hat{r}$	Yaw damping derivative.
$C_{n_{\hat{r}^3}} = \partial^3 C_n / \partial \varepsilon \hat{r}^3$	Cubic yaw damping derivative.
$C_{\ell_{\hat{\omega}_\beta^2 \hat{p}}} = \partial^3 C_\ell / \partial \beta^2 \partial \varepsilon \hat{p} \hat{\omega}_r$	Mixed linear roll damping derivative.
$C_{\ell_{\hat{\omega}_\beta \hat{p}^2}} = \partial^3 C_\ell / \partial \beta \partial^2 \varepsilon \hat{p} \hat{\omega}_r$	Mixed quadratic roll damping derivative.
$C_{n_{\beta^2 \hat{r}}} = \partial^3 C_n / \partial \beta^2 \partial \varepsilon \hat{r}$	Mixed linear yaw damping derivative.
$C_{n_{\beta \hat{r}^2}} = \partial^3 C_n / \partial \beta \partial \varepsilon \hat{r}^2$	Mixed quadratic yaw damping derivative.
d	End plate diameter.
$\mathcal{D}^{(I)}$	Rotational derivative relative to inertial frame (I).
D	Drag force.
$[E]$	Second order unit tensor.
(E)	Earth frame.
$[f_a]$	Aerodynamic force.
$[f_g]$	Gravitational force.
$F_{k,n}$	Fourier coefficients.
g	Earth acceleration constant.
$G_{k,n}$	Fourier coefficients.
g_1, g_2, g_3	Nonlinear aerodynamic functions.
$[H]$	Reflection tensor.

$[I_B^{(B)}]$	Moment-of-inertia tensor of body (B) referred to center of mass B.
I	Transverse moment of inertia.
$I_y \equiv I_z$	Spin moment of inertia.
$\bar{I} = I / \ell^2 \mu^2 m$	Dynamic-normalized transverse moment of inertia.
$\bar{I}_y = I_y / \ell^2 \mu^2 m$	Dynamic-normalized spin moment of inertia.
$[\ell_B^{(B)(I)}]$	Angular momentum of body (B) relative to inertial frame (I) and referred to the mass center B. Axial vector.
$\ell = c/2$	Reference length.
L	Lift force.
L/D	Lift over drag ratio.
$[m_a]$	Aerodynamic moment. Axial vector.
MR	Magnus rotor.
m	Mass of MR.
M_R	Mach number of reference flight.
$\mathcal{O}\{\ \}$	Order of magnitude.
$[p^{(B)(I)}]$	Linear momentum of body (B) relative to inertial frame (I).
$\varepsilon\hat{p}, \varepsilon\hat{q}, \varepsilon\hat{r}$	Perturbations of the angular velocity components.
$q = \rho V_R^2 / 2$	Dynamic pressure.
$[R_p^{(S)} {}_R^{(S)}]$	Rotation tensor of the perturbed stability frame relative to the reference stability frame.
(R)	Reference frame.
R_R	Reynolds number of reference flight.
S	Reference area.
(S)	Stability frame.

$[s_{\ell B}]$	Displacement vector of element ℓ relative to point B.
$\mathcal{S}$	Summation sign over a continuum.
$\bar{s}_N = \bar{\xi}_N \pm i\eta_N$	Roots of nutation mode.
$\bar{s}_u = \bar{\xi}_u \pm \eta_u$	Roots of undulation mode.
t	Time.
$\bar{t} = \frac{1}{\tau} t$	Dynamic-normalized time.
$\hat{t} = \frac{V_R}{\ell} t$	Aero-normalized time.
$\varepsilon\hat{u}, \varepsilon\hat{v}, \varepsilon\hat{w}$	Perturbations of the linear velocity components.
V	Flight speed.
V_R	Reference flight speed.
V_{ss}	Steady-state flight speed.
$\delta V = V_p - V_R$	Flight speed perturbation.
$[v_B^{(A)}]$	Velocity vector of center of mass B relative to air frame (A).
$[v_{B_R}^{(I)}]$	Velocity vector of the center of mass during reference flight, B_R, relative to the inertial frame (I).
W	Weight of MR.
(W)	Wind frame.
x_1^B, x_2^B, x_3^B	Body axes.
$x_{1p}^S, x_{2p}^S, x_{3p}^S$	Stability axes during perturbed flight.
$x_{1R}^S, x_{2R}^S, x_{3R}^S$	Stability axes during reference flight.
x_1^Y, x_2^Y, x_3^Y	Yawing axes.
x_1^L, x_2^L, x_3^L	Line of node axes.
x_1^N, x_2^N, x_3^N	Nutation axes.

α	Angle of attack.
$\dot{\alpha}_r = \bar{\omega}_r$	Dynamic-normalized spin rate during reference flight.
β	Angle of sideslip.
γ	Glide angle.
$\delta\gamma = \gamma_p - \gamma_r$	Glide angle perturbation.
Γ	Complex angle of orientation.
δ	Perturbation symbol.
ε	Perturbation symbol.
ζ	Body angle.
η	Cone angle.
$\mu = 2m/\rho S l$	Mass parameter.
ρ	Air density.
ϑ	Node angle.
τ	Time parameter.
ϕ	Roll angle.
Φ	Roll angle referred to earth frame.
ψ	Yaw angle.
Ψ	Yaw angle referred to earth frame.
$[\Omega_p^{(S)(I)}]$	Skew-symmetric angular velocity tensor of perturbed stability frame relative to inertial frame.
$[\omega_p^{(S)(I)}]$	Axial vector of $[\Omega_p^{(S)(I)}]$.
$[\omega^{(B)(A)}]$	Angular velocity axial vector of body frame (B) relative to air frame (A).
$[\varepsilon\omega^{(S)(I)}]$	Perturbations of angular velocity of frame (S) relative to frame (I).

ω	Spin rate. Component of the angular velocity vector along the spin axis.
$\bar{\omega}_r = \mathring{\alpha}_r$	Dynamic-normalized spin rate during reference flight.
$\hat{\omega} = \frac{\omega \ell}{V}$	Tip-speed ratio.
$\hat{\omega}_r = \frac{\omega_r \ell}{V_r}$	Aero-normalized spin rate during reference flight or tip-speed ratio.

SUBSCRIPTS

p	Perturbed flight.
r	Reference flight.
ss	Steady-state flight.

SUPERSCRIPTS

$\wedge$	Aero-normalized.
$-$	Dynamic-normalized.
$\sim$	Averaged value.
T	Transposed.

LITERATURE CITED

1. Brunk, J.; Davidson, W.L.; Rakestraw, R.W. — "The Dynamics of Spinning Bodies at Large Angle of Attack." AFOSR/DRA-62-3. January 1962. AD 275 437.

2. Brunk, J. — "The Dynamics and Aerodynamics of Self-Sustained Large Angle of Attack Body Spinning Motions." AFOSR-4596. February 1963. AD 407 183.

3. Boehler, G.D. and Foshag, W.F. — "Wing Rotors." US Patent No. 3262656. Filed October 1964.

4. Foshag, W.F. and Boehler, G.D. — "Review and Preliminary Evaluation of Lifting Horizontal-Axis Rotating-Wing Aeronautical Systems (HARWAS)". USAAVLABS Technical Report 69-13. March 1969. AD 857 462.

5. Maxwell, J.C. — "On A Particular Case of the Descent of a Heavy Body in a Resisting Medium." Cambridge and Dublin Math. J. IX (1854) pp. 115-118.

6. Millevolte, P.L. — "Dynamic Stability of Vortex Gliders." Master's Thesis, University of Minnesota, 1966.

7. Bustamante, A.C. and Stone, G.W. — "Autorotational Characteristics of Flat Plates and Right Circular Cylinders at Subsonic Speeds." Sandia Labs., New Mexico, SC-RR-67-778. November 1967.

8. Bustamante, A.C. — "Free-Fall Rotation and Aerodynamic Motion of Rectangular Plates." Sandia Labs., New Mexico. SC-RR-68-132. August 1968.

9. Bustamante, A.C. and Stone, G.W. — "The Autorotation Characteristics of Various Shapes in Subsonic and Hypersonic Flow." Sandia Labs., New Mexico. SC-RR-69-159. April 1969.

10. Truesdell, C. — "Die rationale Mechanik der Kontinua." ZAMM Band 44 (1964) Heft 8/9 pp. 341-347.

11. Hamel, G. — "Die Axiome der Mechanik." Handbuch der Physik, Band 5 (1929) Springer Verlag, Berlin, p. 6.

12. Noll, W. "On the Continuity of the Solid and Fluid States." J. Rat. Mech. Anal. 4, 1 (1955) p. 19.

13. Jeffreys and Jeffreys "Methods of Mathematical Physics." Cambridge at the University Press, 1956.

14. Wrede, R.C. "Introduction to Vector and Tensor Analysis." John Wiley and Sons, Inc., 1963.

15. Brillouin, L. "Tensors in Mechanics and Elasticity." Academic Press, 1964.

16. Etkin, B. "Dynamics of Flight." John Wiley & Sons, Inc., 1959.

17. Hopkin, H.R. "A Scheme of Notation and Nomenclature for Aircraft Dynamics and Associated Aerodynamics." June 1966. Royal Aircraft Establishment. TR 66200.

18. Maple, C.G. and Synge, J.L. "Aerodynamic Symmetry of Projectiles." Quarterly of Applied Mathematics Vol. VI No. 4, (1949), pp. 345-366.

19. Charters, A.C. "The Linearized Equations of Motion Underlying The Dynamic Stability of Aircraft, Spinning Projectiles, and Symmetrical Missiles." NACA TN 3350. January 1955.

20. Wright, J. "A Compilation of Aerodynamic Nomenclature and Axes Systems." NOLR 1241. August 1962. AD 284 911.

21. Bogoliubov, N.N. and Mitropolsky, Y.A. "Asymptotic Methods in the Theory of Non-Linear Oscillations." Second Edition. Translated from the Russian. Gordon and Breach Science Publisher, Inc., 1961.

22. Malkin, I.C. "Theorie der Stabilitaet einer Bewegung." Translated from the Russian by W. Hahn. R. Oldenbourg Munic, W. Germany, 1959.

23. Bellman, R. "Stability Theory of Differential Equations." McGraw-Hill Book Company, Inc., 1953.

24. Cesari, L. "Asymptotic Behavior and Stability Problems in Ordinary Differential Equations." Second Edition. Academic Press Inc., 1963.

25. Zubov, V.I. "Mathematical Methods for the Study of Automatic Control Systems." Translated from the Russian by Yaakov Schorr-Kon. MacMillan Company, 1963.

26. Van Aken, R.W. and Kelly, H.R. "The Magnus Force on Spinning Cylinders." IAS Reprint No. 712. January 1957.

27. Swanson, W.M. "An Experimental Investigation of the Two-Dimensional Magnus Effect." Final Report, Contract DA-33-019-ORD-1434. Case Institute of Technology. December 1956. AD 122 945.

28. Ralston, A. and Wilf, H.S. "Mathematical Methods for Digital Computers." John Wiley & Sons, 1960.

APPENDIX A

PROOFS OF SECTION 3.3

PROPERTY 1: The rotational derivative of a vector $[p]$ relative to a frame (R) is a vector; i.e., let $(\bar{M})$ and $(\bar{\bar{M}})$ be any two frames with the associated coordinate systems $]^{\bar{M}}$ and $]^{\bar{\bar{M}}}$ and the transformation matrix $[T]^{\bar{M}\bar{\bar{M}}}$, then

$$[\mathcal{D}^{(R)} p]^{\bar{M}} = [T]^{\bar{M}\bar{\bar{M}}} [\mathcal{D}^{(R)} p]^{\bar{\bar{M}}} \tag{1}$$

PROOF: The proof will be carried out in subscript notation with summation convention. We shall use the following notation:

$\vec{p}_i \longleftrightarrow [p]$		arbitrary vector
$p_i \longleftrightarrow [p]^R$		components in $]^R$-coordinate system
$\bar{p}_i \longleftrightarrow [p]^{\bar{M}}$		components in $]^{\bar{M}}$-coordinate system
$\bar{\bar{p}}_i \longleftrightarrow [p]^{\bar{\bar{M}}}$		components in $]^{\bar{\bar{M}}}$-coordinate system
$r_i \longleftrightarrow [r]^R$		vector fixed in reference frame but otherwise arbitrary ; $\frac{d}{dt} r_i = 0$
$\bar{t}_{ij} \longleftrightarrow [T]^{\bar{M}R}$		transformation matrix
$\bar{\bar{t}}_{ij} \longleftrightarrow [T]^{\bar{\bar{M}}R}$		transformation matrix
$t^*_{ij} = \bar{t}_{ik}\bar{\bar{t}}_{jk} \longleftrightarrow [T]^{\bar{M}\bar{\bar{M}}} = [T]^{\bar{M}R}[T]^{\bar{\bar{M}}R^T}$		

To prove Equation (1), we will generate a scalar $p_i r_i$ and take the time derivative:

$$\frac{d}{dt}(p_i r_i) = \frac{d}{dt}(\bar{p}_i \bar{r}_i) = \frac{d}{dt}(\bar{\bar{p}}_i \bar{\bar{r}}_i) \tag{2}$$

Expanding the first relationship of Equation (2), we obtain:

$$r_i \frac{d}{dt} p_i = \bar{p}_k \frac{d}{dt} \bar{r}_k + \bar{r}_s \frac{d}{dt} \bar{p}_s \tag{3}$$

where we used the fact that r_i is a vector fixed in the reference frame, i.e., $\frac{d}{dt} r_i = 0$

Let

$$\bar{r}_k = \bar{t}_{ki} r_i \tag{4}$$

and substitute into Equation (3):

$$r_i \frac{d}{dt} p_i = \left(\frac{d}{dt} \bar{t}_{ki}\right) \bar{p}_k r_i + \bar{t}_{si} \left(\frac{d}{dt} \bar{p}_s\right) r_i \tag{5}$$

Because r_i is arbitrary, we get:

$$\frac{d}{dt} p_i = \left(\frac{d}{dt} \bar{t}_{ki}\right) \bar{p}_k + \bar{t}_{si} \left(\frac{d}{dt} \bar{p}_s\right) \tag{6}$$

Multiply and contract

$$\delta_{li} = \bar{t}_{sl} \bar{t}_{si} \tag{7}$$

on both sides of Equation (6)

$$\delta_{li} \frac{d}{dt} p_i = \bar{t}_{sl} \bar{t}_{si} \left(\frac{d}{dt} \bar{t}_{ki}\right) \bar{p}_k + \delta_{li} \bar{t}_{si} \left(\frac{d}{dt} \bar{p}_s\right) \tag{8}$$

Thus

$$\frac{d}{dt} p_l = \bar{t}_{sl} \left\{ \frac{d}{dt} \bar{p}_s + \bar{t}_{si} \left(\frac{d}{dt} \bar{t}_{ki} \right) \bar{p}_k \right\} \tag{9}$$

The second relationship of Equation (2)

$$\frac{d}{dt} (p_i r_i) = \frac{d}{dt} (\bar{p}_i \bar{r}_i) \tag{10}$$

yields a similar equation using the same procedure:

$$\frac{d}{dt}\rho_\ell = \bar{\bar{t}}_{n\ell}\left\{\frac{d}{dt}\bar{\bar{\rho}}_n + \bar{\bar{t}}_{nj}\left(\frac{d}{dt}\bar{\bar{t}}_{pj}\right)\bar{\bar{\rho}}_p\right\} \tag{11}$$

Set Equation (9) equal to Equation (11)

$$\bar{t}_{s\ell}\left\{\frac{d}{dt}\bar{\rho}_s + \bar{t}_{si}\left(\frac{d}{dt}\bar{t}_{ki}\right)\bar{\rho}_k\right\} = \bar{\bar{t}}_{n\ell}\left\{\frac{d}{dt}\bar{\bar{\rho}}_n + \bar{\bar{t}}_{nj}\left(\frac{d}{dt}\bar{\bar{t}}_{pj}\right)\bar{\bar{\rho}}_p\right\} \tag{12}$$

Multiply and contract $\bar{t}_{t\ell}$ on both sides of Equation (12) and introduce

$$t^*_{tn} = \bar{t}_{t\ell}\,\bar{\bar{t}}_{n\ell} \tag{13}$$

We get

$$\frac{d}{dt}\bar{\rho}_t + \bar{t}_{ti}\left(\frac{d}{dt}\bar{t}_{ki}\right)\bar{\rho}_k = t^*_{tn}\left\{\frac{d}{dt}\bar{\bar{\rho}}_n + \bar{\bar{t}}_{nj}\left(\frac{d}{dt}\bar{\bar{t}}_{pj}\right)\bar{\bar{\rho}}_p\right\} \tag{14}$$

which, in matrix notation, takes the form:

$$\frac{d}{dt}[\rho]^{\bar{R}} + [T]^{\bar{R}R}\left(\frac{d}{dt}[T]^{\bar{R}R^T}\right)[\rho]^{\bar{R}} = [T]^{\bar{R}\bar{\bar{R}}}\left\{\frac{d}{dt}[\rho]^{\bar{\bar{R}}} + [T]^{\bar{\bar{R}}R}\left(\frac{d}{dt}[T]^{\bar{\bar{R}}R^T}\right)[\rho]^{\bar{\bar{R}}}\right\} \tag{15}$$

This can be written according to Equation (3.19):

$$[\mathcal{D}^{(R)}\rho]^{\bar{R}} = [T]^{\bar{R}\bar{\bar{R}}}\,[\mathcal{D}^{(R)}\rho]^{\bar{\bar{R}}} \tag{16}$$

which is exactly the form of Equation (1).

<u>PROPERTY 2</u>: The rotational derivative of a tensor $[P]$ relative to frame (R) is a tensor; i.e., let $(\bar{R})$ and $(\bar{\bar{R}})$ be any two frames with the associated coordinate systems $]^{\bar{R}}$ and $]^{\bar{\bar{R}}}$ and the transformation matrix $[T]^{\bar{R}\bar{\bar{R}}}$, then

$$[\mathcal{D}^{(R)}P]^{\bar{R}} = [T]^{\bar{R}\bar{\bar{R}}}\,[\mathcal{D}^{(R)}P]^{\bar{\bar{R}}}\,[T]^{\bar{R}\bar{\bar{R}}^T} \tag{17}$$

PROOF: The proof is similar to that of Property 1. As additional notation, we need only R_{ij} , a tensor whose components are time invariant with respect to the frame (R) , i.e., $\frac{d}{dt} R_{ij} = 0_{ij}$

We form a scalar with the twice-contracted product of P_{ij} and R_{ij} and take the time derivative

$$\frac{d}{dt}\left(P_{ij} R_{ij}\right) = \frac{d}{dt}\left(\bar{P}_{ij} \bar{R}_{ij}\right) = \frac{d}{dt}\left(\bar{\bar{P}}_{ij} \bar{\bar{R}}_{ij}\right) \tag{18}$$

Expanding the first relationship of Equation (18), we obtain:

$$R_{ij} \frac{d}{dt} P_{ij} = \bar{R}_{\ell m} \frac{d}{dt} \bar{P}_{\ell m} + \bar{P}_{kn} \frac{d}{dt} \bar{R}_{kn} \tag{19}$$

Take the time derivative of

$$\bar{R}_{kn} = \bar{t}_{ki} \bar{t}_{nj} R_{ij} \tag{20}$$

$$\frac{d}{dt} \bar{R}_{kn} = \left\{ \bar{t}_{ki} \left(\frac{d}{dt} \bar{t}_{nj}\right) + \left(\frac{d}{dt} \bar{t}_{ki}\right) \bar{t}_{nj} \right\} R_{ij} \tag{21}$$

and substitute into Equation (19). Because R_{ij} is arbitrary, we get, in view of Equation (20):

$$\frac{d}{dt} P_{ij} = \bar{t}_{mj} \bar{t}_{\ell j} \frac{d}{dt} \bar{P}_{\ell m} + \bar{t}_{ki} \left(\frac{d}{dt} \bar{t}_{nj}\right) \bar{P}_{kn} + \left(\frac{d}{dt} \bar{t}_{ki}\right) \bar{t}_{nj} \bar{P}_{kn} \tag{22}$$

Multiplying Equation (22) by

$$\delta_{pi} = \bar{t}_{rp} \bar{t}_{ri} \quad ; \quad \delta_{qj} = \bar{t}_{sq} \bar{t}_{sj} \tag{23}$$

and contracting yields:

$$\frac{d}{dt} P_{pq} = \bar{t}_{mq} \bar{t}_{\ell p} \left\{ \frac{d}{dt} \bar{P}_{\ell m} + \bar{t}_{\ell i} \left(\frac{d}{dt} \bar{t}_{ki}\right) \bar{P}_{km} + \bar{P}_{\ell n} \left(\frac{d}{dt} \bar{t}_{nj}\right) \bar{t}_{mj} \right\} \tag{24}$$

The second relationship of Equation (18)

$$\frac{d}{dt}\left(P_{ij}R_{ij}\right) = \frac{d}{dt}\left(\bar{P}_{ij}\bar{\bar{R}}_{ij}\right) \tag{25}$$

yields a similar equation using the same procedure:

$$\frac{d}{dt}P_{pq} = \bar{\bar{t}}_{mq}\bar{\bar{t}}_{lp}\left\{\frac{d}{dt}\bar{\bar{P}}_{lm} + \bar{\bar{t}}_{li}\left(\frac{d}{dt}\bar{\bar{t}}_{ki}\right)\bar{\bar{P}}_{km} + \bar{\bar{P}}_{ln}\left(\frac{d}{dt}\bar{\bar{t}}_{nj}\right)\bar{\bar{t}}_{mj}\right\} \tag{26}$$

Set Equation (25) equal to Equation (26), multiply both sides by $\bar{t}_{aq}\bar{t}_{bp}$, contract, and introduce

$$t^*_{as} = \bar{t}_{aq}\bar{\bar{t}}_{sq} \quad ; \quad t^*_{bt} = \bar{t}_{bp}\bar{\bar{t}}_{tp} \tag{27}$$

The result is:

$$\begin{aligned}&\frac{d}{dt}\bar{P}_{ba} + \bar{t}_{bi}\left(\frac{d}{dt}\bar{t}_{ki}\right)\bar{P}_{ka} + \bar{P}_{bn}\left(\frac{d}{dt}\bar{t}_{nj}\right)\bar{t}_{aj} = \\ &= t^*_{bt}\,t^*_{as}\left\{\frac{d}{dt}\bar{\bar{P}}_{ts} + \bar{\bar{t}}_{tn}\left(\frac{d}{dt}\bar{\bar{t}}_{vn}\right)\bar{\bar{P}}_{vs} + \bar{\bar{P}}_{tn}\left(\frac{d}{dt}\bar{\bar{t}}_{nw}\right)\bar{\bar{t}}_{sw}\right\}\end{aligned} \tag{28}$$

and in matrix notation:

$$\begin{aligned}&\frac{d}{dt}[P]^{\bar{A}} + [T]^{\bar{A}R}\left(\frac{d}{dt}[T]^{\bar{A}R^T}\right)[P]^{\bar{A}} + [P]^{\bar{A}}\left(\frac{d}{dt}[T]^{\bar{A}R}\right)[T]^{\bar{A}R^T} \\ &= [T]^{\bar{A}\bar{\bar{A}}}\left\{\frac{d}{dt}[P]^{\bar{\bar{A}}} + [T]^{\bar{A}R}\left(\frac{d}{dt}[T]^{\bar{A}R^T}\right)[P]^{\bar{\bar{A}}} + [P]^{\bar{\bar{A}}}\left(\frac{d}{dt}[T]^{\bar{\bar{A}}R}\right)[T]^{\bar{A}R^T}\right\}[T]^{\bar{A}\bar{\bar{A}}^T}\end{aligned} \tag{29}$$

This can be written according to Equation (3.20):

$$[\mathcal{D}^{(R)}P]^{\bar{A}} = [T]^{\bar{A}\bar{\bar{A}}}[\mathcal{D}^{(R)}P]^{\bar{\bar{A}}}[T]^{\bar{A}\bar{\bar{A}}^T} \tag{30}$$

which is exactly Equation (17).

<u>PROPERTY 3</u>: If the allowable coordinate systems are right-hand orthogonal Cartesian coordinate systems, then an axial vector $[\ell]$ has the same

rotational derivative as a regular vector; i.e., let $(\bar{M})$ and $(\bar{\bar{M}})$ be any two frames with the associated coordinate systems $]^{\bar{M}}$ and $]^{\bar{\bar{M}}}$ and the transformation matrix $[T]^{\bar{M}\bar{\bar{M}}}$, then

$$[\mathcal{D}^{(R)} \ell]^{\bar{M}} = [T]^{\bar{M}\bar{\bar{M}}} [\mathcal{D}^{(R)} \ell]^{\bar{\bar{M}}} \tag{31}$$

<u>PROOF</u>: It is sufficient to show that, if P_{ij} of Equation (22) is a skew-symmetric second-order tensor, say L_{ij}, Equation (22) can be reduced to Equation (9) with axial vector ℓ_i. Rewrite Equation (22) for L_{ij}:

$$\frac{d}{dt} L_{ij} = \bar{t}_{mj} \bar{t}_{\ell i} \frac{d}{dt} \bar{L}_{\ell m} + \bar{L}_{kn} \left\{ \bar{t}_{ki} \frac{d}{dt} \bar{t}_{nj} + \left(\frac{d}{dt} \bar{t}_{ki} \right) \bar{t}_{nj} \right\} \tag{32}$$

Introduce the definition

$$L_{ij} = \varepsilon_{ijp} \ell_p \quad ; \quad \bar{L}_{ij} = \bar{\varepsilon}_{ijp} \bar{\ell}_p \tag{33}$$

into Equation (32):

$$\varepsilon_{ijp} \frac{d}{dt} \ell_p = \bar{t}_{mj} \bar{t}_{\ell i} \bar{\varepsilon}_{\ell m q} \frac{d}{dt} \bar{\ell}_q + \bar{\varepsilon}_{knn} \bar{\ell}_n \left\{ \bar{t}_{ki} \frac{d}{dt} \bar{t}_{nj} + \left(\frac{d}{dt} \bar{t}_{ki} \right) \bar{t}_{nj} \right\} \tag{34}$$

To reduce further the second term on the right-hand side of Equation (34), we use the transformation relation

$$\bar{\varepsilon}_{pqr} = |\bar{t}| \, \bar{t}_{pi} \, \bar{t}_{qk} \, \bar{t}_{rm} \, \varepsilon_{ikm} \tag{35}$$

Multiplying both sides by $\bar{t}_{ps} \bar{t}_{qt}$ and taking the time derivative yields:

$$\bar{\varepsilon}_{knn} \left\{ \bar{t}_{ki} \frac{d}{dt} \bar{t}_{nj} + \left(\frac{d}{dt} \bar{t}_{ki} \right) \bar{t}_{nj} \right\} = |\bar{t}| \, \varepsilon_{ijs} \frac{d}{dt} \bar{t}_{ns} \tag{36}$$

Substitute Equation (36) into Equation (34)

$$\varepsilon_{ijp} \frac{d}{dt} \ell_p = \bar{t}_{mj} \bar{t}_{\ell i} \bar{\varepsilon}_{\ell m q} \frac{d}{dt} \bar{\ell}_q + |\bar{t}| \, \varepsilon_{ijs} \left(\frac{d}{dt} \bar{t}_{ns} \right) \bar{\ell}_n \tag{37}$$

and use the inverse of Equation (35)

$$\varepsilon_{ijs} = \frac{1}{|\bar{t}|} \bar{\varepsilon}_{lmq} \bar{t}_{li} \bar{t}_{mj} \bar{t}_{qs} \tag{38}$$

to combine the terms on the right-hand side of Equation (37):

$$\varepsilon_{ijp} \frac{d}{dt} l_p = \bar{\varepsilon}_{lmq} \bar{t}_{mj} \bar{t}_{li} \left\{ \frac{d}{dt} \bar{l}_q + \bar{t}_{qs} \left(\frac{d}{dt} \bar{t}_{rs} \right) \bar{l}_r \right\} \tag{39}$$

In view of

$$\bar{\varepsilon}_{lmq} \bar{t}_{mj} \bar{t}_{li} = |\bar{t}| \varepsilon_{ijp} \bar{t}_{qp} \tag{40}$$

we get:

$$\varepsilon_{ijp} \frac{d}{dt} l_p = \varepsilon_{ijp} |\bar{t}| \bar{t}_{qp} \left\{ \frac{d}{dt} \bar{l}_q + \bar{t}_{qs} \left(\frac{d}{dt} \bar{t}_{rs} \right) \bar{l}_r \right\} \tag{41}$$

For right-hand orthogonal Cartesian coordinate systems, $|\bar{t}| = +1$. Furthermore, because i, j are free indices, there will be for each $p = 1, 2, 3$ a combination of i, j such that $\varepsilon_{ijp} \neq 0$. Therefore, Equation (41) becomes

$$\frac{d}{dt} l_p = \bar{t}_{qp} \left\{ \frac{d}{dt} \bar{l}_q + \bar{t}_{qs} \left(\frac{d}{dt} \bar{t}_{rs} \right) \bar{l}_r \right\} \tag{42}$$

which is exactly in the form of Equation (9).

<u>THEOREM OF TRANSFORMATION OF FRAMES</u>. Let (A) and (B) be two arbitrary frames related by the angular velocity tensor $[\Omega^{(B)(A)}]$. Then, for any vector $[p]$, the following relationship holds:

$$[\mathcal{D}^{(A)} p] = [\mathcal{D}^{(B)} p] + [\Omega^{(B)(A)}][p] \tag{43}$$

where every term is a first-order tensor.

<u>PROOF</u>: We shall use the following notation:

$p_i \longleftrightarrow [p]$	arbitrary vector
a_i	vector fixed in frame (A) but otherwise arbitrary
b_i	vector fixed in frame (B) but otherwise arbitrary
$\bar{p}_i \longleftrightarrow [p]^{\bar{M}}$	components in first arbitrary coordinate system $]^{\bar{M}}$
$\bar{\bar{p}}_i \longleftrightarrow [p]^{\bar{\bar{M}}}$	components in second arbitrary coordinate system $]^{\bar{\bar{M}}}$
$\tilde{a}_i$	components in coordinate system $]^A$ associated with frame (A) ; note: $\frac{d}{dt}\tilde{a}_i = 0$
$\tilde{\tilde{b}}_i$	components in coordinate system $]^B$ associated with frame (B) ; note: $\frac{d}{dt}\tilde{\tilde{b}}_i = 0$

$$\left.\begin{aligned}
\bar{p}_i &= t^1_{ij}\,\tilde{p}_j && \longleftrightarrow [p]^{\bar{M}} = [T]^{\bar{M}A}[p]^A \\
\bar{\bar{p}}_i &= t^2_{ij}\,\tilde{p}_i && \longleftrightarrow [p]^{\bar{\bar{M}}} = [T]^{\bar{\bar{M}}A}[p]^A \\
\bar{\bar{p}}_i &= t^2_{ij}\,t^1_{kj}\,\bar{p}_k = t^3_{ik}\,\bar{p}_k && \longleftrightarrow [p]^{\bar{\bar{M}}} = [T]^{\bar{\bar{M}}\bar{M}^T}[p]^{\bar{M}} \\
\bar{\bar{p}}_i &= t^4_{ij}\,\tilde{\tilde{p}}_j && \longleftrightarrow [p]^{\bar{\bar{M}}} = [T]^{\bar{\bar{M}}B}[p]^B
\end{aligned}\right\}\ \text{coordinate transformations}$$

Equation (3.45) permits us to introduce the components of two angular velocity tensors:

$$\frac{d}{dt}\tilde{b}_i = \tilde{\Omega}^{(B)(A)}_{ij}\,\tilde{b}_j \tag{44}$$

$$\frac{d}{dt}\tilde{\tilde{a}}_i = \tilde{\tilde{\Omega}}^{(A)(B)}_{ij}\,\tilde{\tilde{a}}_j \tag{45}$$

To prove the theorem, generate two scalars $a_i p_i$ and $b_i p_i$, take their time derivatives and add:

$$\frac{d}{dt}(\tilde{a}_i \tilde{p}_i) + \frac{d}{dt}(\tilde{b}_i \tilde{p}_i) = \frac{d}{dt}(\tilde{\tilde{a}}_i \tilde{\tilde{p}}_i) + \frac{d}{dt}(\tilde{\tilde{b}}_i \tilde{\tilde{p}}_i) \tag{46}$$

$$(\tilde{a}_i + \tilde{b}_i)\frac{d}{dt}\tilde{p}_i + \tilde{p}_i \frac{d}{dt}\tilde{b}_i = (\tilde{\tilde{a}}_i + \tilde{\tilde{b}}_i)\frac{d}{dt}\tilde{\tilde{p}}_i + \tilde{\tilde{p}}_i \frac{d}{dt}\tilde{\tilde{a}}_i \tag{47}$$

Substitute Equations (44) and (45) into Equation (47) and get:

$$(\tilde{a}_i + \tilde{b}_i)\frac{d}{dt}\tilde{p}_i = (\tilde{\tilde{a}}_i + \tilde{\tilde{b}}_i)\frac{d}{dt}\tilde{\tilde{p}}_i + \tilde{\tilde{p}}_i \tilde{\tilde{\Omega}}_{ij}^{(A)(B)}\tilde{\tilde{a}}_j - \tilde{p}_j \tilde{\Omega}_{ij}^{(B)(A)}\tilde{b}_j \tag{48}$$

This can be simplified, noting that each term is a scalar and that:

$$\tilde{\tilde{\Omega}}_{ij}^{(A)(B)} = -\tilde{\tilde{\Omega}}_{ij}^{(B)(A)} = +\tilde{\tilde{\Omega}}_{ji}^{(B)(A)} \tag{49}$$

$$(\tilde{a}_i + \tilde{b}_i)\frac{d}{dt}\tilde{p}_i = (\tilde{\tilde{a}}_i + \tilde{\tilde{b}}_i)\frac{d}{dt}\tilde{\tilde{p}}_i + (\bar{\bar{a}}_j + \bar{\bar{b}}_j)\bar{\bar{\Omega}}_{ji}^{(B)(A)}\bar{\bar{p}}_i \tag{50}$$

We will express the first factor of every term as $(\bar{a}_i + \bar{b}_i)$, using the appropriate coordinate transformations, and convert the arbitrary vector p_i into $\bar{p}_i$, $\bar{\bar{p}}_i$ components by

$$\tilde{p}_i = t^1_{ji}\bar{p}_j \quad ; \quad \tilde{\tilde{p}}_i = t^4_{ji}\bar{\bar{p}}_j \tag{51}$$

We obtain:

$$(\bar{a}_\ell + \bar{b}_\ell)\left\{t^1_{\ell i}\, t^1_{ji}\frac{d}{dt}\bar{p}_j + t^1_{\ell i}\left(\frac{d}{dt}t^1_{ji}\right)\bar{p}_j\right\} =$$

$$= (\bar{a}_\ell + \bar{b}_\ell)\, t^3_{k\ell}\left\{t^4_{ki}\, t^4_{ji}\frac{d}{dt}\bar{\bar{p}}_j + t^4_{ki}\left(\frac{d}{dt}t^4_{ji}\right)\bar{\bar{p}}_j + \bar{\bar{\Omega}}_{kj}^{(B)(A)}\bar{\bar{p}}_j\right\} \tag{52}$$

Because $\bar{a}_\ell$ and $\bar{b}_\ell$ are the components of arbitrary vectors contained in (A) and (B), respectively, $(\bar{a}_\ell + \bar{b}_\ell)$ are the components of an arbitrary vector. From Equation (52) it follows:

$$\frac{d}{dt}\bar{p}_\ell + t^1_{\ell i}\left(\frac{d}{dt}t^1_{ji}\right)\bar{p}_j = t^3_{k\ell}\left\{\frac{d}{dt}\bar{\bar{p}}_k + t^4_{ki}\left(\frac{d}{dt}t^4_{ji}\right)\bar{\bar{p}}_j + \bar{\bar{\Omega}}^{(B)(A)}_{kj}\,\bar{\bar{p}}_j\right\} \tag{53}$$

and in matrix notation:

$$\frac{d}{dt}[p]^{\bar{M}} + [T]^{\bar{M}A}\left(\frac{d}{dt}[T]^{\bar{M}A^T}\right)[p]^{\bar{M}} =$$

$$= [T]^{\bar{M}\bar{\bar{M}}}\left\{\frac{d}{dt}[p]^{\bar{\bar{M}}} + [T]^{\bar{\bar{M}}B}\left(\frac{d}{dt}[T]^{\bar{\bar{M}}B^T}\right)[p]^{\bar{\bar{M}}} + [\Omega^{(B)(A)}]^{\bar{\bar{M}}}[p]^{\bar{\bar{M}}}\right\} \tag{54}$$

which, in view of Equation (3.19), becomes:

$$[\mathcal{D}^{(A)}p]^{\bar{M}} = [T]^{\bar{M}\bar{\bar{M}}}\left\{[\mathcal{D}^{(B)}p]^{\bar{\bar{M}}} + [\Omega^{(B)(A)}]^{\bar{\bar{M}}}[p]^{\bar{\bar{M}}}\right\} \tag{55}$$

Because $]^{\bar{M}}$ and $]^{\bar{\bar{M}}}$ are arbitrary coordinate systems, we can write Equation (55) in the tensorial form of Equation (43).

APPENDIX B

COMPUTER PROGRAM MAGSIX

The equations of motion of a Magnus rotor in perturbed planar glide phase, Table 12.1, were programmed in Fortran IV for the Control Data Corporation Computer CDC 3150. It was assumed that the air density and the aerodynamic coefficients are constant. To solve the differential equations, a fourth-order Runge-Kutta method was used because it is stable, self-starting, and adjusts the time increment so that a specified upper error bound is not exceeded (see Ralston and Wilf (28)).

The functional operation of the program is shown in Figure B.1. The main program MAGSIX reads the data, controls the computational process, and writes the headings, input parameters, and initial conditions. The input data are given in the dimensions K_g(mass), m, sec, while the calculation is performed in dynamic-normalized (DN) units. To convert from one system to the other, the subroutine CONVERT is used. The actual calculations are executed in the subroutines RKGS and FCT. They start at the initial time specified by PRMT (1) and proceed in time intervals not to exceed the value PRMT (2) until the final time PRMT (3) is reached. Then the control is transferred back to MAGSIX for new input data. The results of the calculations are written by the subroutine OUTPUT in row form, following the initial conditions.

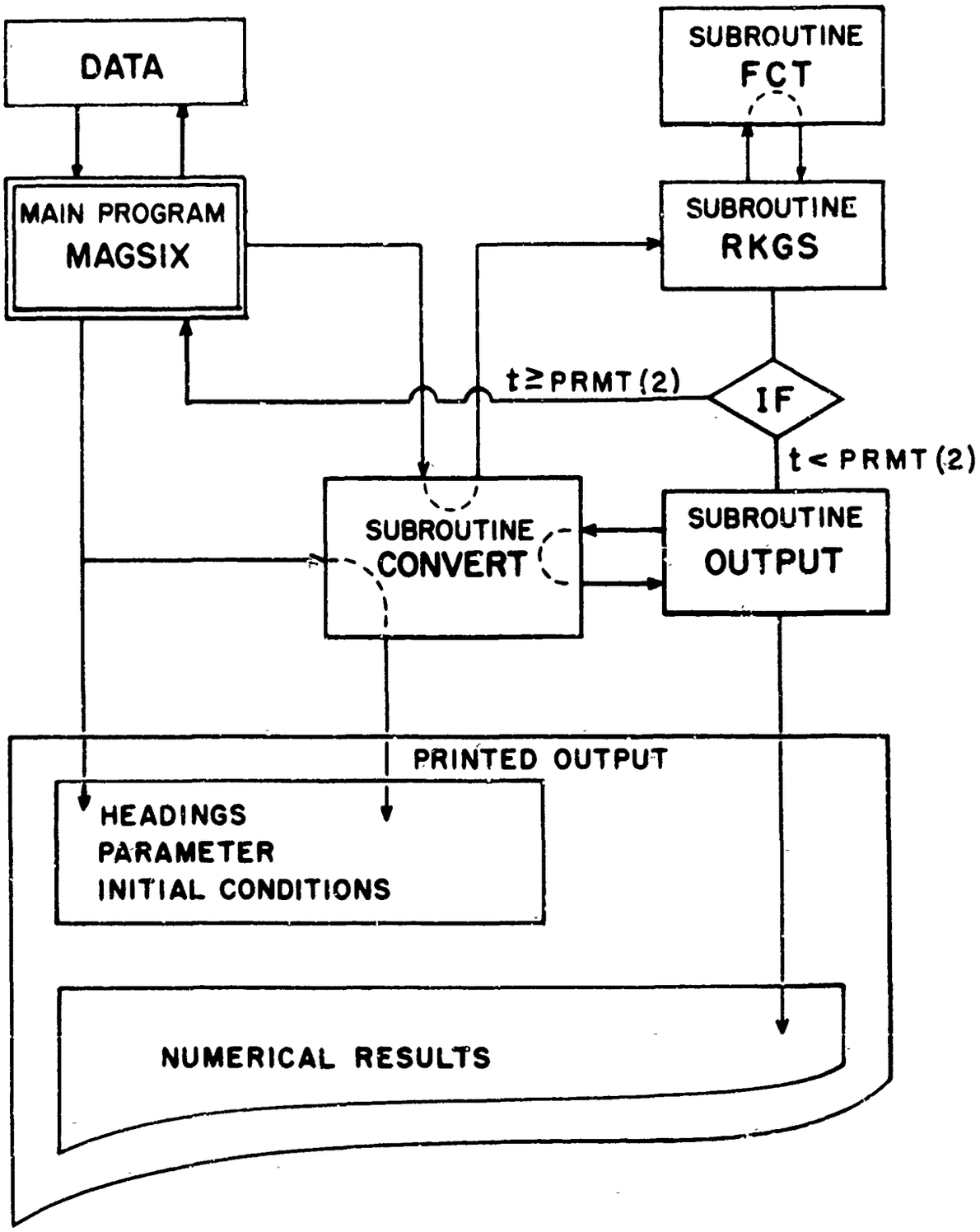

FIGURE B.1 MAGSIX FUNCTIONAL CHART

Table B. 1 summarizes all the required input data. The accuracy of the computations is controlled by the upper error bound, PRMT (4), and the error weights W(I); I = 1, ..., 10. At each time step the total error is calculated by the formula

$$\delta = \frac{1}{15} \sum_{I=1}^{10} W(I)\, \Delta P(I) \tag{B.1}$$

If $\delta > PRMT(4)$, the time interval is halved and the calculation repeated. The number of these bisections is given on the print-out in the column IHLF. The maximum error incurred at each time step by the I's state variable is

$$E(I) \leqq \frac{15}{W(I)} PRMT\ (4) \tag{B.2}$$

Some of the symbols used in the program have already been given in Table B.1. The remaining definitions are collected in Table B.2. The Fortran IV statements follow on pages 234 through 238, with the first portion of a print-out sheet on page 239.

RUN NO.:

IDENTIFICATION:

MAGNUS ROTOR PARAMETERS

SYMBOL	COMP.SY.*	VALUE	DIM.
ρ	RHO		KG/M^3
S	S		M^2
c/ℓ	RL		M
m	BM		KG
I	TMOI		$KG\ M^2$
I_y	SMOI		$KG\ M^2$
γ_{ss}	GSS		DEG
C_D	C(1)		ALL DERIVATIVES IN RADIANS
$C_{L\hat{\omega}}$	C(2)		
C_{M_a}	C(3)		
$C_{M_d\hat{\omega}}$	C(4)		
$C_{y\beta}$	C(5)		
$C_{y\beta^3}$	C(6)		
$C_{\ell\hat{\omega}\beta}$	C(7)		
$C_{\ell\hat{p}}$	C(8)		
$C_{\ell\hat{\omega}\beta^3}$	C(9)		
$C_{\ell\hat{p}^3}$	C(10)		
$C_{\ell\hat{\omega}\beta^2\hat{p}}$	C(11)		
$C_{\ell\hat{\omega}\beta\hat{p}^2}$	C(12)		
$C_{n\beta}$	C(13)		
$C_{n\hat{r}}$	C(14)		
$C_{n\beta^3}$	C(15)		
$C_{n\hat{r}^3}$	C(16)		
$C_{n\beta^2\hat{r}}$	C(17)		
$C_{n\beta\hat{r}^2}$	C(18)		

CONTROL PARAMETERS

	COMP.SY.*	VALUE	DIM.
No. of Equations	NDIM	10	-
Initial Time	PRMT(1)		DNT
Final Time	PRMT(2)		DNT
Upper Time Incr.	PRMT(3)		DNT
Upper Error Bd.	PRMT(4)		-

INITIAL CONDITIONS				ERROR WEIGHTS		
SYM.	CO.S	VALUE	DIM.	SYM.	VAL.	DIM.
V_r	P(1)		M/SEC	$\Delta\bar{V}_r$	.05	DNL/DNT
γ_r	P(2)		DEG	$\Delta\gamma_r$	.049	RAD
ω_r	P(3)		RPM	$\Delta\bar{\omega}_r$	.001	RAD/DNT
β	P(4)		DEG	$\Delta\beta$	.2	RAD
ϕ	P(5)		DEG	$\Delta\phi$	.2	RAD
$\dot{\phi}$	P(6)		DEG/SEC	$\Delta\dot{\phi}$	.05	RAD/DNT
ψ	P(7)		DEG	$\Delta\psi$	.2	RAD
$\dot{\psi}$	P(8)		DEG/SEC	$\Delta\dot{\psi}$	.05	RAD/DNT
x	P(9)		M	$\Delta\bar{x}$	.1	DNL
z	P(10)		M	$\Delta\bar{z}$	.1	DNL

REMARKS:

* COMP.SY. means: Computer Symbol

SYM.	COMP. SY.	EXPLANATION
γ_{ss}	GSS	steady-state glide angle
V_{ss}	VSS	steady-state flight speed
τ	TAU	time parameter
$\bar{I}$	TMOIDN	transverse M.O.I. dynamic norm.
$\bar{I}_y$	SMOIDN	spin M.O.I. dynamic norm.
V_n	VR	flight speed
γ_n	GAMR	glide angle
β	BETA	side slip angle
ϕ	PHI	rolling angle
$\dot{\phi}$	PHI.	
ψ	PSI	yawing angle
$\dot{\psi}$	PSI.	
x	XX	range
z	ZZ	vertical drop
$\hat{\omega}_n$	WRAN	tip speed ratio
	DNT	dynamic-norm. time
	DNL	dynamic-norm. length

TABLE B.2 COMPUTER SYMBOLS

```
                                   MS FORTRAN (4.0)/MSOS          06/19/70

      PROGRAM MAGSIX
      DIMENSION Y(10),P(10),DERY(10),PRMT(7),AUX(8,10),AAA(50)
      COMMON BM,RHO,S,RL,TMOI,SMOI,GSS,G,BMU,VSS,TAU,TMOIDN,SMOIDN,C(18)
     C,ACCEL
      EXTERNAL FCT,OUTP
    1 CALL GREEN
      READ(60,11) IRUN
      GOTO(10,2),EOFCKE(60)
    2 READ(60,12)AAA
      READ(60,13) RHO,S,RL,BM,TMOI,SMOI,GSS,(C(I),I=1,18)
      READ(60,14)NDIM,(PRMT(I),I=1,6)
      READ(60,15)(P(I),DERY(I),I=1,NDIM)
      ACCEL=0.
      RGSS=GSS*0.01745
      G=9.8066
      BMU=(2.*BM)/(RHO*S*RL)
      DUM1=SIN(RGSS)
      DUM2=ABS(DUM1)
      DUM3=S*RL*BMU*DUM2/C(1)
      VSS=SQRT(DUM3)
      TAU=BML*RL/VSS
      TMOIDN=TMOI/(BM*(RL*BMU)**2)
      SMOIDN=SMOI/(BM*(RL*BMU)**2)
      CALL CONVERT(P,Y,1,NDIM)
      WRITE(61,16) IRUN,AAA,RHO,GSS,S,VSS,RL,TAU,BM,BMU,TMOI,TMOIDN,
     CSMOI,SMOIDN,(C(I),I=1,18)
      WRITE(61,17)(P(I),Y(I),I=1,10)
      WRITE(61,18)
      CALL RKGS(PRMT,Y,DERY,NDIM,IHLF,FCT,OUTP,AUX)
      CALL REW(ITIME)
   11 FORMAT(I2)
   12 FORMAT(50A1)
   13 FORMAT(F20.6)
   14 FORMAT(I2,6X,6E10.3)
   15 FORMAT(2F20.6)
   16 FORMAT(1H1,9X,6H RUN NO ,I2,50A1,////
     C/,9H     RHO =,E10.2,20H KG/CUM          GSS =,E10.2,6H DEG  ,
     C/,9H       S =,E10.2,20H SQM             VSS =,E10.2,6H M/SEC,
     C/,9H      RL =,E10.2,20H M               TAU =,E10.2,6H SEC  ,
     C/,9H      BM =,E10.2,20H KG              BMU =,E10.2,
     C/,9H    TMOI =,E10.2,20H KG.SQM       TMOIDN =,E10.2,
     C/,9H    SMOI =,E10.2,20H KG.SQM       SMOIDN =,E10.2,///
     C/,8H      CD =,E10.2,8H   CLW =,E10.2,8H   CMA =,E10.2,8H  CMDW =,
     CE10.2,8H   CYB =,E10.2,8H  CYB3 =,E10.2,/,8H  CLBW =,E10.2,
     CEH   CLP =,E10.2,8H  CLB3 =,E10.2,8H  CLP3 =,E10.2,8H CLB2P =,
     CE10.2,8H CLBP2 =,E10.2,/,8H   CNB =,E10.2,8H   CNR =,E10.2,
     CEH  CNB3 =,E10.2,8H  CNR3 =,E10.2,8H CNB2R =,E10.2,8H CNBR2 =,
     CE10.2,//////)
   17 FORMAT(20X,20H INITIAL CONDITIONS ,//
     C/,20X,9H      VR =,E10.2,16H M/SEC     VRDN =,E10.2,9H DNL/DNT ,
     C/,20X,9H    GAMR =,E10.2,16H DEG       GAMR =,E10.2,9H RAD     ,
     C/,20X,9H      WR =,E10.2,16H RPM       WRDN =,E10.2,9H RAD/DNT ,
```

```
C/,20X,9H   BETA =,E10.2,16H DEG       BETA =,E10.2,9H RAD      ,
C/,20X,9H    PHI =,E10.2,16H DEG        PHI =,E10.2,9H RAD      ,
C/,20X,9H   PHI. =,E10.2,16H DEG/SEC  PHI. =,E10.2,9H RAD/DNT ,
C/,20X,9H    PSI =,E10.2,16H DEG        PSI =,E10.2,9H RAD      ,
C/,20X,9H   PSI. =,E10.2,16H DEG/SEC  PSI. =,E10.2,9H RAD/DN  ,
C/,20X,9H     XX =,E10.2,16H M         XXDN =,E10.2,9H DNL      ,
C/,20X,9H     ZZ =,E10.2,16H M         ZZDN =,E10.2,9H DNL      )
18 FORMAT(1H1,40X,52H TRAJECTORY AND ATTITUDE MOTIONS OF THE MAGNUS R
C OTOR,///,2X,10HDYN.-NORM.,3X,6HACTUAL,4X,2HXX,5X,2HZZ,3X,2HVR,3X,
C4HGAMR,4X,2HWR,4X,4HVRDN,4X,4HWRDN,4X,4HWRAN,4X4HBETA,5X,3HPHI,5X,
C3HPSI,6X,4HPHI.,7X,4HPSI.,3X,4HIHLF,/,4X,4HTIME,8X,4HTIME,//,4X,
C3HDNT,10X,3HSEC,6X,1HM,5X,1HM,2X,5HM/SEC,3X,3HDEG,3X,3HRPM,3X,7HDN
CL/DNT,6H RAD/DNT,8H RAD/ANT,3X,3HDEG,5X,3HDEG,5X,3HDEG,4X,7HDEG/SE
CC,4X,7HDEG/SEC,///)
  ISEC=ITIME/1000
  IMIN=ISEC/60
  ISEC=FLOAT(ISEC)-60.*FLOAT(IMIN)
  WRITE(61,19)IMIN,ISEC
19 FORMAT(14H1RUNNING TIME I3,9H MIN AND I3,4H SEC)
  GO TO 1
10 CALL RED(ITIME)
  STOP
  END
```

```
  SUBROUTINE CONVERT(P,Y,NCODE,NDIM)
  DIMENSION P(10),Y(10),A(10)
  COMMON BM,RHO,S,RL,TMOI,SMOI,GSS,G,BMU,VSS,TAU,TMOIDN,SMOIDN,C(18)
 C,ACCEL
  RAD=57.2958 $ A(1)=1/VSS $ A(2)=1/RAD $ A(3)=TAU*0.10472
  A(4)=1/RAD $ A(5)= 1/RAD $ A(6)=TAU/RAD $ A(7)=1/RAD
  A(8)=TAU/RAD $ A(9)=1/(BMU*RL) $ A(10)=1/(BMU*RL)
  GO TO (100,200)NCODE
100 DO 101 I=1,NDIM
101 Y(I)=P(I)*A(I)
  RETURN
200 DO 201 I=1,NDIM
201 P(I)=Y(I)/A(I)
  RETURN
  END
```

```
      SUBROUTINE RKGS(PRMT,Y,DERY,NDIM,IHLF,FCT,OUTP,AUX)
      DIMENSION Y(1),DERY(1),AUX(8,1),A(4),B(4),C(4),PRMT(1)
      DO 1 I=1,NDIM
    1 AUX(8,I)=.0555556*DERY(I)
      PRMT(5)=0
      X=PRMT(1) $ XEND=PRMT(2) $ H=PRMT(3) $ CALL FCT(X,Y,DERY)
      IF(H*(XEND-X))36,37,2
    2 A(1)=.5 $ A(2)=.2928932 $ A(3)=1.707107 $ A(4)=.1666667
      B(1)=B(4)=2.0 $ B(2)=B(3)=1.0
      C(1)=C(4)=0.5 $ C(2)=.2928932 $ C(3)=1.707107
      DO 3 I=1,NDIM
      AUX(1,I)=Y(I) $ AUX(2,I)=DERY(I)
    3 AUX(3,I)=AUX(5,I)=0.0
      IREC=0 $ H=H+H $ IHLF=-1 $ ISTEP=IEND=0
    4 IF((X+H-XEND)*H)7,6,5
    5 H=XEND-X
    6 IEND=1
    7 CALL OUTP(X,Y,DERY,IREC,NDIM,PRMT)
      IF(PRMT(5))40,8,40
    8 ITEST=0
    9 ISTEP=ISTEP+1 $ J=1
   10 AJ=A(J) $ BJ=B(J) $ CJ=C(J)
      DO 11 I=1,NDIM
      R1=H*DERY(I) $ R2=AJ*(R1-BJ*AUX(6,I))
      Y(I)=Y(I)+R2 $ R2=R2+R2+R2
   11 AUX(5,I)=AUX(5,I)+R2-CJ*R1
      IF(J-4)12,13,13
   12 J=J+1
      IF(J-3)13,14,13
   13 X=X+.5*H
   14 CALL FCT(X,Y,DERY) $ GO TO 10
   15 IF(ITEST)16,16,20
   16 DO 17 I=1,NDIM
   17 AUX(4,I)=Y(I)
      ITEST=1 $ ISTEP=ISTEP+ISTEP-2
   18 IHLF=IHLF+1 $ X=X-H $ H=.5*H
      DO 19 I=1,NDIM
      Y(I)=AUX(1,I) $ DERY(I)=AUX(2,I)
   19 AUX(6,I)=AUX(3,I)
      GO TO 9
   20 IMOD=ISTEP/2
      IF(ISTEP-1-IMOD-IMOD)21,23,21
   21 CALL FCT(X,Y,DERY)
      DO 22 I=1,NDIM
      AUX(5,I)=Y(I)
   22 AUX(7,I)=DERY(I)
      GO TO 9
   23 DELT=0
      DO 24 I=1,NDIM
   24 DELT=DELT+AUX(8,I)*ABS(AUX(4,I)-Y(I))
      IF(DELT-PRMT(4))28,28,25
   25 IF(IHLF-10)26,30,30
   26 DO 27 I=1,NDIM
   27 AUX(4,I)=AUX(1,I)
      ISTEP=ISTEP+ISTEP-4 $ X=X+H $ IEND=0 $ GO TO 18
   28 CALL FCT(X,Y,DERY)
```

```
      DO 29 I=1,NDIM
      AUX(1,I)=Y(I) $ AUX(2,I)=DERY(I) $ AUX(3,I)=AUX(6,I)$Y(I)=AUX(5,I)
   29 DERY(I)=AUX(7,I)
      CALL OUTP(X,H,Y,DERY,IHLF,NDIM,PRMT)
      IF(PRMT(5))40,30,40
   30 DO 31 I=1,NDIM
      Y(I)=AUX(1,I)
   31 DERY(I)=AUX(2,I)
      IREC=IHLF
      IF(IEND)32,32,39
   32 IHLF=IHLF-1 $ ISTEP=ISTEP/2 $ H=H+H
      IF(IHLF)4,33,33
   33 IMOD=ISTEP/2
      IF(ISTEP-IMOD-IMOD)4,34,4
   34 IF(DELT-.02*PRMT(4))35,35,4
   35 IHLF=IHLF-1 $ ISTEP=ISTEP/2 $ H=H+H $ GO TO 4
   36 IHLF=11 $ CALL FCT(X,Y,DERY) $ GO TO 39
   37 IHLF=12 $ GO TO 39
   38 IHLF=13
   39 CALL OUTP(X,Y,DERY,IHLF,NDIM,PRMT)
   40 RETURN
      END
```

```
      SUBROUTINE FCT(X,Y,DERY)
      DIMENSION Y(10),DERY(10)
      COMMON BM,RMU,S,RL,TMOI,SMOI,GSS,G,BMU,VSS,TAU,TMOIDN,SMOIDN,C(18)
     C,ACCEL
      DERY(1)=-C(1)*Y(1)**2-(TAU*G/VSS)*SIN(Y(2))
      DERY(2)=C(2)*Y(3)/BMU-TAU*G*COS(Y(2))/(VSS*Y(1))
      DERY(3)=C(3)*Y(1)**2/(BMU*SMOIDN)+C(4)*Y(1)*Y(3)/(SMOIDN*BMU**2)
      DERY(4)=  (-ACCEL/Y(1) +Y(1)*C(5))*Y(4)-Y(6)+TAU*G*COS(Y(2))*Y(5)/
     C(VSS*Y(1))+TAU*G*SIN(Y(2))*Y(7)/(VSS*Y(1))+C(6)*Y(1)*Y(4)**3/6.
      DERY(5)=Y(6)
      DERY(6)=C(7)*Y(1)*Y(5)*Y(4)/(TMOIDN*BMU**2)+C(8)*Y(1)*Y(6)/(TMOIDN
     C*BMU**2)+SMOIDN*Y(3)*Y(6)/TMOIDN+C(9)*Y(1)*Y(3)*Y(4)**3/(6.*TMOIDN
     C*BMU**2)+C(10)*Y(6)**3/(6.*Y(1)*TMOIDN*BMU**4)+C(11)*Y(3)*Y(4)**2*
     CY(6)/(6.*TMOIDN*BMU**3)+C(12)*Y(4)*Y(6)**2*Y(3)/(6.*TMOIDN*BMU**4*
     CY(1))
      DERY(7)=Y(8)
      DERY(8)=(1/TMOIDN)*(C(13)*Y(1)**2*Y(4)/BMU - SMOIDN*Y(3)*Y(6)+
     CC(14)*Y(1)*Y(5)/BMU**2 + C(15)*Y(1)**2*Y(4)**3/(6.*BMU) + C(16)*
     CY(3)**3/(6.*BMU**4*Y(1)) + C(17)*Y(1)*Y(4)**2*Y(8)/(6.*BMU**2)+
     CC(18)*Y(4)*Y(8)**2/(6.*BMU**3))
      DERY(9)=Y(1)*COS(Y(2))
      DERY(10)=-Y(1)*SIN(Y(2))
      RETURN
      END
```

```
      SUBROUTINE OUTP(X,Y,DERY,IHLF,NDIM,PRMT)
      DIMENSION Y(10),P(10),DERY(10),PRMT(7),
      COMMON BM,RHO,S,RL,TMOI,SMOI,GSS,G,BMU,VSS,TAU,TMOIDN,SMOIDN,C(18)
C*ACCEL
      ACCEL=DERY(1)
      T=TAU*X
      CALL CONVERT(P,Y,2,NDIM)
      WRAN=Y(3)/(BMU*Y(1))
      WRITE(61,1)X,T,P(9),P(10),P(1),P(2),P(3),Y(1),Y(3),WRAN,P(4),P(5),
C P(7),P(6),P(8),IHLF
    1 FORMAT(1X,E10.3,F10.0,2F6.0,F7.1,2F6.0,F8.3,F8.0,F8.3,3F8.2,2E11.2
C,I5)
      RETURN
      END
```

```
NO ERRORS
LOAD,56
RUN,10
```

RUN NO 19 RECTANGULAR MAGNUS ROTOR ONE

RHO =	1.16E 00 KG/CUM	GSS =	-2.47E 01 DEG
S =	4.68E-02 SQM	VSS =	1.31E 01 M/SEC
RL =	6.25E-02 M	TAU =	4.20E 00 SEC
RM =	1.50E 00 KG	BHU =	8.81E 02
TMOI =	2.68E-02 KG.SQM	TMOIDN =	5.89E-06
SMOI =	4.00E-03 KG.SQM	SMOIDN =	8.79E-07

CD =	1.31E 00	CLW =	2.51E 00	CMA =	5.08E-01	CMDW =	-4.50E-01	CYB =	-3.82E 00	CYB3 =	0		
CLBW =	-3.57E-01	CLP =	-5.82E 00	CLB3 =	0	CLP3 =	0	CLR2P =	0	CLBP2 =	0		
CNB =	-7.37E-01	CNR =	-1.38E 01	CNA3 =	0	CNR3 =	0	CNR2R =	0	CNBR2 =	0		

INITIAL CONDITIONS

VR =	8.50E 00 M/SEC	VRDN =	6.48E-01 DNL/DNT
GAMR =	-8.50E 01 DEG	GAMR =	-1.48E 00 RAD
WR =	3.60E 02 RPM	WRDN =	1.58E 02 RAD/DNT
BETA =	0 DEG	BETA =	0 RAD
PHI =	-2.50E 01 DEG	PHI =	-4.36E-01 RAD
PHI. =	0 DEG/SEC	PHI. =	0 RAD/DNT
PSI =	0 DEG	PSI =	0 RAD
PSI. =	1.41E 02 DEG/SEC	PSI. =	1.03E 01 RAD/DNT
XX =	2.00E 00 M	XXDN =	3.63E-02 DNL
ZZ =	2.00E 01 M	ZZDN =	3.63E-01 DNL

TRAJECTORY AND ATTITUDE MOTIONS OF THE MAGNUS ROTOR

DYN.-NOSM. TIME DNT	ACTUAL TIME SEC	XX M	ZZ M	VR M/SEC	GAMR DEG	WR RPM	VRDN DNL/DNT	WRDN RAD/DNT	WRAN RAD/ANT	BETA DEG	PHI DEG	PSI DEG	PHI. DEG/SEC	PSI. DEG/SEC	IHLF
2.381E-01	.999117	2	20	8.5	-85	360	.648	158	.277	0	-25.00	0	0	1.41E 02	0
2.481E-01	1.041079	2	20	8.8	-85	365	.673	160	.270	-5.86	-24.31	5.81	3.28E 01	1.35E 02	0
2.581E-01	1.083041	2	21	9.2	-85	370	.698	163	.264	-11.20	-22.27	11.21	6.36E 01	1.22E 02	0
2.681E-01	1.125003	2	21	9.5	-85	376	.723	165	.259	-15.77	-19.02	15.94	9.08E 01	1.03E 02	0
2.781E-01	1.166965	2	22	9.8	-85	382	.747	168	.255	-19.32	-14.73	19.76	1.13E 02	7.84E 01	0
2.881E-01	1.208927	2	22	10.1	-85	389	.771	171	.252	-21.70	-9.64	22.47	1.29E 02	5.03E 01	0
2.981E-01	1.250889	2	22	10.4	-85	396	.794	174	.249	-22.78	-4.04	23.95	1.37E 02	1.90E 01	0

CONTINUED

APPENDIX C

MAGNUS ROTOR DATA

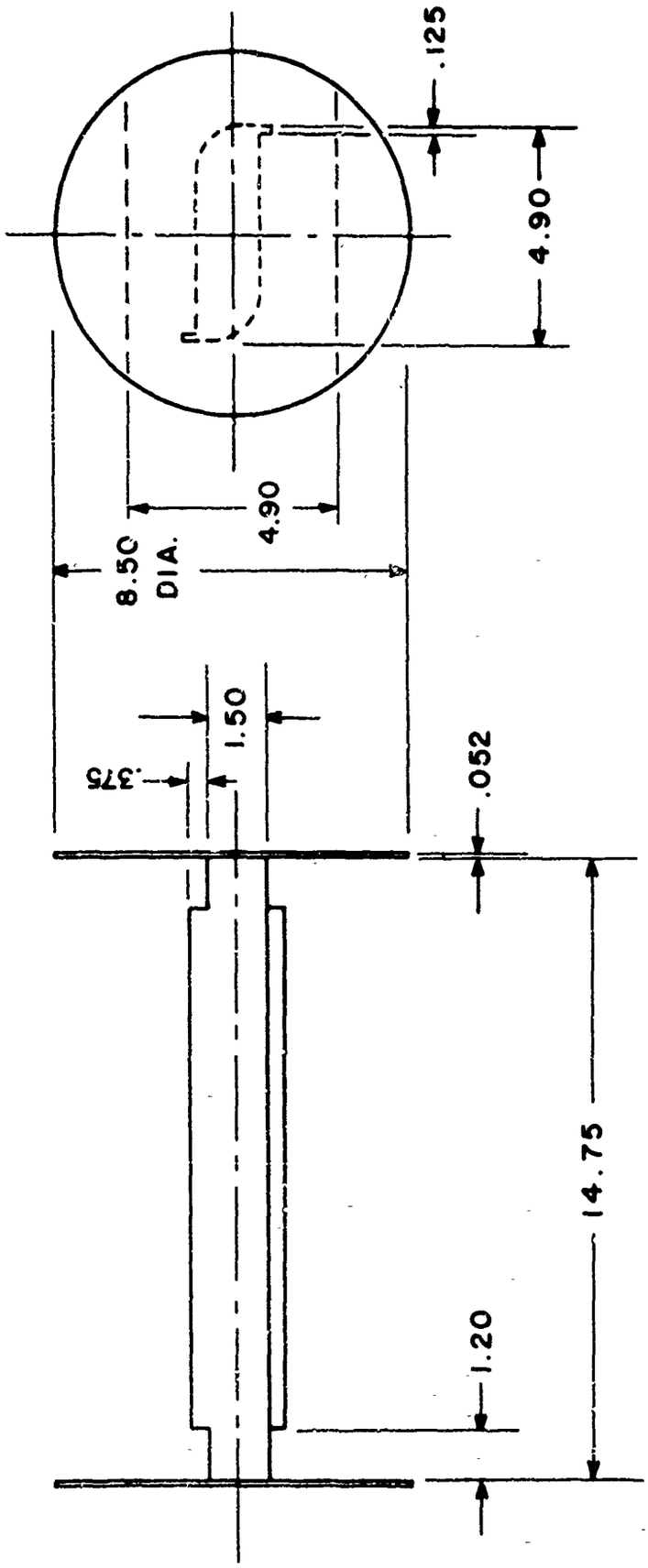

FIGURE C.1 RECTANGULAR MAGNUS ROTORS 1, 2, and 3. DIMENSIONS IN INCHES

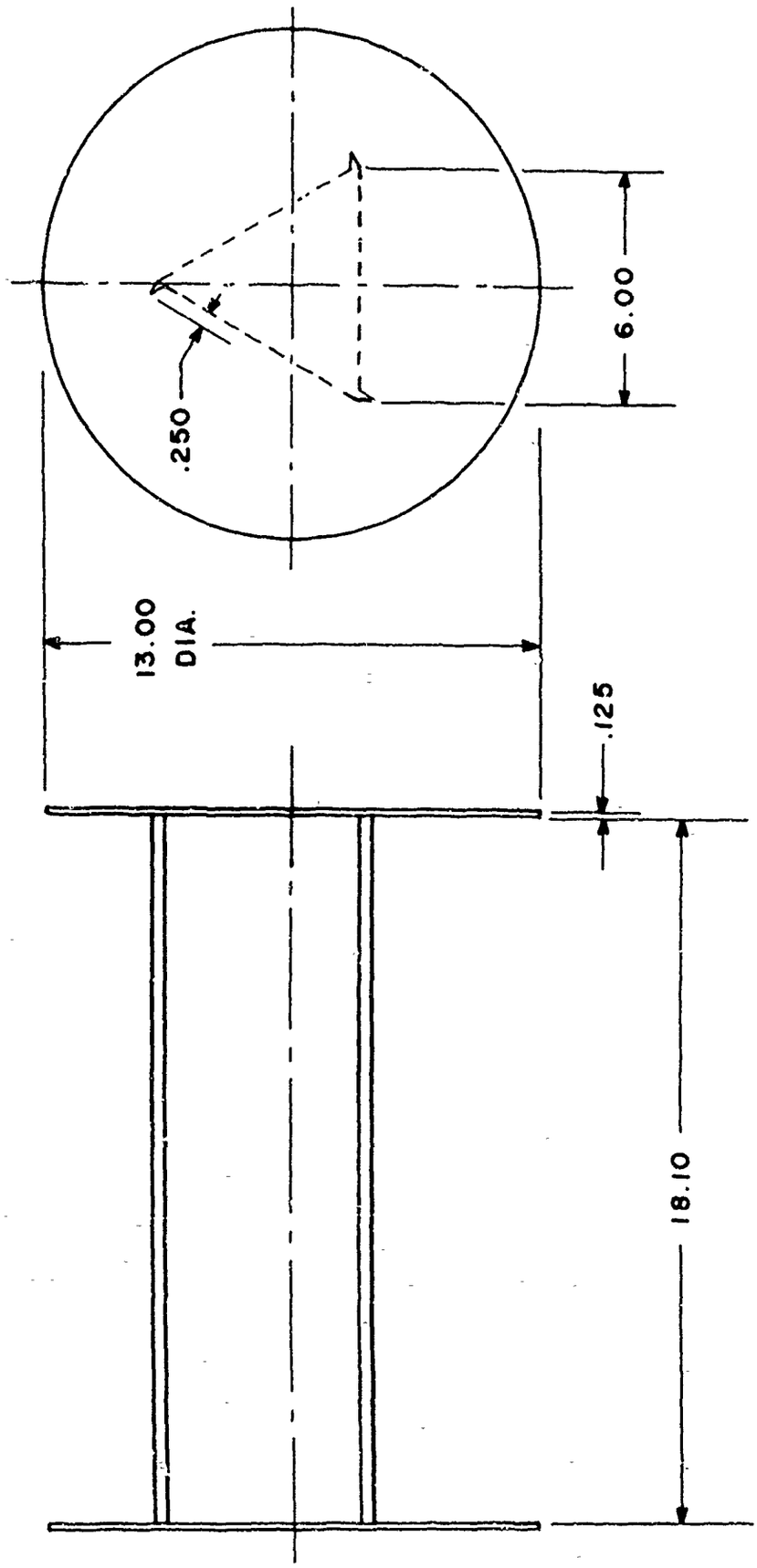

FIGURE C.2 TRIANGULAR MAGNUS ROTOR 1. DIMENSIONS IN INCHES

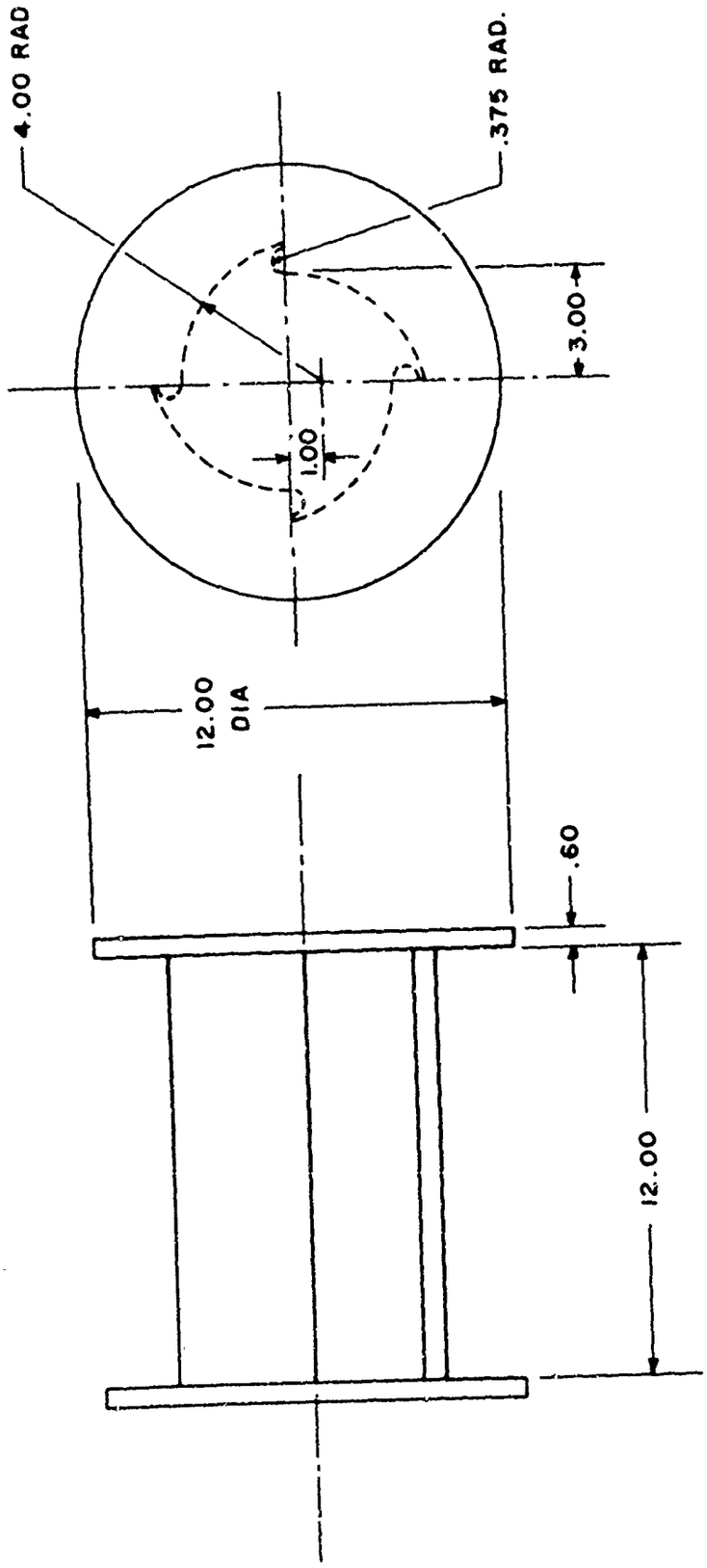

FIGURE C.3 CYLINDRICAL MAGNUS ROTORS 1, 3, 4A, and 11. DIMENSIONS IN INCHES

RUN NO.: 13

IDENTIFICATION: RECT. MR 1

MAGNUS ROTOR PARAMETERS

SYMBOL	COMP.SY.	VALUE	DIM.
ρ	RHO	1.225	KG/M^3
S	S	.0468	M^2
c/ℓ	RL	.0625	M
m	BM	1.50	KG
I	TMOI	.0268	$KG \cdot M^2$
I_y	SMOI	.0040	$KG\ M^2$
γ_{ss}	GSS	-24.7	DEG
C_D	C(1)	1.31	ALL DERIVATIVES IN RADIANS
$C_{L_{\hat{\omega}}}$	C(2)	2.51	
C_{M_α}	C(3)	.508	
$C_{M_{d\hat{\omega}}}$	C(4)	-.450	
C_{y_β}	C(5)	-3.82	
$C_{y_{\beta^3}}$	C(6)	0	
$C_{\ell_{\hat{\omega}\beta}}$	C(7)	-.357	
$C_{\ell_{\hat{p}}}$	C(8)	-5.82	
$C_{\ell_{\hat{\omega}\beta^3}}$	C(9)	0	
$C_{\ell_{\hat{p}^3}}$	C(10)	0	
$C_{\ell_{\hat{\omega}\beta^2\hat{p}}}$	C(11)	0	
$C_{\ell_{\hat{\omega}\beta\hat{p}^2}}$	C(12)	0	
C_{n_β}	C(13)	-.737	
$C_{n_{\hat{r}}}$	C(14)	-13.80	
$C_{n_{\beta^3}}$	C(15)	0	
$C_{n_{\hat{r}^3}}$	C(16)	0	
$C_{n_{\beta^2\hat{r}}}$	C(17)	0	
$C_{n_{\beta\hat{r}^2}}$	C(18)	0	

CONTROL PARAMETERS

	COMP.SY.	VALUE	DIM.
No. of Equations	NDIM	10	-
Initial Time	PRMT(1)	0	DNT
Final Time	PRMT(2)	10	DNT
Upper Time Incr.	PRMT(3)	10^{-1}	DNT
Upper Error Bd.	PRMT(4)	10^{-6}	-

INITIAL CONDITIONS				ERROR WEIGHTS		
SYM.	CO.S	VALUE	DIM.	SYM.	VAL.	DIM.
V_R	P(1)	16.6	M/SEC	$\Delta\bar{V}_R$	.05	DNL/DNT
γ_R	P(2)	-77	DEG	$\Delta\gamma_R$	.049	RAD
ω_R	P(3)	850	RPM	$\Delta\bar{\omega}_R$	.001	RAD/DNT
β	P(4)	0	DEG	$\Delta\beta$	.2	RAD
ϕ	P(5)	3	DEG	$\Delta\phi$	.2	RAD
$\dot{\phi}$	P(6)	0	DEG/SEC	$\Delta\mathring{\phi}$	.05	RAD/DNT
ψ	P(7)	0	DEG	$\Delta\psi$	.2	RAD
$\dot{\psi}$	P(8)	-40	DEG/SEC	$\Delta\mathring{\psi}$	.05	RAD/DNT
X	P(9)	0	M	$\Delta\bar{X}$	.1	DNL
Z	P(10)	0	M	$\Delta\bar{Z}$	.1	DNL

REMARKS:

Aerodynamic data from NACA
Langley Stability Tunnel
Test RM SL 55 J 26
November 1955

RUN NO.: 15

IDENTIFICATION: RECT. MR 1

MAGNUS ROTOR PARAMETERS

SYMBOL	COMP.SY.	VALUE	DIM.
ρ	RHO	SEE RUN 13	KG/M^3
S	S		M^2
c/ℓ	RL		M
m	BM		KG
I	TMOI		$KG\ M^2$
I_y	SMOI		$KG\ M^2$
γ_{ss}	GSS		DEG
C_D	C(1)	SEE RUN 13	ALL DERIVATIVES IN RADIANS
$C_{L\hat{\omega}}$	C(2)		
C_{M_a}	C(3)		
$C_{M_{d\hat{\omega}}}$	C(4)		
C_{y_β}	C(5)		
$C_{y_{\beta^3}}$	C(6)		
$C_{\ell_{\hat{\omega}\beta}}$	C(7)		
$C_{\ell_{\hat{p}}}$	C(8)		
$C_{\ell_{\hat{\omega}\beta^3}}$	C(9)		
$C_{\ell_{\hat{p}^3}}$	C(10)		
$C_{\ell_{\hat{\omega}\beta^2\hat{p}}}$	C(11)		
$C_{\ell_{\hat{\omega}\beta\hat{p}^2}}$	C(12)		
C_{n_β}	C(13)		
$C_{n_{\hat{R}}}$	C(14)		
$C_{n_{\beta^2}}$	C(15)		
$C_{n_{\hat{R}^3}}$	C(16)		
$C_{n_{\beta^2\hat{R}}}$	C(17)		
$C_{n_{\beta\hat{R}^2}}$	C(18)		

CONTROL PARAMETERS

	COMP.SY.	VALUE	DIM.
No. of Equations	NDIM	10	-
Initial Time	PRMT(1)	0.	DNT
Final Time	PRMT(2)	5.	DNT
Upper Time Incr.	PRMT(3)	10^{-1}	DNT
Upper Error Bd.	PRMT(4)	10^{-5}	-

INITIAL CONDITIONS				ERROR WEIGHTS		
SYM.	CO.S	VALUE	DIM.	SYM.	VAL.	DIM.
V_R	P(1)	100	M/SEC	$\Delta\bar{V}_R$	.05	DNL/DNT
γ_R	P(2)	0	DEG	$\Delta\gamma_R$	.049	RAD
ω_R	P(3)	4000	RPM	$\Delta\bar{\omega}_R$	.001	RAD/DNT
β	P(4)	0	DEG	$\Delta\beta$	.2	RAD
ϕ	P(5)	3	DEG	$\Delta\phi$	.2	RAD
$\dot{\phi}$	P(6)	0	DEG/SEC	$\Delta\dot{\phi}$	.05	RAD/DNT
ψ	P(7)	0	DEG	$\Delta\psi$	.2	RAD
$\dot{\psi}$	P(8)	0	DEG/SEC	$\Delta\dot{\psi}$	.05	RAD/DNT
x	P(9)	0	M	$\Delta\bar{x}$	.1	DNL
z	P(10)	0	M	$\Delta\bar{z}$	.1	DNL

REMARKS:

RUN NO.: 19

IDENTIFICATION: RECT. MR 1

MAGNUS ROTOR PARAMETERS

SYMBOL	COMP.SY.	VALUE	DIM.
ρ	RHO	1.164	KG/M^3
S	S	.0468	M^2
c/ℓ	RL	.0625	M
m	BM	1.50	KG
I	TMOI	.0268	$KG\ M^2$
I_y	SMOI	.0040	$KG\ M^2$
γ_{ss}	GSS	-24.7	DEG
C_D	C(1)	SEE RUN 13	ALL DERIVATIVES IN RADIANS
$C_{L_{\hat{\omega}}}$	C(2)		
C_{M_α}	C(3)		
$C_{M_{d\hat{\omega}}}$	C(4)		
C_{y_β}	C(5)		
$C_{y_{\beta^3}}$	C(6)		
$C_{\ell_{\hat{\omega}\beta}}$	C(7)		
$C_{\ell_{\hat{p}}}$	C(8)		
$C_{\ell_{\hat{\omega}\beta^3}}$	C(9)		
$C_{\ell_{\hat{p}^3}}$	C(10)		
$C_{\ell_{\hat{\omega}\beta^2\hat{p}}}$	C(11)		
$C_{\ell_{\hat{\omega}\beta\hat{p}^2}}$	C(12)		
C_{n_β}	C(13)		
$C_{n_{\hat{R}}}$	C(14)		
$C_{n_{\beta^3}}$	C(15)		
$C_{n_{\hat{R}^3}}$	C(16)		
$C_{n_{\beta^2\hat{R}}}$	C(17)		
$C_{n_{\beta\hat{R}^2}}$	C(18)		

CONTROL PARAMETERS

	COMP.SY.	VALUE	DIM.
No. of Equations	NDIM	10	-
Initial Time	PRMT(1)	0.238	DNT
Final Time	PRMT(2)	6.	DNT
Upper Time Incr.	PRMT(3)	10^{-2}	DNT
Upper Error Bd.	PRMT(4)	10^{-5}	-

INITIAL CONDITIONS				ERROR WEIGHTS		
SYM.	CO.S	VALUE	DIM.	SYM.	VAL.	DIM.
V_R	P(1)	8.5	M/SEC	$\Delta\bar{V}_R$	.05	DNL/DNT
γ_R	P(2)	-85	DEG	$\Delta\gamma_R$	.049	RAD
ω_R	P(3)	360	RPM	$\Delta\bar{\omega}_R$	.001	RAD/DNT
β	P(4)	0	DEG	$\Delta\beta$	.2	RAD
ϕ	P(5)	-25	DEG	$\Delta\phi$	.2	RAD
$\dot{\phi}$	P(6)	0	DEG/SEC	$\Delta\dot{\phi}$	.05	RAD/DNT
ψ	P(7)	0	DEG	$\Delta\psi$	.2	RAD
$\dot{\psi}$	P(8)	141	DEG/SEC	$\Delta\dot{\psi}$	.05	RAD/DNT
x	P(9)	2	M	$\Delta\bar{x}$	.1	DNL
z	P(10)	20	M	$\Delta\bar{z}$	.1	DNL

REMARKS:

RUN NO.: 21

IDENTIFICATION: RECT. MR 1

MAGNUS ROTOR PARAMETERS

SYMBOL	COMP.SY.	VALUE	DIM.
ρ	RHO	SEE RUN 13	KG/M^3
S	S		M^2
c/ℓ	RL		M
m	BM		KG
I	TMOI		$KG\ M^2$
I_y	SMOI		$KG\ M^2$
γ_{ss}	GSS		DEG
C_D	C(1)	SEE RUN 13	ALL DERIVATIVES IN RADIANS
$C_{L\hat{\omega}}$	C(2)		
C_{M_α}	C(3)		
$C_{M_{\alpha\hat{\omega}}}$	C(4)		
C_{y_β}	C(5)		
$C_{y_{\beta^3}}$	C(6)		
$C_{\ell_{\hat{\omega}\beta}}$	C(7)		
$C_{\ell_{\hat{p}}}$	C(8)		
$C_{\ell_{\hat{\omega}\beta^3}}$	C(9)		
$C_{\ell_{\hat{p}^3}}$	C(10)		
$C_{\ell_{\hat{\omega}\beta^2\hat{p}}}$	C(11)		
$C_{\ell_{\hat{\omega}\beta\hat{p}^2}}$	C(12)		
C_{n_β}	C(13)		
$C_{n_{\hat{r}}}$	C(14)		
$C_{n_{\beta^3}}$	C(15)		
$C_{n_{\hat{r}^3}}$	C(16)		
$C_{n_{\beta^2\hat{r}}}$	C(17)		
$C_{n_{\beta\hat{r}^2}}$	C(18)		

CONTROL PARAMETERS

	COMP.SY.	VALUE	DIM.
No. of Equations	NDIM	10	-
Initial Time	PRMT(1)	0	DNT
Final Time	PRMT(2)	5	DNT
Upper Time Incr.	PRMT(3)	10^{-1}	DNT
Upper Error Bd.	PRMT(4)	10^{-5}	-

INITIAL CONDITIONS				ERROR WEIGHTS		
SYM.	CO.S	VALUE	DIM.	SYM.	VAL.	DIM.
V_R	P(1)	100	M/SEC	$\Delta\bar{V}_R$	.05	DNL/DNT
γ_R	P(2)	180	DEG	$\Delta\gamma_R$	.049	RAD
ω_R	P(3)	4000	RPM	$\Delta\bar{\omega}_R$	.001	RAD/DNT
β	P(4)	0	DEG	$\Delta\beta$	.2	RAD
ϕ	P(5)	3	DEG	$\Delta\phi$	.2	RAD
$\dot{\phi}$	P(6)	0	DEG/SEC	$\Delta\dot{\phi}$	.05	RAD/DNT
ψ	P(7)	0	DEG	$\Delta\psi$	.2	RAD
$\dot{\psi}$	P(8)	0	DEG/SEC	$\Delta\dot{\psi}$	.05	RAD/DNT
x	P(9)	0	M	$\Delta\bar{x}$	.1	DNL
z	P(10)	0	M	$\Delta\bar{z}$	.1	DNL

REMARKS:

RUN NO.: 23

IDENTIFICATION: RECT. MR 1

MAGNUS ROTOR PARAMETERS			
SYMBOL	COMP.SY.	VALUE	DIM.
ρ	RHO	SEE RUN 13	KG/M^3
S	S		M^2
$c/2$	RL		M
m	BM		KG
I	TMOI		$KG\ M^2$
I_y	SMOI		$KG\ M^2$
γ_{ss}	GSS		DEG
C_D	C(1)	SEE RUN 13	ALL DERIVATIVES IN RADIANS
$C_{L\hat{\omega}}$	C(2)		
C_{M_α}	C(3)		
$C_{M_{d\hat{\omega}}}$	C(4)		
C_{y_β}	C(5)		
$C_{y_{\beta^3}}$	C(6)		
$C_{L_{\hat{\omega}\beta}}$	C(7)		
$C_{L_{\hat{p}}}$	C(8)		
$C_{L_{\hat{\omega}\beta^2}}$	C(9)		
$C_{L_{\hat{p}^3}}$	C(10)		
$C_{L_{\hat{\omega}\beta^2\hat{p}}}$	C(11)		
$C_{L_{\hat{\omega}\beta\hat{p}^2}}$	C(12)		
C_{n_β}	C(13)		
$C_{n_{\hat{R}}}$	C(14)		
$C_{n_{\beta^3}}$	C(15)		
$C_{n_{\hat{R}^3}}$	C(16)		
$C_{n_{\beta^2\hat{R}}}$	C(17)		
$C_{n_{\beta\hat{R}^2}}$	C(18)		

CONTROL PARAMETERS			
	COMP.SY.	VALUE	DIM.
No. of Equations	NDIM	10	-
Initial Time	PRMT(1)	0	DNT
Final Time	PRMT(2)	5	DNT
Upper Time Incr.	PRMT(3)	10^{-2}	DNT
Upper Error Bd.	PRMT(4)	10^{-5}	-

INITIAL CONDITIONS				ERROR WEIGHTS		
SYM.	CO.S	VALUE	DIM.	SYM.	VAL.	DIM.
V_R	P(1)	100	M/SEC	$\Delta\bar{V}_R$	.05	DNL/DNT
γ_R	P(2)	0	DEG	$\Delta\gamma_R$	.049	RAD
ω_R	P(3)	4000	RPM	$\Delta\bar{\omega}_R$	.001	RAD/DNT
β	P(4)	0	DEG	$\Delta\beta$	.2	RAD
ϕ	P(5)	3	DEG	$\Delta\phi$	.2	RAD
$\dot{\phi}$	P(6)	0	DEG/SEC	$\Delta\dot{\phi}$	.05	RAD/DNT
ψ	P(7)	0	DEG	$\Delta\psi$	.2	RAD
$\dot{\psi}$	P(8)	0	DEG/SEC	$\Delta\dot{\psi}$	.05	RAD/DNT
x	P(9)	0	M	$\Delta\bar{x}$	.1	DNL
z	P(10)	0	M	$\Delta\bar{z}$	.1	DNL

REMARKS:

RUN NO.: 24

IDENTIFICATION: RECT. MR 1

MAGNUS ROTOR PARAMETERS

SYMBOL	COMP.SY.	VALUE	DIM.
ρ	RHO	SEE RUN 1	KG/M^3
S	S		M^2
c/ℓ	RL		M
m	BM		KG
I	TMOI		$KG\ M^2$
I_y	SMOI		$KG\ M^2$
γ_{ss}	GSS		DEG
C_D	C(1)	SEE RUN 13	ALL DERIVATIVES IN RADIANS
$C_{L\hat{\omega}}$	C(2)		
C_{M_0}	C(3)		
$C_{M_{d\hat{\omega}}}$	C(4)		
$C_{y\beta}$	C(5)		
$C_{y\beta^3}$	C(6)		
$C_{\ell\hat{\omega}\beta}$	C(7)		
$C_{\ell\hat{p}}$	C(8)		
$C_{\ell\hat{\omega}\beta^3}$	C(9)		
$C_{\ell\hat{p}^3}$	C(10)		
$C_{\ell\hat{\omega}\beta^2\hat{p}}$	C(11)		
$C_{\ell\hat{\omega}\beta\hat{p}^2}$	C(12)		
$C_{n\beta}$	C(13)		
$C_{n\hat{R}}$	C(14)		
$C_{n\beta^2}$	C(15)		
$C_{n\hat{R}^3}$	C(16)		
$C_{n\beta^2\hat{R}}$	C(17)		
$C_{n\beta\hat{R}^2}$	C(18)		

CONTROL PARAMETERS

	COMP.SY.	VALUE	DIM.
No. of Equations	NDIM	10	-
Initial Time	PRMT(1)	0	DNT
Final Time	PRMT(2)	5	DNT
Upper Time Incr.	PRMT(3)	10^{-2}	DNT
Upper Error Bd.	PRMT(4)	10^{-5}	-

INITIAL CONDITIONS				ERROR WEIGHTS		
SYM.	CO.S	VALUE	DIM.	SYM.	VAL.	DIM.
V_R	P(1)	0.1	M/SEC	$\Delta\bar{V}_R$	.05	DNL/DNT
γ_R	P(2)	- 90	DEG	$\Delta\gamma_R$	.049	RAD
ω_R	P(3)	200	RPM	$\Delta\bar{\omega}_R$	.001	RAD/DNT
β	P(4)	5	DEG	$\Delta\beta$	.2	RAD
ϕ	P(5)	0	DEG	$\Delta\phi$	.2	RAD
$\dot{\phi}$	P(6)	0	DEG/SEC	$\Delta\dot{\phi}$	.05	RAD/DNT
ψ	P(7)	0	DEG	$\Delta\psi$	.2	RAD
$\dot{\psi}$	P(8)	0	DEG/SEC	$\Delta\dot{\psi}$	.05	RAD/DNT
x	P(9)	0	M	$\Delta\bar{x}$	.1	DNL
z	P(10)	0	M	$\Delta\bar{z}$	.1	DNL

REMARKS:

RUN NO.: 25

IDENTIFICATION: RECT. MR 1

MAGNUS ROTOR PARAMETERS			
SYMBOL	COMP.SY.	VALUE	DIM.
ρ	RHO	SEE RUN 13	KG/M^3
S	S		M^2
$c/2$	RL		M
m	BM		KG
I	TMOI		$KG\ M^2$
I_y	SMOI		$KG\ M^2$
γ_{ss}	GSS		DEG
C_D	C(1)	SEE RUN 13	ALL DERIVATIVES IN RADIANS
$C_{L_{\hat{\omega}}}$	C(2)		
C_{M_0}	C(3)		
$C_{M_{\alpha}\hat{\omega}}$	C(4)		
C_{y_β}	C(5)		
$C_{y_{\beta^3}}$	C(6)		
$C_{l_{\hat{\omega}\beta}}$	C(7)		
$C_{l_{\hat{p}}}$	C(8)		
$C_{l_{\hat{\omega}\beta^3}}$	C(9)		
$C_{l_{\hat{p}^3}}$	C(10)		
$C_{l_{\hat{\omega}\beta^2\hat{p}}}$	C(11)		
$C_{l_{\hat{\omega}\beta\hat{p}^2}}$	C(12)		
C_{n_β}	C(13)		
$C_{n_{\hat{R}}}$	C(14)		
$C_{n_{\beta^3}}$	C(15)		
$C_{n_{\hat{R}^3}}$	C(16)		
$C_{n_{\beta^2\hat{R}}}$	C(17)		
$C_{n_{\beta\hat{R}^2}}$	C(18)		

CONTROL PARAMETERS			
	COMP.SY.	VALUE	DIM
No. of Equations	NDIM	10	-
Initial Time	PRMT(1)	0	DNT
Final Time	PRMT(2)	5	DNT
Upper Time Incr.	PRMT(3)	10^{-2}	DNT
Upper Error Bd.	PRMT(4)	10^{-5}	-

INITIAL CONDITIONS				ERROR WEIGHTS		
SYM.	CO.S	VALUE	DIM.	SYM.	VAL.	DIM.
V_R	P(1)	0.1	M/SEC	$\Delta\bar{V}_R$	.05	DNL/DNT
γ_R	P(2)	-90	DEG	$\Delta\gamma_R$	.049	RAD
ω_R	P(3)	200	RPM	$\Delta\bar{\omega}_R$	.001	RAD/DNT
β	P(4)	5	DEG	$\Delta\beta$	.2	RAD
ϕ	P(5)	0	DEG	$\Delta\phi$	.2	RAD
$\dot{\phi}$	P(6)	0	DEG/SEC	$\Delta\dot{\phi}$	.05	RAD/DNT
ψ	P(7)	0	DEG	$\Delta\psi$	.2	RAD
$\dot{\psi}$	P(8)	0	DEG/SEC	$\Delta\dot{\psi}$	.05	RAD/DNT
x	P(9)	0	M	$\Delta\bar{x}$	.1	DNL
z	P(10)	0	M	$\Delta\bar{z}$	.1	DNL

REMARKS:

RUN NO.: 30

IDENTIFICATION: CYL. MK 4A

MAGNUS ROTOR PARAMETERS

SYMBOL	COMP.SY.	VALUE	DIM.
ρ	RHO	1.139	KG/M^3
S	S	.0464	M^2
c/ℓ	RL	.0762	M
m	BM	2.137	KG
I	TMOI	.0267	$KG\ M^2$
I_y	SMOI	.0122	$KG\ M^2$
γ_{ss}	GSS	-57	DEG
C_D	C(1)	1.2	ALL DERIVATIVES IN RADIANS
$C_{L\hat{\omega}}$	C(2)	1.6	
C_{M_α}	C(3)	.22	
$C_{M_{d\hat{\omega}}}$	C(4)	-.55	
C_{y_β}	C(5)	-1.0	
$C_{y_{\beta^3}}$	C(6)	0	
$C_{\ell_{\hat{\omega}\beta}}$	C(7)	-2.11	
$C_{\ell_{\hat{p}}}$	C(8)	-1.5 1/	
$C_{\ell_{\hat{\omega}\beta^3}}$	C(9)	104	
$C_{\ell_{\hat{p}^3}}$	C(10)	0	
$C_{\ell_{\hat{\omega}\beta^2\hat{p}}}$	C(11)	0	
$C_{\ell_{\hat{\omega}\beta\hat{p}^2}}$	C(12)	0	
C_{n_β}	C(13)	.47	
$C_{n_{\hat{r}}}$	C(14)	-1.7 1/	
$C_{n_{\beta^3}}$	C(15)	0	
$C_{n_{\hat{r}^3}}$	C(16)	0	
$C_{n_{\beta^2\hat{r}}}$	C(17)	0	
$C_{n_{\beta\hat{r}^2}}$	C(18)	0	

CONTROL PARAMETERS

	COMP.SY.	VALUE	DIM.
No. of Equations	NDIM	10	-
Initial Time	PRMT(1)	0	DNT
Final Time	PRMT(2)	2	DNT
Upper Time Incr.	PRMT(3)	10^{-2}	DNT
Upper Error Bd.	PRMT(4)	10^{-5}	-

INITIAL CONDITIONS				ERROR WEIGHTS		
SYM.	CO.S	VALUE	DIM.	SYM.	VAL.	DIM.
V_R	P(1)	24	M/SEC	$\Delta\bar{V}_R$	.05	DNL/DNT
γ_R	P(2)	-57	DEG	$\Delta\gamma_R$	.049	RAD
ω_R	P(3)	1290	RPM	$\Delta\bar{\omega}_R$	.001	RAD/DNT
β	P(4)	0	DEG	$\Delta\beta$	.2	RAD
ϕ	P(5)	12.5	DEG	$\Delta\phi$	.2	RAD
$\dot{\phi}$	P(6)	0	DEG/SEC	$\Delta\mathring{\phi}$	.05	RAD/DNT
ψ	P(7)	0	DEG	$\Delta\psi$	.2	RAD
$\dot{\psi}$	P(8)	-768	DEG/SEC	$\Delta\mathring{\psi}$	.05	RAD/DNT
x	P(9)	0	M	$\Delta\bar{x}$	.1	DNL
z	P(10)	0	M	$\Delta\bar{z}$	.1	DNL

REMARKS:

Aerodynamic data from ARO, Inc., Wind Tunnel Test PC 0037, May 1970

1/ from Flight Test, June 1970

RUN NO.: 31

IDENTIFICATION: CYL. MR 11

MAGNUS ROTOR PARAMETERS			
SYMBOL	COMP.SY.	VALUE	DIM.
ρ	RHO	1.139	KG/M^3
S	S	.0464	M^2
c/ℓ	RL	.0762	M
m	BM	2.580	KG
I	TMOI	.0170	$KG\ M^2$
I_y	SMOI	.0133	$KG\ M^2$
γ_{ss}	GSS	-57	DEG
C_D	C(1)	SEE RUN 30	ALL DERIVATIVES IN RADIANS
$C_{L\hat{\omega}}$	C(2)		
C_{M_α}	C(3)		
$C_{M_{d\hat{\omega}}}$	C(4)		
C_{y_β}	C(5)		
$C_{y_{\beta^3}}$	C(6)		
$C_{\ell_{\hat{\omega}\beta}}$	C(7)		
$C_{\ell_{\hat{p}}}$	C(8)		
$C_{\ell_{\hat{\omega}\beta^3}}$	C(9)		
$C_{\ell_{\hat{p}^3}}$	C(10)		
$C_{\ell_{\hat{\omega}\beta^2\hat{p}}}$	C(11)		
$C_{\ell_{\hat{\omega}\beta\hat{p}^2}}$	C(12)		
C_{n_β}	C(13)		
$C_{n_{\hat{r}}}$	C(14)		
$C_{n_{\beta^3}}$	C(15)		
$C_{n_{\hat{r}^3}}$	C(16)		
$C_{n_{\beta^2\hat{r}}}$	C(17)		
$C_{n_{\beta\hat{r}^2}}$	C(18)		

CONTROL PARAMETERS			
	COMP.SY.	VALUE	DIM.
No. of Equations	NDIM	10	-
Initial Time	PRMT(1)	0	DNT
Final Time	PRMT(2)	2	DNT
Upper Time Incr.	PRMT(3)	10^{-2}	DNT
Upper Error Bd.	PRMT(4)	10^{-5}	-

INITIAL CONDITIONS				ERROR WEIGHTS		
SYM.	CO.S.	VALUE	DIM.	SYM.	VAL.	DIM.
V_R	P(1)	26	M/SEC	$\Delta\bar{V}_R$	.05	DNL/DNT
γ_R	P(2)	-57	DEG	$\Delta\gamma_R$	.049	RAD
ω_R	P(3)	1290	RPM	$\Delta\bar{\omega}_R$	.001	RAD/DNT
β	P(4)	0	DEG	$\Delta\beta$	.2	RAD
ϕ	P(5)	12.5	DEG	$\Delta\phi$	.2	RAD
$\dot{\phi}$	P(6)	0	DEG/SEC	$\Delta\mathring{\phi}$	.05	RAD/DNT
ψ	P(7)	0	DEG	$\Delta\psi$	.2	RAD
$\dot{\psi}$	P(8)	-768	DEG/SEC	$\Delta\mathring{\psi}$	.05	RAD/DNT
x	P(9)	0	M	$\Delta\bar{x}$	.1	DNL
z	P(10)	0	M	$\Delta\bar{z}$	.1	DNL

REMARKS:

RUN NO.: 32

IDENTIFICATION: RECT. MR 3

MAGNUS ROTOR PARAMETERS

SYMBOL	COMP.SY.	VALUE	DIM.
ρ	RHO	1.127	KG/M^3
S	S	.0468	M^2
$c/2$	RL	.0625	M
m	BM	1.367	KG
I	TMOI	.0238	$KG\ M^2$
I_y	SMOI	.0028	$KG\ M^2$
γ_{ss}	GSS	-27.7	DEG
C_D	C(1)	1.42	ALL DERIVATIVES IN RADIANS
$C_{L\hat{\omega}}$	C(2)	2.39	
C_{M_a}	C(3)	.508	
$C_{M_{\dot{\alpha}}\hat{\omega}}$	C(4)	-.45	
$C_{y\beta}$	C(5)	-2.51	
$C_{y\beta^3}$	C(6)	0	
$C_{L\hat{\omega}\beta}$	C(7)	-1.23	
$C_{l\hat{p}}$	C(8)	-4.24	
$C_{l\hat{\omega}\beta^3}$	C(9)	345	
$C_{l\hat{p}^3}$	C(10)	0	
$C_{l\hat{\omega}\beta^2\hat{p}}$	C(11)	0	
$C_{l\hat{\omega}\beta\hat{p}^2}$	C(12)	0	
$C_{n\beta}$	C(13)	1.30	
$C_{n\hat{r}}$	C(14)	-10	
$C_{n\beta^2}$	C(15)	-212	
$C_{n\hat{r}^3}$	C(16)	0	
$C_{n\beta^2\hat{r}}$	C(17)	0	
$C_{n\beta\hat{r}^2}$	C(18)	0	

CONTROL PARAMETERS

	COMP.SY.	VALUE	DIM.
No. of Equations	NDIM	10	-
Initial Time	PRMT(1)	0	DNT
Final Time	PRMT(2)	.6	DNT
Upper Time Incr.	PRMT(3)	10^{-2}	DNT
Upper Error Bd.	PRMT(4)	10^{-5}	-

INITIAL CONDITIONS				ERROR WEIGHTS		
SYM.	CO.S	VALUE	DIM.	SYM.	VAL.	DIM.
V_R	P(1)	7	M/SEC	$\Delta\bar{V}_R$	.05	DNL/DNT
γ_R	P(2)	-50	DEG	$\Delta\gamma_R$	.049	RAD
ω_R	P(3)	300	RPM	$\Delta\bar{\omega}_R$	.001	RAD/DNT
β	P(4)	3	DEG	$\Delta\beta$	.2	RAD
ϕ	P(5)	0	DEG	$\Delta\phi$	.2	RAD
$\dot{\phi}$	P(6)	0	DEG/SEC	$\Delta\dot{\phi}$	.05	RAD/DNT
ψ	P(7)	0	DEG	$\Delta\psi$	.2	RAD
$\dot{\psi}$	P(8)	0	DEG/SEC	$\Delta\dot{\psi}$	.05	RAD/DNT
x	P(9)	0	M	$\Delta\bar{x}$	.1	DNL
z	P(10)	0	M	$\Delta\bar{z}$	.1	DNL

REMARKS:

Aerodynamic data from NACA Langley Stability Tunnel Test RM SL 55J26. November 1955

RUN NO.: 34

IDENTIFICATION: CYL. MR 1

MAGNUS ROTOR PARAMETERS

SYMBOL	COMP.SY.	VALUE	DIM.
ρ	RHO	1.127	KG/M^3
S	S	.0464	M^2
c/ℓ	RL	.0762	M
m	BM	3.148	KG
I	TMOI	.0598	$KG\ M^2$
I_y	SMOI	.0248	$KG\ M^2$
γ_{ss}	GSS	-42.3	DEG
C_D	C(1)	1.3	ALL DERIVATIVES IN RADIANS
$C_{L\hat{\omega}}$	C(2)	2.64	
C_{M_α}	C(3)	.21	
$C_{M_{\alpha\hat{\omega}}}$	C(4)	-.40	
C_{y_β}	C(5)	-4.9	
$C_{y_{\beta^3}}$	C(6)	0	
$C_{\ell_{\hat{\omega}\beta}}$	C(7)	-2.0	
$C_{\ell_{\hat{p}}}$	C(8)	-10 1/	
$C_{\ell_{\hat{\omega}\beta^3}}$	C(9)	0	
$C_{\ell_{\hat{p}^3}}$	C(10)	0	
$C_{\ell_{\hat{\omega}\beta^2\hat{p}}}$	C(11)	0	
$C_{\ell_{\hat{\omega}\beta\hat{p}^2}}$	C(12)	0	
C_{n_β}	C(13)	-2.0	
$C_{n_{\hat{r}}}$	C(14)	-20 1/	
$C_{n_{\beta^3}}$	C(15)	0	
$C_{n_{\hat{r}^3}}$	C(16)	0	
$C_{n_{\beta^2\hat{r}}}$	C(17)	0	
$C_{n_{\beta\hat{r}^2}}$	C(18)	0	

CONTROL PARAMETERS

	COMP.SY.	VALUE	DIM.
No. of Equations	NDIM	10	-
Initial Time	PRMT(1)	0	DNT
Final Time	PRMT(2)	7	DNT
Upper Time Incr.	PRMT(3)	10^{-2}	DNT
Upper Error Bd.	PRMT(4)	10^{-5}	-

INITIAL CONDITIONS				ERROR WEIGHTS		
SYM.	CO.S	VALUE	DIM.	SYM.	VAL.	DIM.
V_R	P(1)	13.5	M/SEC	$\Delta\bar{V}_R$	.05	DNL/DNT
γ_R	P(2)	-32	DEG	$\Delta\gamma_R$	.049	RAD
ω_R	P(3)	470	RPM	$\Delta\bar{\omega}_R$	.001	RAD/DNT
β	P(4)	0	DEG	$\Delta\beta$	.2	RAD
ϕ	P(5)	0	DEG	$\Delta\phi$	.2	RAD
$\dot{\phi}$	P(6)	0	DEG/SEC	$\Delta\mathring{\phi}$	.05	RAD/DNT
ψ	P(7)	0	DEG	$\Delta\psi$	.2	RAD
$\dot{\psi}$	P(8)	0	DEG/SEC	$\Delta\mathring{\psi}$	.05	RAD/DNT
x	P(9)	0	M	$\Delta\bar{x}$	.1	DNL
z	P(10)	0	M	$\Delta\bar{z}$	.1	DNL

REMARKS:

Aerodynamic data from ARO, Inc.
Wind Tunnel Test PC 0037. May 1970

1/ from Flight Test, June 1970

RUN NO.: 35

IDENTIFICATION: TRIANG. MR 1

MAGNUS ROTOR PARAMETERS

SYMBOL	COMP.SY.	VALUE	DIM.
ρ	RHO	1.127	KG/M^3
S	S	.0810	M^2
c/ℓ	RL	.0880	M
m	BM	2.395	KG
I	TMOI	.0541	$KG\ M^2$
I_y	SMOI	.0123	$KG\ M^2$
γ_{ss}	GSS	-33.7	DEG
C_D	C(1)	1.03	ALL DERIVATIVES IN RADIANS
$C_{L\hat{\omega}}$	C(2)	2.0	
C_{M_α}	C(3)	.247	
$C_{M_{d\hat{\omega}}}$	C(4)	-.325	
C_{y_β}	C(5)	-3.85	
$C_{y_{\beta^3}}$	C(6)	0	
$C_{L\hat{\omega}\beta}$	C(7)	-.35	
$C_{L\hat{p}}$	C(8)	-5.4	
$C_{L\hat{\omega}\beta^3}$	C(9)	0	
$C_{L\hat{p}^3}$	C(10)	0	
$C_{L\hat{\omega}\beta^2\hat{p}}$	C(11)	0	
$C_{L\hat{\omega}\beta\hat{p}^2}$	C(12)	0	
C_{n_β}	C(13)	-2.0	
$C_{n_{\hat{R}}}$	C(14)	-13.1	
$C_{n_{\beta^3}}$	C(15)	0	
$C_{n_{\hat{R}^3}}$	C(16)	0	
$C_{n_{\beta^2\hat{R}}}$	C(17)	0	
$C_{n_{\beta\hat{R}^2}}$	C(18)	0	

CONTROL PARAMETERS

	COMP.SY.	VALUE	DIM.
No. of Equations	NDIM	10	-
Initial Time	PRMT(1)	0	DNT
Final Time	PRMT(2)	5	DNT
Upper Time Incr.	PRMT(3)	10^{-2}	DNT
Upper Error Bd.	PRMT(4)	10^{-5}	-

INITIAL CONDITIONS				ERROR WEIGHTS		
SYM.	CO.S	VALUE	DIM.	SYM.	VAL.	DIM.
V_R	P(1)	19	M/SEC	$\Delta\bar{V}_R$	.05	DNL/DNT
γ_R	P(2)	-40	DEG	$\Delta\gamma_R$	.049	RAD
ω_R	P(3)	200	RPM	$\Delta\bar{\omega}_R$	.001	RAD/DNT
β	P(4)	0	DEG	$\Delta\beta$	.2	RAD
ϕ	P(5)	3	DEG	$\Delta\phi$	.2	RAD
$\dot{\phi}$	P(6)	0	DEG/SEC	$\Delta\dot{\phi}$	.05	RAD/DNT
ψ	P(7)	0	DEG	$\Delta\psi$	.2	RAD
$\dot{\psi}$	P(8)	0	DEG/SEC	$\Delta\dot{\psi}$	.05	RAD/DNT
x	P(9)	0	M	$\Delta\bar{x}$	.1	DNL
z	P(10)	0	M	$\Delta\bar{z}$	.1	DNL

REMARKS:

Aerodynamic data from Aerojet General Corp., IR & D Report 8706-23(01)FP April 1965

RUN NO.: 36

IDENTIFICATION: RECT. MR 2

MAGNUS ROTOR PARAMETERS			
SYMBOL	COMP.SY.	VALUE	DIM.
ρ	RHO	1.140	KG/M^3
S	S	.0468	M^2
c/ℓ	RL	.0625	M
m	BM	1.607	KG
I	TMOI	.0336	$KG\ M^2$
I_y	SMOI	.0028	$KG\ M^2$
γ_{ss}	GSS	-27.7	DEG
C_D	C(1)	SEE RUN 32	ALL DERIVATIVES IN RADIANS
$C_{L_{\hat{\omega}}}$	C(2)		
C_{M_a}	C(3)		
$C_{M_{d\hat{\omega}}}$	C(4)		
C_{y_β}	C(5)		
$C_{y_{\beta^3}}$	C(6)		
$C_{\ell_{\hat{\omega}\beta}}$	C(7)		
$C_{\ell_{\hat{p}}}$	C(8)		
$C_{\ell_{\hat{\omega}\beta^3}}$	C(9)		
$C_{\ell_{\hat{p}^3}}$	C(10)		
$C_{\ell_{\hat{\omega}\beta^2\hat{p}}}$	C(11)		
$C_{\ell_{\hat{\omega}\beta\hat{p}^2}}$	C(12)		
C_{n_β}	C(13)		
$C_{n_{\hat{R}}}$	C(14)		
$C_{n_{\beta^3}}$	C(15)		
$C_{n_{\hat{R}^3}}$	C(16)		
$C_{n_{\beta^2\hat{R}}}$	C(17)		
$C_{n_{\beta\hat{R}^2}}$	C(18)		

CONTROL PARAMETERS			
	COMP.SY.	VALUE	DIM.
No. of Equations	NDIM	10	-
Initial Time	PRMT(1)	0	DNT
Final Time	PRMT(2)	1	DNT
Upper Time Incr.	PRMT(3)	10^{-2}	DNT
Upper Error Bd.	PRMT(4)	10^{-5}	-

INITIAL CONDITIONS				ERROR WEIGHTS		
SYM.	CO.S	VALUE	DIM.	SYM.	VAL.	DIM.
V_R	P(1)	13.9	M/SEC	$\Delta\bar{V}_R$	.05	DNL/DNT
γ_R	P(2)	-27.7	DEG	$\Delta\gamma_R$	.049	RAD
ω_R	P(3)	2400	RPM	$\Delta\bar{\omega}_R$	.001	RAD/DNT
β	P(4)	0	DEG	$\Delta\beta$	.2	RAD
ϕ	P(5)	1.5	DEG	$\Delta\phi$	.2	RAD
$\dot{\phi}$	P(6)	0	DEG/SEC	$\Delta\dot{\phi}$	.05	RAD/DNT
ψ	P(7)	0	DEG	$\Delta\psi$	.2	RAD
$\dot{\psi}$	P(8)	-30	DEG/SEC	$\Delta\dot{\psi}$	.05	RAD/DNT
X	P(9)	0	M	$\Delta\bar{X}$	.1	DNL
Z	P(10)	0	M	$\Delta\bar{Z}$	.1	DNL

REMARKS:

RUN NO.: 37

IDENTIFICATION: RECT. MR 4

MAGNUS ROTOR PARAMETERS

SYMBOL	COMP.SY.	VALUE	DIM.
ρ	RHO	SEE RUN 32	KG/M^3
S	S		M^2
c/ℓ	RL		M
m	BM		KG
I	TMOI		$KG\ M^2$
I_y	SMOI		$KG\ M^2$
γ_{ss}	GSS		DEG
C_D	C(1)	SEE RUN 32	ALL DERIVATIVES IN RADIANS
$C_{L\hat{\omega}}$	C(2)		
C_{M_0}	C(3)		
$C_{M_d\hat{\omega}}$	C(4)		
$C_{y_\gamma\beta}$	C(5)		
$C_{y_\gamma\beta^3}$	C(6)		
$C_{\ell\hat{\omega}\beta}$	C(7)		
$C_{\ell\hat{p}}$	C(8)		
$C_{\ell\hat{\omega}\beta^3}$	C(9)		
$C_{\ell\hat{p}^3}$	C(10)		
$C_{\ell\hat{\omega}\beta^2\hat{p}}$	C(11)		
$C_{\ell\hat{\omega}\beta\hat{p}^2}$	C(12)		
$C_{n\beta}$	C(13)		
$C_{n\hat{R}}$	C(14)		
$C_{n\beta^3}$	C(15)		
$C_{n\hat{R}^3}$	C(16)		
$C_{n\beta^2\hat{R}}$	C(17)		
$C_{n\beta\hat{R}^2}$	C(18)		

CONTROL PARAMETERS

	COMP.SY.	VALUE	DIM.
No. of Equations	NDIM	10	-
Initial Time	PRMT(1)	0	DNT
Final Time	PRMT(2)	1	DNT
Upper Time Incr.	PRMT(3)	10^{-2}	DNT
Upper Error Bd.	PRMT(4)	10^{-5}	-

INITIAL CONDITIONS				ERROR WEIGHTS		
SYM.	CO.S	VALUE	DIM.	SYM.	VAL.	DIM.
V_R	P(1)	12.9	M/SEC	$\Delta\bar{V}_R$	.05	DNL/DNT
γ_R	P(2)	-27.7	DEG	$\Delta\gamma_R$	.049	RAD
ω_R	P(3)	2227	RPM	$\Delta\bar{\omega}_R$	.001	RAD/DNT
β	P(4)	0	DEG	$\Delta\beta$	.2	RAD
ϕ	P(5)	1.5	DEG	$\Delta\phi$	.2	RAD
$\dot{\phi}$	P(6)	0	DEG/SEC	$\Delta\mathring{\phi}$	.05	RAD/DNT
ψ	P(7)	0	DEG	$\Delta\psi$	.2	RAD
$\dot{\psi}$	P(8)	-27.8	DEG/SEC	$\Delta\mathring{\psi}$	.05	RAD/DNT
X	P(9)	0	M	$\Delta\bar{X}$	.1	DNL
Z	P(10)	0	M	$\Delta\bar{Z}$	.1	DNL

REMARKS:

RUN NO.: 38

IDENTIFICATION: CYL. MR 11

MAGNUS ROTOR PARAMETERS

SYMBOL	COMP.SY.	VALUE	DIM.
ρ	RHO	SEE RUN 31	KG/M^3
S	S		M^2
c/ℓ	RL		M
m	BM		KG
I	TMOI		$KG\ M^2$
I_y	SMOI		$KG\ M^2$
γ_{ss}	GSS		DEG
C_D	C(1)	SEE RUN 30	ALL DERIVATIVES IN RADIANS
$C_{L_{\hat{\omega}}}$	C(2)		
C_{M_m}	C(3)		
$C_{M_{d\hat{\omega}}}$	C(4)		
C_{y_β}	C(5)		
$C_{y_{\beta^3}}$	C(6)		
$C_{\ell_{\hat{\omega}\beta}}$	C(7)		
$C_{\ell_{\hat{p}}}$	C(8)		
$C_{\ell_{\hat{\omega}\beta^3}}$	C(9)		
$C_{\ell_{\hat{p}^3}}$	C(10)		
$C_{\ell_{\hat{\omega}\beta^2\hat{p}}}$	C(11)		
$C_{\ell_{\hat{\omega}\beta\hat{p}^2}}$	C(12)		
C_{n_β}	C(13)		
$C_{n_{\hat{r}}}$	C(14)		
$C_{n_{\beta^3}}$	C(15)		
$C_{n_{\hat{r}^3}}$	C(16)		
$C_{n_{\beta^2\hat{r}}}$	C(17)		
$C_{n_{\beta\hat{r}^2}}$	C(18)		

CONTROL PARAMETERS

	COMP.SY.	VALUE	DIM.
No. of Equations	NDIM	10	-
Initial Time	PRMT(1)	.53	DNT
Final Time	PRMT(2)	7	DNT
Upper Time Incr.	PRMT(3)	10^{-1}	DNT
Upper Error Bd.	PRMT(4)	10^{-5}	-

INITIAL CONDITIONS				ERROR WEIGHTS		
SYM.	CO.S	VALUE	DIM.	SYM.	VAL.	DIM.
V_R	P(1)	18	M/SEC	$\Delta\bar{V}_R$	.05	DNL/DNT
γ_R	P(2)	-51	DEG	$\Delta\gamma_R$	.049	RAD
ω_R	P(3)	230	RPM	$\Delta\bar{\omega}_R$	.001	RAD/DNT
β	P(4)	0	DEG	$\Delta\beta$	.2	RAD
ϕ	P(5)	0	DEG	$\Delta\phi$	.2	RAD
$\dot{\phi}$	P(6)	0	DEG/SEC	$\Delta\dot{\phi}$	.05	RAD/DNT
ψ	P(7)	0	DEG	$\Delta\psi$	.2	RAD
$\dot{\psi}$	P(8)	0	DEG/SEC	$\Delta\dot{\psi}$	.05	RAD/DNT
x	P(9)	0	M	$\Delta\bar{x}$	.1	DNL
z	P(10)	0	M	$\Delta\bar{z}$	.1	DNL

REMARKS:

RUN NO.: 39

IDENTIFICATION: TRIANG. MR 1

MAGNUS ROTOR PARAMETERS

SYMBOL	COMP.SY.	VALUE	DIM.
ρ	RHO	1.225	KG/M^3
S	S	.0810	M^2
c/ℓ	RL	.0880	M
m	BM	2.395	KG
I	TMOI	.0541	$KG\ M^2$
I_y	SMOI	.0123	$KG\ M^2$
γ_{ss}	GSS	-33.7	DEG
C_D	C(1)	SEE RUN 35	ALL DERIVATIVES IN RADIANS
$C_{L\hat{\omega}}$	C(2)		
C_{M_α}	C(3)		
$C_{M_{d\hat{\omega}}}$	C(4)		
C_{Y_β}	C(5)		
$C_{Y_{\beta^3}}$	C(6)		
$C_{\ell_{\hat{\omega}\beta}}$	C(7)		
$C_{\ell_{\hat{p}}}$	C(8)		
$C_{\ell_{\hat{\omega}\beta^3}}$	C(9)		
$C_{\ell_{\hat{p}^3}}$	C(10)		
$C_{\ell_{\hat{\omega}\beta^2\hat{p}}}$	C(11)		
$C_{\ell_{\hat{\omega}\beta\hat{p}^2}}$	C(12)		
C_{n_β}	C(13)		
$C_{n_{\hat{r}}}$	C(14)		
$C_{n_{\beta^3}}$	C(15)		
$C_{n_{\hat{r}^3}}$	C(16)		
$C_{n_{\beta^2\hat{r}}}$	C(17)		
$C_{n_{\beta\hat{r}^2}}$	C(18)		

CONTROL PARAMETERS

	COMP.SY.	VALUE	DIM.
No. of Equations	NDIM	10	-
Initial Time	PRMT(1)	0	DNT
Final Time	PRMT(2)	7	DNT
Upper Time Incr.	PRMT(3)	10^{-2}	DNT
Upper Error Bd.	PRMT(4)	10^{-5}	-

INITIAL CONDITIONS				ERROR WEIGHTS		
SYM.	CO.S	VALUE	DIM.	SYM.	VAL.	DIM.
V_R	P(1)	100	M/SEC	$\Delta\bar{V}_R$	.05	DNL/DNT
γ_R	P(2)	0	DEG	$\Delta\gamma_R$	.049	RAD
ω_R	P(3)	200	RPM	$\Delta\bar{\omega}_R$	.001	RAD/DNT
β	P(4)	0	DEG	$\Delta\beta$	.2	RAD
ϕ	P(5)	3	DEG	$\Delta\phi$	.2	RAD
$\dot{\phi}$	P(6)	0	DEG/SEC	$\Delta\mathring{\phi}$	.05	RAD/DNT
ψ	P(7)	0	DEG	$\Delta\psi$	.2	RAD
$\dot{\psi}$	P(8)	0	DEG/SEC	$\Delta\mathring{\psi}$	.05	RAD/DNT
x	P(9)	0	M	$\Delta\bar{x}$	.1	DNL
z	P(10)	0	M	$\Delta\bar{z}$	.1	DNL

REMARKS:

RUN NO.: 40

IDENTIFICATION: CYL. MR 1

MAGNUS ROTOR PARAMETERS

SYMBOL	COMP.SY.	VALUE	DIM.
ρ	RHO	1.225	KG/M^3
S	S	.0464	M^2
c/ℓ	RL	.0762	M
m	BM	3.148	KG
I	TMOI	.0598	$KG\ M^2$
I_y	SMOI	.0248	$KG\ M^2$
γ_{ss}	GSS	-42.3	DEG
C_D	C(1)	SEE RUN 34	ALL DERIVATIVES IN RADIANS
$C_{L\hat{\omega}}$	C(2)		
C_{M_α}	C(3)		
$C_{M_{d\hat{\omega}}}$	C(4)		
C_{y_β}	C(5)		
$C_{y_{\beta^3}}$	C(6)		
$C_{L\hat{\omega}\beta}$	C(7)		
$C_{L\hat{p}}$	C(8)		
$C_{L\hat{\omega}\beta^3}$	C(9)		
$C_{L\hat{p}^3}$	C(10)		
$C_{L\hat{\omega}\beta^2\hat{p}}$	C(11)		
$C_{L\hat{\omega}\beta\hat{p}^2}$	C(12)		
$C_{n\beta}$	C(13)		
$C_{n\hat{R}}$	C(14)		
$C_{n\beta^3}$	C(15)		
$C_{n\hat{R}^3}$	C(16)		
$C_{n\beta^2\hat{R}}$	C(17)		
$C_{n\beta\hat{R}^2}$	C(18)		

CONTROL PARAMETERS

	COMP.SY.	VALUE	DIM.
No. of Equations	NDIM	10	-
Initial Time	PRMT(1)	0	DNT
Final Time	PRMT(2)	7	DNT
Upper Time Incr.	PRMT(3)	10^{-2}	DNT
Upper Error Bd.	PRMT(4)	10^{-5}	-

INITIAL CONDITIONS				ERROR WEIGHTS		
SYM.	CO.S	VALUE	DIM.	SYM.	VAL.	DIM.
V_R	P(1)	1	M/SEC	$\Delta\bar{V}_R$	.05	DNL/DNT
γ_R	P(2)	0	DEG	$\Delta\gamma_R$	.049	RAD
ω_R	P(3)	4000	RPM	$\Delta\bar{\omega}_R$	.001	RAD/DNT
β	P(4)	3	DEG	$\Delta\beta$	.2	RAD
ϕ	P(5)	0	DEG	$\Delta\phi$	.2	RAD
$\dot{\phi}$	P(6)	0	DEG/SEC	$\Delta\dot{\phi}$	.05	RAD/DNT
ψ	P(7)	0	DEG	$\Delta\psi$	.2	RAD
$\dot{\psi}$	P(8)	0	DEG/SEC	$\Delta\dot{\psi}$	.05	RAD/DNT
x	P(9)	0	M	$\Delta\bar{x}$	.1	DNL
z	P(10)	0	M	$\Delta\bar{z}$	.1	DNL

REMARKS:

RUN NO.: 41

IDENTIFICATION: CYL. MR 3

MAGNUS ROTOR PARAMETERS			
SYMBOL	COMP.SY.	VALUE	DIM.
ρ	RHO	1.127	KG/M^3
S	S	.0464	M^2
c/ℓ	RL	.0762	M
m	BM	3.242	KG
I	TMOI	.0617	$KG\ M^2$
I_y	SMOI	.0247	$KG\ M^2$
γ_{ss}	GSS	-42.3	DEG
C_D	C(1)	SEE RUN 34	ALL DERIVATIVES IN RADIANS
$C_{L_{\hat{\omega}}}$	C(2)		
C_{M_0}	C(3)		
$C_{M_{d\hat{\omega}}}$	C(4)		
C_{y_β}	C(5)		
$C_{y_{\beta^3}}$	C(6)		
$C_{\ell_{\hat{\omega}\beta}}$	C(7)		
$C_{\ell_{\hat{p}}}$	C(8)		
$C_{\ell_{\hat{\omega}\beta^3}}$	C(9)		
$C_{\ell_{\hat{p}^3}}$	C(10)		
$C_{\ell_{\hat{\omega}\beta^2\hat{p}}}$	C(11)		
$C_{\ell_{\hat{\omega}\beta\hat{p}^2}}$	C(12)		
C_{n_β}	C(13)		
$C_{n_{\hat{R}}}$	C(14)		
$C_{n_{\beta^3}}$	C(15)		
$C_{n_{\hat{R}^3}}$	C(16)		
$C_{n_{\beta^2\hat{R}}}$	C(17)		
$C_{n_{\beta\hat{R}^2}}$	C(18)		

CONTROL PARAMETERS			
	COMP.SY.	VALUE	DIM.
No. of Equations	NDIM	10	-
Initial Time	PRMT(1)		DNT
Final Time	PRMT(2)		DNT
Upper Time Incr.	PRMT(3)		DNT
Upper Error Bd.	PRMT(4)		-

INITIAL CONDITIONS				ERROR WEIGHTS		
SYM.	CO.S	VALUE	DIM.	SYM.	VAL.	DIM.
V_R	P(1)		M/SEC	$\Delta\bar{V}_R$	.05	DNL/DNT
γ_R	P(2)		DEG	$\Delta\gamma_R$	.049	RAD
ω_R	P(3)		RPM	$\Delta\bar{\omega}_R$	.001	RAD/DNT
β	P(4)		DEG	$\Delta\beta$	.2	RAD
ϕ	P(5)		DEG	$\Delta\phi$	.2	RAD
$\dot{\phi}$	P(6)		DEG/SEC	$\Delta\dot{\phi}$	.05	RAD/DNT
ψ	P(7)		DEG	$\Delta\psi$	.2	RAD
$\dot{\psi}$	P(8)		DEG/SEC	$\Delta\dot{\psi}$	.05	RAD/DNT
x	P(9)		M	$\Delta\bar{x}$	.1	DNL
z	P(10)		M	$\Delta\bar{z}$	.1	DNL

REMARKS:

CYL. MR 3 was flight tested only. It is similar to CYL. MR 1 with small changes in mass distribution.

Unclassified
Security Classification

DOCUMENT CONTROL DATA - R & D

(Security classification of title, body of abstract and indexing annotation must be entered when the overall report is classified)

1. ORIGINATING ACTIVITY (Corporate author) Department of the Army Fort Detrick Frederick, Maryland 21701	2a. REPORT SECURITY CLASSIFICATION Unclassified 2b. GROUP

3. REPORT TITLE

ON FLIGHT DYNAMICS OF MAGNUS ROTORS

4. DESCRIPTIVE NOTES (Type of report and inclusive dates)

5. AUTHOR(S) (First name, middle initial, last name)

Peter H. Zipfel

6. REPORT DATE November 1970	7a. TOTAL NO. OF PAGES 264	7b. NO. OF REFS 28
8a. CONTRACT OR GRANT NO b. PROJECT NO 1T061101A91A c. d.	9a. ORIGINATOR'S REPORT NUMBER(S) Technical Report 117 9b. OTHER REPORT NO(S) (Any other numbers that may be assigned this report) AMXFD-AE-T 50403	

10. DISTRIBUTION STATEMENT Distribution of this publication is unlimited; it has been cleared for release to the general public. Non-DOD agencies may purchase this publication from Clearinghouse, ATTN: Storage and Dissemination Section, Springfield, Virginia, 22151.

11. SUPPLEMENTARY NOTE Munitions Development Division	12. SPONSORING MILITARY ACTIVITY Department of the Army Fort Detrick Frederick, Maryland 21701

13. ABSTRACT

A Magnus rotor is an autorotating flight vehicle, designed to develop a Magnus force efficiently and to employ it as the major lift force in free flight. In this report the equations of motion of Magnus rotors are derived and their performance and stability analyzed and correlated with free flight tests. Tensor concepts are used extensively in formulating the flight dynamical problem. In particular, the ordinary time derivative is replaced by the Rotational Derivative, thus permitting an invariant formulation of the equations of motion, even under time-dependent coordinate transformations. The perturbation equations are nonlinear nonautonomous ordinary differential equations of fifth-order with three degrees-of-freedom: rolling, yawing, and sideslipping. Their stability is analyzed. A reduction to one degree-of-freedom is achieved by combining the roll and yaw angles to form the nutation angle and by employing the method of averaging. The stability of the resulting first-order equation is discussed. Necessary and sufficient conditions for limit cycles are derived, and it is shown how limit cycles can be avoided by proper design of the Magnus rotor. Thirty models were flight tested. Their trajectories and attitude motions are correlated with computer simulations whose aerodynamic input data are solely based on wind tunnel tests. The agreement is satisfactory. Two different Magnus shapes were tested for limit cycles. The test results agree well with predictions.

DD FORM 1 NOV 65 1473 REPLACES DD FORM 1473, 1 JAN 64, WHICH IS OBSOLETE FOR ARMY USE.

Unclassified
Security Classification

Unclassified
Security Classification

14 KEY WORDS	LINK A ROLE	LINK A WT	LINK B ROLE	LINK B WT	LINK C ROLE	LINK C WT
Magnus rotors						
Flight dynamics						
Flight testing						
Aeroballistics						
Equations of Motion						
Aerodynamic derivative						
Tensor analysis						
Time derivative						
Perturbation equations						
Aerial delivery						
Decelerator						
Spinning bodies						
Rigid body dynamics						

Unclassified
Security Classification